



UNIVERSITÉ
F R A N C O
I T A L I E N N E

UNIVERSITÀ
I T A L O
F R A N C E S E



**Università
degli Studi
di Ferrara**

Memoire 1 for the double degree Master in:

Mention Archéologie, sciences pour l'archéologie parcours
Arts, Sociétés, Environnements de la Préhistoire et de la
Protohistoire: Europe, Afrique

***Micromorphological contribution to the
anthropogenic structures issue at Mas Des Caves
archaeological site (Hérault, Occitanie, FR)***

Directors: Bruxelles Laurent

Lejay Mathieu

Fontana Federica

Student: Esposito Corrado

2022 - 2023

Table of Contents

Abstract	7
Résumé	8
1. Introduction	9
1.1 State of the art	9
1.2 New excavation programs	13
1.3 Geological and geographical background	14
1.3.1 Geomorphology	14
1.3.2 Speleogenesis and cavity infilling	16
1.3.3 Stratigraphy	18
1.4 Anthropogenic structures issue	19
2. Methodology	24
2.1 State of the art	24
2.2 General principles of Soil Micromorphology	26
2.3 Technical aspects.....	27
2.3.1 Sampling.....	27
2.3.2 Thin section preparation and observation	28
2.4 Elements of descriptions	29
2.4.1 Mesoscale observation	29
2.4.2 Microscale observation	30
2.5 Common micromorphological features in cave sites	36
2.5.1 Common geogenic depositional features	36
2.5.2 Common pedofeatures in caves' deposits	37
2.5.3 Biogenetic features	38
2.5.4 Traces of anthropogenic activities.....	39
2.6 Sampling at Mas des Caves.....	41
2.6.1 Sampling technique	41

2.6.2 Sampling strategy	42
2.6.3 Methodology applied for the analysis of Mas des Caves' thin sections	46
3. Results	48
MM1	50
MM2.....	52
MM3.....	54
MM4.....	56
MM5.....	58
4. Discussions.....	61
4.1 Stratigraphic position of the thin sections	61
4.2 Facies correlations and microlayers	62
4.3 Depositional and post-depositional processes of microlayers.....	67
4.4 Carnivore activities	71
4.5 Human activities.....	72
4.5.1 Anthropogenic structures issue	75
5. Conclusions and future perspectives	76
5.1 Conclusions	76
5.2 Future perspectives.....	78
Bibliography.....	81
APPENDIX	86
MM1	87
Stratigraphic description of the block	87
Mesoscopic description of the section	90
Microscopic description of facies.....	92
MM2.....	105
Stratigraphic description of the block	105
Mesoscopic description of the thin section	107

Microscopic description of facies.....	109
MM3.....	122
Stratigraphic description of the block	122
Mesoscopic description of the thin section	125
Microscopic description of facies.....	128
MM4.....	149
Stratigraphic description of the block	149
Mesoscopic description of the thin section	152
Microscopic description of facies.....	155
MM5.....	168
Stratigraphic description of the block	168
Mesoscopic description of the thin section	171
Microscopic description of facies.....	173
Appendix bibliography.....	185
Acknowledgements	187

Abstract

In this Memoire, it will be presented a micromorphological analysis done at the archaeological site of Mas Des Caves (Hérault, Occitanie, FR). The primary objective is to investigate a specific layer (*couche 9*) which contains a complex of pebbles previously identified as an anthropogenic structure (*Sol 76*) by former director, notably Bonifay between the 1960s and the 1980s. Nowadays this interpretation of the structure is in doubt and several studies and methodologies are currently ongoing aimed at validating or rejecting it. To address this issue, however, the use of a multidisciplinary approach is needed.

Thus, this micromorphological analysis falls into a boarder project, resulting to be a piece of the puzzle rather than a standalone element.

The Memoire is structured into an introduction, in which the site and the objective are exposed. Successively the methodology is presented. Only a summary of the results is presented in the main body of the Memoire, the complete observations made on the thin sections can be find in the appendix. Finally, before a short conclusion, the results will be discussed.

Résumé

Ce mémoire présente une analyse micromorphologique réalisée sur le site archéologique du Mas Des Caves (Hérault, Occitanie, FR). L'objectif principal est d'étudier une couche spécifique (couche 9) qui contient un complexe de galets précédemment identifié comme une structure anthropique (Sol 76) par l'ancien directeur, notamment Bonifay entre les années 1960 et 1980. Aujourd'hui, cette interprétation de la structure est remise en question et plusieurs études et méthodologies sont actuellement en cours afin de la valider ou de la rejeter. Pour répondre à cette question, l'utilisation d'une approche multidisciplinaire est nécessaire, y compris la perspective micromorphologique présentée dans ce mémoire.

Cette analyse micromorphologique s'inscrit donc dans le cadre d'un projet frontalier et constitue une pièce du puzzle plutôt qu'un élément autonome.

Le mémoire est structuré en une introduction, dans laquelle le site et l'objectif sont exposés. La méthodologie est ensuite présentée. Seul un résumé des résultats est présenté dans le corps du Mémoire, les observations complètes faites sur les lames minces se trouvent en annexe. Enfin, avant une brève conclusion, les résultats seront discutés.

1. Introduction

1.1 State of the art

The archaeological site of Mas des Caves n° 1 or Lunel Viel 1 (LV I) is located within the cave of the same name, situated inside Lunel Viel commune's borders (Hérault, Occitanie, FR; lat. = 43,683421 ; long. = 4,080298, fig.1), on the left bank of Dardaillon river (fig.2).



Fig.1: Geographical location of Mas des Cave (modified from FranceTopo.fr).

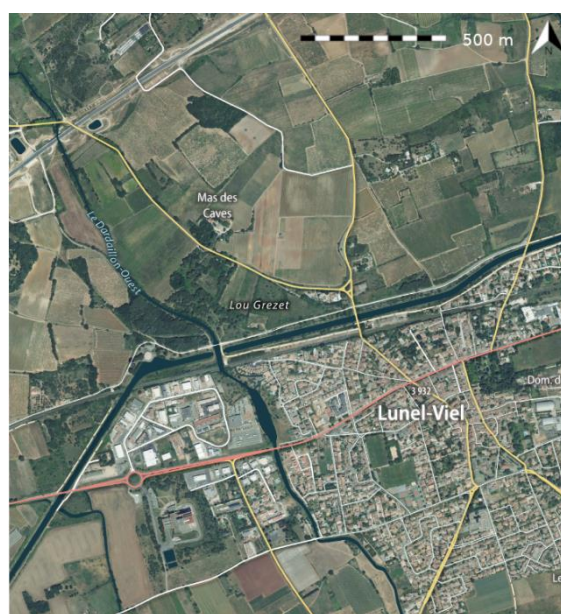


Fig.2: Zoom on the location of Mas des Cave (modified from FranceTopo.fr).

The archaeological site was discovered in 1800 during quarrying activities aimed at exploiting the local Miocene molasse. The first excavation activities were carried out by Marcel de Serres between 1824 and 1827, during which a trench was made (Tranchée M. de Serre in fig.3) (Brugal et al., 2022b, p. 9). After 1827 the archaeological site was completely abandoned until 1962, when Eugène Bonifay resumed research and excavation activities that would have last continuously until 1982.

The researches allowed the discover of the original entrance of the cave (dolina) in order to explore the karst network, from which allochthonous sediments get accumulated and completely filled the cavity (Brugal et al., 2021b, p. 9). Excavation activities by Bonifay, which last in around 20 years, led to the discovery of numerous paleontological finds and lithic artifacts that, in some cases, are still under study.

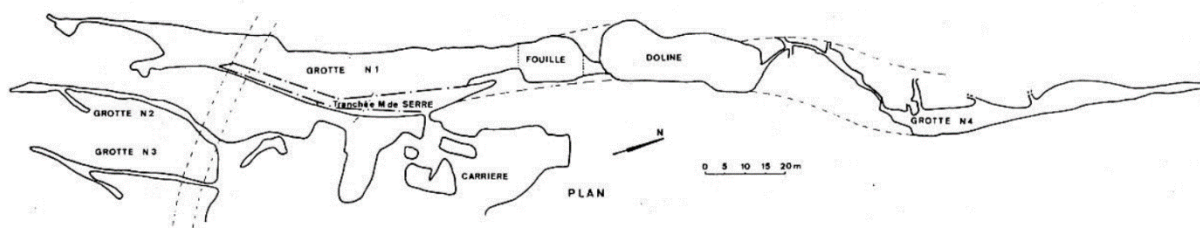


Fig.3: Map of the cave: on the left are visible the smaller cavities (LV II and LV III), in cave number 1 (LV I) is visible the trench excavated by M. de Serre. The area indicated with "fouille" indicate instead the area excavated during Bonifay's activities. Toward the north, the sinkhole (doline) and cave number 4 are visible. (Document of E. Bonifay in Brugal et al., 2021b, p. 10)

After Bonifay's researches, excavation activities were interrupted until 2019, when Jean-Philip Brugal (University of Aix Marseille) resumed the direction of the investigations with the aim of better clarify Bonifay's choices and his interpretations, aside to document and excavate Mas des Caves with modern and interdisciplinary techniques, approaches, and methodologies.

The observations and studies made under Bonifay's direction were thus the starting point for current research activities. Although, these results are currently under review as they have been carried out with non-modern techniques and methodologies. However, a brief summary of the discoveries and interpretations made by Bonifay turns out to be indispensable to well understand the starting point of the new excavation activities. All the following information concerns the research activities carried out in cave number 1 (LV I).

- Stratigraphy and sedimentology (Brugal et al., 2021b, p. 10):

The integrity of the stratigraphy has a significant thickness (about 12 m), but only its upper part has been observed. The base of the known part (2-3 m) consists of reddish clays (*argiles rouges*), sandy, with some large blocks of limestone inside, more or less lithified and sterile sediments. Their mode of emplacement was attributed to the presence of an underground paleo lake (Bonifay, 1976), presents throughout the karst network, while the origin of these clayish reddish sediments has been linked to open air alterites deposited in the cave by runoff phenomena through cave's paleo entrances, at the time of the red clays deposition the dolina (LV V) was still sealed.

On the top of this, we find a 2 to 5 m thick series of silts, sands, and gravels, generally reddish or yellowish in color. It originates exclusively from runoff phenomena coming from the dolina and the series has been subdivided into twelve levels according to

grain size and color changes. These levels are discontinuous, lenticular, and sometimes difficult to follow over large areas. All along this upper sequence elements pointing both to human occupations and to hyena dens have been found, it appears to be richer in hyena dens towards the base, while human occupation is more frequent towards the top.

This second phase of cavity filling also appears to have occurred fairly continuously and in a relatively short time (Bonnet, 1967).

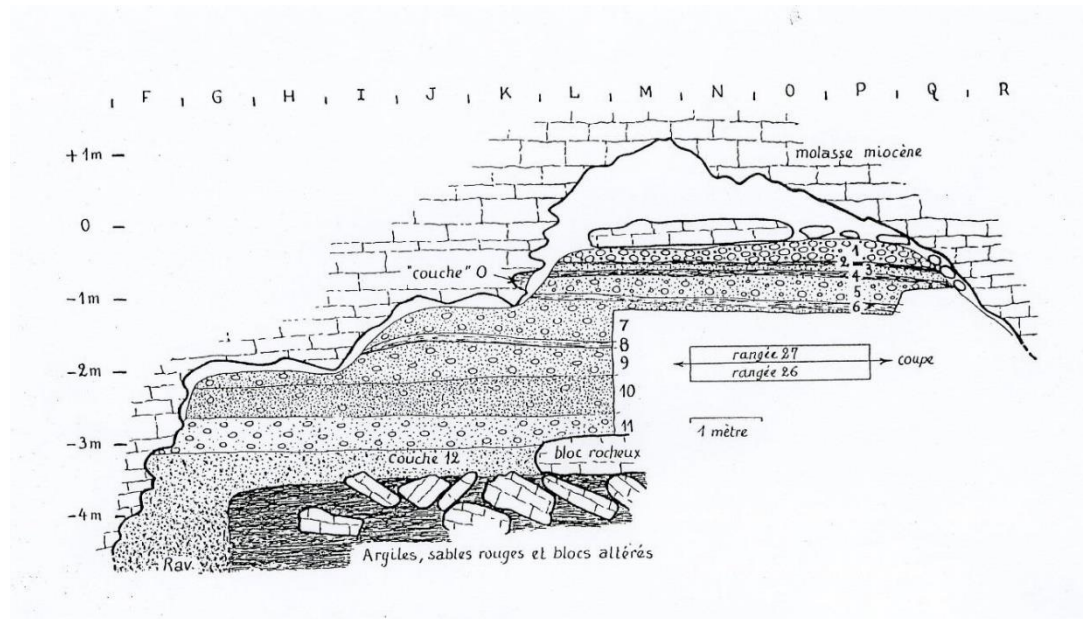


Fig.4: Stratigraphic section along the short axis of the cavity (east-west). Visible at the base of the sequence are the sterile reddish clays, on which the fossiliferous levels rest. (Document of E. Bonifay in Brugal et al., 2021b, p. 11)

- Human occupations (Brugal et al., 2021b, p. 12):

A relatively small amount of lithic industry was found (a few hundred pieces) during Bonifay's excavation campaigns. The lithic ensemble turns out to consist of numerous Levallois flakes and cores, scrapers, few denticulates, and a single possible biface fragment; the industry was attributed to the Mediterranean Acheulean facies. In addition, some bone remains have been interpreted as tools. Beyond the lithic industry an important element of Bonifay's observations and interpretations is the presence of habitation structures, including hut bottoms, combustion features of various types, paved areas, stone walls, and anthropogenic bone accumulations (waste deposits). The issue of these structures identified as anthropogenic by Bonifay will be better discussed later in the dedicated section. Anthropogenic frequentations of the cave were also interpreted as sporadic and related to main occupations located in the sinkhole area and on the plateau surrounding the cavity.

- Paleobiology and paleoenvironmental reconstruction (Brugal et al., 2021b, pp. 11–12): Paleontological remains represent most of the materials found in the cavity, they are in an excellent state of preservation, representing a wide variability of mammal species (both carnivores and herbivores) as well as birds, fishes, and reptiles. To be noted the high and varied presence of carnivores (including *Canidae*, *Felidae*, *Ursidae*, etc.) and in particular the presence of hyenas (both genus *Crocuta* and genus *Hyaena*), the latter also attested by the abandoned presence of coprolites associated with them.

The presence of hyenas is also very interesting in the occupational history of the site since, thanks to the findings associated with them (coprolites, digested and chewed bones, and bone remains of both adult and sub-adult hyena individuals), it has been possible to define the cave as a dwelling site of hyenas (Fosse, 1996).

Among the paleobotanical remains, on the other hand, the presence of hackberry seeds (genus *Celtis*) is noted, which (also integrated with faunal data) allowed the reconstruction of the paleoenvironment surrounding the cave. The latter was defined as composed of alternating forested and open-areas biotypes and characterized by a temperate climate, humid in winter and dry in summer.

- Chronology (Brugal et al., 2021b, p. 11):

Bonifay established a chronology of the upper portion of the infilling based on the stratigraphy, archeological materials and fossil fauna found in the site. Its formation was contextualized in a temperate and humid climate between the end of the Middle Pleistocene and the early beginning of the Upper Pleistocene (based on identified faunal taxons). In absolute value a large interval was considered, between 300 000 and 500 000 years ago.

Once Bonifay's excavation activities were completed, the materials continued to be studied, including the previously mentioned study on hyena activity in the cave (Fosse, 1996) and the technological and taphonomic study on the spatial distribution of the artifacts, which also brought to light questions about the issue of structures interpreted as anthropogenic by Bonifay (Le Grand, 1994). Even now, the materials recovered from Bonifay's activities are still being studied, particularly the paleontological materials (among them, one of the most recent is Uzunidis, 2020), which highlights the richness and very high potential of information that can be obtained from the Mas des Caves site.

All the information described before briefly reflect the state of research from which the new activities started, with the aim of clarifying and resolving the doubts that these information

have raised, particularly about the real degree of anthropization of the cave (Brugal et al., 2021b, p. 13).

1.2 New excavation programs

Succeeding the years-long stop of field research at the Mas des Caves site, in 2019, excavations resumed under the direction of Jean Philippe Brugal, mainly with the aim of using new techniques and investigation methodologies developed in archaeological research in recent decades to investigate the already known archaeological and paleontological potential of the site. These objectives, as already mentioned, precisely represent the starting point of the new investigations and that is why they necessarily need to be integrated into the new project, even if they inevitably need (considering the limited technologies available in those years) to be reviewed under a new perspective.

Several stages are prioritized to provide the best reconstruction of what happened in Mas des Caves. Below are some of the goals of the new research project (Brugal et al., 2021b).

Geochronological and stratigraphical redefinition, and reconstruction of sediments deposition patterns. Extensive and complete study of paleontological remains. Paleoenvironmental reconstruction based on the materials present at the site (fauna and flora, charcoals, and coprolites). Typological, technological, and spatial study of the lithic industry present in the cavity to understand the anthropogenic occupation patterns of the site. Taphonomic study of the deposit, with the aim of better understanding the post-depositional history of the materials, both lithic and faunal. Reconstruction of the karst history of the cavity, from its speleogenesis, through the opening of the cave following the collapse of the sinkhole, to its complete sealing. Development of an investigation methodology aimed at evaluating and reinterpreting the structures interpreted as anthropogenic by Bonifay.

In these first three years of research already great progress has been made on all fronts previously described, within the scope of this Memoire we will, however, limit ourselves to describing those most significant for our research, in particular we will focus on the new geological, karstological, stratigraphic and geomorphological informations of the site and on the renewed observations made on structures interpreted as anthropogenic by Bonifay.

1.3 Geological and geographical background

LV I cave is a relatively straight gallery with NE-SW orientation and measuring 150 m in length, 10-12 m in width, and nearly 6 m (variable) in height. Three other cavities are present in the same karstic network (fig.3): two narrower ones (LV II and LV III) running parallel to LV I, and LV IV, which is in continuity with LV I and presents speleothems inside (which are absent in LV I). Another geomorphological unit of the karstic network is the dolina (LV V), which generated from the collapse of the vault between the two cavities in continuity with each other (LV I and LV IV), thus becoming the original entrance of both these cavities (Brugal et al., 2021a).

1.3.1 Geomorphology

The information presented in this paragraph were synthesized from geomorphological observations made by Laurent Bruxelles and presented in the 2020 Mas des Caves excavation report (Bruxelles in Brugal et al., 2020, pp. 26–34).

From a geomorphological point of view, the landscape surrounding Mas des Caves appears to be composed of three different geomorphological units. The first geomorphological unit consist of limestone outcrops formed during the Burdigalian age and is the unit where Mas des Caves was excavated. In the NW of the cavity, there are the two Dardaillon valleys (the Dardaillon Est and the Dardaillon Ouest), which cut into about thirty meters below the surrounding relief (that has an elevation of about 50 m above sea level) and also excavate the Burdigalian limestones. On the other hand, above the cavity the reliefs are surmounted by remains of Rhône fluvial terraces with quartzite pebbles.

These last two geomorphological units described reflect the surface formations found near the Mas de Caves cave:

- Rhodaniens pebble colluviums (*colluvions à galets Rhodaniens*):

This surface formation turns out to be composed of heavily degraded quartz pebbles embedded in a reddish sandy-clay matrix. Their genesis appears to be related to a reworking of Rhône's alluvial sediments in the form of colluviums. The original alluvial terraces are still visible in the higher areas, thus testifying their reworking and redeposition in the more depressed areas. These reworking processes have been mainly chronologically placed during the Pleistocene (their formation, however,

appears to be polyphasic and occurred throughout the Quaternary). The development of a soil and its subsequent erosion on these colluviums has also been hypothesized. They also appear to have acted as a water storage sponge that would thus have favored karst dissolution of the limestone substrate at preferential locations.

- Silty colluviums at the bottom of the slopes (*colluvions limoneuses de bas de versant*): The bottom of the slopes and the opening of the plain, on the other hand, appears to be characterized by the presence of colluviums of various types, incorporating archaeological materials (*terracotta* from the modern period) which are evidence of their young age of formation, which is probably related to agricultural activities. To note the local presence also of colluviums that are visibly older but whose chronological attribution is more problematic.

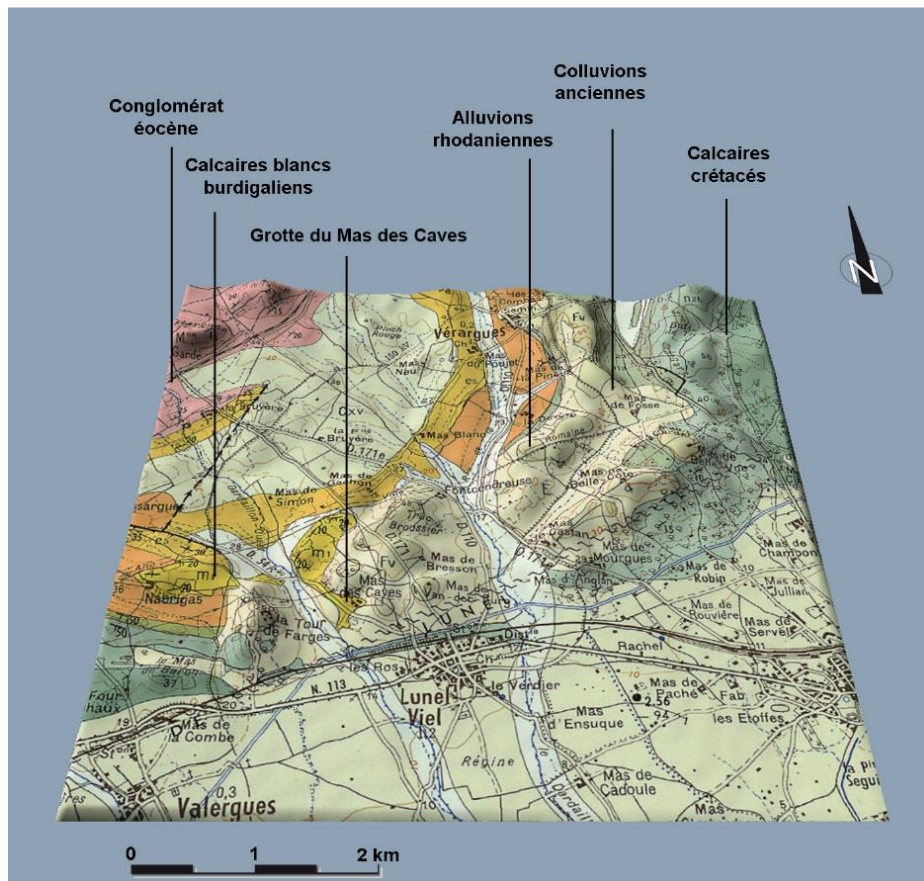


Fig.5: Geological and geomorphological context of Mas des Caves (Bruxelles in Brugal et al., 2020, p. 26)

1.3.2 Speleogenesis and cavity infilling

The information presented in this paragraph (where not explicitly stated), about the speleogenesis and filling of the cavity, were taken from observations and studies made by Laurent Bruxelles based on previous excavation reports, INRAP works in the framework of the construction of the Nîmes-Montpellier high-speed rail line, and present in the 2021 excavation report of Mas des Caves (Bruxelles in Brugal et al., 2021b, pp. 65–70).

The karstic network of Mas des Caves is located inside bioclastic limestone (*molasse*) from Burdigalian age (Lower Miocene). These are white limestones, more or less sandy, which locally contain numerous fossils.

The speleogenesis of the network has been chronologically located between the middle of the Miocene and the end of the Pliocene. Specifically, its formation is related to the lowering of the base level of hydrological regimes flowing into the Mediterranean Sea during the Messinian crisis (end of Miocene), which led to major waves of regressive erosion and to the development of deep underground networks in karsts.

Later, with the reestablishment of the base levels of the Mediterranean basin, previously eroded areas were sealed by marine and continental detrital sediments, thus generating drainage malfunction in the deep karst networks, leading to their progressive filling with clayish and sandy-clayish sediments.

The series of reddish clays (*argiles rouges*) present at the base of the sequence at Mas des Caves were therefore related to this geological phase. The deposition of these reddish clays thus appears to have occurred during a phase of complete flooding of the cavity, they would turn out to be insoluble karst clays released by the dissolution of the Miocene *molasse* in which the cavity is excavated. Their presence in the cavity then turns out to have influenced the morphology of the cavity as well, covering in fact the base of the latter they limited the dissolution at the base, which then occurred mainly on the walls and vault, thus allowing the development of the cavity by dissolution from the bottom to the top and contributing to the progressive accumulation of the clays, until the complete filling of the cavity by these. The deposition of these clays would then result simultaneous with a volumetric expansion phase of the cavity.

Once filled with red clays, the cavity appears to have undergone an erosive event, which carried away some of the clay sediments previously deposited, leaving room for a second phase of filling by the sediment series composed of gravels, sands, and sandy clays; the contact between the two series results in fact to be uncomfortable. The emplacement of this second

series of sediments appears to be related to runoff processes that introduced allochthonous sediments into the cavity, the chronology of this second phase of sedimentation has been assigned (preliminary data) to either MIS 9 (approximately 330-300 Ky) or MIS 7 (approximately 240-186 Ky) (Brugal et al., 2022a). The entrance through which these sediments entered is the geomorphological unit called LV V or *dolina* (sinkhole), which was formed due to a progressive thinning and subsequent collapse of the vault, and which divided LV I from LV IV (originally connected to each other). The opening of this sinkhole thus allowed allochthonous sediments to enter the karst network for the first time and gradually fill it until it was completely sealed, the main agent of transport and accumulation turns out to be water. In particular, the sediments that filled the cavity seem to correlate with the rhodaniens colluviums described earlier, reworked from runoff phenomena.

The presence of bats is also a factor to be noted, as their bio corrosive action has helped shape the morphology of the cavity, leaving recognizable traces (Bigot and Dardenne in Brugal et al., 2021b, pp. 42–46).

Once the cavity was completely obstructed by these sediments it underwent no further changes (except for eventual post-depositional processes) until its discovery in 1800.

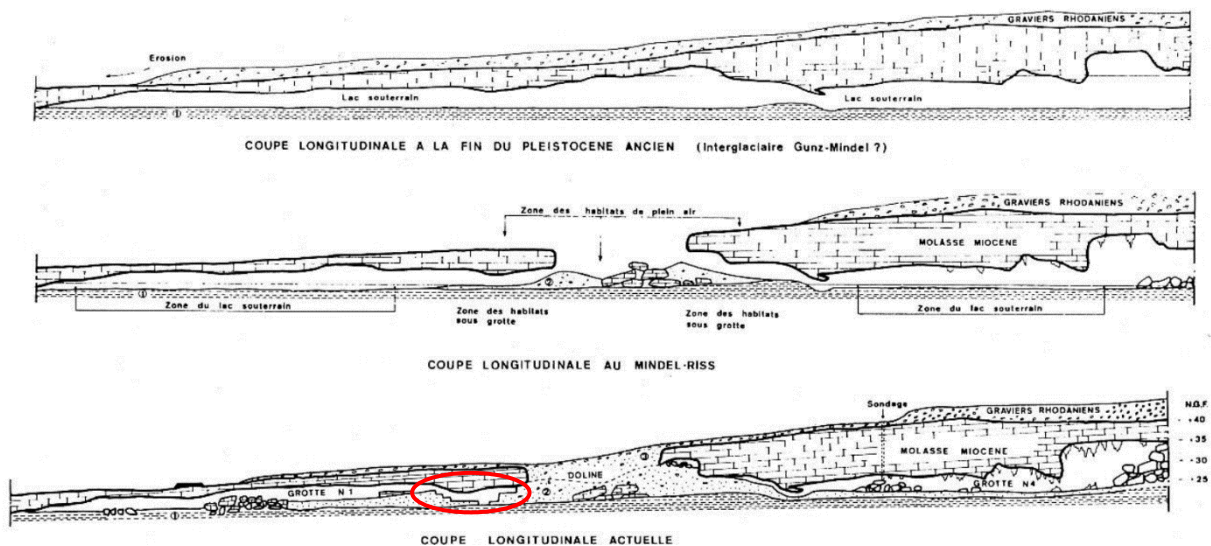


Fig.6: Explanatory scheme of cave infilling dynamics proposed by Bonifay. From top to bottom one can see the collapse of the sinkhole that divided a single cavity into LV I and LV IV and later their complete filling. With the red ellipse is marked the approximate excavation area, note the progressive decrease of the deposit's slope from the dolina toward the bottom of the cave (modified from document of E. Bonifay in Brugal et al., 2021b, p. 10).

1.3.3 Stratigraphy

In the series of silts, sands, and gravels located above the series of sterile reddish clays (*argiles rouges*), Bonifay identified 14 levels (*couches*), 12 of which are fossiliferous over a thickness of about 5 meters (fig.7). These levels appear to vary in thickness (on the order of centimeters or decimeters) and show a descending slope, clearly visible in the field, from the sinkhole toward the bottom of the cavity (Brugal, André and Guiliani in Brugal et al., 2020, p. 52). At a general level, this series has been divided into an upper ensemble (*couche 1-5*) and a lower ensemble (*couche 6-12*) (ibid.); however, the whole series appears to have been deposited by runoff phenomena that introduced sediments into the cavity through the sinkhole (Bruxelles in Brugal et al., 2021b, pp. 65–70). At present, further studies to clarify and expand the information about the stratigraphy of the site are ongoing, in particular sedimentological analyses to reconstruct sedimentary dynamics and a renewed stratigraphic analysis.

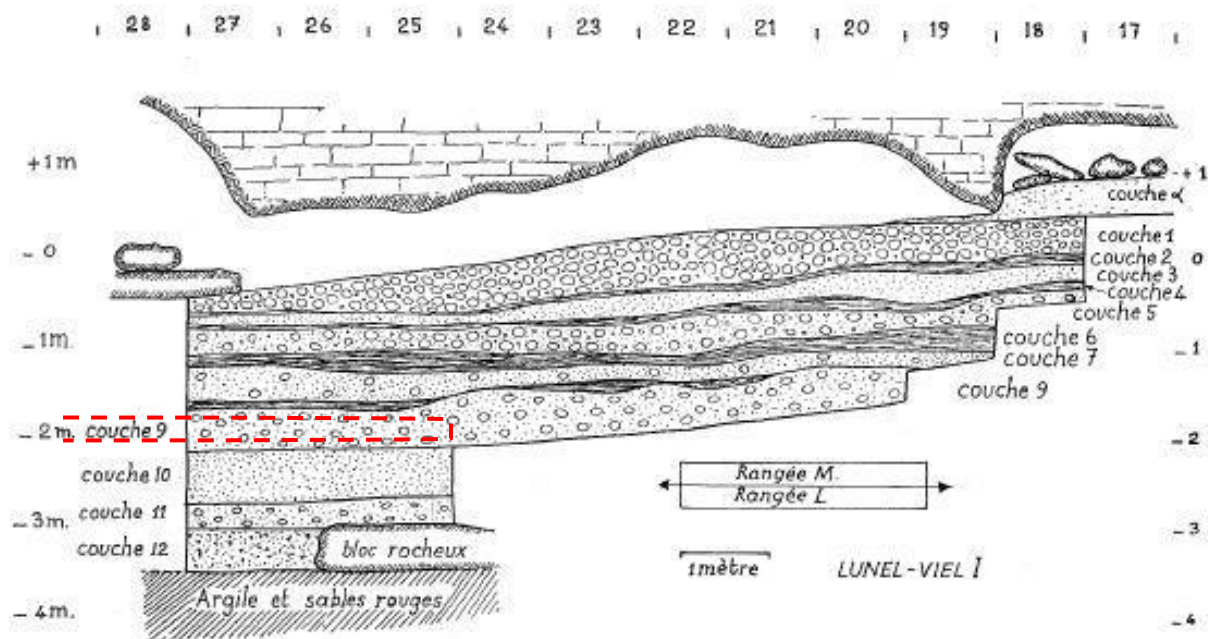


Fig.7: Stratigraphic section along the long axis of the cavity, from the doline entrance (square 17, North) towards the interior (square 28, South). Sol 76 approximate location is marked by the red dashed line. Note the reddish clays at the base and the slope of the upper layers (*couches*) (modified from document of E. Bonifay in Brugal et al., 2020, p. 52).

1.4 Anthropogenic structures issue

In addition to numerous lithic and paleontological finds during his campaigns Bonifay also identified the oldest anthropogenic habitational structures ever found in caves. In particular he identified habitation structures such as hut bottoms made from pebbles and combined with imprints of woody remains; several types of combustion features (fireplaces on flat stones, on the ground or in pits, and located outside the huts); trampled and paved surfaces close to the fireplaces; stone walls for diverting the rainwater and accumulations of bones identified as anthropogenic (Bruxelles in Brugal et al., 2021b, p. 65).

However, the anthropic character of these structures turns out to be in doubt; the interpretations provided by Bonifay were in fact also contested in later research such as Le Grand's doctoral thesis in which the need for further studies before their actual anthropicity can be affirmed is underlined (Le Grand, 1994, p. 287).

Unfortunately, many of these structures were excavated by Bonifay himself, thus making it impossible to study them in order to prove, or disprove, their anthropogenic character. Others possible structures, however, were exposed but left in place, such as the *Sol 76* located in the *couche 9*, in which bones, rare tools, seeds, and woody debris were found, and was interpreted by Bonifay as a pavement made up of loose pebbles (Brugal et al., 2021b, pp. 19–20).

With the start of new excavation activities therefore, one of the issues to be addressed turns out to be precisely to better understand the elements that constitute these structures so that they can then be reinterpreted in the light of research done on the basis of modern knowledge, techniques, and investigative methodologies.

In the context of this Memoire, we will focus on the structure named *Sol 76* by Bonifay.

It is located within *couche 9* (Brugal et al., 2022, p. 34), within quadrants O-M 25-29, between about 15 and 20 meters from the sinkhole (fig.8) and is composed of large pebbles, not in contact with each other, which are resting in a fine matrix. This archaeological level (*couche 9*, fig.7) regroups several accumulation events (Giuliani, thesis in progress in Brugal et al., 2022, p. 20) that gave rise to several sub-horizontal levels (or lenticular facies (Le Grand, 1994, p. 65) with alternating sandy, sandy-silt and gravelly beds of millimeter or centimeter thickness (Bonifay, 1979 in Brugal et al., 2021b, p. 20). This alternation of lenticular facies that compose *couche 9* includes both facies with archaeological evidence and

facies of natural origin, with evidence of use of the cavity by hyenas, presence of more than 100 coprolites in the entire couche (Brugal et al., 2021b, p. 94). The couche is developed over a thickness varying from 30 to 80 centimeters (Bonifay in Le Grand, 1994 Annex 2), decreasing from the cave entrance (doline) toward the bottom; beyond the thickness, the grain size and slope of the couche is also decreasing in the same direction (Le Grand, 1994, p. 25).

Sol 76 was interpreted by Bonifay as a habitation structure, however this interpretation given by Bonifay needs to be verified.

In order to verify this interpretation, it is first necessary to validate the anthropicity of the elements that make up the above structure, that is, to understand whether their deposition can be linked to natural sedimentary dynamics or not. The first step in being able to address this issue is, of course, field observations, these were carried out by Laurent Bruxelles and presented in the Mas des Caves excavation report of 2021 and allowed to highlight the not obvious natural origin of these elements.

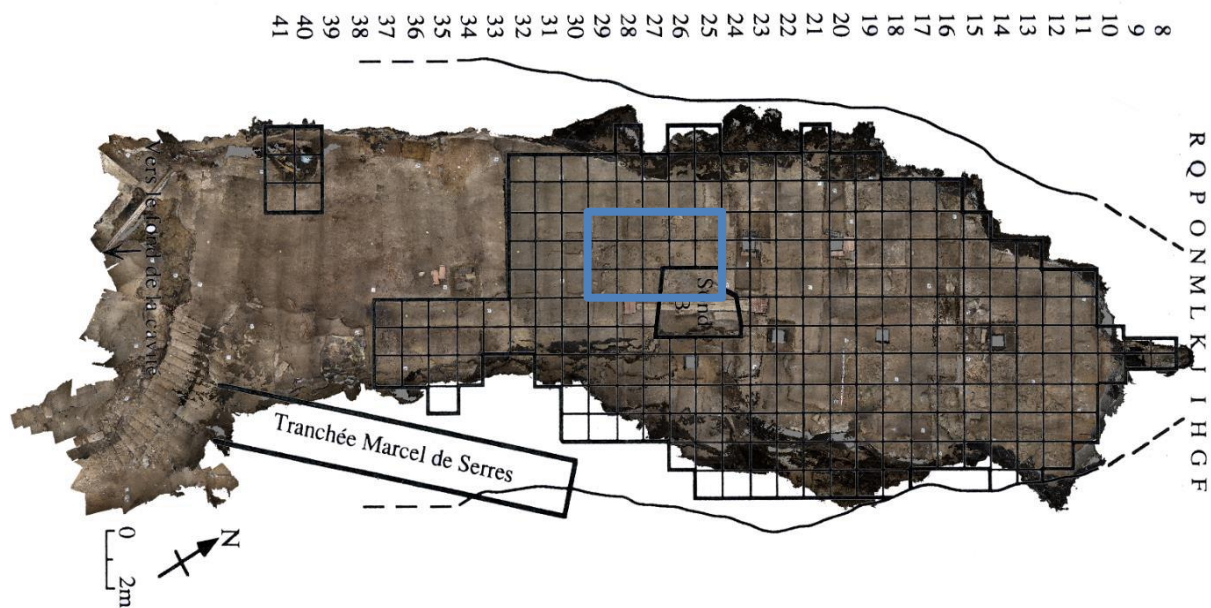


Fig.8: Plan of the cave, the blue rectangle indicates the surface of *Sol 76*. The dolina is located beyond line 8. (Modified from Brugal et al., 2020, p. 21).

The elements composing *Sol 76* have been identified as a sedimentary anomaly (Bruxelles in Brugal et al., 2021b, pp. 65–70). Being in fact the dynamics of filling the cavity closely related to runoff phenomena, sedimentary forms related to them are clearly visible in the field. In particular, there is a very characteristic grain size variation of individual layers.

Within each layer the general grain size of each layer decreases from north to south, in other words, from the original entrance of the sediments (sinkhole or LV V) toward the bottom of the cave (ibid.). This type of grain-size sorting turns out to be in line with the loss of runoff-water competence, which is linked to the decrease in the slope of the layers (also clearly visible in the field and following the same direction, from north to south, fig.7-6) (ibid.).

Given the internal position of the structure therefore the position of its elements (large pebbles) is anomalous in relation to the pattern of natural sorting described earlier (ibid.). These are in fact embedded in a fine matrix (in line with sedimentary dynamics) to which their size does not correspond at all to the average granulometry of the matrix. From a physical point of view therefore it seems impossible that the runoff-water capable of transporting only fine material (sand and few small pebbles) could have deposited these large pebbles; furthermore, neither coarse granulometric procession nor sedimentary features (such as blocking features) are present in association with these elements (ibid.).

To summarize the situation, we are faced with turns out to be as follows: a sedimentary unit (*couche 9*) is characterized by a spatial grain size difference (related to its emplacement dynamics) that results in a progressive average grain size decrease of its sediments from north to south. This grain-size pattern appears to be always reflected in the unit, except for the elements (large pebbles) constituting the structure *Sol 76*, which are located at a point where the average grain size of the unit is visibly finer than the pebbles in question.

On the base of field observations, hence the *Sol 76* elements appear not to have been deposited by natural phenomena, the hypothesis of anthropogenic deposition of these elements therefore seems plausible. However, this remains only a hypothesis, which although plausible, needs further study and observation to be validated.

In order to provide an answer to this question it is therefore necessary to thoroughly understand the depositional history of the site (in order to definitively reject the possibility of a natural deposition of the elements), and to search for archaeological sites in caves that can provide comparisons and insights into the Mas des Caves site. A bilateral approach appears necessary, one geoarchaeological and one more strictly archaeological.

As far as the geoarchaeological approach is concerned, several studies carried out at different scales of observation and with diversified techniques are necessary to be able to obtain a broad spectrum of data on which to reason about the issue.

Therefore, an approach that is multiscale and multidisciplinary:

- Stratigraphic analysis

This analysis is necessary in order to obtain a comprehensive view of the cavity infilling, through a continuous reading of the stratigraphy, from the sinkhole to, and beyond, the *Sol 76* placement area.

- 3D modeling

On the other hand, 3D reconstruction of the cavity (both its morphology and its infilling) will allow visualization and study of the geometry of the levels and their spatial variations in three dimensions. They will also make it possible to project and precisely observe the *Sol 76* within the stratigraphy.

- Sedimentological and mineralogical analyses

These analyses will make it possible to obtain information and reconstruct the sedimentary dynamics that led to the filling of the cave and possibly also to reconstruct the origin of the components that constitute the stratigraphy.

- Micromorphological analysis

The scale of microscopic observation will allow the evaluation of how the sediments were put in place, the post-depositional processes they underwent and to observe (if present) any microscopic anthropogenic or carnivore traces. It will also enable us to identify the individual accumulation events (microstratigraphy) that led to the formation of the deposit, to observe each of them separately and to observe their contacts in order to understand their mutual relationships.

This multiscale and multidisciplinary approach is necessary to provide a more comprehensive answer to the question of anthropogenic structures at the Mas des Caves site. In fact, a single point of view could lead to misleading interpretations; data obtained from a single type of analysis could in fact be interpreted differently once integrated with data from the other analyses. Thus, this investigation plan should be carried out in a simulated manner.

Currently, sedimentological, and mineralogical analyses of sediments are being carried out by researcher Vincent Ollivier. The stratigraphic study of the cavity, on the other hand, is being carried out as part of a master's degree work at the University of Toulouse (by Marie-Eléa Coustures under the direction of Laurent Bruxelles). 3D modeling is also in progress. While micromorphological observations of the sediment were carried out within the scope of this memoir.

2. Methodology

In the context of this memoire the study of the Mas Des Caves deposit will be approached through a microscopic approach. The methodology used will be archaeological micromorphology. This methodology is derived from the application of a microscopic study method developed within the earth sciences, more specifically soil science, called Soil Micromorphology.

Soil Micromorphology can be summarized as the study of undisturbed sediments with microscopic (and ultramicroscopic) techniques, by which different soil constituents can be identified and their mutual spatial and temporal interrelationships determined (Stoops, 2021 [2003], p. 5).

Within this chapter, the history, development and archaeological application of Soil Micromorphology, its general principles and technical aspects will be briefly described. This description is not intended to be exhaustive, for any further details one can refer to the bibliography cited in the text.

Following this, the elements for describing thin sections will be reviewed, with more focus on those most relevant to this memoire. Finally, the sampling method and strategy used at the Mas des Caves site will be described.

2.1 State of the art

Micropedology, or soil micromorphology, as a discipline, was developed by W. L. Kubiëna in the 1930s (Stoops and Nicosia, 2017a) with the publication of a handbook entitled "Micropedology" in 1938. It was created with the aim of helping to solve problems related to the genesis, classification, and management of soils (Stoops et al., 2010, p. 1).

The applications of this new discipline in archaeology did not take long to arrive, in fact after about 20 years, it was Cornwall who was the first to leave a trace of this application (Stoops and Nicosia, 2017a) by publishing "Soils and Micromorphology in Archaeology" in 1958 with the aim of improving the understanding of paleoenvironments, and so beginning the micromorphological study of anthropogenic deposits (Macphail et al., 1990).

However, this new approach of analyzing archaeological sediments remains sporadic in the following years, during which the analysis of thin sections taken from archaeological deposits remains relegated to the curiosity of earth scientists, often connected to geological or

pedological surveys (Stoops and Nicosia, 2017a). It was not until the late 1970s that soil micromorphology began to be applied expressly to archaeological deposits, notably by Goldberg, Macphail and Stoops (ibid.).

Finally, in 1989, the first handbook specifically written for an application of pedology and micromorphology to archaeology was published, titled "Soils and Micromorphology in Archaeology," written by those who can be considered the founders of micromorphology archaeology: Marie-Agnès Courty, Richard Macphail and Paul Goldberg (Bronnikova et al., 2016).

From the perspective of the application of micromorphology in different fields, it is interesting to note that since 1990 there has been a decrease in the absolute number of publications making use of micromorphology, but during the same period an increase in archaeological publications using it (Stoops, 2014 in Stoops and Nicosia, 2017a). Now archaeologists can in fact be counted as among the most frequent users of this methodology (Stoops and Nicosia, 2017a).

The high potential of archaeological micromorphology can be attributable to the fact that many processes (physical, chemical, biological and human) create microfeatures, observable only through the study of thin sections (Macphail et al., 1990).

Currently, micromorphology in archaeology is used to address a wide variety of problems, often specific depending on the site studied and the problematic being investigated. In general, the following fields of application can be distinguished, often overlapping during micromorphological investigations (Stoops and Nicosia, 2017a):

- Study of archaeological material
- Investigation of ancient technology (ex. combustion features or manufacturing techniques)
- Reconstruction of the archaeological context, microstratigraphy, syn- and post-depositional changes
- Impact of man on the environment (discussed in “Common micromorphological features in cave sites” paragraph)

As regarding this memoire, the field of context reconstruction and depositional changes turns out to be the most revealing.

It is important to emphasize that micromorphological studies always fit within a wider geoarchaeological approach that needs different scales of observation (Stein and Linse, 1993

in Goldberg and Macphail, 2006, p. 2) in order to provide correct answers and interpretations about the history of deposits. In fact, micromorphology should not be considered as a stand-alone technique but rather as one of the different scales (or tool) of observation in a multiscale geoarchaeological study (Stoops and Nicosia, 2017b).

2.2 General principles of Soil Micromorphology

The principles on which micromorphological investigation is based on are two (Stoops, 2021 [2003], p.5):

- *Preservation of the fabric and structure*: this principle turns out to be fundamental in micromorphological analysis because the great potential of this methodology lies precisely in the possibility of observing features which other investigative methodologies, that can be carried out on sediments (ex. granulometric or geochemical analyses), do not allow to analyze, because of limitations intrinsic to the methodologies themselves (ibid.). For example, to perform a grain size analysis it is necessary to treat the sample with methods that inevitably lead to the loss of some information. Like the disaggregation of the soil for dispersion of clay particles, it is a necessary treatment, but it eliminates information regarding any aggregates present in the sediment (Goldberg and Macphail, 2006, p. 339), which are visible instead in thin section. Therefore, sampling must be done by specific methods to allow preservation, and future observation, of sediment features invisible to other survey methods.
- *Functional investigation*: “all observations should be directed to the understanding of the function of each soil constituent or fabric within the soil as a whole” (Stoops, 2021 [2003], p. 6). In fact, it should not be forgotten that soil is an open physical system (substances can be added or removed), which has functionally interconnected properties (if one property changes, others will also change consequently) derived from five independent variables, defined as soil-forming factors: climate, organisms, topography, parent material, time (Jenny, 1994, p. 11). Given such complexity of the soil system, therefore, it would be misleading to conduct an investigation which is not aimed at a functional understanding of soil as a whole. Regarding cave deposits lacking pedogenetic processes (as in the case of Mas des Caves), the discussion is similar, although obviously the factors and properties will certainly be different.

A normal micromorphological study can therefore be defined as the study of sedimentary and stratigraphic structures at a finer scale than with field observations (Karkanis and Goldberg, 2008) and consists of 4 consequential steps (Stoops 2021 [2003], p.9):

- Sampling: samples should be taken while keeping the sediment undisturbed for the reasons seen before.
- Preparation of the thin sections.
- Analysis and description of the thin sections: carried out using different microscopic techniques depending on the need and problematic of the study. The description of the observed features should be carried out with terminologies that are unambiguous and possibly referable to an existing terminological system, to allow comparisons and correct interpretations (Stoops and Nicosia, 2017a).
- Interpretation and reporting: in particular, interpretation must be based on observed features and data from literature, while also always considering information available in the field and from other analysis methodologies applied to the site (Stoops 2021 [2003], p.10). It needs a clear explanation and justification and needs to be tested by re-observing the thin sections based on the interpretative hypotheses developed and comparing the results with those from studies from other disciplines, such as bulk chemistry, palynology, etc. (Goldberg and Macphail, 2006, p. 356).

2.3 Technical aspects

2.3.1 Sampling

Techniques for taking undisturbed samples are varied and range from the use of metal boxes (Kubiěna boxes) to simply digging out a block of the desired size or the use of plaster bands to consolidate the sample, the choice of technique applied is mainly related to the type of sediment (Stoops and Nicosia, 2017b).

The sampling strategy (how many and where to take the samples) is extremely specific to each case study and strongly related to the problematic to be answered through the micromorphological study (Ibid.).

A crucial aspect of monolith sampling is the recording of the context of the block (Goldberg and Macphail, 2003). Before the block is removed, it is critically important to mark on it the name of the sample and its orientation (the way up of the block and, if needed, the north).

2.3.2 Thin section preparation and observation

Microscopic techniques used for micromorphological investigation are carried out on thin sections: undisturbed sediment slices about 30 microns thick. Preparation of a thin section requires three crucial stages, which are: sampling, removal of water in the sample and impregnation of the sample with resin. Once the sample is completely filled with resin and the resin solidified it is treated as a rock (Murphy, 1986). A slice can then be cut and reduced to the desired thickness. To then provide a physical structure to such a thin section, and allow it to be observed under a microscope, it is bonded between two glass slides.

Such a fine thickness is necessary for light to pass through it, allowing observation under a petrographic microscope (transmitted light microscope) through which both the mineralogical characteristics of the components and the structural characteristics (fabric) of the sample can be observed.

The microscopic and ultramicroscopic techniques by which a thin section can be observed and analyzed are varied and often specific to the problematic (for further information see Stoops, 2021 [2003] and, in the case of archaeological micromorphology, (Nicosia and Stoops, 2017). Within the context of this memoire, only the techniques applied to the Mas des Caves site will be described, which are polarized light microscope observation (petrographic microscope) with standard techniques: plane-polarized light (PPL), cross-polarized light (XPL) and oblique incident light (OIL).

The polarized light microscope allows the magnification of an optical microscope to be coupled with the polarization of light induced by a polarizer (placed between the light source and the thin section) and an analyzer (placed between the thin section and the binocular) (Verrecchia and Trombino, 2021, p. 9) that can be inserted (XPL vision) or removed (PPL vision) depending on the need of the observer, and the elements and features that one wants to observe.

When observing the section without the analyzer inserted the setting is called PPL and allows the observation of properties such as color, texture, fabric, grain size and shape. While the insertion of the analyzer allows XPL observation, providing the possibility to distinguish

isotropic and opaque bodies from anisotropic and birefringent elements, a quality that enables the recognition of mineralogical species.

Observations made by these two techniques involve light passing through the section (transmitted light); the OIL technique, on the other hand, involves observing the thin section without a transmitted light source but with an external light source with a direction oblique to the thin section; this technique is applied for the observation of opaque bodies or features. These, in fact, cannot be observed in transmitted light, as they do not allow light to pass through them, while they can be observed with an external, oblique light source (Stoops, 2021 [2003], p. 23).

2.4 Elements of descriptions

Observing and describing thin sections is a key step to then allow proper interpretation of the events that took place during and after sediment deposition. Fundamental to the description of a thin section is also to use terminology that is clear and unambiguous, possibly based on existing models to allow comparisons and revisiting of the investigation.

For the description of the thin sections studied in this memoir, we will use terminology provided by Stoops (2021 [2003]). For the interpretations, presented in the Results chapter, we will base mainly on the publications found in Nicosia and Stoops (2017) and additional articles cited within the chapter reference.

2.4.1 Mesoscale observation

The first step in observing a thin section is what is referred to as the mesoscopic approach, which provides a visual transition between the field and microscopic scales of observation (Goldberg and Aldeias, 2018). This mesoscopic viewpoint is critical for a micromorphological investigation, as it will allow no observational gap between the field and the microscale (Macphail et al., 1990) and to observe large and complex features that may not be observable with microscopic techniques (Goldberg and Aldeias, 2018; Stoops 2021 [2003] p. 190). It also makes it possible to make an initial subdivision of the deposit present in the section, which will facilitate the microscopic description of the section. The mesoscopic approach can be done in two ways: by observing the section with the naked eye or by digitalizing (scanning) it and observing it on a computer screen.

There are several techniques for high-resolution scanning of thin sections (Haaland et al., 2018), and all of them allow for more efficient mesoscopic observation, compared to naked-eye observation, as they provide additional possibilities such as zooming in, editing the scan using photo editing software and sharing it.

2.4.2 Microscale observation

Once a mesoscopic observation and description has been made, we will move on to microscopic observation and description, which will be done with a polarized light microscope based on the descriptive elements defined by Stoops 2021 [2003]. It is important that the description is done in advance of interpretations, in fact if they are placed within this analytical step, they can undermine the systematic collection of data and alter them (Goldberg and Macphail, 2006, p. 355).

Micromorphological investigation can be divided into two main branches: compositional study and fabric study (Stoops 2021 [2003]). Beyond the theoretical division between these two branches, micromorphological units are described based on both characteristics, compositional and fabric (*ibid.*).

Compositional study consists of identifying data such as the mineralogical and chemical composition of elements and their associated characteristics (color, refractive index or interference colors). On the other hand, the study of fabric focuses on the study of two different types of data: scalar data (such as the size, shape and homogeneity of features) and vector data, that is, the orientation and distribution of features (both from a general point of view and with reference to specific observed features) (Stoops, 2021 [2003], p. 37).

Before proceeding with the various steps leading to an objective observation and description of the sections, it is necessary to clarify the concept of fabric. Defined by Stoops (2021 [2003], p. 38) on the basis of Bullock et al. (1985) as the "total organization of a soil, expressed by the spatial arrangements of the soil constituents (solid, liquid and gaseous), their shape, size and frequency, considered from a configurational, functional and genetic viewpoint", it turns out to be the result of all the syn- and post-depositional processes that have led to the current aspect of the deposit, its study can therefore allow the identification of the events that have contributed to the deposition and modification of the sediments, by both natural and anthropogenic agents.

It is important to note that the concept of fabric is a multiscalar concept used to describe homogeneous and heterogeneous areas (Verrecchia and Trombino, 2021, p. 21) and therefore strongly related to the degree of magnification used in the observation. This concept of multiscalarity is central to micromorphological investigation, because at each degree of magnification used the features observed are different, and a homogeneous body may turn out to be heterogeneous when observed at a larger magnification (Stoops, 2021 [2003], p. 39).

Moreover, given the complex nature of sediments it is impossible to describe exhaustively the total fabric present in a sample (ibid.), it is therefore of fundamental importance to choose the fabric elements to describe in such a way that they correlate with the characteristics studied (ibid.).

In summary, fabric can be considered "as the arrangement and/or organization of soil constituents" and as a concept can be applied in several circumstances and scales (Verrecchia and Trombino, 2021, p. 19).

During micromorphological investigation then an initial observation of thin sections is aimed (except for specific problematics) at the objective description of the spatial organization, and composition of the sediment studied. To accomplish this goal, the following features should be described:

Groundmass

The groundmass is defined by Stoops (2021 [2003], p. 127) based on Bullock et al. (1985) as a "general term used for the coarse and fine material and associated packing voids, which forms the base material of the soil in thin section, other than that in pedofeatures". His description results to be very important since it reflects the lithology, homogeneity, and degree of weathering of the parent material (ibid.). It is described by the following elements:

- *Limit between coarse and fine material*: based on the granulometry, the limit is arbitrary and should be chosen on the type of sediments studied and the magnification used.
- *Coarse/fine related distribution*: which express the space organization of the coarse elements in relation to the micromass and associated voids (Stoops and Jongerius, 1975 in Stoops, 2021 [2003], p. 52). The c/f related distribution usually show itself as patterns, the main types are presented in fig.9.

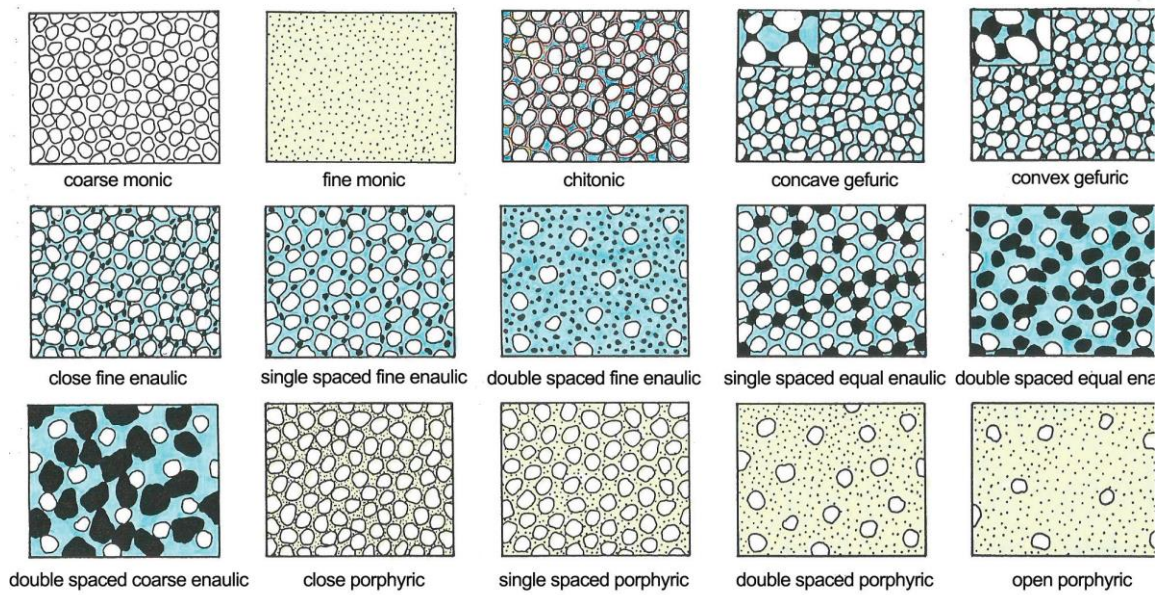


Fig.9: Different types of c/f related distribution patterns (blue color indicates voids). (Stoops, 2021 [2003], p.49)

- *Coarse material*: described through their composition, size, shape, sorting and their arrangement in the space. For what concerns the size of the elements they can be described both with pure numerical data or as size classes. For the size classes, in the framework of this memoire, we will refer to the recommended terms provided by Stoops (2021 [2003], p. 57, tab.4.1) resumed in the following table:

Class	Size limits (in μm)
Clay	< 2
Silt	2-50
Very fine sand	50-100
Fine sand	100-200
Medium sand	200-500
Coarse sand	500-1,000
Very coarse sand	1,000-2,000
Fine gravel	>2,000

Tab.1: Size classes terms (modified from Stoops, 2021 [2003], pag.57, tab.4.1)

- *Micromass, or fine material*: described through its color, limpidity and fabric. The fabric of the micromass cannot be observed directly (due to the size of the single elements) so it is deduced from its b-fabric (birefringence-fabric), which is the “pattern of orientation and distribution of interference colors in the micromass” (Stoops, 2021 [2003], p. 131)

- *Voids*: defined as space unoccupied by materials (Stoops, 2021 [2003], p. 68), they are divided in different categories based on their genesis, development, morphology and distribution (Lejay, 2018, p. 50). The main types are presented in fig.10.

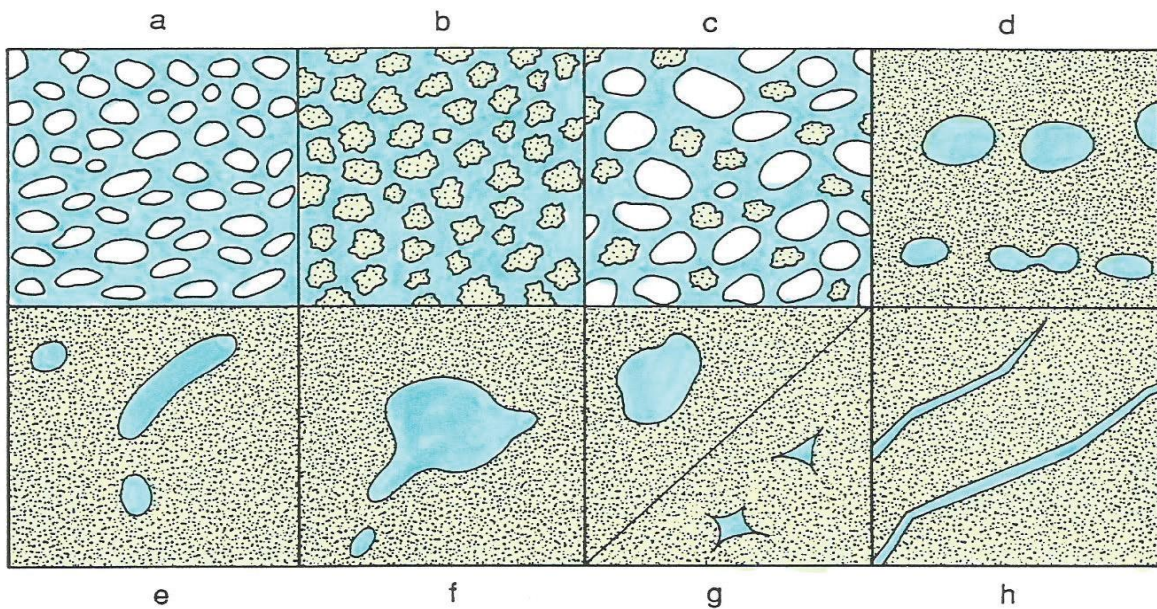


Fig.10: Different types of voids: (a) simple packing voids, (b) compound packing voids, (c) complex packing voids, (d) vesicles, (e) channels, (f) chamber, (g) regular and star-shaped vughs, and (h) planes. (Stoops, 2021 [2003], p. 69)

Microstructure

The soil microstructure is a part of soil fabric which take in account only the relation between the solid material (both coarse and fine fractions) and the voids (porosity) (Stoops, 2021 [2003] p. 67). Given the complexity of the soil system, the types of microstructures that can be observed are potentially infinite; moreover, two or more different microstructures may overlap (Stoops, 2021 [2003] p. 83).

It is defined based on the morphology of aggregates and voids, the degree of aggregate separation, and the relationship between voids, aggregates and mineral grains (Verrecchia and Trombino 2021, p. 39). Examples in fig.11.

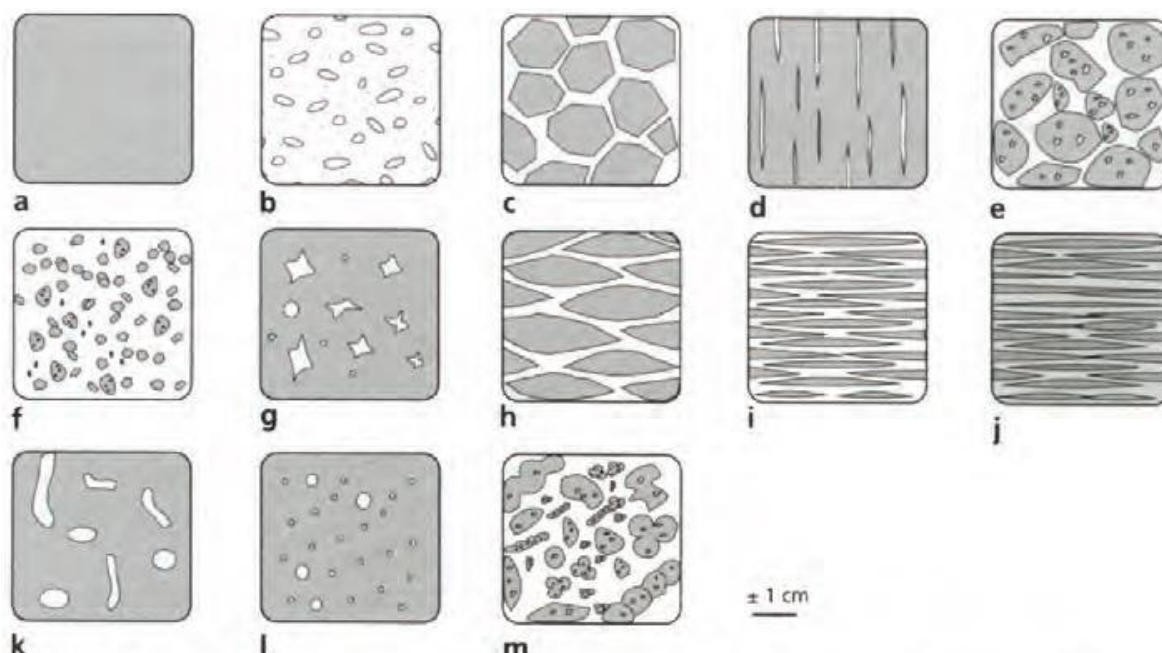


Fig.11: Different types of microstructures: (a) massive, (b) granular, (c) polyhedral, (d) prismatic, (e) crumb, (f) microaggregated, (g) spongy, (h) lenticular, (i) laminated, (j) “microlitée”, (k) channel and chamber, (l) vesicular, (m) bioturbated (Sordollet, 2009 in Lejay, 2018, p. 52)

Contacts

The contacts between the layers (both archaeological and natural) are a central element to gain a good understanding of the processes that contributed to the current appearance of the deposits. Their genesis may be a result of a change in depositional processes or a result of post-depositional processes (e.g., diagenesis or human activities such as combustion) (Mallol and Mentzer, 2017). In archaeological sites they may be (from a genetic point of view) geogenic, pedogenetic, biogenetic or anthropogenic and may be of two different natures conformable (from abrupt to gradational) or unconformable (ibid.).

Their correct identification (both on the nature of contact and their genesis) is not always possible in the field, whereas a micromorphological analysis has the potential to do so. Their correct interpretation is crucial in archaeology since a visible stratigraphic contact in the field could indicate a geogenic process largely disconnected from human activity (ibid.), or even a diagenetic process, extremely disconnected from the latter.

This descriptive element seems very important for the study of Mas des Caves thin sections due to the density of stratigraphic contacts present in the studied *couche*.

Pedofeatures

Defined as “discrete fabric units present in soil materials that are recognizable from groundmass by a difference in concentration in one or more components or by a difference in internal fabric” (Bullock et al., 1985 in Stoops, 2021 [2003], p. 142). They are subdivided based on their genesis and physical characteristics and can be both formed *in situ* or inherited from a previous pedogenetic process (ibid.). The first distinction of pedofeatures is made on the base of their constituents in relationship with the groundmass, two types are presents: matrix pedofeatures (which still present the general characteristics of the groundmass) and intrusive pedofeatures (whose material is not related to the groundmass). The matrix pedofeatures are then subdivided on the base of the relationship present between their material and the groundmass, three subtypes are present: depletion pedofeatures (lower concentration of one or more components in comparison with the groundmass), impregnative pedofeatures (higher concentration of one or more components in comparison with the groundmass) and fabric pedofeatures (distinct from groundmass in having a different fabric) (Stoops, 2021 [2003], p. 144).

It is important to be noted that the pedofeatures observed during micromorphological investigations are not necessarily related to pedological processes.

As it is said in the definition in fact, the term indicates a micromorphological feature which is characterized by differences with the groundmass, this implies that also processes and activities not strictly linked to pedogenesis may leave in the microscopic record such features. Thus, during (or after) a micromorphological investigation it is possible to distinguish these features based on their genesis, for examples: strictly pedological features, anthropogenic features, climatic features, etc. Within the scope of this memoire, we will use the term “pedofeature” to indicate all the discrete units that displays differences with the groundmass, beyond their type of genesis.

This description of pedofeatures is not exhaustive, additional classifications and subdivisions of pedofeatures are based on their morphology, fabric, material, etc. For further information refer to Stoops, 2021 [2003].

2.5 Common micromorphological features in cave sites

2.5.1 Common geogenic depositional features

Caves deposits results to have a high degree of complexity as the geogenic input sources are various and closely related to individual case studies. However, some processes are shared by most caves' environments, and they leave behind common features and fabrics observable at a microscopic scale:

- Graded facies displaying an interbedded fabric, composed by an alternation of laminae. These laminae may have different thickness and be composed of different materials (usually they result to be composed of sand, silt and clay). Their formation usually points to water deposition dynamics and the characteristics of these laminae (thickness, extension, material, sorting, etc.) gives the possibility to reconstruct the processes involved (such as static water body with sediment pulses or low energy transport, like runoff or sheet wash), (Karkanis and Goldberg, 2013). The material that compose these features usually comes from the caves' overlying plateau (Mallol and Goldberg, 2017).
- Facies characterized by the presence of well sorted sand or silt. These features are usually related to an aeolian deposition, but their structure results to be highly subjected to syn- and post-depositional physical modification such as mixing with other sediments during or before burial, voids' infilling by percolation of finer sediments (notably clay) or compaction due to trampling or the weight of overlying sediments. In addition these aeolian sediments may also be deposited by the wind outside the cave and then, through the transport of other agents (notably water), they can be deposited inside the cave already incorporated with other sediments (Mallol and Goldberg, 2017).
- Gravitational input. Clasts detached from the roof or walls of the cavity and accumulate on the cave floor, due to processes such as dissolution, freeze-thaw and tectonic movements. The characteristics of these clasts are highly related to the lithology of the cave, the processes that produce their detachment and the post-depositional processes (such as dissolution) that they underwent once buried. So, their size is also very variable and usually their observation is more functional at a field scale. However, microscopical observation of these elements can provide information

on their possible post-depositional movements or chemical processes undergone (Goldberg and Sherwood, 2006).

2.5.2 Common pedofeatures in caves' deposits

The formation of pedofeatures results to be mostly linked to pedogenetic processes which change the structure and the microstructure of the parent material. Even though the Mas des Caves deposit does not appear to be influenced by direct pedogenetic processes (given constant lack of light), some pedofeatures (not necessarily linked to pedogenesis) may still be present. As already mentioned in fact, within the scope of this memoire, we will use the term "pedofeature" to indicate all the discrete units that displays differences with the groundmass, beyond their type of genesis.

In the case of caves systems, characteristic pedofeatures can develop due to the chemical and physical processes (both depositional and post-depositional) that take place in them. Some of these are the follows:

- Capping: matrix pedofeatures consisting of fine material laying on top and supported by a coarser element, such as a clast or an aggregate. Also link cappings exist, in this case the fine material results to be capping two or more elements (Stoops, 2021 [2003]). The formation of these pedofeatures in cave systems results to be linked to processes involving freezing and thawing of the water within the sediment which by redistributing the fine groundmass creates these features, thus pointing to a formation related to cold climate (Mallol and Goldberg, 2017). These pedofeatures are also often present in relationship to planar voids resulting by the melting of ice lenses. Moreover, the formation of these features often take place close to the sediment's surface since the changes in the atmospheric temperature effect the surface layers the most.
- Typic void's coating: pedofeature consisting in the coverage of voids' walls by micromass. Their presence in cave systems results to be pointing to water as source of input (Karkanis and Goldberg, 2013). To be noted that this does not exclude the possible presence of simultaneous additional input sources such as wind or gravity.
- Matrix cementation and secondary deposited calcite: pedofeatures related to the chemical behavior of calcite. This mineral can in fact be dissolved by water and transported deep into sediments and redeposited in the form of secondary calcite, usually under the form of sparite or micrite (Mallol and Goldberg, 2017). The

deposition of this secondary calcite can bring to the cementing of the matrix (as in Sefunim Cave, Israel (Friesem et al., 2022) or can form calcitic hypocoatings of voids (as in Pech de l'Azè IV, France (Mallol and Goldberg, 2017). The form under which the calcite is redeposited, and its areal extension are identifiers of different involved processes such as dripping-water or groundwater related (ibid.). The precipitation of secondary calcite, depending on the processes involved in its precipitation, may also form flowstone or travertine. Alongside with calcite other minerals are subject to dissolution and precipitation, such as phosphates or gypsum.

- Dissolution features: the same process described above can also have an opposite effect on sediment. That is, to remove soluble minerals (both primary and secondary) from defined areas through dissolution. Thus, leaving depletion pedofeatures characterized by the absence of the above minerals (Mallol and Goldberg, 2017).

2.5.3 Biogenetic features

Biological activities may act as depositional as well as syn- and post-depositional processes. Different types of animals generate different processes and features both at macro and microscopic scale of observation:

- Bats' guano: the deposition of guano in caves systems can be one of the most important agents of organic deposition in caves and it generates several features and processes both at a microscopic and macroscopic scale. The accumulation of guano may present itself in several aspects, from microscopic crusts to thick layers. Due to its chemical composition fresh guano is unlikely to be preserved in prehistoric archaeological site but its part presence may be identified through the identification of its alteration products such as apatite, gypsum and phosphate minerals (Karkanas, 2017), visible at a microscopic scale of observation. The effects of guano on the sediments can be quite heavy, its chemical composition can in fact trigger diagenetic processes affecting archaeological remains, notably bones, which could be completely dissolved (Mallol and Goldberg, 2017), but also other material such as flint. Its presence in the stratigraphical record also indicates stable surface with lack of sedimentation, usually also pointing to human absence (Karkanas, 2017).
- Carnivore activities: man's ability to enter caves often implies the ability of other animals to do so as well and some animals, such as bears and hyenas, result to search

caves for hibernation or dwelling sites. Here we will focus mostly on hyenas due to the high presence of this specie at Mas des Caves (Brugal et al., 2021a). When hyenas occupy caves as a dwelling site they act as a major sedimentary agent of biogenic material, notably their presence is associated with coprolites (characterized by a pale yellow-grayish color of the groundmass, isotropic behavior in XPL linked to their phosphatic composition, the presence of bone fragments and quartz grains embedded in them, and a porosity composed of numerous vesicular pores) and bones (usually presenting also traces of digestive process such as rounded edges and a low interference color under the microscope (XPL) (Brönnimann et al., 2017). Besides the accumulation of material, carnivores activities in caves may also generate a reworking and a compression of the sediments, thus obliterating or reworking human traces (Mallol and Goldberg, 2017) or creating trampling features which could be similar to the human's ones. Although it might be logical to think that the presence of carnivores in the cave implies the simultaneous absence of humans this mutual exclusion does not always turn out to be respected. Particularly at the site of Sefunim Cave, Israel (Friesem et al., 2022) a close interaction between carnivores and humans has been identified through a micromorphological analysis, which displayed that the time between the two occupation was shorter than could be traced even microscopically, giving rise to some sort of human-carnivore palimpsests.

- Burrowing animals activities: the presence of animals such as rodents which burrow their dens in the sediments will bring to a post-depositional redistribution of the material or to the obliteration of depositional structures and anthropogenic features (Mallol and Goldberg, 2017).
- Mesofauna activities: soil mesofauna such as worms and insects may also change the structure or microstructure of the sediments, in particular their activity can create microaggregates, increase the sediment porosity, create granular microstructures and simultaneously allow artifact movement (Mallol and Goldberg, 2017).

2.5.4 Traces of anthropogenic activities

As we know human occupation of caves has left behind a great amount of traces visible at different scales of observation. Beyond the ones visible from a field point of view some anthropogenic activities leave visible traces, even or only microscopically, under the form of micromorphological features and fabrics. Some of these features are:

- Trampling: this term refers to the transformation and modification of artifacts and deposits resulting from the movement of humans or animals across a surface. The results that this activity has on the sediments vary in function of several variables such as: its intensity, nature of the substrate, thickness of the deposit overlaying the trampled pieces and morphological and morphometrical characteristics of the pieces (Miller, 2017). The effect of trampling can be seen both macroscopically (since it can leave traces on artifacts and bones) and microscopically (Rentzel et al., 2017). Within the scope of this text, we will focus on the effects visible microscopically.

Three main types of microscopical modifications are attributed to this process: microstructural modification of the sediment, development of fabrics like laminations or bedding and effects on coarser elements like charcoals, bones and flint such as the *in situ* fracturing of the fragile materials or their pressing into the underlying sediments (Rentzel et al., 2017). Quite a few studies, both archaeological and experimental, have been carried out about the formation of these microscopic features as a consequence of trampling activities. However, these researches turn out to be strongly linked to situations characterized by the sedentary behavior of anthropogenic communities (hence Neolithic or post-Neolithic sites), during which the floors (both those of external spaces and those constructed inside buildings) are regularly trampled (for some examples, please refer to Cammas, 1998; Wattez and Onfray, 2012), while regarding older sites there do not seem to be any reference studies.

It is important to specify that the features generated by trampling activity, as an activity that is not exclusive to humans, could also be the result of trampling by large animals, notably domestic animals (Shahack-Gross, 2017); but also carnivores, as in the case of Zhoukoudian Cave (northeastern China), where signs of trampling (based on the cracked nature of the components) were recognized in association with rich coprolite concentrations (Goldberg et al., 2001).

- Combustion features: defined as “sedimentary deposits or structures that contain physical remnants of fire” (Mallol et al., 2017), these features results to be very well visible through micromorphological observations thanks to the possibility to observe combustion products, the thermal alteration of the sediment and any anthropogenic actions that modified the combustion feature at a later time, such as trampling, dumping and sweeping (Miller et al., 2010).
- Knapped lithic artefacts: while from a macroscopic and three-dimensional point of

view a piece of lithics turns out to be easily identifiable as natural or produced by intentional human activity, greater difficulty is presented when it is within the thin section, as we would have the possibility to observe only a random two-dimensional section of it. Several characteristics may help to distinguish between the two (Angelucci, 2017): the grain size often results to be unrelated to the typical grain size of the matrix in which they are embedded; the lithological composition has to be a material suitable for knapping (such as flint, quartz or quartzite) and often exotic to local geological setting (having been imported by humans); the shape results to be mostly tabular or platy and very angular to angular, with sharp boundaries and regular surface.

2.6 Sampling at Mas des Caves

2.6.1 Sampling technique

Sampling at the Mas des Caves site was done on January 6 2023; five undisturbed sediment samples were taken using plaster bands to allow detachment and transport of the monoliths (Goldberg and Macphail, 2006, p. 331). Before collection, all samples were marked with identifying information for each one: sample name (MM1 to MM5), vertical orientation (top of the monolith) and horizontal orientation (north orientation relative to the monolith).

All samples were taken from exposed stratigraphic sections except for sample MM5, taken directly from the exposed excavation surface, by the Bonifay excavations of *Sol 76*.

The sampling procedure was the same for all five samples: excavation of a "frame" with the objective of exposing five surfaces of the monolith, application of the plaster to all exposed surfaces of the block, marking with indelible marker of the attributes necessary for sample identification, detachment of the monolith and covering the last exposed surface from the detachment with additional plaster.

The monoliths were then shipped to the PACEA laboratory in Bordeaux (UMR 5199) for preparation of thin sections, which by April 2023 were ready for the study. Information about how the samples were processed can be found on the laboratory's website (PACEA-Transfert Sédiments & Matériaux | PACEA, 2023).

2.6.2 Sampling strategy

The strategy applied for sampling was chosen to respond to the problematic presented in the first chapter of this memoire, regarding the deposition of the elements from the presupposed anthropogenic structure, *Sol 76*.

The micromorphological investigation carried out as within the scope of this memoire has as its object the facies of *couche 9* contemporary with *Sol 76*, with the aim of studying their spatial differences.

Given the high variability of the facies (both granulometric and geometric), which sometimes makes it difficult to distinguish them in the field (Bonifay, 1979 in Le Grand, 1994, p. 25), it was necessary to make stratigraphic field connections (from the doline to *Sol 76*) prior to sampling in order to take the same sedimentary facies. These connections were made in the field by Laurent Bruxelles and Vincent Ollivier prior to sampling.

In summary, facies contemporary with *Sol 76* (which acts as the stratigraphic connection between them) is present within all samples; instead, the upper facies are represented more in samples MM1 to MM4, and the lower facies more by sample MM5.

Spatially, the choice of location along the east-west axis of the cavity was strongly limited to exposed sections that still had *couche 9* within them; while along the north-south axis, samples were taken to cover about 12 meters from the doline toward *Sol 76*.

The location of the samples is better described in the following figures, the size of the rectangles which indicate the samples are not in scale.



Fig.12: Interior view of the cave, the rectangles roughly represent the positions of the samples: MM1 red, MM2 yellow, MM3 green, MM4 blue, MM5 purple. Sol 76 can be seen in the close-up. The photo was taken in the direction of the doline (north direction).



Fig.13: Detail of the stratigraphic section of samples MM1 (red) and MM2 (yellow). The white wire running through the two samples indicates the stratigraphic correlation made before sampling.



Fig.14: Detail of samples MM3 (green) and MM4 (blue).

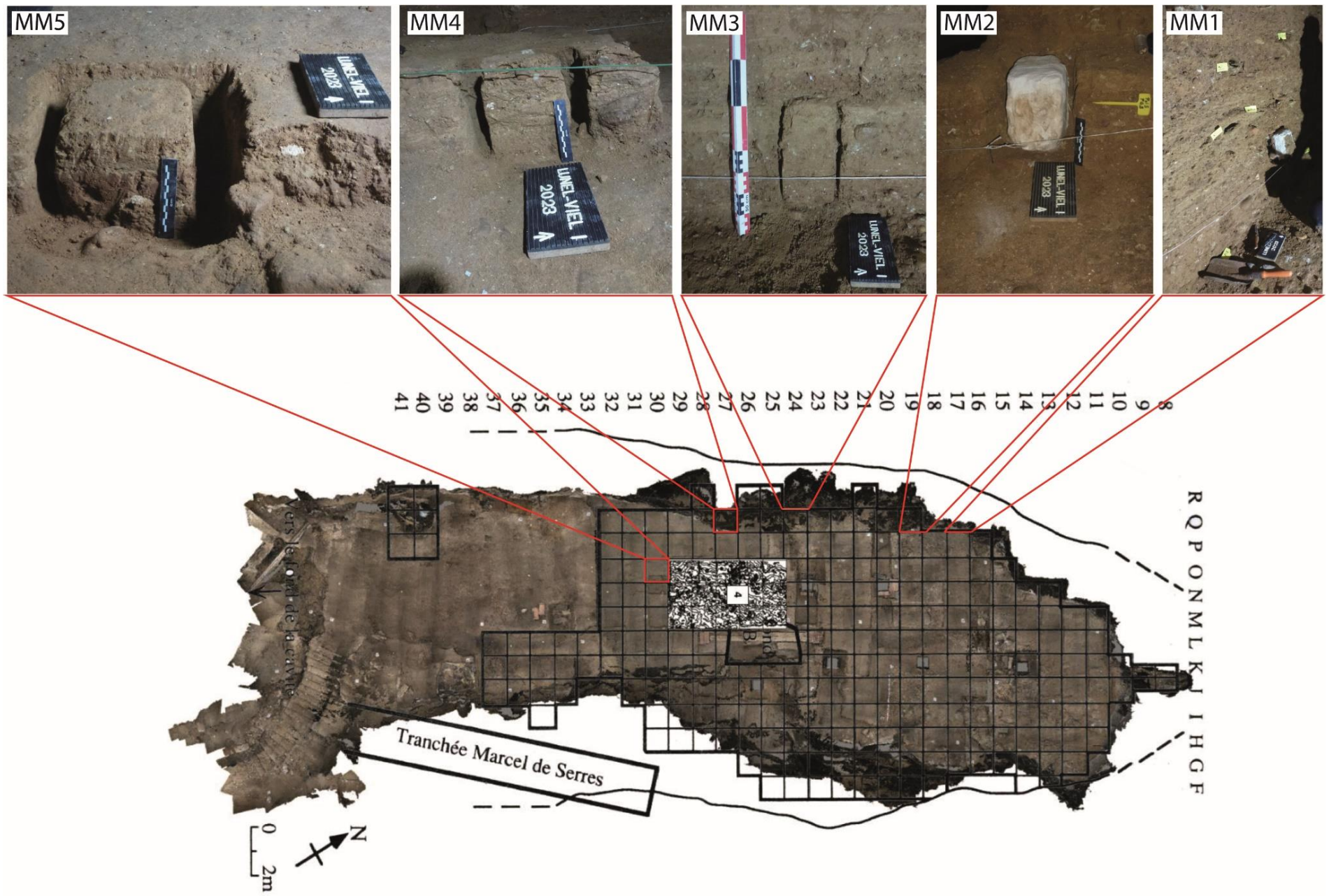


Fig.15: Plan of the cave, the topographic survey (identified by the number 4 indicates the surface of Sol 76). (Modified from Brugal et al., 2022).

2.6.3 Methodology applied for the analysis of Mas des Caves' thin sections

To describe the thin sections sampled at the archaeological site of Mas des Caves the following procedure has been applied:

- Macroscale description of the blocks. The first step took for this analysis was the stratigraphical description of the blocks, with the aim to find the approximative location of the thin section inside of it. This description was made through the optical observation of the stratigraphy present in the block with naked eye and with the help of a magnifying lens. Since the blocks are impregnated with resin the texture of the sediment could not be tested by touch, due to this reason it was impossible to define a difference between clayish or silty material; because of this both of them will be referred as *fine material*.
- Mesoscale description of the thin sections. Before moving to the microscope and begin the microscopical observation of the thin sections a mesoscale observation of the thin sections has been made in order to identify the different facies present in them. This step results to be crucial to the effectiveness of the analysis since the bigger features results impossible to be observed only at a microscale.
- Microscopical description of the identified facies. The description was made based on the guidelines provided by Stoops (2021, [2003]) and described earlier in this chapter. The micromorphological descriptions were done objectively, trying not to give interpretations on the observed features, which were made only after the observations were finished and discussed in the chapter *Discussions*.
- Cross-sections correlations. Once the descriptions of the sections were finished, the facies identified in the different sections were correlated with each other based on the features observed within them, with the aim of analyzing their spatial differences and thus understanding how they change as a result of their distance from the doline.
- Interpretation of the identified features. After identifying the stratigraphically related facies groups, we moved on to the interpretation of the identified features with the goal of understanding their mode of deposition, the presence of any traces of anthropogenic or carnivore activity, and the post-depositional processes that changed their original aspect.

To save space, full descriptions of the blocks and thin sections will be placed in the appendix,

while only a summary of the investigation will be presented in the “Results” chapter.

3. Results

This chapter will present descriptive data collected during microscopic observations of thin sections, done at the TRACES laboratory in Toulouse. These data will be presented here briefly in the form of tables, alongside the scans of the thin sections and some more significant micrographs. For the complete descriptions of the thin sections and more micrographs please refer to the appendix.

The data of the stratigraphic descriptions of the blocks will not be presented here, for these too, please refer to the appendix.

Reading keys for tables:

- Microstructure: general microstructure identified in the facies.
- Banded fabric: facies composed by an alteration of bands, well distinguishable (with naked eyes or under the microscope), mostly based on the elements size that compose them. Banded fabric present (+); banded fabric absent (-). The banded fabrics are marked in the scans of the thin sections with green dashed lines. On the other hand, the blue lines in the scans mark the contact between the facies, the dashed ones mark a comfortable contact, while the continuous ones an abrupt contact.
- c/f r.d.p.: (coarse/fine related distribution pattern): most representative assemblage identified in the facies.
- Constituents: summary of the most representative materials that compose the facies.
- Aggregates of cemented matrix: presence (+) or absence (-) of aggregates composed of a calcitic matrix (micrite showing calcitic crystallitic b-fabric) cementing coarser elements.
- Opaque micromass: presence (+) or absence (-) of micromass with opaque behavior (no light passing through them, black both in PPL and in XPL) and displaying a reddish to orange color in OIL. This material results to be mostly present as cores of micromass aggregates.
- Bioturbation features: features identified as results of mesofauna activities, such as biospheroids, fecal pellets and bow-like features.

- Taphonomic features: features identified as results of taphonomic processes.
- Carnivore features: features identified as results of carnivore activities, such as coprolites, chewed and digested bones (characterized by smooth boundaries and a low interference color) and phosphatic grains.

The latter elements have been identified as phosphatic grains based on their pale yellowish color (in PPL) and their isotropic behavior (in XPL); since it has not been possible to use fluorescence microscopy to test them, their attribution is still to be confirmed. The number of * in brackets indicate a quantitative assessment of their presence.

- Anthropogenic features: elements that may be pointing to an anthropogenic origin, such as ashes and flint or quartzite element with angular and sharp boundaries.

MM1

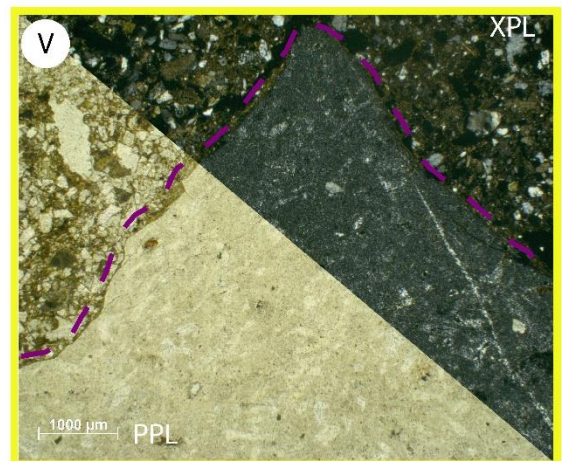
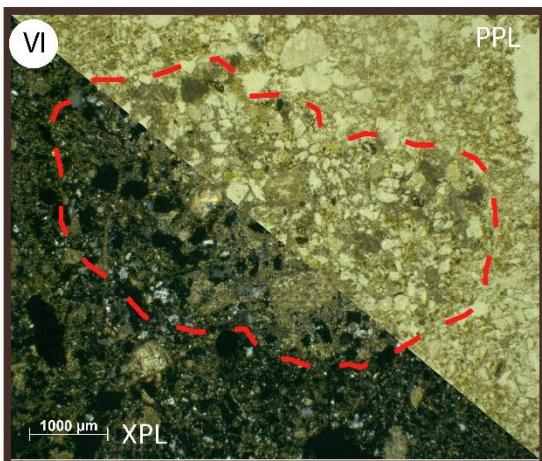
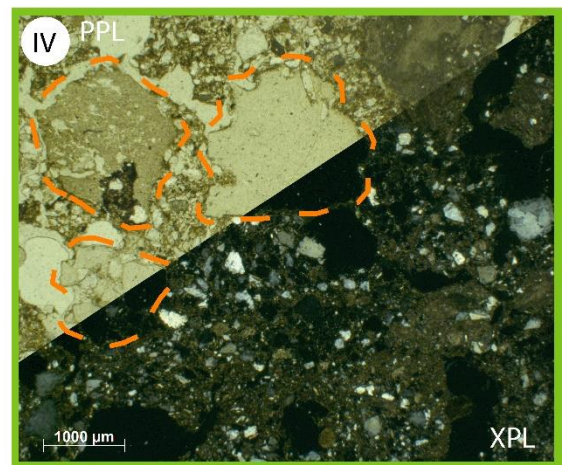
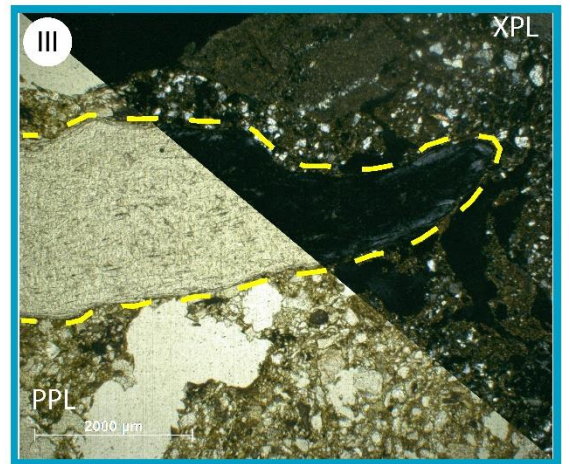
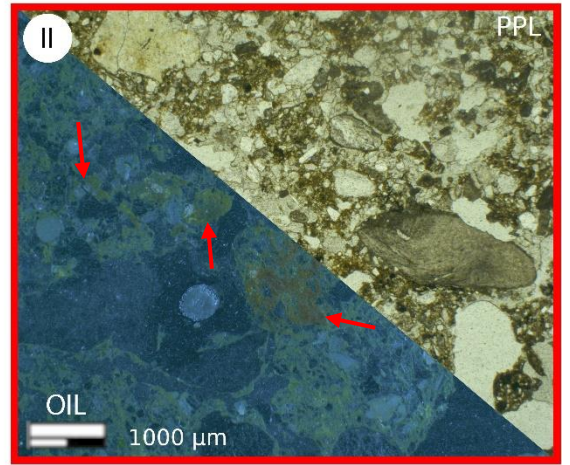
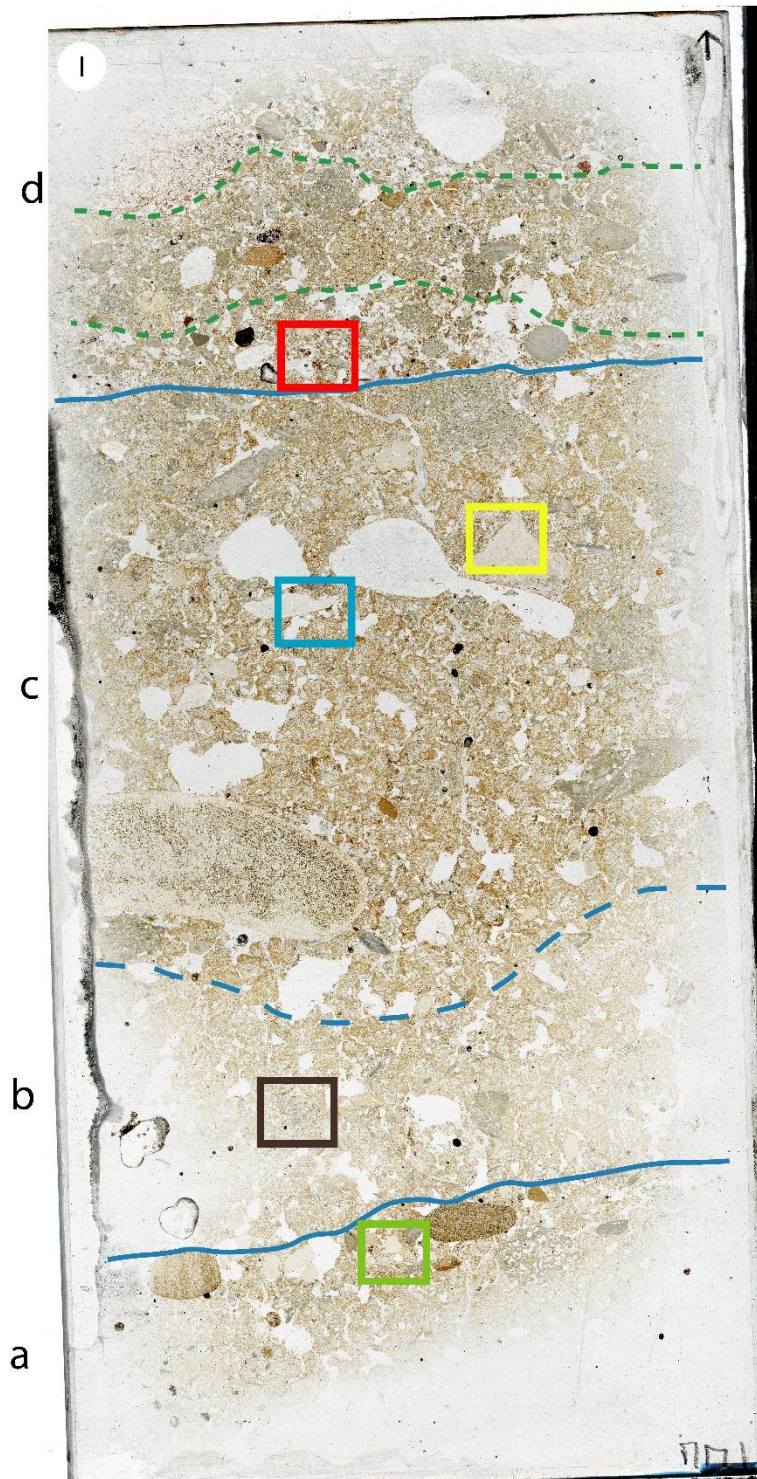
Four facies have been identified in MM1, two of which show a banded fabric (*d* and *a*), even though the lowest one (*a*) results to be too thin to be well observed. The thin section presents both anthropogenic and carnivore's traces, but they are not present throughout all the thin section. It should be noted that the division between facies *c* and *b* was made according to their color, the change of which could also be related simply to the lower thickness of facies *b* compared to facies *c*.

MM1	<i>d</i>	<i>c</i>	<i>b</i>	<i>a</i>
Microstructure	massive / vesicular	channel / chamber	vughy / vesicular	vesicular / planar
Banded fabric	+	-	-	-
c/f r.d.p.	enaulic to porphyric	porphyric	gefuric to chitonic	close porphyric
Constituents	fine to coarse sand	silt / sand / fine gravel	silt / medium sand	silt / sand / fine gravel
Aggregates of cemented matrix	+	-	+	-
Opaque micromass	+	-	-	+
Bioturbation features	biospheroid	-	-	-
Taphonomic features	-	cappings / voids' coating	-	-
Carnivore features	-	(****) bones / phosphatic grains / coprolites	(**) phosphatic grains	(**) phosphatic grains / bones
Anthropogenic features	-	knapped flint (?)	-	-

Tab.2: Summery of MM1 micromorphological analysis.

Sheet 1 (next page): MM1

I) Scan of MM1 thin section (14 x 6,5 cm) and its facies. II) Opaque micromass (red arrows), note their reddish to orange color in OIL. III) Bone element, note its smooth boundaries and its low interference color in XPL, characteristics which usually point to chewed and digested bones. IV) Phosphatic grains, note their isotropic behavior in XPL. V) Flint element with sharp boundaries, identified as a possible artifact. VI) Aggregate of cemented matrix.



MM2

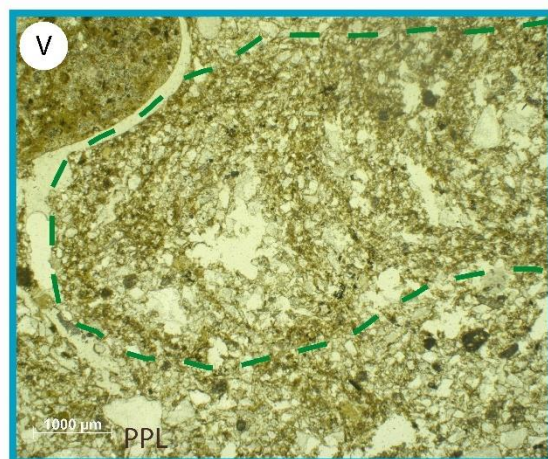
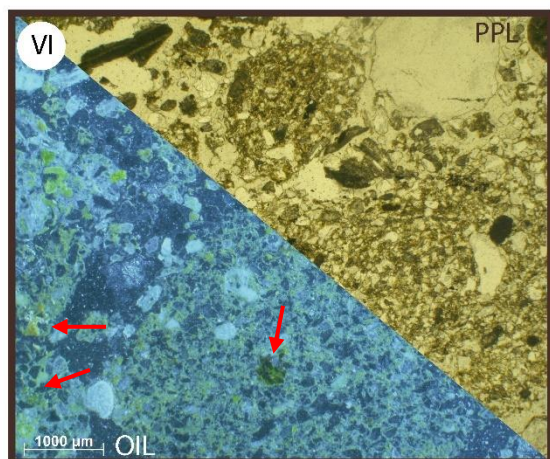
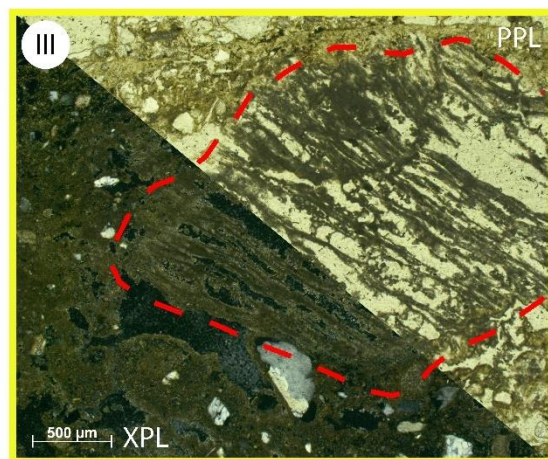
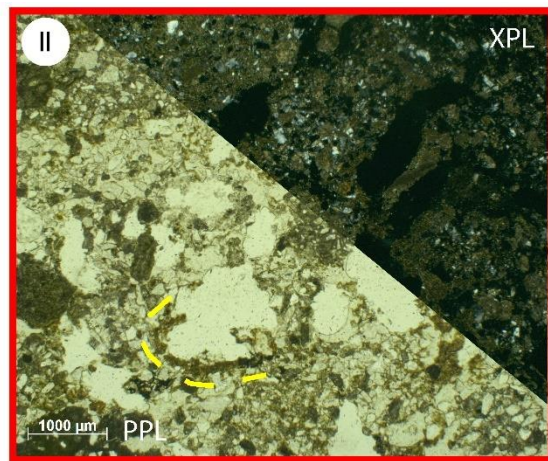
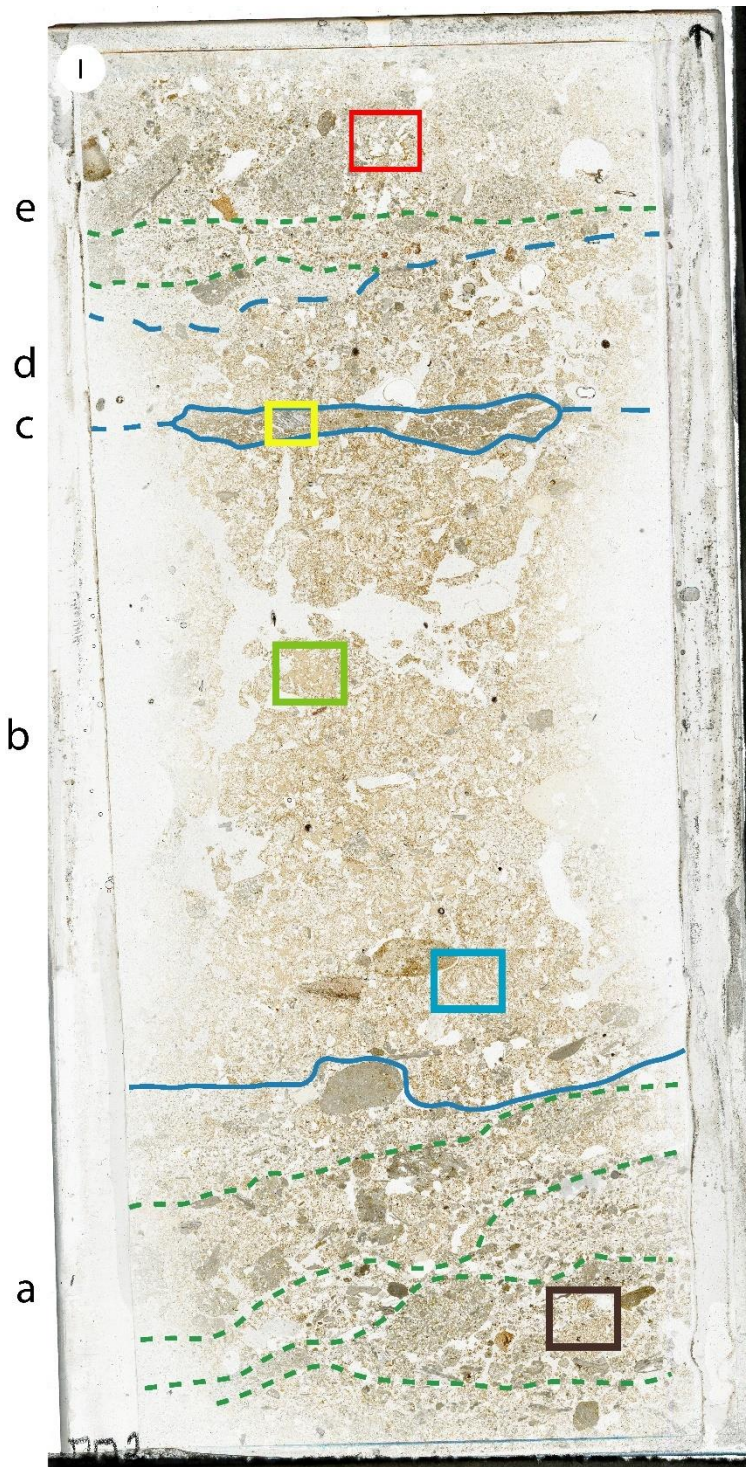
MM2 thin section has been subdivided into five facies, two of which show a banded fabric, also in this case, as in MM1, these facies are the uppermost and the lowest ones (*e* and *a*). The material between these two facies has been divided into three facies even if facies *d* and facies *b* present very similar characteristics; they have been separated due to the presence of a lenticular facies (*c*) between them. The latter (facies *c*) is very characteristics since it is very discrete (sharp contacts with the other facies) and presents features not observed in other sections. Moreover, it presents a grayish calcitic matrix (calcitic crystallitic b-fabric) that sometimes displays fabric and porosity very similar to a vegetal structure, notably wood (sheet 2,III).

MM2	<i>e</i>	<i>d</i>	<i>c</i>	<i>b</i>	<i>a</i>
Microstructure	basic / intergrain	channel / vughy	complex	channel / vesicular	basic / intergrain
Banded fabric	+	-	-	-	+
c/f r.d.p.	monic to enaulic	Porphyric to gefuric / sporadic monic	porphyric to chitonic	close porphyric / sporadic gefuric	monic to enaulic
Constituents	fine to coarse sand	fibrous silt / sand	calcitic micromass / fine sand	fibrous silt / fine sand	fine to coarse sand
Aggregates of cemented matrix	+	+	+	+	+
Opaque micromass	-	+	-	-	-
Bioturbation features	-	-	-	bow-like feature	-
Taphonomic features	micromass voids' coating	micromass voids' coating	-	voids' coating	-
Carnivore features	-	(*) phosphatic grains	-	(***) bones / phosphatic grains	-
Anthropogenic features	-	-	ashes	-	-

Tab.3: Summery of MM2 micromorphological analysis.

Sheet 2 (next page): MM2

I) Scan of MM2 thin section (14 x 6,5 cm) and its facies. II) Micromass coating in vesicles. III) Ash displaying wood structure aspect. IV) Group of phosphatic grains with sub-spherical shape. Note its isotropic behavior in XPL. V) Bow-like feature with crescent striated internal fabric, probably formed by an earthworm. VI) Opaque micromass (red arrows) displaying reddish to orange color in OIL.



MM3

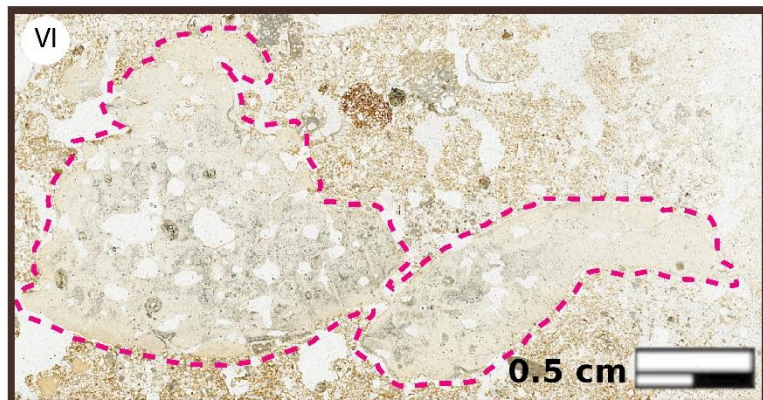
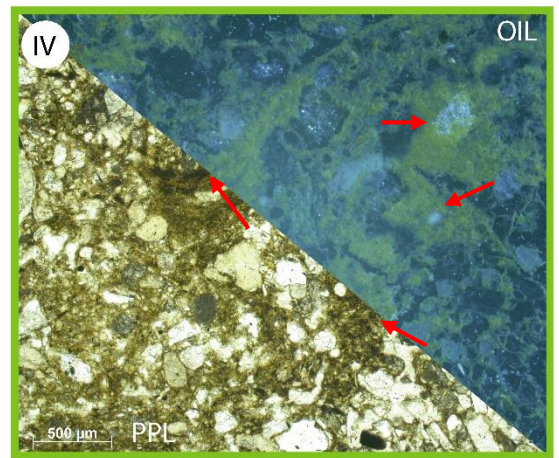
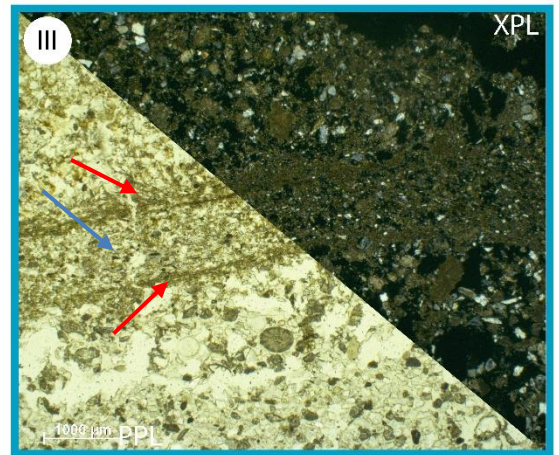
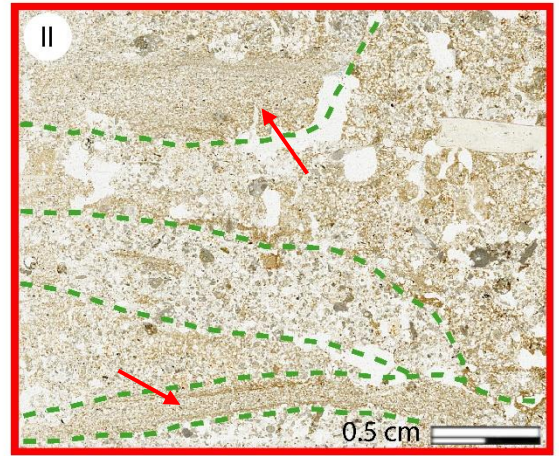
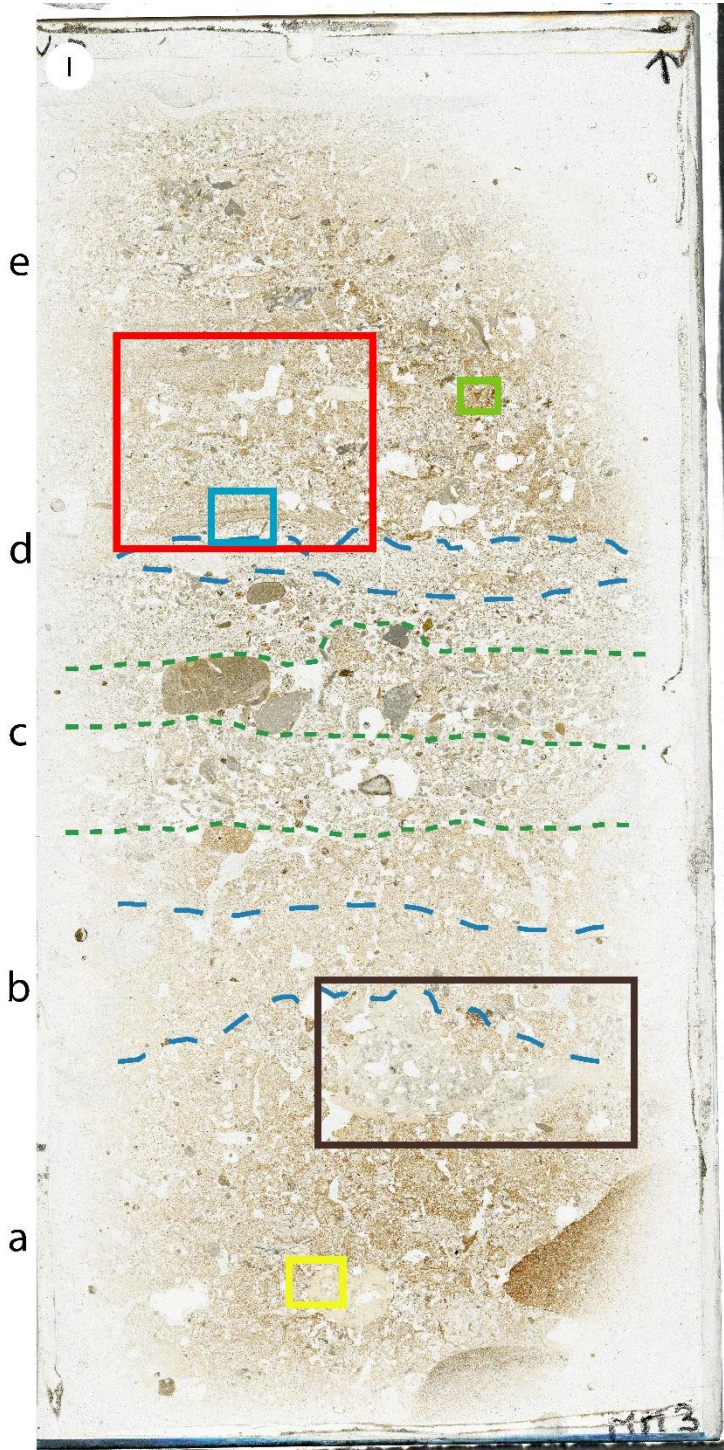
MM3 thin section has been subdivided into five facies, also in this case two of them show a banded fabric even if for facies *e* the situation results to be slightly different. The banded fabric identified in this facies is in fact formed by peculiar a partial fabric called *sandwich partial fabric* (sheet 3,II and III; see appendix for more details) which results to be present only on the left side of the facies. Another important thing to be noted regards facies *d*, this part of the thin section has been identified as a separate facies, however it could also be seen as one of the bands composing the banded fabric of facies *c*. Moreover, for what concerns the carnivore traces, facies *a* of this thin section presents the biggest coprolites identified during this investigation (sheet 3,VI).

MM3	<i>e</i>	<i>d</i>	<i>c</i>	<i>b</i>	<i>a</i>
Microstructure	massive / vughy	basic (single grain)	vughy / vesicular	spongy	massive / channel
Banded fabric	+	-	+	-	-
c/f r.d.p.	porphyric	coarse monic	enaulic to coarse monic	open porphyric	monic to porphyric
Constituents	fibrous silt (<i>sandwich partial fabric</i>) / sand	well sorted sand	fibrous silt / medium to coarse sand	silt / few sand	silt / sand / pebbles
Aggregates of cemented matrix	-	-	+	-	-
Opaque micromass	+	-	-	-	-
Bioturbation features	-	bow-like feature	fecal pellets	fecal pellets	fecal pellets
Taphonomic features	micromass voids' coating	micromass voids' coating	weathering of coarse fraction / cappings	-	-
Carnivore features	(**) phosphatic grains / bones	phosphatic grains (in bioturbation)	-	phosphatic grains (in bioturbation)	(****) coprolites / phosphatic grains
Anthropogenic features	-	-	-	-	-

Tab.4: Summary of MM3 micromorphological analysis.

Sheet 3 (next page): MM3

I) Scan of MM3 thin section (14 x 6,5 cm) and its facies. II) Banded fabric of facies *e* marked by the green dashed lines. Sandwich partial fabric indicated with red arrows. III) Sandwich partial fabric, note the differences between the bread (red arrows) and the inside (blue arrow). IV) Opaque micromass (red arrows) displaying reddish to orange color in OIL. V) Hyena coprolite, note the characteristic vesicular porosity and its isotropic behavior in XPL. VI) Scan zoom of two hyena coprolites in contact with each other. Note their characteristic vesicular porosity and their yellowish-greyish color.



MM4

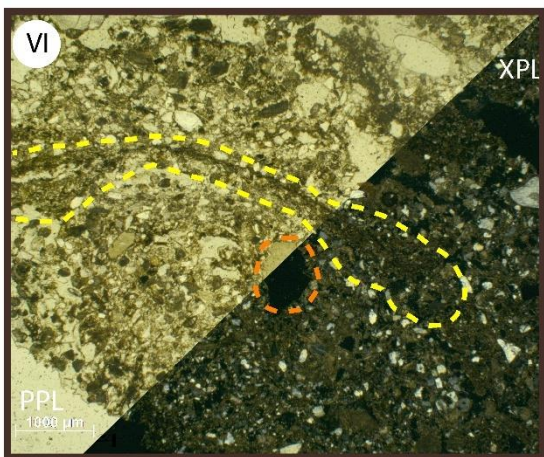
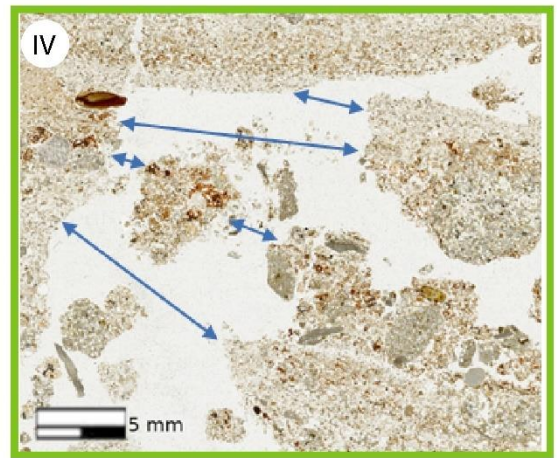
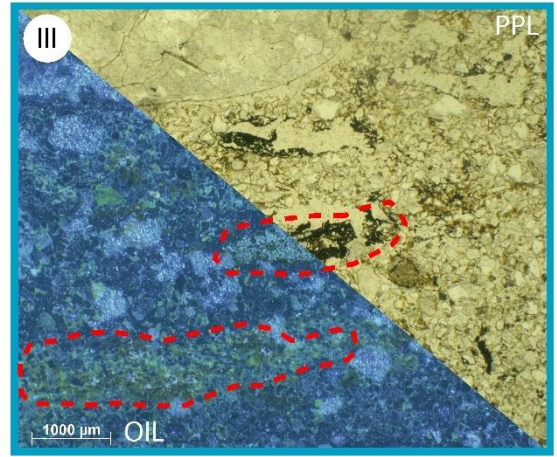
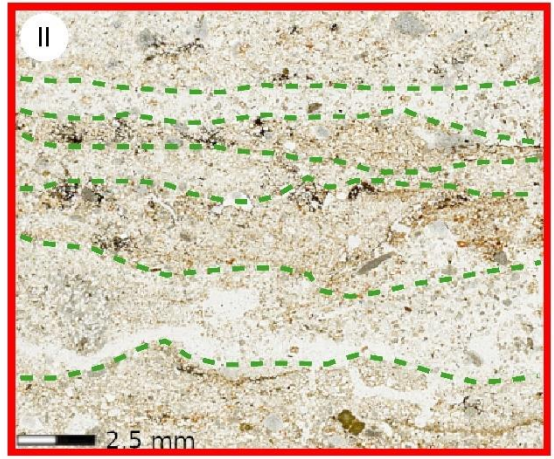
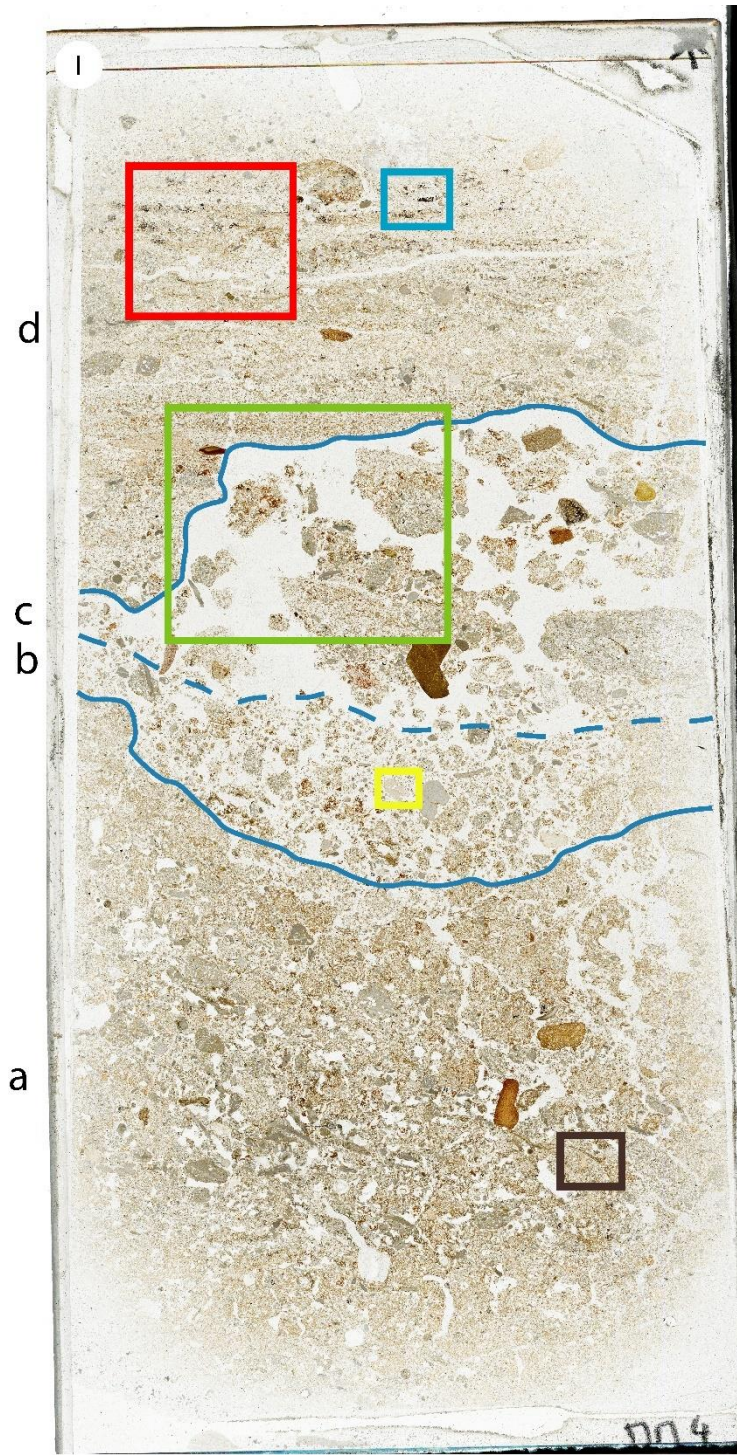
The subdivision of MM4 has been mostly based on its porosity. Facies *d* and *a* show a massive microstructure, while facies *c* and *b* a granular one. Even though the granular microstructure may be linked to specific processes (such as mesofauna activities) facies *c* presents a peculiar aspect. It is indeed composed of large aggregates with a banded inner fabric that results to be in continuity with the upper facies (sheet 4,IV). This characteristic, integrated with the observations made on the block, allowed to argue that the formation of this granular microstructure could be linked to a problem in the fabrication of the thin section, thus excluding a possible natural formation of it (see appendix for more details).

MM4	<i>d</i>	<i>c</i>	<i>b</i>	<i>a</i>
Microstructure	basic / massive	granular (coarse)	granular (fine) / intergrain	massive / channel /vesicular
Banded fabric	+	+	-	-
c/f r.d.p.	porphyric	enaulic	equal enaulic	porphyric / sporadic gefuric
Constituents	well sorted fine to medium sand / silt	aggregates of fine to coarse sand / silt	sand	fibrous silt / fine to coarse sand
Aggregates of cemented matrix	+	+	+	+
Opaque micromass	+	-	+	+
Bioturbation features	-	biospheroids	biospheroids	-
Taphonomic features	micromass voids' coating	-	-	-
Carnivore features	-	-	(*) coprolites / phosphatic grains	(*) phosphatic grains
Anthropogenic features	-	-	-	-

Tab.5: Summery of MM4 micromorphological analysis.

Sheet 4 (next page): MM4

I) Scan of MM4 thin section (14 x 6,5 cm) and its facies. II) Scan zoom of the banded fabric of facies *d* marked by the green dashed lines. III) Opaque micromass (red dashed lines) displaying reddish to orange color in OIL. IV) Scan zoom of the granular microstructure of facies *c*, note how it displays a banded fabric in continuity with the upper facies (continuity marked by the arrows). V) Micrograph of a coprolite. Note its vesicular porosity. VI) Phosphatic grain (orange dashed line) with isotropic behavior in XPL. Linear accumulation of micromass (yellow dashed line) giving the facies' micromass a fibrous aspect.



MM5

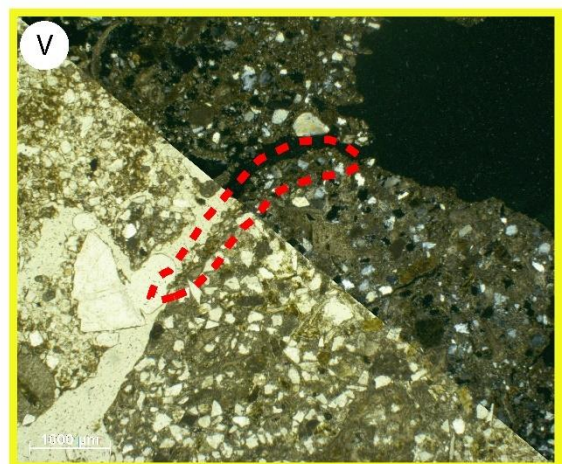
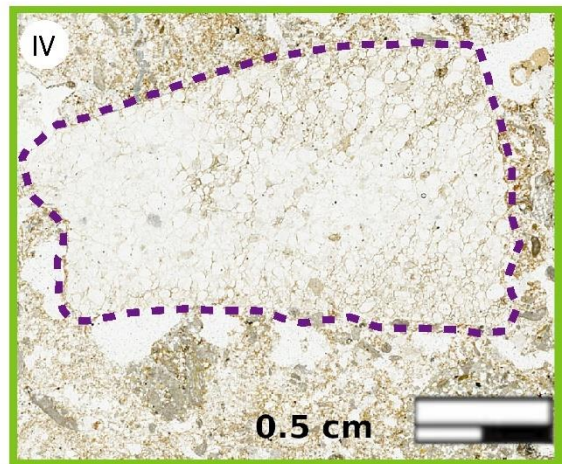
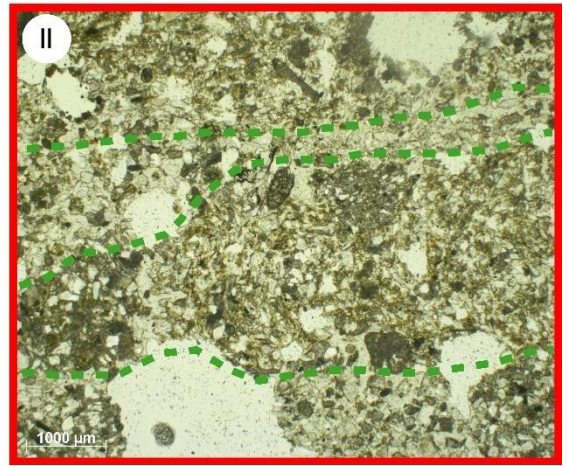
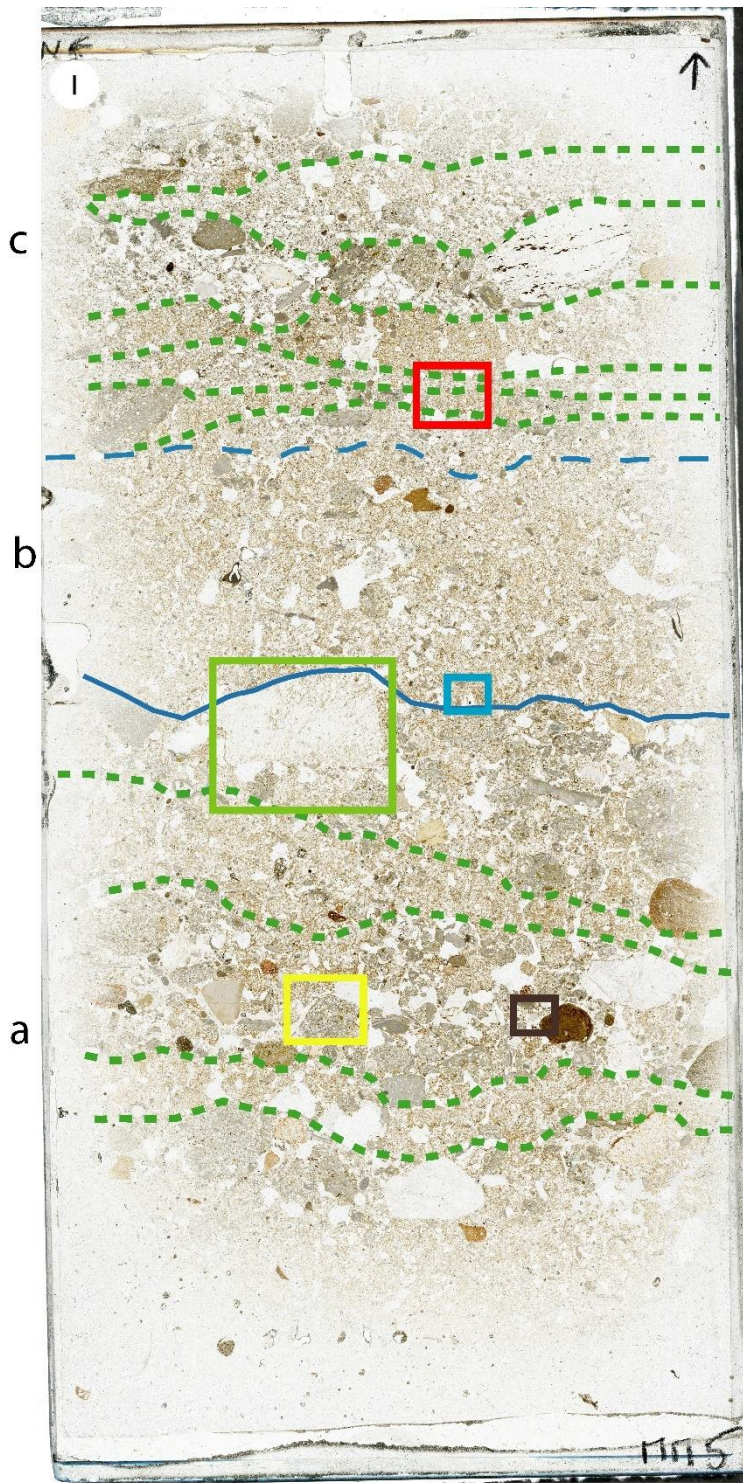
MM5 has been subdivided into three facies, two of which present a banded fabric. This thin section results to be quite interesting for what concerns the anthropogenic elements since it was sampled close to *Sol 76* and it included (in facies *a*) a possible anthropogenic elements (knapped quartzite, sheet 5,IV).

MM5	c	b	a
Microstructure	massive / basic	massive / vesicular	massive / chamber / channel
Banded fabric	+	-	+
c/f r.d.p.	porphyric / gefuric	porphyric	porphyric / sporadic gefuric
Constituents	fibrous silt / fine to coarse sand	silt / fine sand	fibrous silt / fine to medium sand
Aggregates of cemented matrix	+	+	+
Opaque micromass	-	-	+
Bioturbation features	-	chitin	biospheroids
Taphonomic features	-	micromass voids' coating	cappings / channel micromass coating
Carnivore features	-	(*) bones	-
Anthropogenic features	-	-	knapped quartzite (?)

Tab.6: Summary of MM5 micromorphological analysis.

Sheet 5 (next page): MM5

I) Scan of MM5 thin section (14 x 6,5 cm) and its facies. II) Scan zoom of the banded fabric of facies *d* marked by the green dashed lines. III) Bone fragment displaying a very low interference color in XPL. IV) Quartzite rock fragment, note the very angular shape and the regular and smooth surfaces with sharp boundaries. These characteristics are not present in other elements and often point to a knapped artifact. V) Capping of fine material (red dashed line) on aggregate of cemented calcitic matrix. VI) Micrograph of earthworm's biospheroid.



4. Discussions

Based on the observations made on the blocks and thin sections, it is possible to deduce information about the stratigraphy of the *couche* examined through microstratigraphic correlations and an analysis of spatial differences in sediments.

4.1 Stratigraphic position of the thin sections

Stratigraphic description of the blocks made it possible to place sections within them, thus obtaining a general view of the area they represent.

Since the sampling of the blocks was done with the help of stratigraphic connections made in the field, this initial placement of the sections in the blocks turns out to be critical in order to then make stratigraphic connections between the facies. When these connections with a macroscopic scale of observation are absent in fact, the risk of committing errors and wrong stratigraphic connections is higher.

Based on the observations made we can argue that (see mesoscopic descriptions of the thin sections in the appendix for more details):

- For MM1 and MM2, the sections turn out to be representative of almost the entirety of the blocks; in particular, both represent their upper portions. Thus, only a few lower centimeters of the respective blocks remain outside the sections.
- In contrast, the situation for MM3 is slightly more complex, as the block is much higher than the section obtained from it. In this case the section turns out to be representative of the lower portion of the block.
- For MM4 and MM5, on the other hand, the height of the blocks turns out to be the same as the sections, so in both cases the sections result to be representative of the entire stratigraphic portion taken during sampling.

As we have seen in the sampling methodology, all the blocks should contain within them the archaeological layer attributed to the *Sol 76* structure, more specifically sample MM5 should contain the mentioned layer plus lower layers, while the other samples should also have within them upper layers.

Integrating these field informations with the observations made on the samples (both sections and blocks), we can therefore expect a nearly linear stratigraphic connection between MM1, MM2 and MM4, while MM5 and MM3 should be located in a slightly lower stratigraphic position, but still being in connections with the other samples.

4.2 Facies correlations and microlayers

Based on the mesoscopic and microscopic observations made on the thin sections and with the support of the informations presented in the previous paragraph, it was possible to identify the stratigraphic correlations between the different sections.

In order to make these correlations we relied primarily on specific characteristics identified in the different facies. In particular we relied on the presence/absence of a banded fabric and the presence/absence of features identified as traces of carnivore activity.

Facies constituents were excluded in this phase of stratigraphic connections for two main reasons:

- The first reason is related to observations made in the field; in fact, we know that the layers that make up the site infilling present a high spatial variability (mostly linked to their sorting and granulometry). The characteristics of the material within a layer in fact vary in relation to its distance from the original entrance of the cave (dolina); therefore, it does not seem functional to look for microstratigraphic relationships between the different sections on the basis of their constituents.
- The second reason, on the other hand, is related to the mineralogical nature of the facies constituents. Based on the micromorphological descriptions carried within the scope of this Memoire, it was in fact possible to observe a pretty marked homogeneity in the mineralogical nature of the geogenic elements. All facies appear to be composed mainly of quartz, carbonate rock fragments, and silt.

The stratigraphic correlations then allowed us to relate the thin sections through the identification of five microlayers that will be called, from top to bottom: E, D, C, B, A (in capital letters, to distinguish them from the facies identified in the individual sections). Tab.7 summarizes these correlations, which can also be appreciated in fig.17 where the different microlayers are marked by different colored square brackets beside each thin section.

Microlayers	Thin sections				
	MM5	MM4	MM3	MM2	MM1
E	–	<i>d, c</i>	–	<i>e</i>	<i>d</i>
D	–	<i>b, a</i>	<i>e</i>	<i>d, c, b</i>	<i>c, b</i>
C	<i>c</i>	–	<i>d, c</i>	<i>a</i>	<i>a</i>
B	<i>b</i>	–	<i>b, a</i>	–	–
A	<i>a</i>	–	–	–	–

Tab.7: Microlayers identified through the microstratigraphic connections made between the thin sections. In the table are visible the different facies composing the microlayers.

The identified microlayers will be described below, the facies will be named by their letter preceded by the reference thin section number (*1d* will therefore be facies *d* identified in section MM1):

- E: microlayer composed of facies *1d*; *2e*; *4d*, *c*.

All these facies share a banded fabric and none of them presents any carnivore's traces.

1d and *2e* are very similar to each other, they both presents bands displaying comparable features, such as their constituent's granulometry (both fine to coarse sand). On the other hand, MM4 presents bands which are quite different from the previous ones, these bands are in fact much thinner and are composed by a constituent's finer granulometry; *4c* has been included into this microlayer due to its aggregates' banded fabric displaying a straight continuity with *4d*'s banded fabric (Sheet 4,IV).

Thus, an inner spatial variability (mostly linked to the differences between the two thin sections MM1 and MM2 and thin section MM4) seems to characterize this microlayer.

This kind of inner spatial variability of the microlayer, however, results to be coherent with their points of sampling in the field, MM1 and MM2 are in fact very close to each other (about two meters apart), while MM4 has been taken relatively far from them (about nine meters from MM1, fig.15), also confirming the spatial differences of the cave's infilling observed in the field.

- D: microlayer composed of facies *1c, b; 2d, c, b; 3e; 4b, a*.

These facies present a general massive microstructure, whose continuity results to be interrupted by different kind of voids, in particular MM1 and MM2 are characterized by big poroids and channels and MM4 mostly by channels; on the other hand, MM3 presents a slightly different situation, *3e* results in fact to be characterized by a complex microstructure which also presents a banded fabric on its left side (see appendix for more details); *3e* is the only facies of this microlayers which presents a banded fabric (Sheet 3,II).

All the facies, in addition, share the presence of elements identified as traces of carnivore activities (phosphatic grains, chewed and digested bones and coprolite fragments (Sheet 1,III; 2,IV; 4,V). These elements result to be smaller compared to the ones present in microlayer B and their granulometry is coherent with the granulometry of their embedding matrix. To be noted also the presence of anthropogenic elements: a hypothetical knapped flint artifact (Sheet 1,V) in *1c* and ashes in facies *2c* (Sheet 2,III). The latter, however, needs to be considered by itself due to its peculiar features, it has been included into this microlayer since it is located between *2b* and *2d* (both attributed to microlayer D); facies *2c* will be better discussed in the paragraph dedicated to the anthropogenic traces.

- C: microlayer composed of facies *1a; 2a; 3d, c; 5c*.

The situation of the microlayer results to be quite similar to the one presented in E: all the facies present a banded fabric and no elements linked to carnivore activities are present, the only exception are *3d* and *1a* however in *3d* they are only present inside a mesofauna bioturbation feature (fig.16), while in *1a* they are present in contact with facies *1b*, which also presents the same kind of elements.

For what concerns the banded fabrics, facies *1a* is quite problematic since it presents an observational problem linked to thickness of the section, its lower part is in fact too thin to be observed, however a change in the constituents between its upper and lower part is slightly visible, which may be pointing to a banded fabric. The facies of MM3 which are included in this microlayer, on the other hand, may be reconsidered as part of the same facies, with *3d* as a band included in the banded fabric of *3c*.

- B: microlayer composed of facies *3b, a; 5b*.

The facies that compose this microlayer present a massive microstructure with no visible bands (both from a mesoscopic and microscopic point of view), the components of these facies are very homogenous, they all result to be mostly composed of silt and fine sand

medium sand. All the facies also present elements of carnivore activities, in particular *3a* presents big coprolites (two of which are in contact with each other, Sheet 3,VI) and a high number of phosphatic grains, while *5b* presents a bone fragment (Sheet 5,III). To be noted absence of coherence between the coprolites in *3a* and the matrix embedding them.

- A: microlayer composed of facies *5a*

This microlayer is composed of only the lowest facies of MM5, which is coherent with the lower stratigraphic position of MM5 block in relationship with the other blocks.

This microlayer presents a banded fabric with similar characteristics to the ones presented in microlayers E and C. Unlikely, not having other facies to be compared with *5a*, it results impossible to observe eventual spatial differences of the microlayer.

To be noted the presence of a quartzite fragment interpreted as anthropogenic (Sheet 5,IV) due to its angular shape, which is not coherent with the shapes of the other elements present in the facies (mostly rounded to sub-rounded).

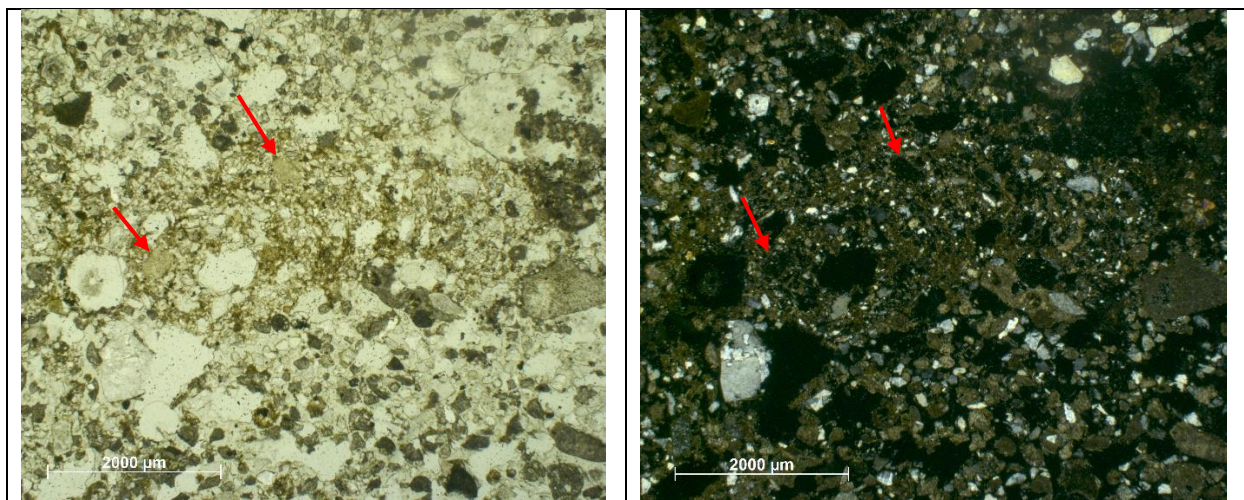


Fig.16: Bowl-like feature in 3d presenting phosphatic grains inside (red arrows). Note their isotropic behavior in XPL.

Fig.17 (next page): Microstratigraphic connections between the thin sections. Each microlayer is marked by different colored square brackets beside each thin section, refer to the legend for the color-microlayer correlation. The red dashed lines mark the correlations between the thin sections. The blue lines (both dashed and straight) mark the contacts between the facies, which are named with the letters at the left side of each thin section. The green dashed lines mark the different bands in the facies displaying a banded fabric. The north direction also indicates the direction toward the dolina.

Microlayers legend:

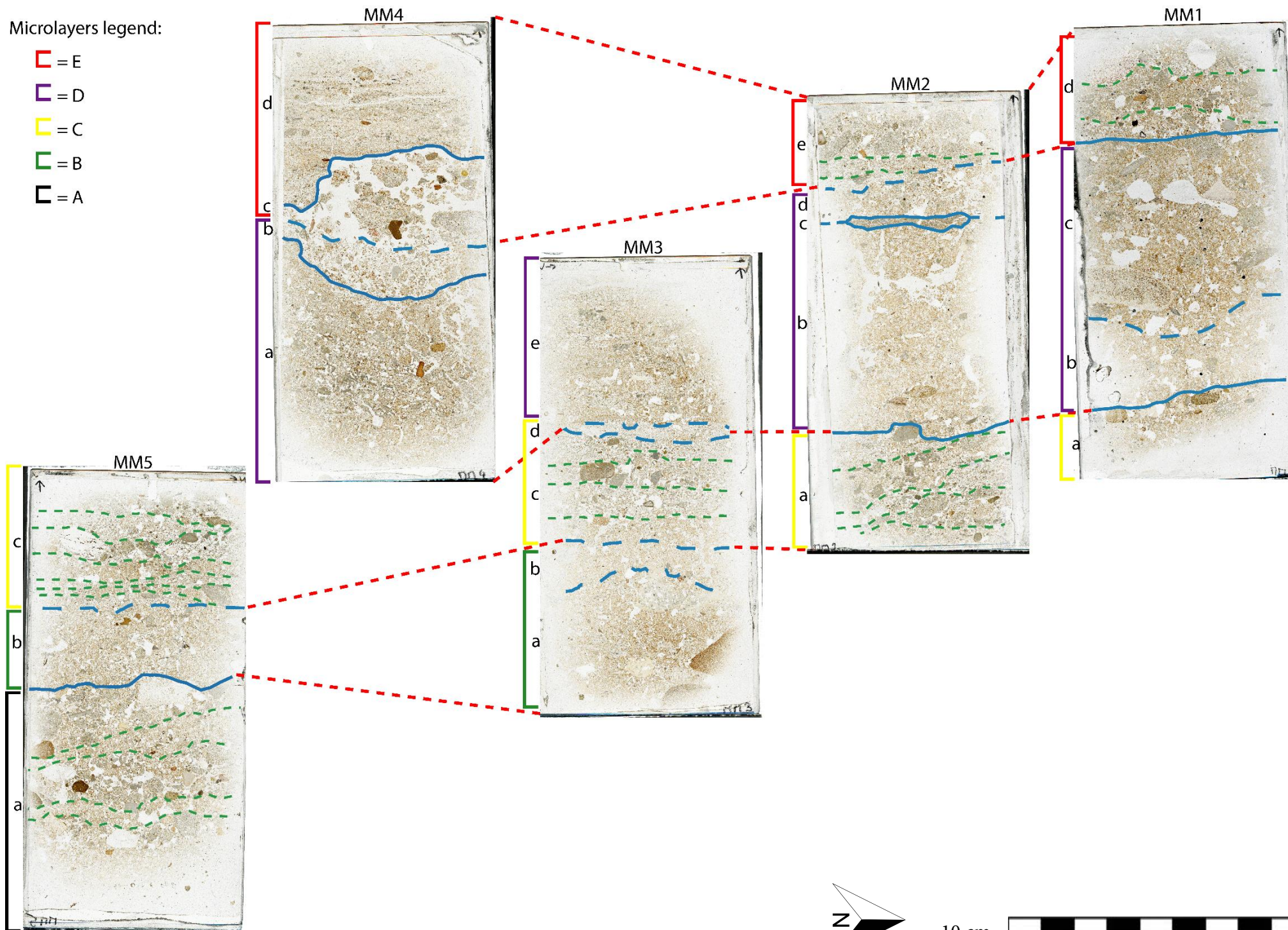
■ = E

■ = D

■ = C

■ = B

■ = A



10 cm



4.3 Depositional and post-depositional processes of microlayers

Based on the features observed in the different microlayers it is possible to argue their mode of emplacement. Two different sets of microlayers can be identified:

- Microlayers displaying a banded fabric (E, C and A): beyond their differences these microlayers are all composed of bands with different degree of sorting; their coarse geogenic components are also quite similar to each other, in fact they all present rounded to sub-rounded elements (of heterogeneous mineralogical nature) and angular to sub-angular elements (all these elements have the same mineralogical nature, which is carbonate rocks with fossils inside).

An interpretation of the depositional history of these sediments can be deduced from these microlayers' features, which seem to be pointing to a deposition linked to water dynamics. Cyclic accumulation phenomena linked to water dynamics tend in fact to create accumulation bands (Karkanas and Goldberg, 2013) composed of allochthonous material taken in charge by the water before it entered the cave.

Since the material often results to be well rounded two hypothesis could be formulated. Due to the close position of the original entrance of the cave to the Dardaillon river, it may seem plausible to assume that this material could be a direct deposition of river paleofloods; or, on the other hand it could be a reworking of fluvial deposits previously deposited outside the cave entrance.

However, as observed during the geomorphological analysis made in the area surrounding the cave, at that time (contemporaneous to the fulfillment of the cavity) the Dardaillon river was already lower in its valley, so eventual paleofloods could not reach the cave entrance. Therefore, the second hypothesis of a reworking of fluvial deposits appears to be more plausible. Particularly, as already mentioned in the introduction (cap. 1.3 "Geological and geographical background") they appear to come from the reworking of old alluvial terraces formed by the Rhône river. In this case the characteristics of the sediments could be related to the Rhône previous transportation (therefore, displaying typical features such as high roundness and alteration surfaces) and may have covered only a short distance to reach the dolina (through processes such as colluvium).

This hypothesis results also to be supported by the high degree of alteration identified in coarse elements, such as the flint pebble displaying an alteration rim (fig.18) which could

be interpreted as a neocortex formed during the fluvial transport.

On the other hand, for what concerns the angular to sub-angular elements, due to their lithology, they can be interpreted as autochthonous sediments coming from the vault and walls erosion of the cave.

Another interesting element observed in these microlayers is their spatial variability in relationship to their material distance from the dolina (fig.15). As a reminder MM1 was the sample closer to the dolina, while MM5 was the one taken the farthest from it; it should also be kept in mind that the cave deposit shows a decreasing slope from the dolina towards the bottom of the cave.

As seen before this matter (microlayers spatial variability) is impossible to be discussed for microlayer A, since there is only one facies representing it. On the other hand, for E and C enough data are present. Microlayer C does not present significant differences between the facies that compose it, so it can be argued that the competence of the water was strong enough to deposit the same kind of material in all the interested area. In contrast microlayer E displays a marked difference between its facies close to the dolina (MM1 and MM2) and the ones further from it (MM4), in this case it can be assumed that the water may have lost competence due to the decreasing slope of the surface of deposition and so also the granulometry of its deposited material progressively decreases. In this case, the original competence of the water depositing E should have been lower compared to the one depositing C.

- Microlayers displaying a massive microstructure with a lack of bands (D and B): the aspect of these microlayers is more complex compared to the previous ones. The lack of bands in fact does not permit an immediate interpretation of their mode of emplacement. The geogenic constituents of this set of microlayers are very peculiar. These in fact result to be fine materials but it does not present a high degree of sorting (from a microscopic point of view), both silt size and sand size elements are present, and their related distribution seems to be random. This lack of sorting and of lamination (fig.19) may be pointing to a shallow water deposition linked to phenomena such as shallow sheetwash or runoff. In this case the vesicular voids may be formed as a result of trapped air (Karkanas and Goldberg, 2013, p. 288).

Moreover, the bands present on the right side of facies *3e* may be pointing to a stabilization of these waters, that may have formed restricted areas of standing water (such as puddles or ponds) (Karkanas and Goldberg, 2013, fig. 1b).

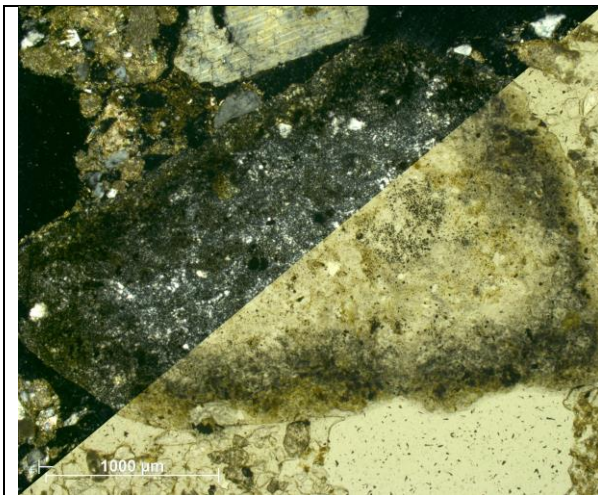


Fig.18: Flint pebble displaying an alteration rim along its contour.

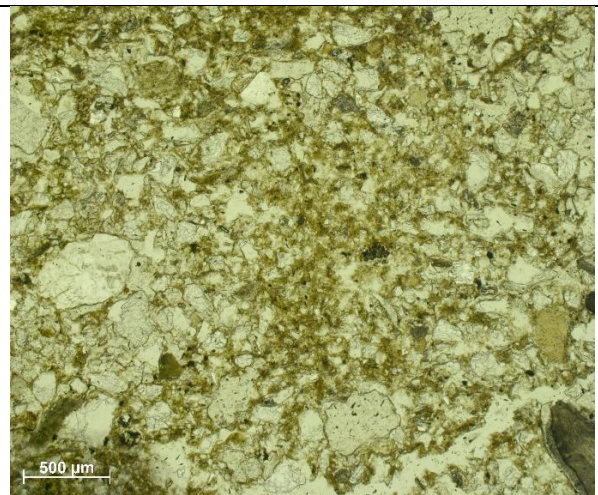


Fig.19: General matrix of 2b (microlayer D). Note the absence of microscopic sorting.

Other elements present in all the thin sections are the aggregates of cemented matrix (Sheet 1,VI; 5,V) and the opaque micromass (Sheets 1,II; 2,VI; 3,IV; 4,III) the interpretation of these elements will be discussed here since these features are shared by both sets of microlayers. The presence of both these elements may correspond to a reworked calcareous topsoil such as *calcosols* (Baize and Girard, 2009, p. 109), the formation of the calcareous soils is usually linked to a calcareous bedrock (such as limestones), which is present in Mas des Caves' area. The pedological development of these soils in fact, usually brings to the decarbonization of the upper horizons (horizons *Aca* or *Sca*), with consequence residual accumulation in these horizons of the insoluble elements such as iron; and the reprecipitation of the soluble elements (secondary carbonates) in the lower horizons (horizons *C* or *K*) (Baize and Girard, 2009, pp. 109–110). Thus, a possible erosion, transport and redeposition of these horizons may have brought into the cave both insoluble materials (which can be linked to the opaque micromass identified in the thin sections, since the elements such as iron are opaque in PPL and XPL, and reddish to orange in OIL) and elements of cemented secondary calcite (these elements, due to their soft and soluble nature, may have been rounded by the water transport they underwent, and they can be linked to the aggregates of cemented matrix identified in the thin sections). In particular, the specific horizon *Sca* present in calcareous soils may show both redox staining and calcareous elements (Baize and Girard, 2009, p. 15), which could be respectively the opaque micromass and the aggregates of cemented matrix identified in the thin sections.

For what concerns the post-depositional processes the following elements have been observed in all the thin sections:

- Bioturbation

Even if traces of mesofaunal activities have not been found in every facies, they are present in all the microlayers. These traces vary from biospheroids (sheet 5,VI) and simple channels, up to more complex features such as bow-like features (sheet 2,V). The random pattern that these elements show throughout all the observed stratigraphy may be pointing to a bioturbation that took place after the deposition of all the observed sequence.

- Water dynamics

Post-depositional processes linked to water dynamics have also been observed in all the thin sections. The features attributed to these processes are: the micromass voids' coatings, linked to the percolation in the sediments of fine materials charge water and its associated deposition on the voids' walls (sheet 5,V); the partial dissolution of carbonate rock fragments (fig.20) and the consequent precipitation of secondary calcite, still as voids' coatings (fig.21).

All these post-depositional processes can be linked to underground water movements.

- Post-depositional movements

Beyond the micromass displacement linked to the water dynamics and the movements of the material linked to mesofauna activity (fine and localized elements) no other vertical movements have been observed.

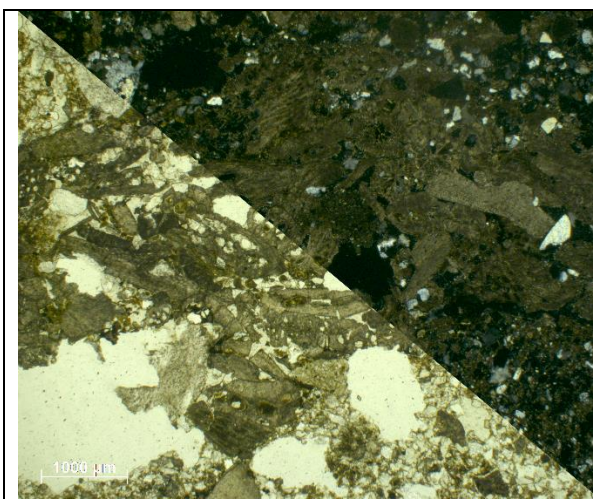


Fig.20: Carbonate rock fragment integrating quartz grains and fossils. Notice its rough surface, that may be pointing to dissolution processes.

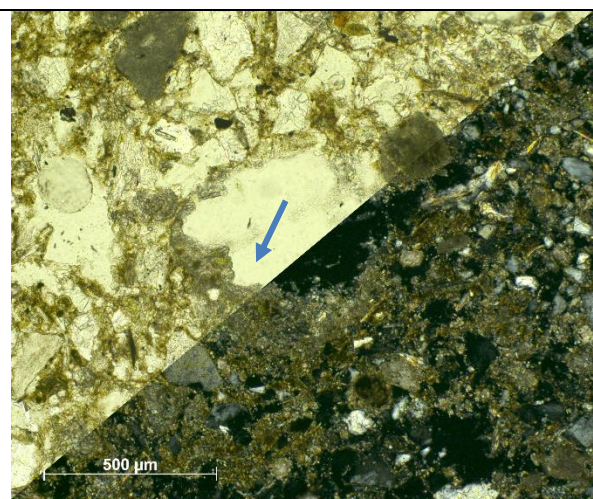


Fig.21: Calcite void coating (blue arrow), which may be pointing to a secondary calcite deposition.

4.4 Carnivore activities

A high presence of traces from carnivore activities has been identified in the studied thin sections. In particular the interested microlayers are D and B, however, even if they both present carnivore activity's traces, the situation is quite different between the two.

In both microlayers these traces are composed of phosphatic grains (sheets 1,IV; 2,IV), bone fragments (sheets 1,III; 5,III) and coprolites (sheets 3,V,VI; 4,V). However, focusing on the granulometry of these elements, it is possible to observe that in D their granulometry results to be coherent with the matrix that embeds them, while in B they result to be quite bigger in comparison with the matrix; this argument applies especially to the coprolites. These in fact, are present both under integral and fragmented form in B, while in D only small fragments have been identified. For microlayer B it must be noted the presence of two big pebbles at the right-low corner of MM3 section, however, these pebbles result to be quite far from the coprolites, and being at the very bottom of the thin section they could be part of a facies not included in the section.

This situation may be pointing to two different scenarios of deposition of these biogenetic elements. In facies D they may have a natural geological deposition, in this case they could have been taken in charge by the same processes that deposited the microlayer and so have been sorted together with their matrix (thus, they should be in a secondary position); while in B they may have a biological deposition, thus being in a primary position. Moreover, the two biggest coprolites found in 3a are in contact with each other, this characteristic may also be pointing to a primary position of these elements.

Following this hypothesis, we could argue that microlayer B could be a carnivore occupational surface, which may have integrated these big coprolites into a finer matrix. Moreover, if this hypothesis results to be correct, it may be possible to question whether the massive microstructure of the microlayer might be linked to carnivores trampling activities; however, no bibliographical comparisons have been found to better support this hypothesis. Indeed, the most common feature indicating trampling in caves results to be the presence of *in situ* crashed components such as charcoal or bones (as in Goldberg et al., 2001; Karkanas and Goldberg, 2010; Bergadà et al., 2023), which were not identified in the studied thin sections.

The above argument is valid for the coprolites that has been identified as hyenas' ones, but it must be noted also the presence of another type of coprolite (fig.22) which attribution results to be complicated, even though it should still be a carnivore's one due to the elongated

poroids present in it, the latter usually identified as “pseudomorphic voids after decomposed hair, fur or wool” (Brönnimann et al., 2017).

For what concerns the traces identified as generated by carnivore activities, it has to be noted that the phosphatic grains have been identified as such only on the base of their color in PPL, their behavior in XPL and the fact that they often results to be present in relationship with carnivore coprolites (Goldberg, 1979; Friesem et al., 2022). However, confirming their true nature would require the use of fluorescence microscopy (Stoops, 2017).

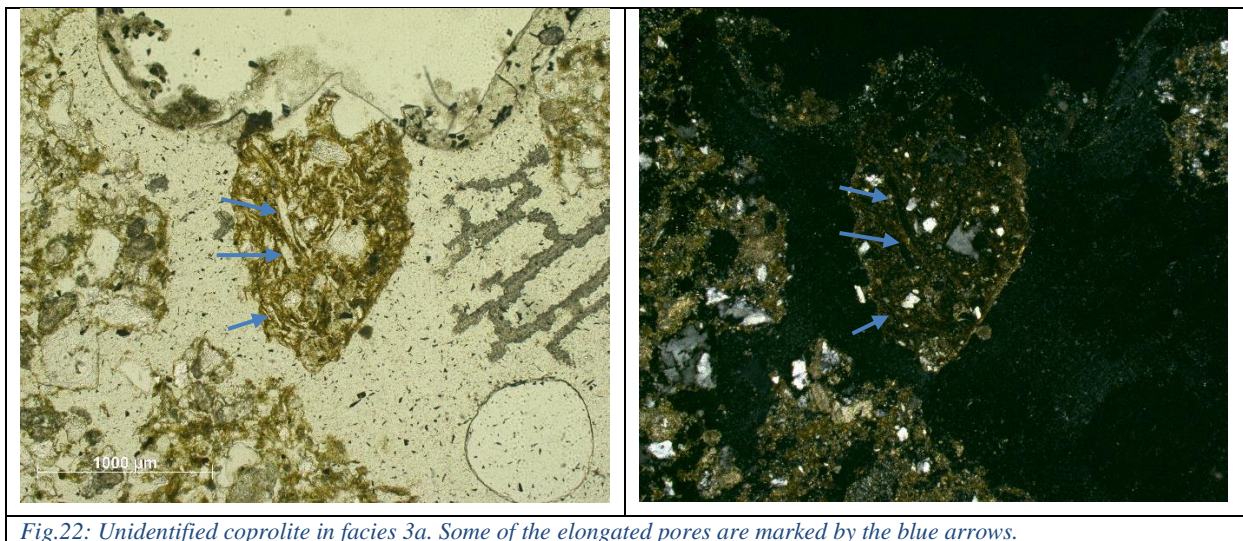


Fig.22: Unidentified coprolite in facies 3a. Some of the elongated pores are marked by the blue arrows.

4.5 Human activities

The anthropogenic traces identified during the observation of the thin sections need to be better discussed since their anthropicity is not obvious and may need further investigations.

Two elements have been identified during the descriptions as knapped artifacts due to their angular shape and their sharp boundaries (sheets 1,V; 5, IV).

However, some problems about this interpretation are present, in fact according to Angelucci (2017) the knapped artifacts (beyond their material) in thin section are “usually tabular or platy”, they can present “scars or crests along the object’s contour or the occurrence of very acute angles at its corners” and they are “almost always very angular to angular, usually with regular and smooth surfaces and sharp and prominent boundaries [...] with a more-or-less regularly curved or straight outline”.

Confronting these guidelines with our elements it is clearly visible how the latter presents some characteristics such as the angular shape and the sharp boundaries, but they do not

present a tabular nor a platy shape.

However, since the observed section of the real elements results to be completely random (due to the aleatory cut made for the fabrication of the thin section) a tabular three-dimensional body may be cut into a two-dimensional section of itself with more or less equidimensional measures, or even into a completely different polygon such as a triangle (Stoops, 2021, pp. 11–17). Moreover, the angular shape of these elements has been identified in no other coarse elements, so it therefore seems anomalous that they underwent the same depositional history as the other elements (which have a rounded to sub-rounded shape).

Thus, it seems plausible to hypnotize the anthropicity of these elements, however, it is important to keep in mind that “in thin section it is exceedingly difficult to distinguish natural from human worked fragments” (Angelucci, 2017). Furthermore, it is crucial to underline that their anthropogenic origin does not exclude a possible natural deposition of these elements inside the cave, due to processes such a water transport that may have moved them from their original point of fabrication.

Other traces of hypothetical human origin that have been identified during the analysis is facies 2c, in which ashes have been identified. Due to the complex microstructure of this facies (see appendix for more details) it results difficult to give it an interpretation without further analysis. However, a visual comparison has been found in Abrigo de la Quebrada site (Valencia, Spain) in which a micromorphological investigation allowed the observation of a combustion feature (heart) with a very similar appearance to facies 2c (fig.23-26). In the case of Abrigo de la Quebrada (Bergadà et al., 2023) these features have been identified as slightly phosphatized calcitic ashes.

Beyond the similar appearance of the two, however, it must be noted that in the case of Abrigo de la Quebrada the combustion feature presents (below it) a layer of thermoaltered silty clays (fig.23) which is completely missing in facies 2c. Thus, its interpretation (of 2c) as a combustion feature is very hypothetical.

If the facies is actually a combustion feature the lack of these underlying thermoaltered layer may be explained in two ways. The first one may be linked to the nature of the substrate, which could be highly resistant to thermoalteration, and thus the combustion may not leave any visible traces in the sediment; or facies 2c could be a fragment of a combustion feature which could have reached its actual position due to its erosion and transportation (after its consolidation or cementation due to post-depositional processes), in this case, anyway, in order to preserve its integrity, the transport should not have covered great distances.

In order to confirm or discard the hypothesis of 2c being a combustion feature further analysis can be very helpful. For example, the use of X-ray microanalysis techniques (such as SEM), may allow the correct identification of the material composing the facies, or the use of micro-FTIR technique may allow to identify thermoaltered sediments through the comparison with control samples of non-thermoaltered sediments. The latter already proposed by FrieSEM et al. (2022) in Sefunim Cave (Israel).

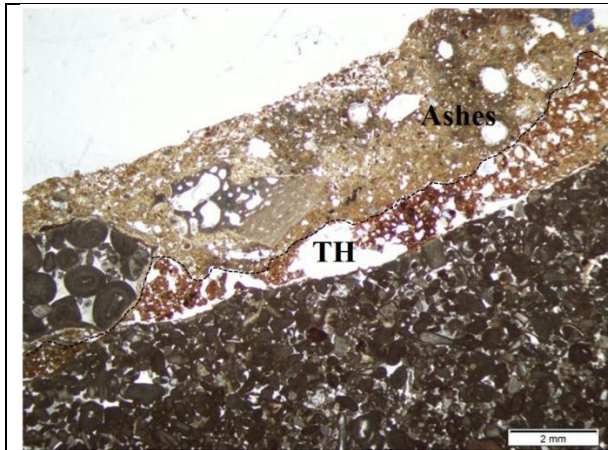


Fig.23: Heart of Abrigo de la Quebrada. Upper, calcitic ashes, slightly phosphatized, and lower, thermoaltered silty clays (TH) (Bergadà et al., 2023, fig. 14 (e)).

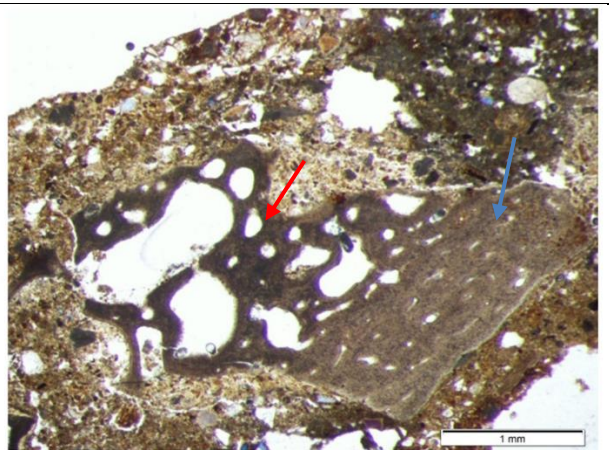


Fig.24: Detail of fig.23, brown to brownish calcined gray bone (blue arrow) and bubble-shaped pores due to high combustion (red arrow) (Modified from Bergadà et al., 2023, fig. 14 (f)).

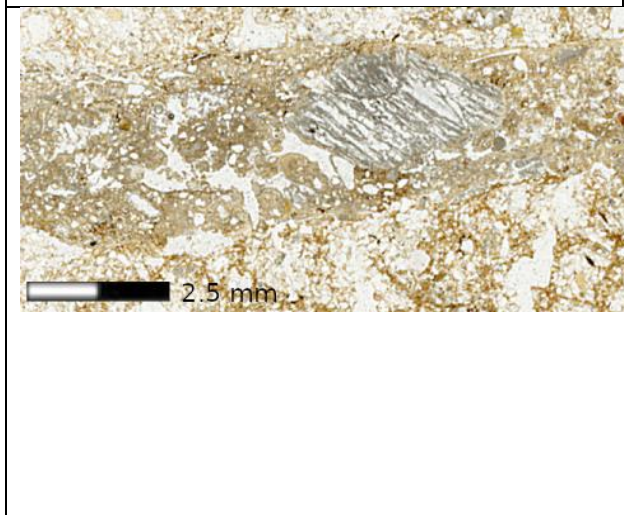


Fig.25: Detail of facies 2c. Note its similar appearance to the calcitic ashes of the heart in fig.23 and the lack of the underlying thermoaltered layer.

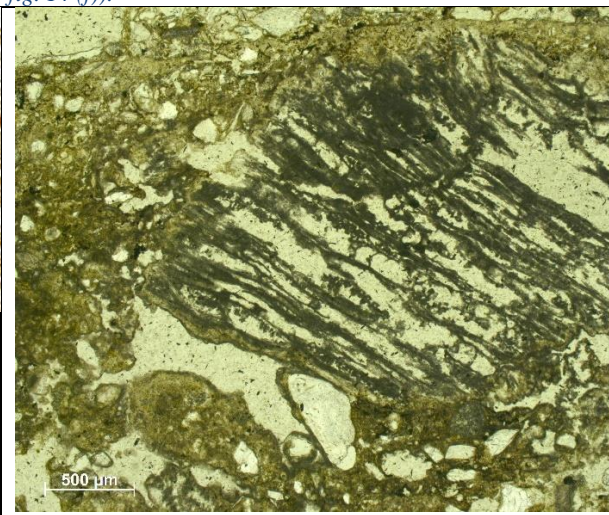


Fig.26: Micrograph of facies 2c. Note the similarity between the microstructure of this facies and the one present in fig.24. Both features present a grayish material (ashes) with a contour of yellowish material.

4.5.1 Anthropogenic structures issue

For what concerns the issue related to the hypothetical anthropogenic structure *Sol76*, the data collected during this study have provided insights into the spatial variability of the studied stratigraphy. This spatial variability is closely associated with the granulometry of the materials, which may or may not change from the dolina to the bottom of the cave (respectively from MM1 to MM5). However, if changes in granulometry occur, they always result in a decrease moving towards the bottom of the cave. Thus, the micromorphological observations appear to support the sedimentary anomaly of *Sol 76* elements observed in the field.

Moreover, no clear erosional surfaces have been observed in the thin sections, so the hypothesis of *Sol 76* elements as residual features does not seem to be plausible.

On the other hand, for what concerns the sample taken close to *Sol 76* (MM5) the only potential anthropogenic trace observed is the quartzite rock fragment. No significant signs of human occupation have been detected.

However, it should be noted that the presence of the hypothesized combustion feature (facies 2c), although not in stratigraphical connection with MM5, may (or may not, depending on its mode of deposition) indicate a direct human occupation of the cave.

5. Conclusions and future perspectives

5.1 Conclusions

The micromorphological investigation of *couche 9* at Mas Des Caves carried out within the scope of this memoire has confirmed the observations made on the field and allowed the discovery of new information about the site's infilling.

Regarding the sedimentological dynamics that filled the cavity the data obtained from this analysis confirm the field observations described in the Introduction chapter. In particular, the sedimentation results to be strongly linked to water dynamics which varied through time. A rhythmic water deposition appears indeed to have taken place, alternating strong water regimes (which deposited the facies with banded fabrics) with weak ones (which deposited the massive facies). For what concerns the origin of the material that filled the cavity two hypotheses have been proposed: the erosion, transportation and deposition of a *calcosols'* topsoil horizon located relatively close to the cave original entrance; and the deposition of fluvial sediments (possibly deposited directly by paleofloods or eroded from already deposited fluvial sediments). The two hypotheses are not mutually exclusive, on the contrary the *calcosols* may have developed on fluvial sediments and later eroded, in this case both hypotheses may be correct. In any case these hypotheses need further studies to be validate.

Another characteristic of the sediments that has been possible to verify through the current analysis is their spatial variability. As for the observation made from a macroscopic point of view (field observations), also under the microscope the microlayers change from the dolina to the bottom of the cave. Precisely the granulometry of the microlayers presenting a banded fabric decrease moving away from the dolina. This suggests a progressive loss of sedimentary dynamics competence linked to the decreasing slope of the depositional surface.

As a result, water progressively deposited elements of its solid load along its path, leading to a gradual sorting of the material and leaving the coarser elements closer to the dolina.

In summary, the slope of the deposits decreases from the dolina to the bottom of the cave. Consequently, the competence of the depositional agent (water) also decreases in the same direction, and as a further consequence, the granulometry of the deposited material decreases with it.

Therefore, the deposition of *couche 9* can be described as follows: all the geogenic sediments

were deposited due to water dynamics, such as runoff or sheet wash processes, which brought allochthonous sediments from the cave's surrounding area into the cavity. Although it is challenging to identify the exact process that generated the couche using only micromorphology, it is reasonable to conclude that the sediments were not introduced into the cave by massive mass movements like mudflows. Elements deposited by such massive displacements cannot achieve the same level of sorting observed in Mas Des Caves, indeed “the sorting of mudflows appears to be independent of grain size” (Pe and Piper, 1975).

The post-depositional processes identified during the analysis are also mostly linked to water dynamics, especially to the percolation of it inside the sediments (which generated the coatings and the infillings). Other post-depositional processes are also present but to a lower degree, in particular traces mesofauna activities have been identified all along the studied sequence but their impact to the sediment resulted to be very small and mainly restricted to the vertical movement of small elements. No vertical movement of coarse elements has been identified.

For what concerns the traces of carnivore’s activities, they result to be highly present in the thin sections. However, their presence seems to be linked to two different types of depositions. Indeed, in microlayer D they appear to have been deposited by water process (as for the matrix in which they are embedded, and thus being in a secondary position), while in microlayer B they may be in their original position. Thus, the presence of a carnivore occupational surface (B) appears to be conceivable, therefore proving the possibility by carnivores to enter the cavity contemporaneous with the deposition of *couche 9*. While this assumption remains a hypothesis it seems to be in line the work of Fosse (1996) and the high presence of coprolite found in *couche 9* (Giuliani and Brugal in Brugal et al., 2020, p. 91).

It also must be noted that the secondary position of these elements in microlayer D does not necessarily mean that they were taken in charge by the transportation agents from outside the cave, indeed they may have been initially deposited by carnivores inside the cave and later reworked and sorted by these agents.

On the other hand, the traces of human activities resulted to be scarcer. Two potentially knapped artifacts and a potential combustion feature have been identified, but their anthropicity cannot be guaranteed by this analysis.

Regarding the issue of anthropogenic structures, instead, no heavy traces of anthropogenic

activities were detected in the sample taken close to *Sol 76* (sample MM5). However, the current micromorphological investigation may have provided new insight to enrich the debate. In addition to the validation of the spatial variability of the sediment observed in the field (described above), no erosional surfaces were detected, therefore it appears that the position of the *Sol 76* pebbles cannot be related to a residual feature. Moreover, the possibility of their deposition connected to massive displacements such as mudflows has been excluded.

Finally, based on the spatial variability observed in the thin sections, it appears that in the area in which *Sol 76* is located the water dynamic was too low to be able to carry large pebbles such as those composing *Sol 76*. This interpretation, however, needs further studies to be confirmed.

5.2 Future perspectives

In order to validate or reject the hypothesis about the depositional history of the deposit described above several steps may be taken.

For what concerns the origin of the sediments, a micromorphological control sample from outside the cave could be collected to determine if the features identified inside the cavity are also present there. However, this needs to be supported by previous pedological and stratigraphic field observations to evaluate the actual potential of the control sample.

On the other hand, the deposition dynamics (such as defining the water competency, and its variations, responsible for depositing the sediments) might be clarified by sedimentological analysis, indeed validating or rejecting the hypothesis made in the scope of this Memoire. These analyses are already underway (by researcher Vincent Ollivier).

Regarding carnivore activity a reexamination of the thin sections with the help of fluorescence microscopy could be very informative. It could verify of the nature of the phosphatic grains and potentially reveal traces related to post-depositional processes, such as phosphatization, which are not observable using only PPL and XPL techniques. Furthermore, the use of the technique may also provide further information about the hypothesized combustion feature (facies 2c), particularly it could be possible to check if it is actually composed of phosphatized ashes (as for the heart of Abrigo de la Quebrada).

Another potential way for study on the same thin sections analyzed here implies the use of X-ray microanalysis or micro-FTIR techniques, which could also provide more detailed insights

into the hypothesized combustion feature.

Regarding the issue of the anthropic structures, the spatial variability of the *couches* appears to be more appreciable from a macroscopic perspective. Thus, a renewed stratigraphic description and analysis will provide better insight; this is also already underway as part of a master's degree work at the University of Toulouse (by Marie-Eléa Coustures under the direction of Laurent Bruxelles).

Moreover, for what concerns future possibilities related to micromorphological analysis, taking a sample directly inside the *Sol 76* area that includes one of its pebbles may provide precise informations about their depositional history.

Lastly, it should be noted that the limited time available for the analyses and my lack of experience (being this my first micromorphological analysis) may have contributed to miss or misinterpret certain features. A renewed investigation of the thin sections by a researcher experienced in cave micromorphology, supported of the upcoming data (such as mineralogical, sedimentological and stratigraphical) may bring more or different elements to light.

Bibliography

- Angelucci, D.E., 2017. Lithic Artefacts. In: Nicosia, C., Stoops, G. (Eds.), *Archaeological Soil and Sediment Micromorphology*. John Wiley & Sons, Ltd, Chichester, UK, pp. 223–230.
doi:10.1002/9781118941065.ch27
- Baize, D., Girard, M.C., 2009. Référentiel pédologique 2008. Éditions Quæ, Versailles.
- Bergadà, M.M., Eixea, A., Villaverde, V., 2023. Geoarchaeological and microstratigraphic view of a Neanderthal settlement at Rambla de Ahíllas in Iberian Range: Abrigo de la Quebrada (Chelva, Valencia, Spain). *Geoarchaeology* *gea.21973*. doi:10.1002/gea.21973
- Bonifay, E., 1976. Grotte du Mas des Caves (Lunel-Viel, Hérault). Presented at the *UISPP IXe congress*, Université de Nice, Nice Parc Valrose, pp. 197–204.
- Bonnet, A., 1967. Un karst limité dans l'espace et le temps : la grotte de Lunel Viel (Hérault). *Spelunca Mémoires* *5*, 47–52.
- Bronnikova, M.A., Panin, A.V., Murasheva, V.V., Golyeva, A.A., 2016. Soil micromorphology in archaeology: history, objectives, possibilities and prospects. *Dokuchaev Soil Bulletin* *86*, 35–45.
doi:10.19047/0136-1694-2016-86-35-45
- Brönnimann, D., Pümpin, C., Ismail-Meyer, K., Rentzel, P., Égüez, N., 2017. Excrements of Omnivores and Carnivores. In: Nicosia, C., Stoops, G. (Eds.), *Archaeological Soil and Sediment Micromorphology*. John Wiley & Sons, Ltd, Chichester, UK, pp. 67–81.
doi:10.1002/9781118941065.ch7
- Brugal, J.P., Fosse, P., Fourvel, J.-B., Magniez, P., Uzunidis, A., Giuliani, C., Ollivier, V., Sirdeys, N., Pascal, L., Derville, B., Guadelli, J.-L., Dauphin, Y., Bruxelles, L., Falguères, C., Bahain, J.-J., Tombret, O., Torres Pérez-Hildago, T. de, Thouveny, N., Paquette, J.-L., Mathias, C., Viallet, C., André, G., Girard, M., Vergoz, T., 2020. Rapport de fouille 2020. Grotte du Mas des Caves n°1 (ou I), Lunel-Viel (Hérault). “ Hommes et Environnements au Pléistocène Moyen ” (Excavation Report). *Laboratoire méditerranéen de préhistoire Europe Afrique (LAMPEA) - UMR 7269 (AMU – CNRS – MCC - IRD)*.
- Brugal, J.-P., Giuliani, C., Fosse, P., Fourvel, J.-B., Magniez, P., Pelletier, M., Uzunidis, A., 2021a. Preliminary data on the Middle Pleistocene site of Lunel-Viel I (Hérault, France). *Alpine and Mediterranean Quaternary* *34*, 75–88. doi:10.26382/AMQ.2021.08
- Brugal, J.P., Magniez, P., Uzunidis, A., Giuliani, C., Guy, A., Ollivier, V., Argant, J., Bendhafer, W., Bahain, J.J., Bigot, J.Y., Braucher, R., Bruxelles, L., Boulbes, N., Lahaye, C., Dardenne, É., Lebrun, B., Falguères, C., Frerebeau, N., Geigl, E.M., Grabge, T., Igreja, M., Mathias, C., Thery, I., Viallet, C., Walles, A., 2021b. Rapport de fouille 2021. Grotte du Mas Des Caves N°1 (ou I), Lunel-Viel (Herault) « Hommes et Environnements au Pléistocène Moyen » (Excavation Report). *Laboratoire méditerranéen de préhistoire Europe Afrique (LAMPEA) - UMR 7269 (AMU – CNRS – MCC - IRD)*.

- Brugal, J.P., André, G., Fourvel, J.-B., Fosse, P., Igreja, M., Magniez, P., Pascal, L., Uzunidis, A., 2022a. Le site archéo-paléontologique du Mas des Caves à Lunel-Viel (Hérault): Historique des recherches et nouveaux travaux. In: *Karstic Sediment, Palaeontology & Archaeology*. Presented at the 18th International Congress of Speleology, Karstologia Mémoires n°25, Savoie Mont Blanc, pp. 339–342.
- Brugal, J.P., Giuliani, C., Fourvel, J.-B., Fosse, P., Argant, J., Argant, A., Baleux, F., Cazes, G., Mathias, C., Viallet, C., 2022b. Rapport de fouille programmée annuelle 2022. Grotte du Mas des Caves n°1 (ou I), Lunel-Viel (Hérault). “ Hommes et Environnements au Pléistocène Moyen ” (Excavation Report). *Laboratoire méditerranéen de préhistoire Europe Afrique (LAMPEA) - UMR 7269 (AMU – CNRS – MCC - IRD)*.
- Bullock, P., Fedoroff, N., Jongerius, A., Stoops, G., Tursina, T., 1985. Handbook for soil thin section description. *Waine Research, Wolverhampton*.
- Cammass, C., 1998. Recherches sur l’habitat ancien de Lattes. Analyse micromorphologique de murs et de sols de la zone 1 et la zone 2. Lattes (Hérault) – *Rapport triannuel 1998–2000*.
- Fosse, P., 1996. La grotte n° 1 de Lunel-Viel (Hérault, France) : Repaire d’hyènes du Pléistocène moyen. Etude taphonomique du matériel osseux. *Paléo* 8, 47–79. doi:10.3406/pal.1996.906
- Friesem, D.E., Shimelmitz, R., Schumacher, M.L., Miller, C.E., Kandel, A.W., 2022. A micro-geoarchaeological view on stratigraphy and site formation processes in the Middle, Upper and Epi-Paleolithic layers of Sefunim Cave, Mt. Carmel, Israel. *Archaeological and Anthropological Sciences* 14, 222. doi:10.1007/s12520-022-01686-0
- Goldberg, P., 1979. Micromorphology of Pech-de-l’Azé II sediments. *Journal of Archaeological Science* 6, 17–47. doi:10.1016/0305-4403(79)90031-1
- Goldberg, P., Aldeias, V., 2018. Why does (archaeological) micromorphology have such little traction in (geo)archaeology? *Archaeological and Anthropological Sciences* 10, 269–278. doi:10.1007/s12520-016-0353-9
- Goldberg, P., Macphail, R., 2006. Practical and theoretical geoarchaeology. *Blackwell Publishing, Malden, MA ; Oxford*.
- Goldberg, P., Macphail, R.I., 2003. Short contribution: Strategies and techniques in collecting micromorphology samples. *Geoarchaeology* 18, 571–578. doi:10.1002/gea.10079
- Goldberg, P., Sherwood, S.C., 2006. Deciphering human prehistory through the geoarchaeological study of cave sediments. *Evolutionary Anthropology: Issues, News, and Reviews* 15, 20–36. doi:10.1002/evan.20094
- Goldberg, P., Weiner, S., Bar-Yosef, O., Xu, Q., Liu, J., 2001. Site formation processes at Zhoukoudian, China. *Journal of Human Evolution* 41, 483–530. doi:10.1006/jhev.2001.0498

- Haaland, M.M., Czechowski, M., Carpentier, F., Lejay, M., Vandermeulen, B., 2018. Documenting archaeological thin sections in high-resolution: A comparison of methods and discussion of applications. *Geoarchaeology* 34, 100–114. doi:10.1002/gea.21706
- Horwitz, L.K., Goldberg, P., 1989. A study of Pleistocene and Holocene hyaena coprolites. *Journal of Archaeological Science* 16, 71–94. doi:10.1016/0305-4403(89)90057-5
- Jenny, H., 1994. Factors of soil formation: a system of quantitative pedology. Dover, New York.
- Karkanias, P., 2017. Guano. In: *Nicosia, C., Stoops, G. (Eds.), Archaeological Soil and Sediment Micromorphology*. John Wiley & Sons, Ltd, Chichester, UK, pp. 83–89. doi:10.1002/9781118941065.ch8
- Karkanias, P., Goldberg, P., 2008. Micromorphology of sediments: deciphering archaeological context. *Isr J Earth Sci* 56, 63–71.
- Karkanias, P., Goldberg, P., 2010. Site formation processes at Pinnacle Point Cave 13B (Mossel Bay, Western Cape Province, South Africa): resolving stratigraphic and depositional complexities with micromorphology. *Journal of Human Evolution* 59, 256–273. doi:10.1016/j.jhevol.2010.07.001
- Karkanias, P., Goldberg, P., 2013. 6.23 Micromorphology of Cave Sediments. In: *Treatise on Geomorphology*. Elsevier, pp. 286–297. doi:10.1016/B978-0-12-374739-6.00120-2
- Kooistra, M.J., Pulleman, M.M., 2010. Features Related to Faunal Activity. In: *Interpretation of Micromorphological Features of Soils and Regoliths*. Elsevier, pp. 397–418. doi:10.1016/B978-0-444-53156-8.00018-0
- Le Grand, Y., 1994. Approche méthodologique et technologique d'un site d'habitat du Pléistocène moyen : la grotte no 1 du Mas des Caves (Lunel-Viel, Hérault) (*These de doctorat*). Aix-Marseille 1.
- Lejay, M., 2018. Approche archéologique et expérimentale des structures de combustion au Paléolithique supérieur ancien. Analyse multiscalaire (micromorphologie et géochimie organique) appliquée aux sites de Régismont-le-Haut et des Bossats.
- Macphail, R.I., Courty, M.-A., Goldberg, P., 1990. Soil micromorphology in archaeology. *Endeavour* 14, 163–171. doi:10.1016/0160-9327(90)90039-T
- Major, J.J., 1998. Pebble orientation on large, experimental debris-flow deposits. *Sedimentary Geology* 117, 151–164. doi:10.1016/S0037-0738(98)00014-1
- Mallol, C., Goldberg, P., 2017. Cave and Rock Shelter Sediments. In: *Nicosia, C., Stoops, G. (Eds.), Archaeological Soil and Sediment Micromorphology*. John Wiley & Sons, Ltd, Chichester, UK, pp. 359–381. doi:10.1002/9781118941065.ch34
- Mallol, C., Mentzer, S.M., 2017. Contacts under the lens: Perspectives on the role of microstratigraphy in archaeological research. *Archaeological and Anthropological Sciences* 9, 1645–1669. doi:10.1007/s12520-015-0288-6

- Mallol, C., Mentzer, S.M., Miller, C.E., 2017. Combustion Features. In: *Nicosia, C., Stoops, G. (Eds.), Archaeological Soil and Sediment Micromorphology*. John Wiley & Sons, Ltd, Chichester, UK, pp. 299–330. doi:10.1002/9781118941065.ch31
- Miller, C.E., 2017. Trampling. In: Gilbert, A.S. (Ed.), *Encyclopedia of Geoarchaeology, Encyclopedia of Earth Sciences Series*. Springer Netherlands, Dordrecht, pp. 981–982. doi:10.1007/978-1-4020-4409-0_128
- Miller, C.E., Conard, N.J., Goldberg, P., Berna, F., 2010. Dumping, Sweeping and Trampling: Experimental Micromorphological Analysis of Anthropogenically Modified Combustion Features. *Palethnologie*. doi:10.4000/palethnologie.8197
- Murphy, C.P., 1986. Thin section preparation of soils and sediments: Soil Survey of England and Wales Rothamsted Experimental Station. A B Acad. Publ, Berkhamsted.
- Nicosia, C., Stoops, G. (Eds.), 2017. *Archaeological Soil and Sediment Micromorphology*, 1st ed. Wiley. doi:10.1002/9781118941065
- PACEA-Transfert Sédiments & Matériaux | PACEA [WWW Document], 2023. URL <https://www.pacea.u-bordeaux.fr/pacea-transfert-sediments-materiaux/> (accessed 9.1.23).
- Pe, G.G., Piper, D.J.W., 1975. Textural recognition of mudflow deposits. *Sedimentary Geology* 13, 303–306. doi:10.1016/0037-0738(75)90039-1
- Rentzel, P., Nicosia, C., Gebhardt, A., Brönnimann, D., Pümpin, C., Ismail-Meyer, K., 2017. Trampling, Poaching and the Effect of Traffic. In: *Nicosia, C., Stoops, G. (Eds.), Archaeological Soil and Sediment Micromorphology*. John Wiley & Sons, Ltd, Chichester, UK, pp. 281–297. doi:10.1002/9781118941065.ch30
- Shahack-Gross, R., 2017. Animal Gathering Enclosures. In: *Nicosia, C., Stoops, G. (Eds.), Archaeological Soil and Sediment Micromorphology*. John Wiley & Sons, Ltd, Chichester, UK, pp. 265–280. doi:10.1002/9781118941065.ch29
- Stoops, G., 2017. Fluorescence Microscopy. In: *Nicosia, C., Stoops, G. (Eds.), Archaeological Soil and Sediment Micromorphology*. John Wiley & Sons, Ltd, Chichester, UK, pp. 393–397. doi:10.1002/9781118941065.ch36
- Stoops, G., 2021. Guidelines for analysis and description of regolith thin sections, Second edition. ed, ASA, CSSA, and SSSA books. Wiley-ACSESS, Hoboken, NJ.
- Stoops, G., Nicosia, C., 2017a. Introduction. In: *Nicosia, C., Stoops, G. (Eds.), Archaeological Soil and Sediment Micromorphology*. John Wiley & Sons, Ltd, Chichester, UK, pp. 1–7. doi:10.1002/9781118941065.ch0
- Stoops, G., Nicosia, C., 2017b. Sampling for Soil Micromorphology. In: *Nicosia, C., Stoops, G. (Eds.), Archaeological Soil and Sediment Micromorphology*. John Wiley & Sons, Ltd, Chichester, UK, pp. 383–391. doi:10.1002/9781118941065.ch35

Stoops, G., Mees, F., Marcelino, V., 2010. Interpretation of micromorphological features of soils and regoliths. Elsevier, Amsterdam.

Uzunidis, A., 2020. Dental wear analyses of Middle Pleistocene site of Lunel-Viel (Hérault, France): Did Equus and Bos live in a wetland? *Quaternary International* 557, 39–46.
doi:10.1016/j.quaint.2020.04.011

Verrecchia, E.P., Trombino, L., 2021. A Visual Atlas for Soil Micromorphologists. Springer International Publishing, Cham. doi:10.1007/978-3-030-67806-7

Wattez, J., Onfray, M., 2012. La question des sols d'occupation néolithiques : apports de la géoarchéologie à leur identification et à leur interprétation. In: I, S., C, B., F, B., I, P., É. (dir), T. (Eds.), Premières Rencontres Nord/Sud de Préhistoire Récente, Méthodologie de La Terrain Sur La Préhistoire Récente En France, Nouveaux Acquis, Nouveaux Outils, 1987-2012. *Éditions Archives d'Écologie Préhistorique*, Marseille, France, pp. 317–331.

APPENDIX

MM1

Stratigraphic description of the block

The block results to be well made and entirely observable. North is not marked on it but taking a closer look at the block it was possible to identify it. The rear part of the block (the side where plaster is still present), results to be the face of the block facing west, so the front part of the block (from which the section has been made, has the north on its right side). This understanding was made possible thanks to the plaster present on the back of the section which was also the last to be applied on the block. This side of the block should therefore be the one opposite to the exposed stratigraphic section from which the block was sampled. To support this hypothesis, it can be noted that the absence of the top of the nail (fig.3) on the back part of the block indicates that this side is facing towards the west (located within the exposed section during sampling)

The position of the MM1 thin section on the block is guaranteed by the presence of a pebble which is present in both elements.

North is also not marked on the section, but thanks to the pebble shared with the block we can argue that north should be on the right side on the section as well.

From a stratigraphical point of view the block has been divided into four units. From top to bottom we find:

- I.* The unit present a banded fabric composed by an alternation of sandy-gravel levels and levels of fine material (fig.2).
- II.* Sandy gravel unit, homogeneous at this scale of observation, which doesn't present any lamination. The coarser elements present a sub-horizontal orientation pattern. All these elements float in a fine dark brown matrix (fig.3).
- III.* New unit displaying a banded fabric composed of an alternation of sandy levels and levels of fine material. To be noted the presence of a coprolite at the bottom (fig.5)
- IV.* Sandy gravel unit presenting the same characteristics as unit *II* (fig.4).

All the stratigraphical contacts identified in the block results to be comfortable.

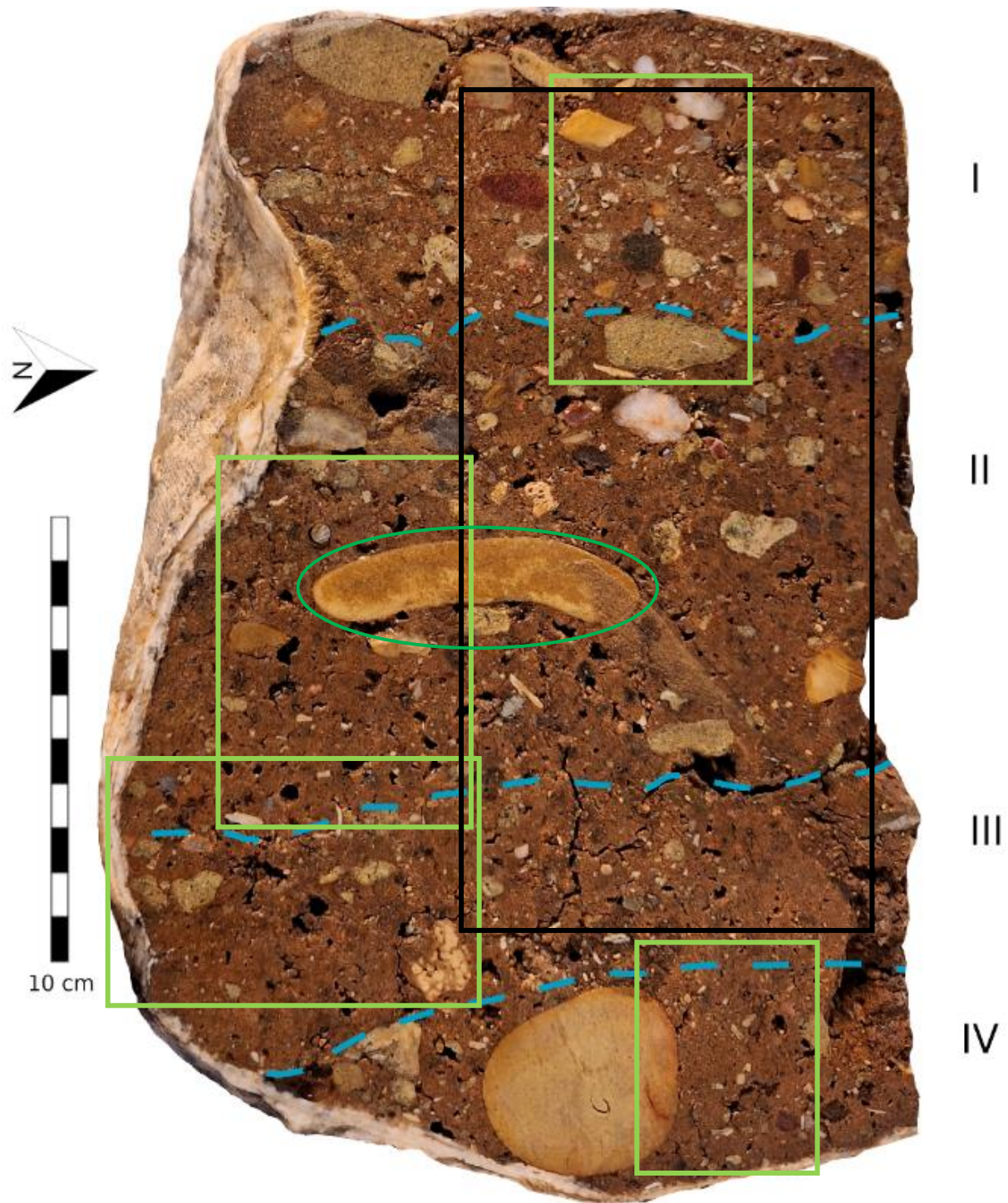


Fig.1: MM1 block. The dashed lines indicate the contact between the identified units. The green rectangles indicate the areas from which the following pictures were taken. The ellipse underlines the pebble shared between the block and the section. The black rectangle indicates the position of the section in the block.



Fig.2: zoom of unit I, note the banded fabric. On the lower is visible the contact with unit II (red arrow) (scale: 2 cm).



Fig.3: detail of unit II, note the absence of bands and the sub-horizontal orientation pattern of the elements (scale: 2 cm).



Fig.4: Detail of unit IV. Note the absence of bands and the similarity in the matrix with fig.3 (scale: 2 cm).

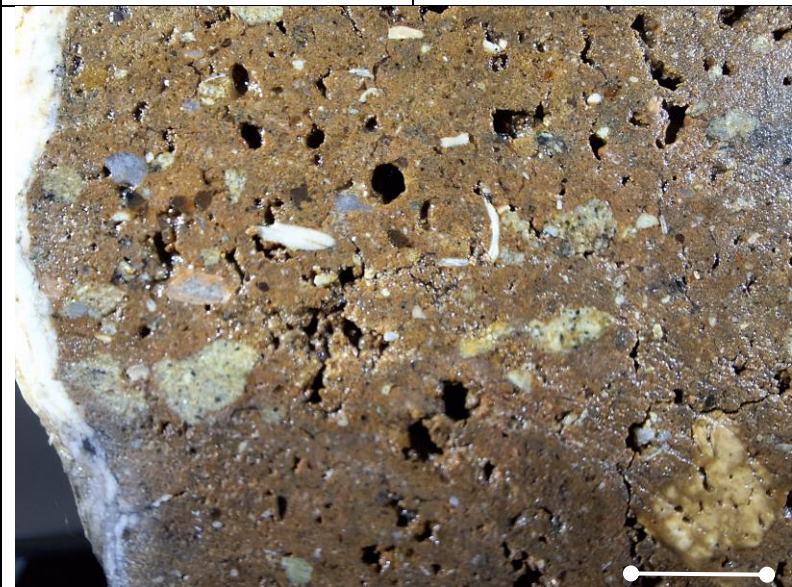


Fig.5: Detail of unit III. Note the banded fabric and the coprolite at the bottom right part (scale: 2cm)

Mesoscopic description of the section

From a mesoscale point of view the thin section has been divided into four facies, from top to bottom we find (fig.6):

- d)* The facies displays a banded fabric composed of two partial fabric alternating each other. One presenting a massive microstructure and located between two bands of the second partial fabric, presenting a more spongy microstructure. Between the three bands comfortable contacts are present.
- c)* The microstructure at this scale of observation ranges from channel to chamber, these voids result to interrupt the continuity of a massive material (structure visible at a mesoscopic scale). A high presence of coarse fraction is noted, it displays a linear basic distribution pattern, with a sub-parallel and sub-horizontal orientation pattern. The matrix is quite homogenous and presents a dark brown color. A variability in the porosity of the facies is noted, it decreases progressively going upwards.
- b)* At this scale of observation, the facies present a vughy to channel microstructure. Presenting almost only fine fraction, the facies results to be very homogenous. The color of the matrix is pale yellow. This color results to be very similar to the color present at the borders of the section, where the thickness of the latter decreases. The yellow of the facies is therefore in doubt, it could be related to a reduced thickness of the section and not to the sediment's natural color.
- a)* Facies characterized by the presence of coarse elements, a banded fabric seems to be slightly visible, we cannot be sure about this due to the low thickness of the lowermost part of the section, which doesn't permit a correct observation.

Based on these observations it was possible to create a stratigraphical connection between the block and the section. The *d* facies of the block results to be the lower part of the *I* unit on the block. Going downwards *c* and *b* result to be both related to *II* unit of the block, while facies *a* corresponds to the top part of unit *III*. Unit *IV* is therefore not described.

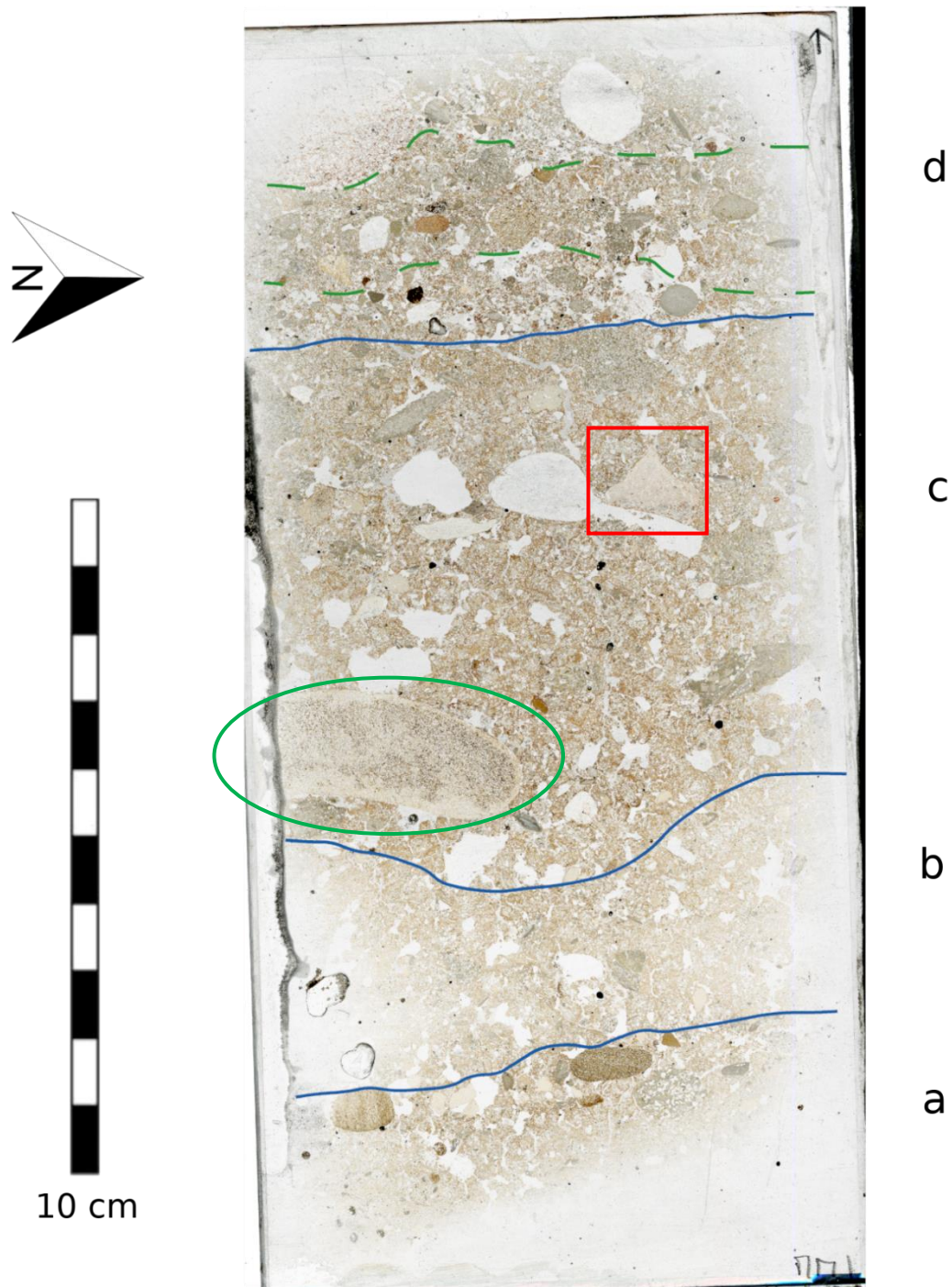


Fig.6: MM1 thin section, the continuous lines mark the limit between the facies while the dashed ones mark the partial fabrics identified in facies *d*. With the ellipse is high lined the pebble shared with the block, while with the square the flint element described in the paragraph dedicated to *c* micromorphological description.

Microscopic description of facies

d)

The facies presents massive to vesicular microstructure with a banded fabric. Due to its banded fabric, it has been subdivided into two partial fabrics to better describe it, these partial fabrics were named after the most representative size present in them (fig.7):

- *Sandy material*: this partial fabric is present at the bottom and at the top of the facies. The microstructure of the partial fabric ranges from basic to intergrain micro-aggregates (fig.8-9). The porosity is composed of simple packing voids, vesicles, and few channels. The fine fraction ($c/f_{20\mu m}$) has a brownish to reddish color, a speckled and granostriated b-fabric, it presents opaque staining in it, and it is present both as aggregates and as free micromass (fig.10). The opaque material displays a reddish to orange color in OIL (fig.16). The related distribution pattern between the coarse and fine fraction is enaulic (equal to coarse) with areas presenting a gerufic one. The coarse fraction is composed by:
 - Aggregates, composed of fine fraction embedding quartz grains, around which the granostriated b-fabric is displayed (fig.11). They have heterogeneous shape that range from elongated to spherical.
 - Lithological elements: heterogeneous lithology presenting quartz grains, carbonate rocks, flint and unidentified elements. Their shape is sub-spherical, and they have heterogeneous sizes, ranging from fine to coarse sand.

Within this partial fabric a variability is present, related to the porosity and the c/f related distribution pattern. The lower fabric unit presents in fact a more compact aspect (the packing voids results to be smaller), and the micromass is only present under aggregates from.

- *Fine material*: only one fabric unit of this partial fabric is present, it is located between the two units of the previous partial fabric. The porosity results to be composed mostly of channels which cut through a matrix with a massive to vesicular microstructure (fig.12-13). The coarse fraction ($c/f_{20\mu m}$) results to be the same present in the previous partial fabric, but the related distribution pattern is close porphyric. The fine fraction displays a dark brown color with opaque stains, it has a crystallitic b-fabric (fig.12). Aggregates of cemented calcitic matrix (micrite showing calcitic crystallitic b-fabric) with have also been identified (fig.14).

For what concerns the biogenetic elements, a biospheroid has been identified in the contact between the two partial fabrics (fig.15).

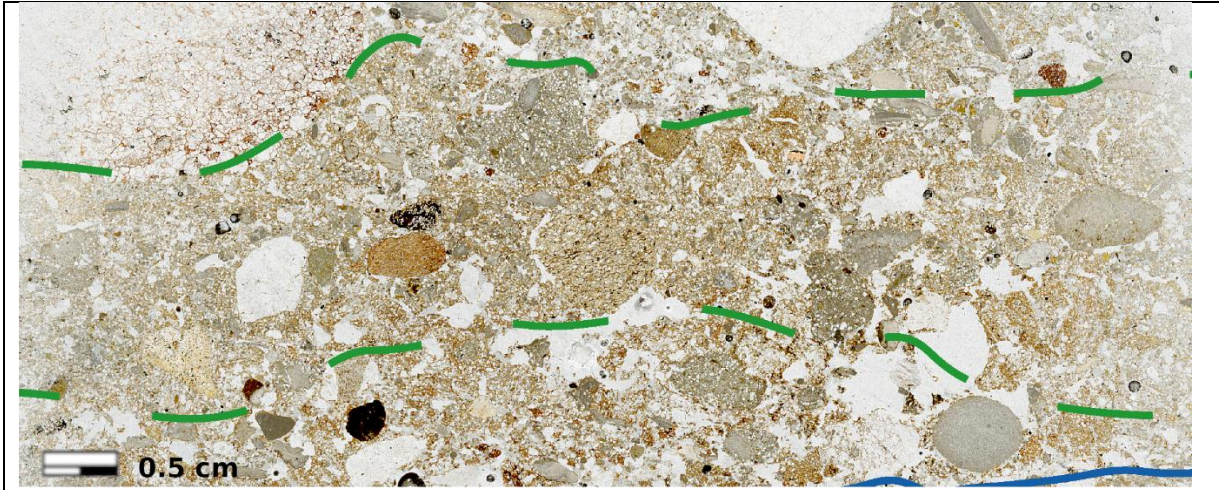


Fig.7: Banded fabric of facies d. The green dashed lines mark the contacts between the bands.

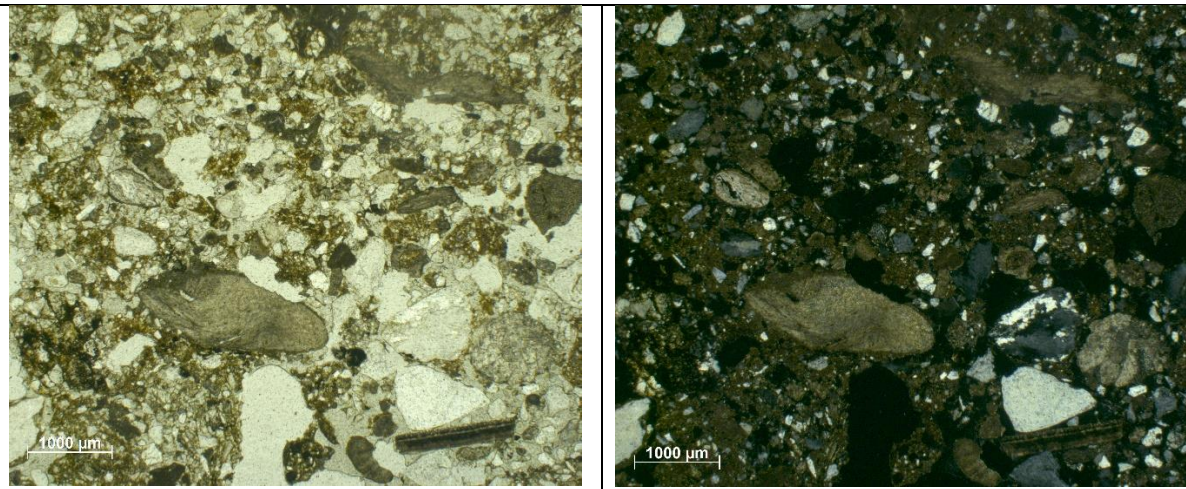


Fig.8: Intergrain micro-aggregates microstructure of the sandy material fabric unit

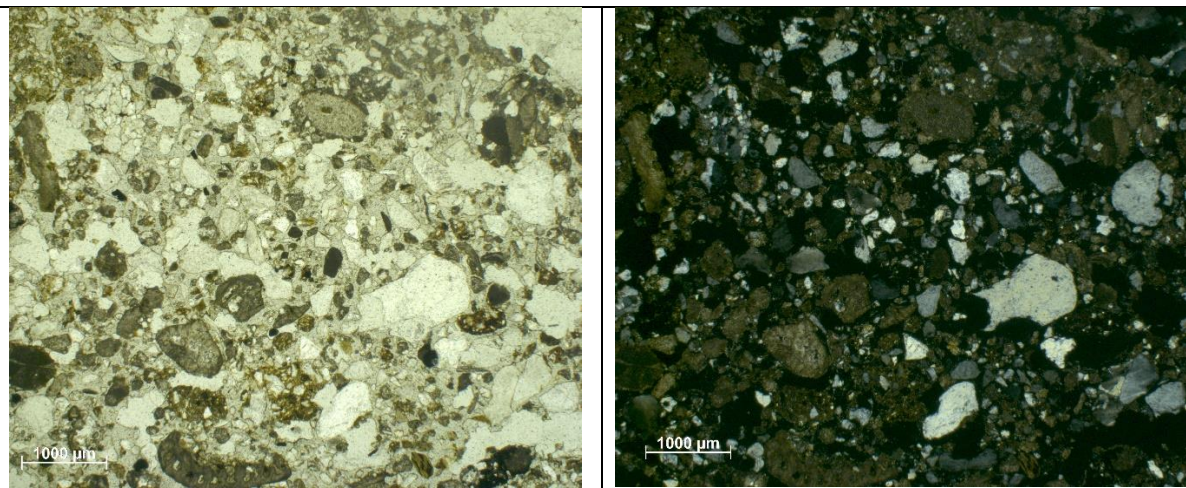


Fig.9: Basic microstructure of the sandy material fabric unit

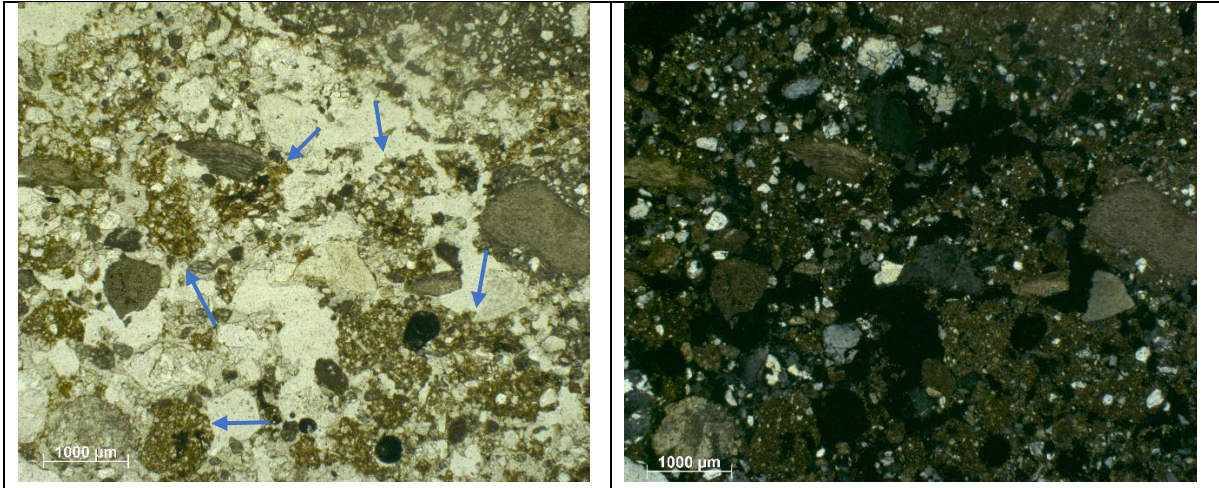


Fig.10: Sandy material partial fabric, aggregates of micromass (arrows). Note the opaque staining at the center of some of them

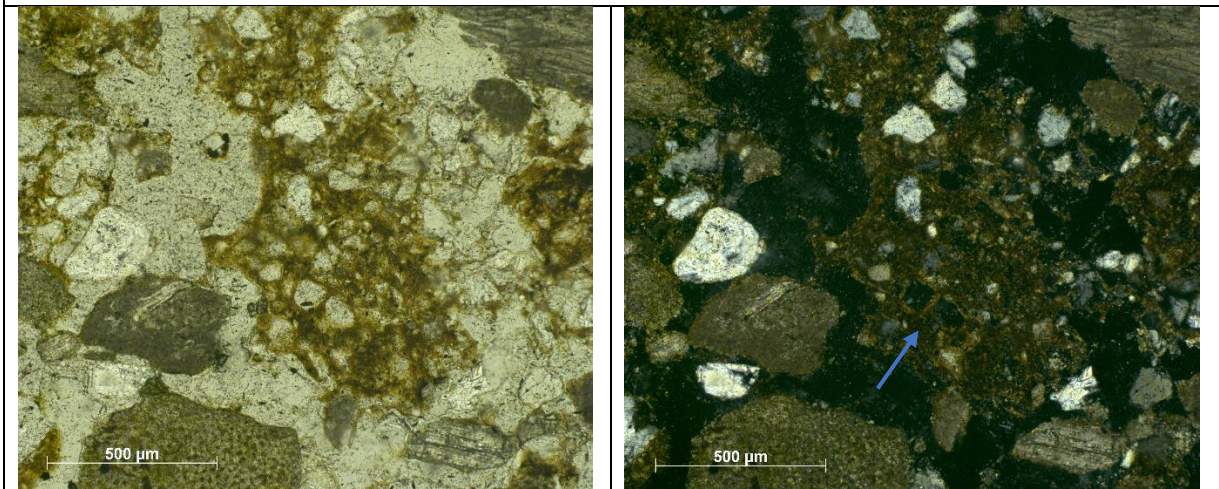


Fig.11: Sandy material partial fabric, aggregate of micromass embedding coarse elements. In XPL note the granostriated b-fabric around these last elements (arrow).

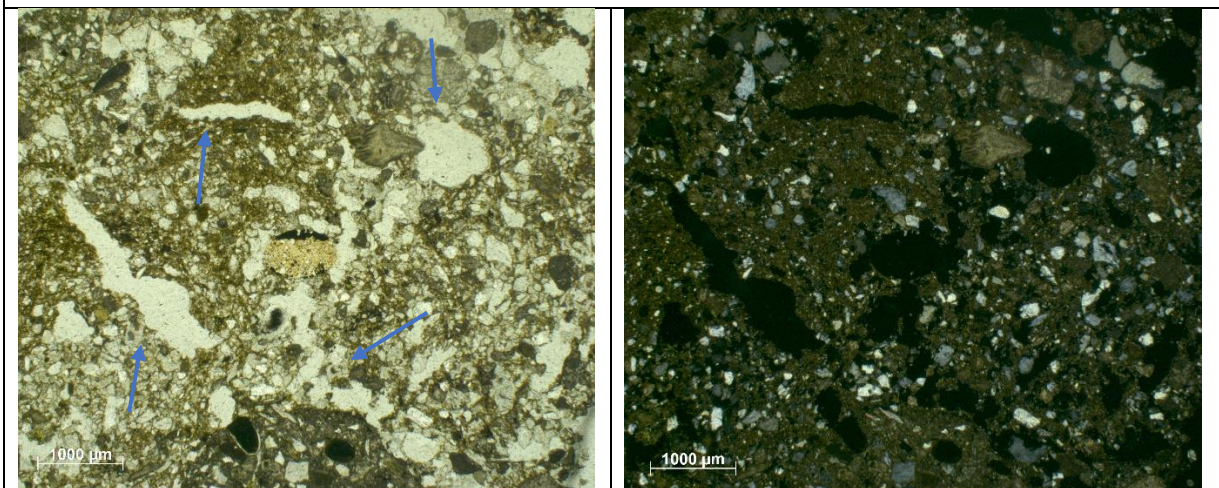


Fig.12: Fine material partial fabric, massive to vesicular microstructure and channels cutting through the matrix (arrows). Note the micromass at the top left part of the micrograph presenting opaque staining in it.

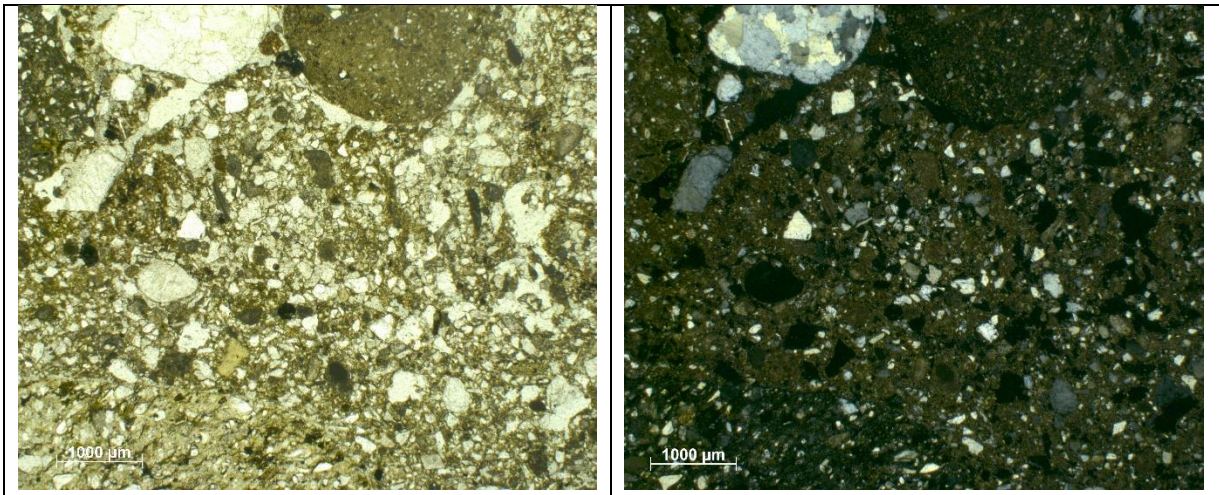


Fig.13: Fine material partial fabric, massive to vesicular microstructure.

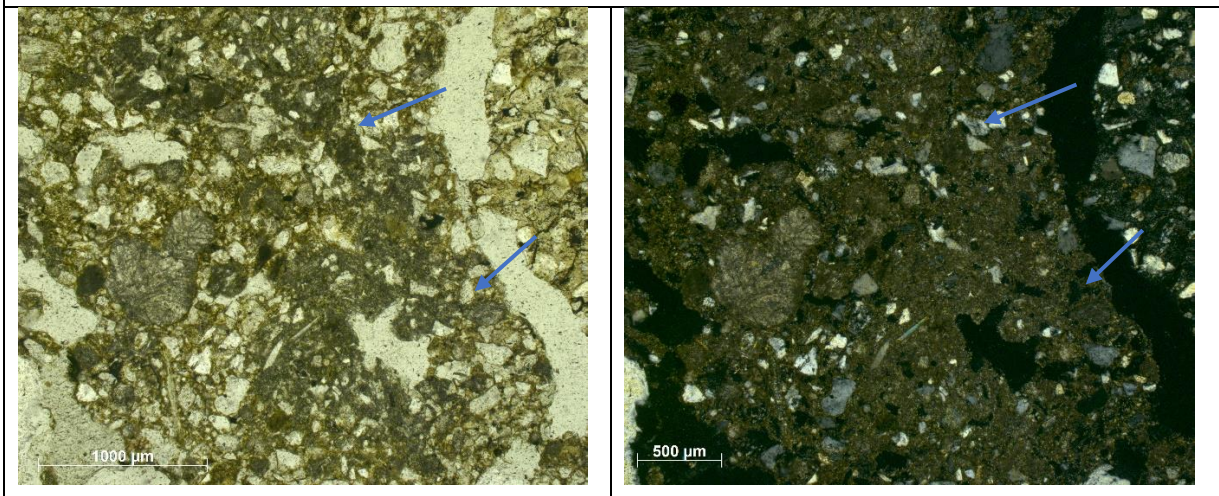


Fig.14: Fine material partial fabric, aggregates of cemented calcitic matrix (arrows).

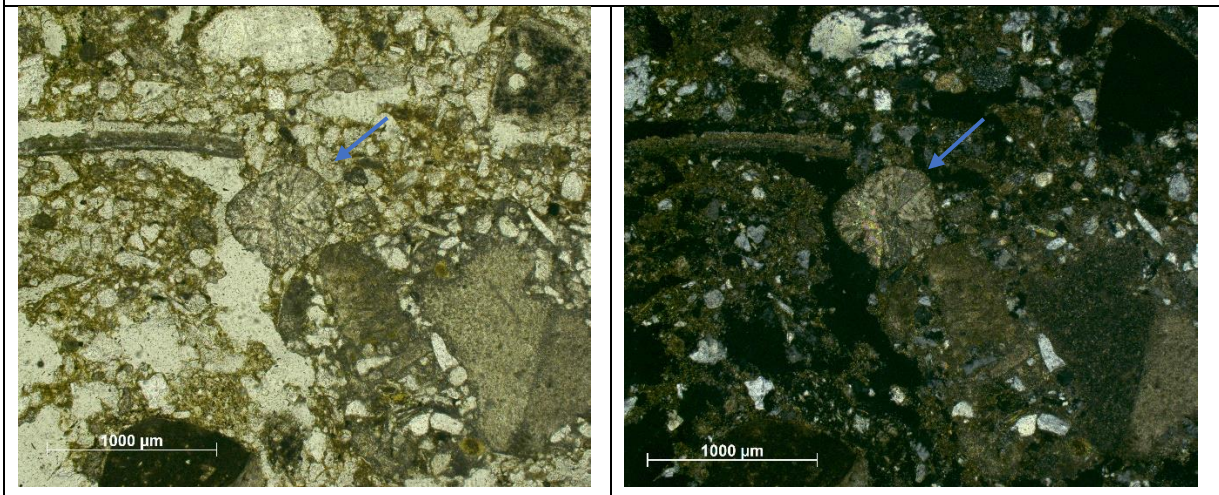


Fig.15: Biospheroid (arrow) produced by earthworms located in the contact between the two partial fabric

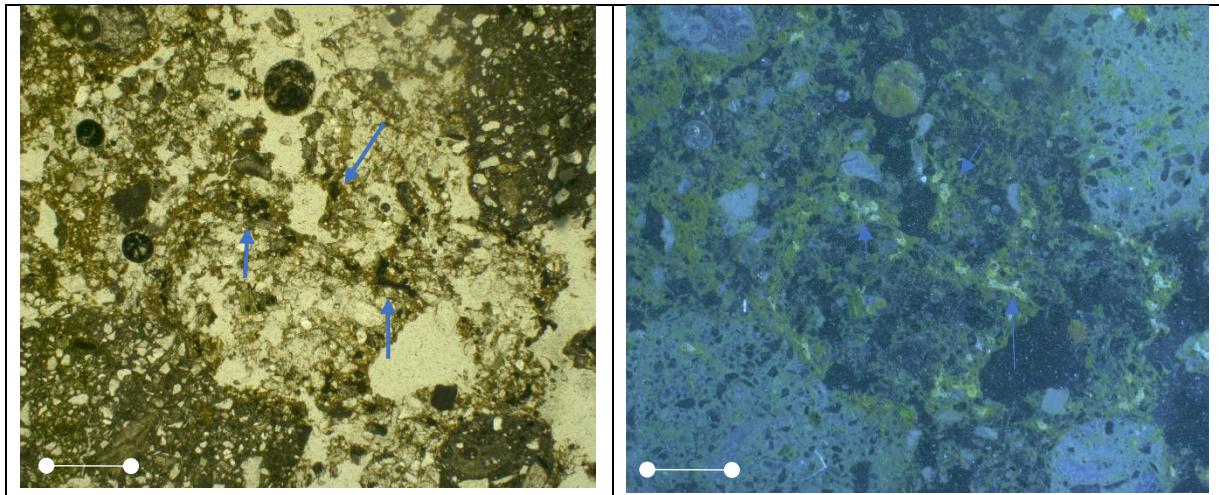


Fig.16: Opaque material (arrows), note the reddish to orange color in OIL. (Scale: 1000 μm).

c)

A channel and chamber microstructures are present in the facies (fig.17). The porosity is mostly composed of channels (with low degree of accommodation, fig.21), often interconnected with chambers, also vesicles are present. These poroids interrupts the continuity of a massive to spongy material (small vughs).

The coarse/fine related distribution pattern ($c/f_{20\mu\text{m}}$) ranges from close to single spaced porphyric. The fine fraction displays a brownish to yellowish color, its change in color sometimes shows a banded fabric (fig.18), aggregates of yellow micromass have also been identified (fig.19). The fine fraction has a fibrous aspect, given by irregular (curved) linear accumulations of micromass with a random distribution pattern (fig.20). Here too opaque material is present and it still displays a reddish to orange color in OIL (fig.26).

The coarse fraction has been divided into two different size classes:

- Elements $< 1000 \mu\text{m}$ (very fine to coarse sand): a low degree of sorting and a random size distribution of the elements are present. These elements are embedded in the micromass. Their lithology is quite homogeneous, quartz minerals result to be the most present, alongside with few carbonate rock fragments and very few micas grains. The general shape of the elements is sub-spherical and sub-rounded, exception made for the smaller quartz minerals, presenting an angular shape.
- Elements $> 1000 \mu\text{m}$: these elements display a high degree of heterogeneity in size, lithology, and shape. For what concerns the lithology no dominant types have identified, alongside with quartz, flint and carbonate rock fragments (also under dissolution) other

unidentified elements are present. On the other hand, for what concerns the size, even if it heterogenous from a general point of view, they present a banded fabric (more appreciable from a mesoscale point of view), the bands present a sub-horizontal distribution pattern. The space between these elements results to be composed of micromass embedding the coarse fraction $< 1000 \mu\text{m}$. To be noted the presence of a flint element (fig.17-25) displaying very angular shape and sharp boundaries, characteristics often pointing to a knapped lithic artifacts (Angelucci, 2017).

In both the size classes are also present biogenetic elements, notably bone and coprolite fragments (fig.22-24), the micromass around these elements displays a granostriated b-fabric, and the bones show a low interference color.

Elements with isotropic behavior in XPL have also been identified (fig.20) in both the size classes, they present a sub-spherical shape, and a pale-yellow color. They often embed in them quartz grains (very fine sand size, presenting in XPL a granostriated b-fabric on their surface). Their degree of roundness is very variable, but a trend has been observed: in general, the smallest these elements are the more round their surfaces are.

For what concerns the pedofeatures, cappings and channel's micromass coating have been identified (fig.23).



Fig.17: Microstructure of facies c. Note the channels (in blue) and the chambers (in red) interrupting the continuity of the material. Other visible elements are: coprolite fragment (in green), digested bone (in black) and the presumed knapped flint element (in purple).

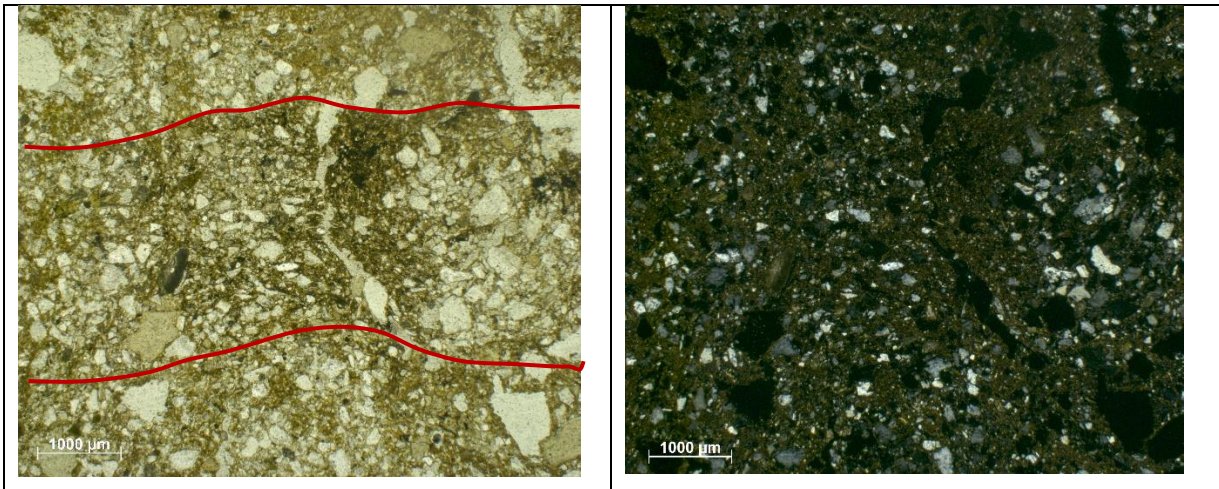


Fig.18: Micromass of facies c. Note the banded fabric related to the changes in its color: from top to bottom (separated by lines) we find clearer, darker and again clearer micromass. Note also the coarse fraction < 1000 µm embedded in the micromass.

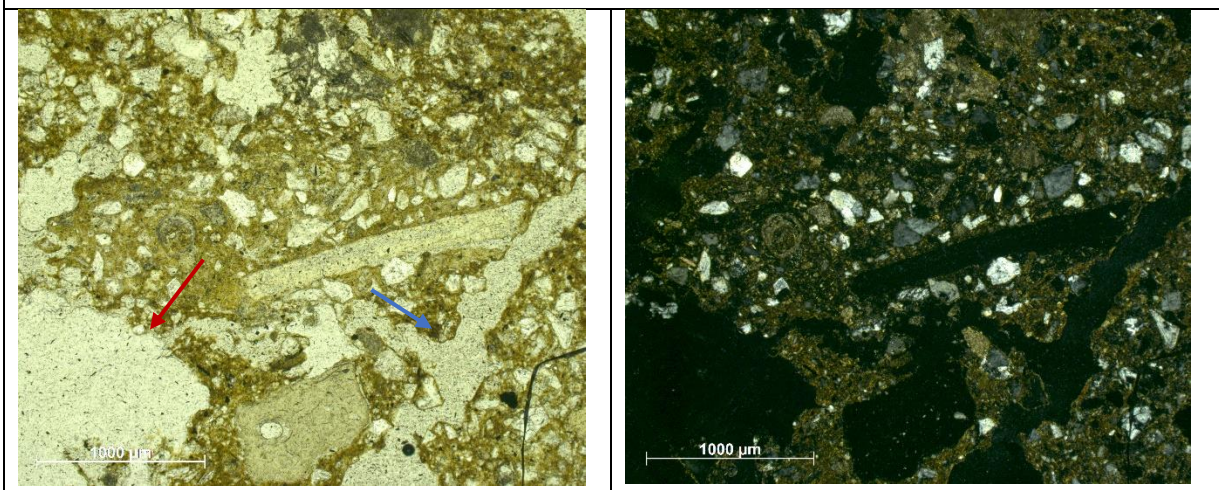


Fig.19: Aggregate of yellowish micromass. Note a channel on the right (blue arrow) and a chamber (red arrow) on the bottom-left of the micrographs.

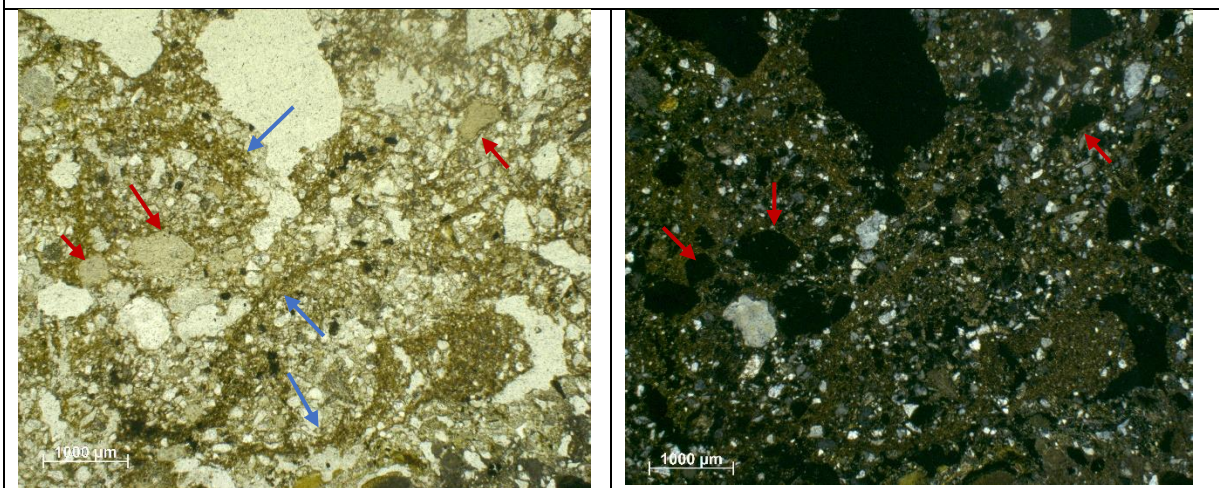


Fig.20: Fibrous aspect of the micromass given by the presence of by irregular (curved) linear accumulations of micromass with a random distribution pattern (blue arrows). The elements with isotropic behavior are also visible (red arrows).

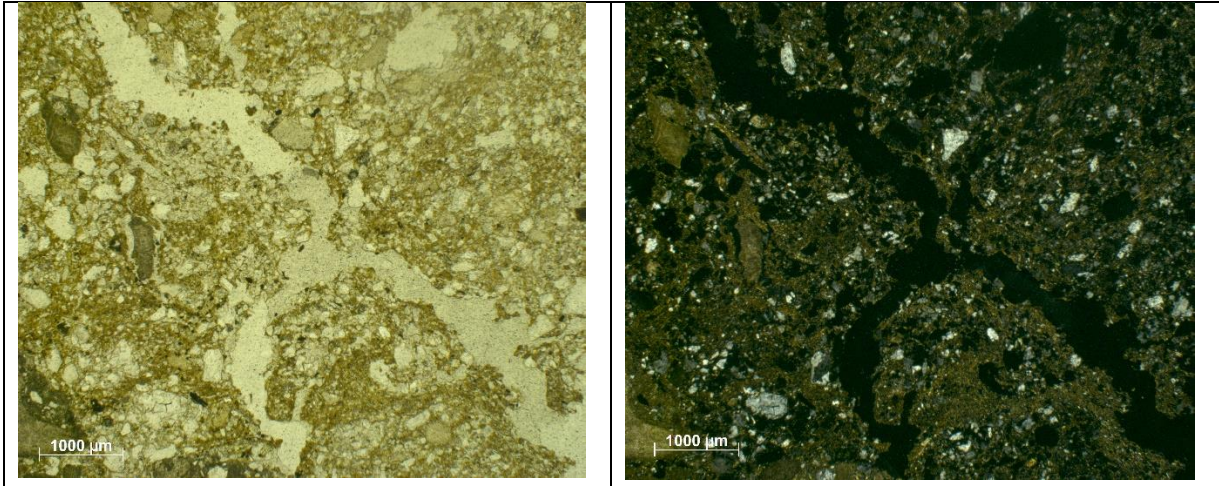


Fig.21: Channel microstructure with a low degree of accommodation.

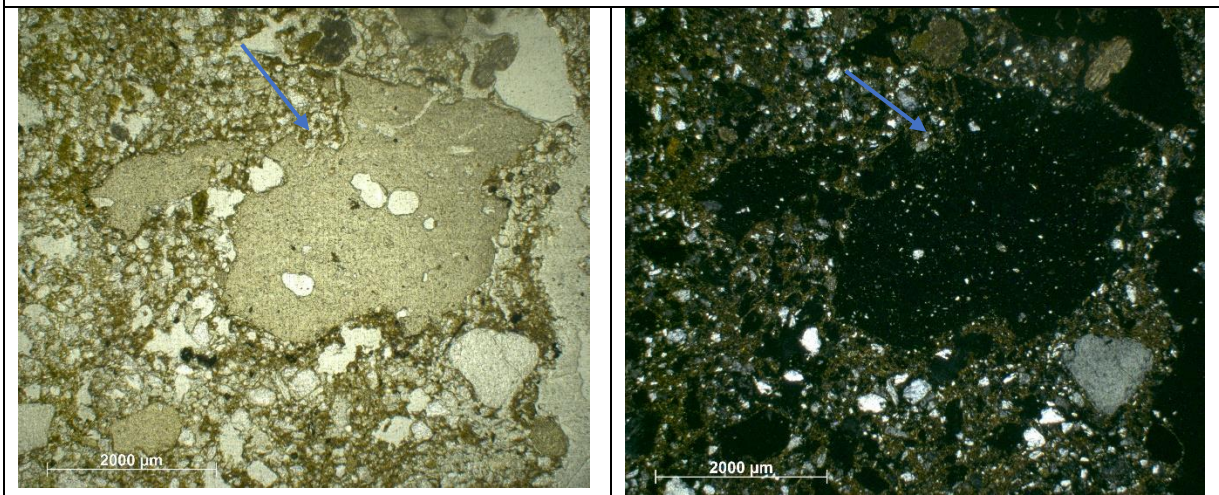


Fig.22: Coprolite fragment (arrow), identified for its characteristic inner porosity.

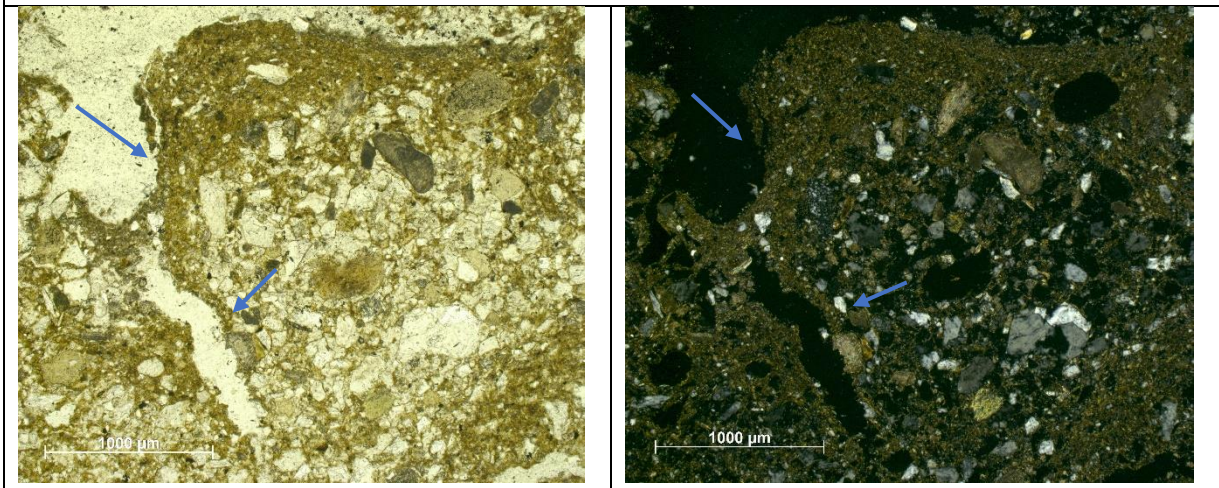


Fig.23: Link capping (upper arrow) and channel coating (lower arrow) of micromass.

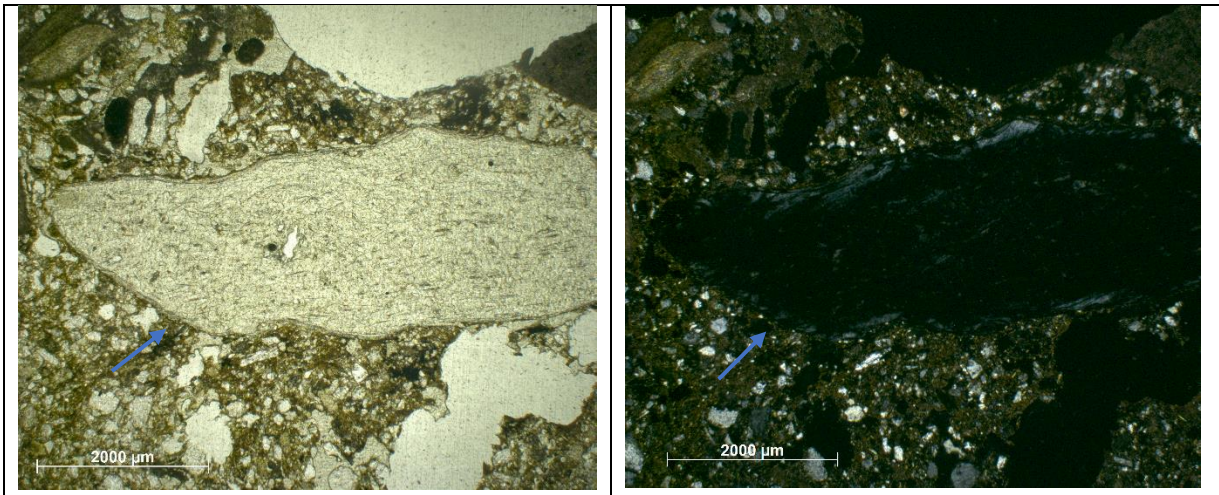


Fig.24: Bone fragment (arrow). Note the smooth surface, the low interference color and the poroid present in it. All these characteristics seem to point to a digestive process undergone by the bone.

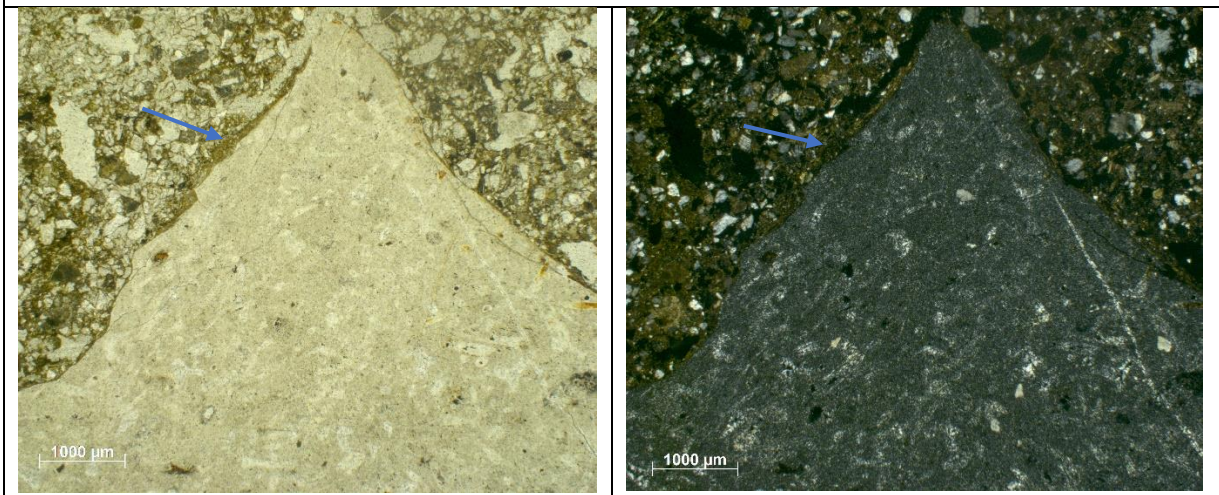


Fig.25: Flint element. Note the very angular shape and the sharp boundaries. A capping (arrow) of micromass is also present on its left side.

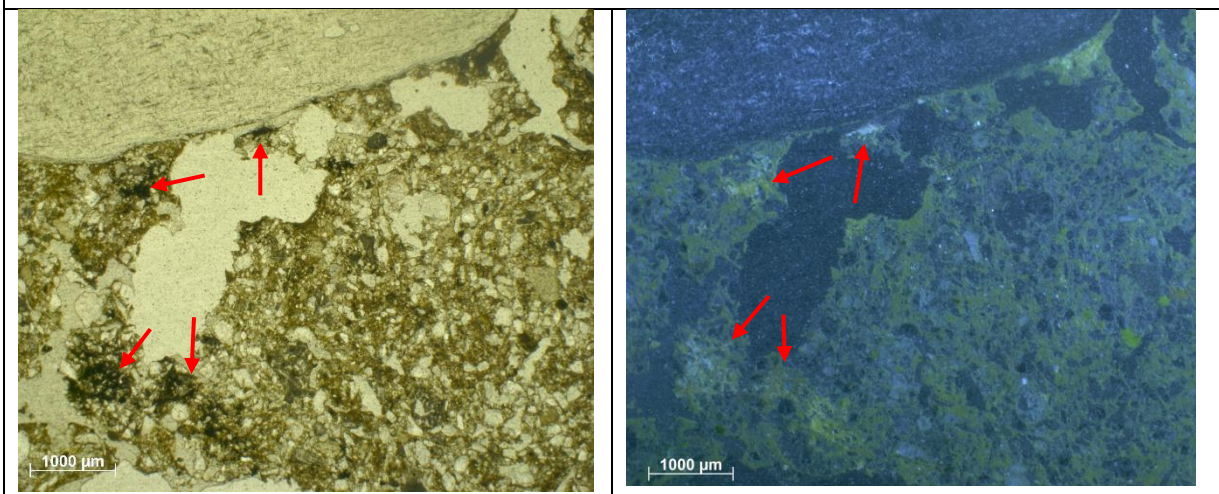


Fig.26: Opaque material (arrow), note the reddish to orange color in OIL.

b)

A spongy microstructure overlapped by bigger poroids is displayed in this facies (fig.27). The porosity is composed of small poroids present all over the groundmass and bigger poroids (few channels, vughs, and vesicles) with heterogenous shape and size. The coarse/fine related distribution pattern ($c/f_{20\mu m}$) range from gerufic to chitonic with sporadic areas displaying a porphyric one (fig.28). The micromass has a pale-yellow color, a limpid aspect and a crystallitic b-fabric, also a granostriated b-fabric is present (mostly present around the isotropic elements, fig.29). For what concerns the coarse elements we find a fraction with a size ranging between 50 and 300 μm , mostly composed of quartz grains and few elements of unidentified lithology (showing a high interference color). Beyond this fraction we also have carbonate rock fragments with heterogeneous size and shape and the same isotropic elements described in facies *c*, these last elements are present both as isolated elements with a clustered distribution pattern (fig.30). Aggregates of cemented calcitic matrix, displaying calcitic crystallitic b-fabric, have also been identified (fig.31).

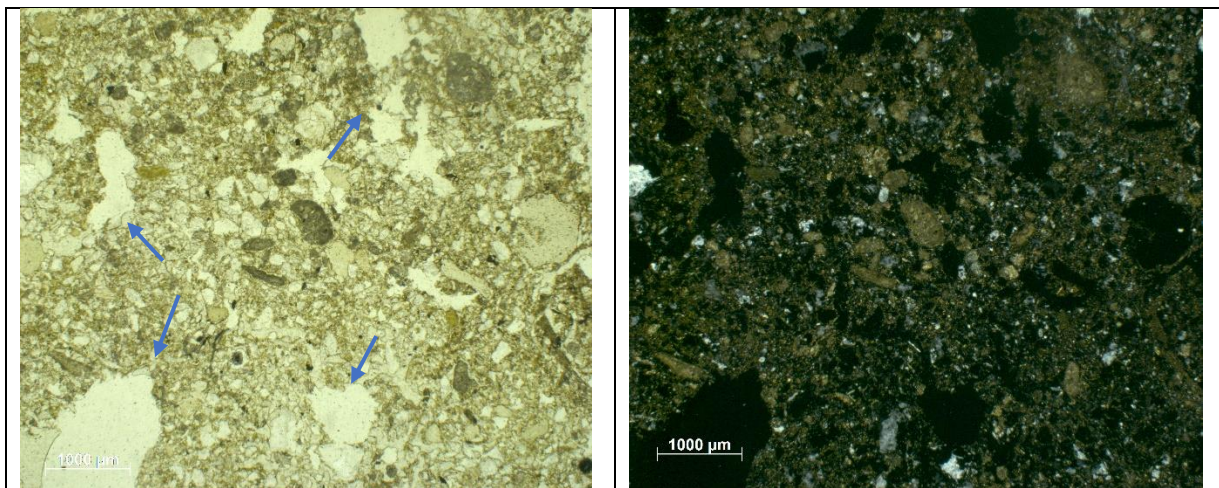


Fig.27: Spongy microstructure, note the bigger poroids (arrows) interrupting the continuity of the material.

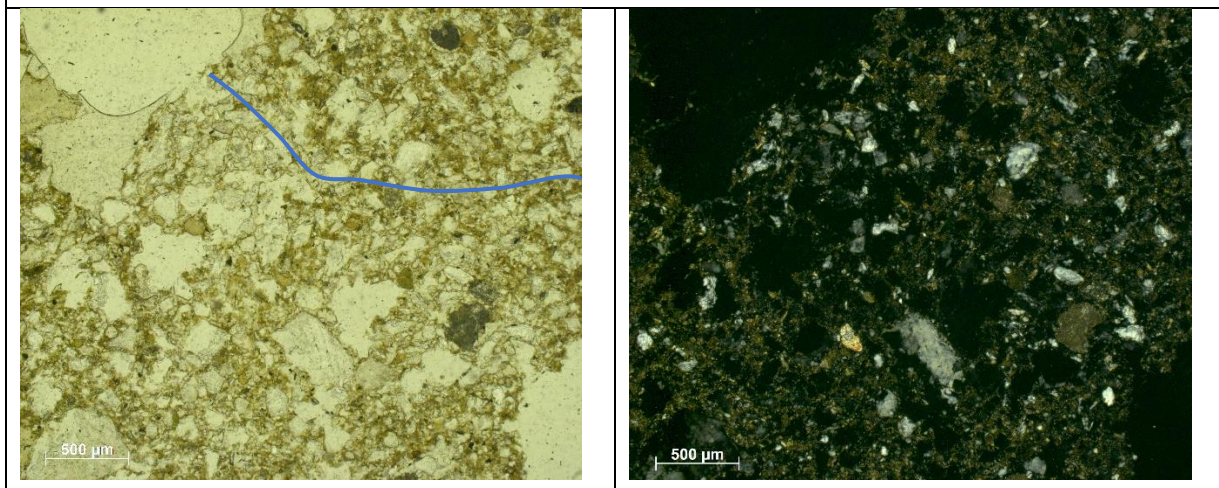


Fig.28: Gerufic (middle of the micrograph) to porphyric (up-right corner and lower part of the micrograph) r.d.p., separated by the line.

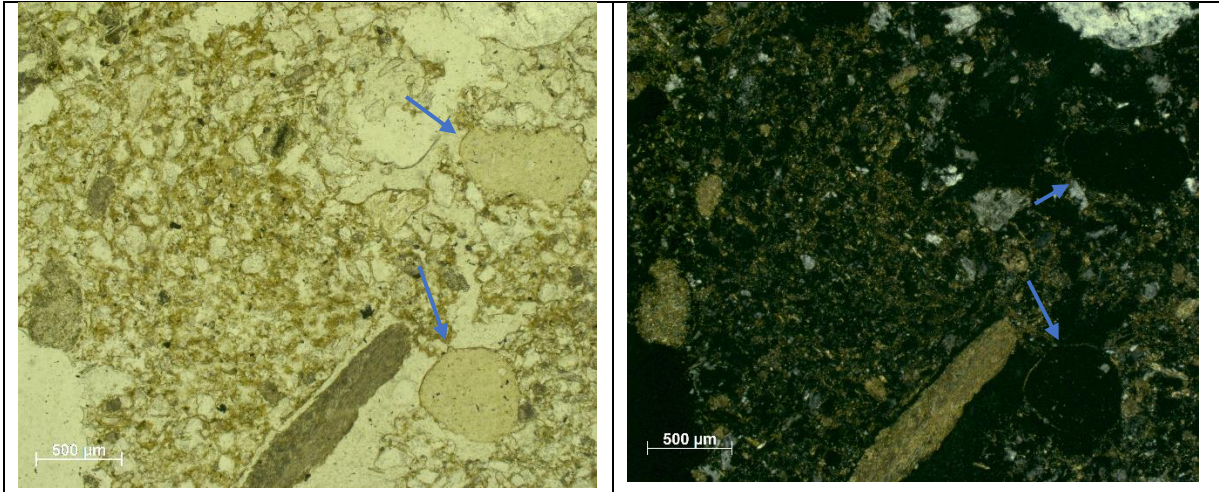


Fig.29: Isotropic elements with spherical shape (arrows). Note the granostriated b-fabric of the micromass around them.

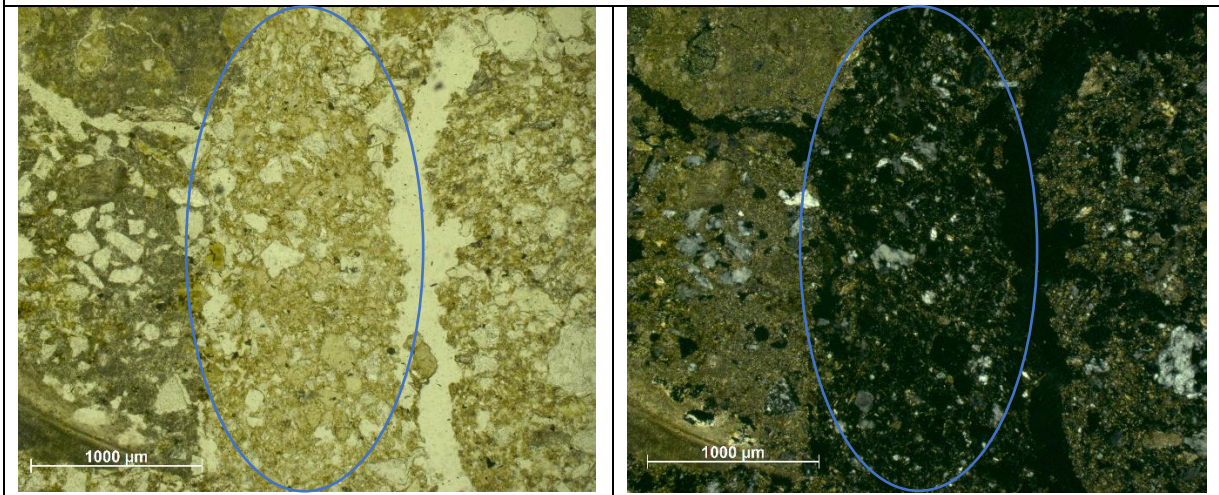


Fig.30: Group of isotropic elements (ellipse) and channel on its right side.

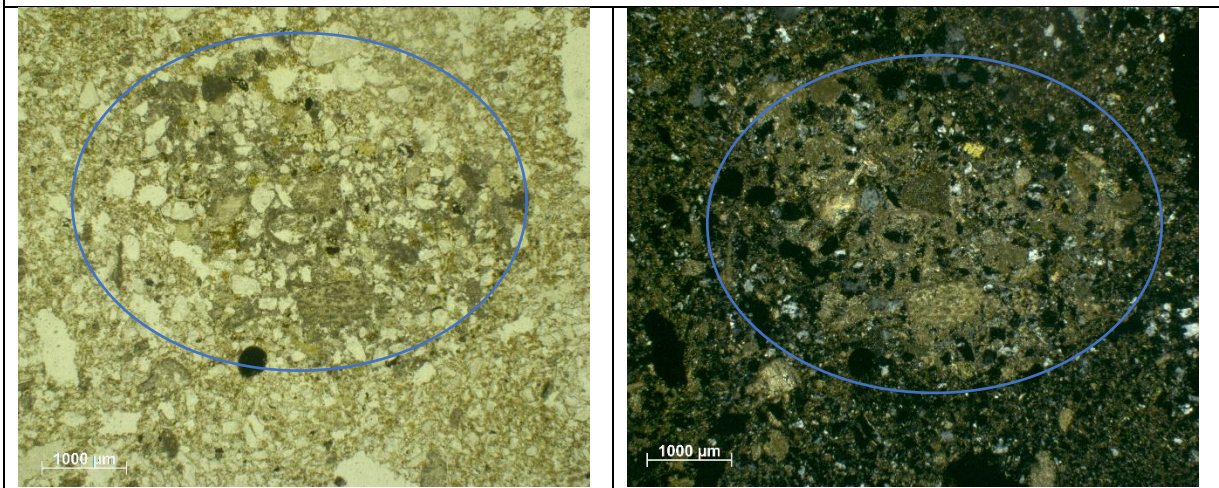


Fig.31: Aggregate of cemented calcitic matrix (ellipse). Note the calcitic crystallitic b-fabric of the matrix.

a)

A vesicular microstructure is displayed in this facies (fig.32). The porosity is mostly composed of vesicles and planes with a sub-vertical orientation pattern (fig.33); few channels are also present. The coarse/fine related distribution pattern ($c/f_{20\mu m}$) results to be close porphyric. The micromass has a dark brown color with dots and stains of opaque material (fig.34). Also in this case the opaque material displays a reddish to orange color in OIL. It usually embeds micas elements and few quartz grains (very fine sand) and present a crystallitic and sporadic granostriated b-fabric. As for the coarse fraction, it has been divided into three different types:

- Isotropic elements, presenting the same characteristics of the ones described in *c*, but here their presence is notably higher (fig.32).
- Quartz grains ranging from 100 to 400 μm (fine to medium sand size).
- Coarse sand size elements: presenting a sub-spherical shape, a well-rounded surface, and a heterogeneous lithology (including quartz, flint and elements with unidentified lithology).

Two bone fragments, with low interference color, have also been identified (fig.35).

To be noted that the lower part of the facies is too thin to be observed, however a change in the constituents between its upper and lower part is slightly visible, which may be pointing to a banded fabric.

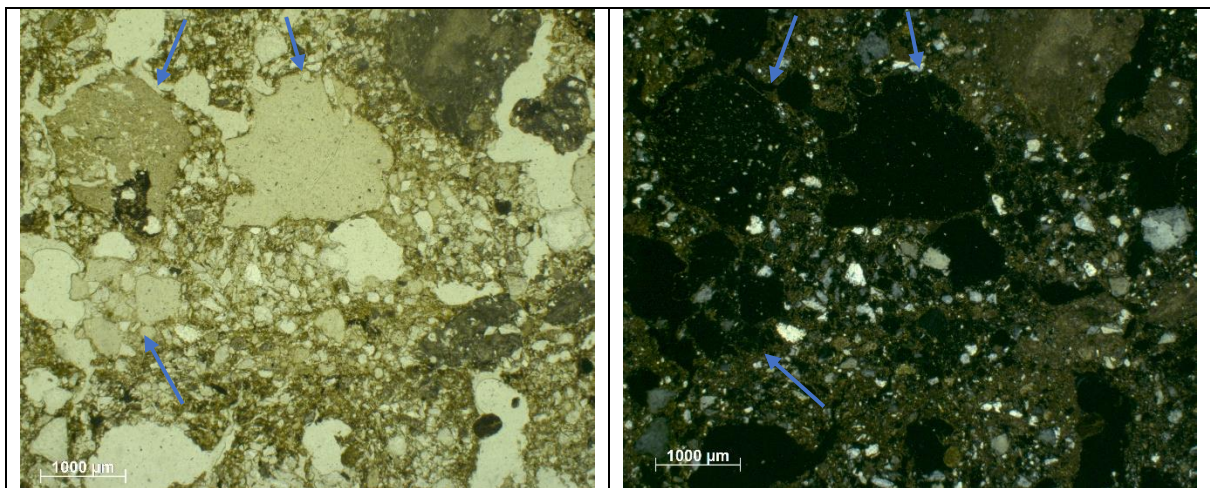


Fig.32: Vesicular microstructure and isotropic elements (arrows).

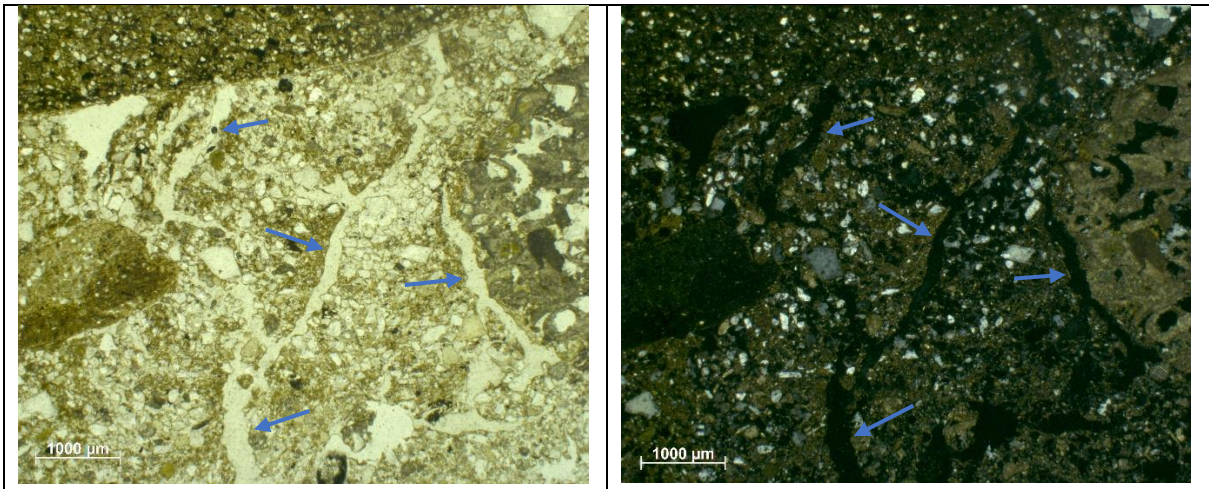


Fig.33: Sub-vertical planes (arrows) cutting through the material.

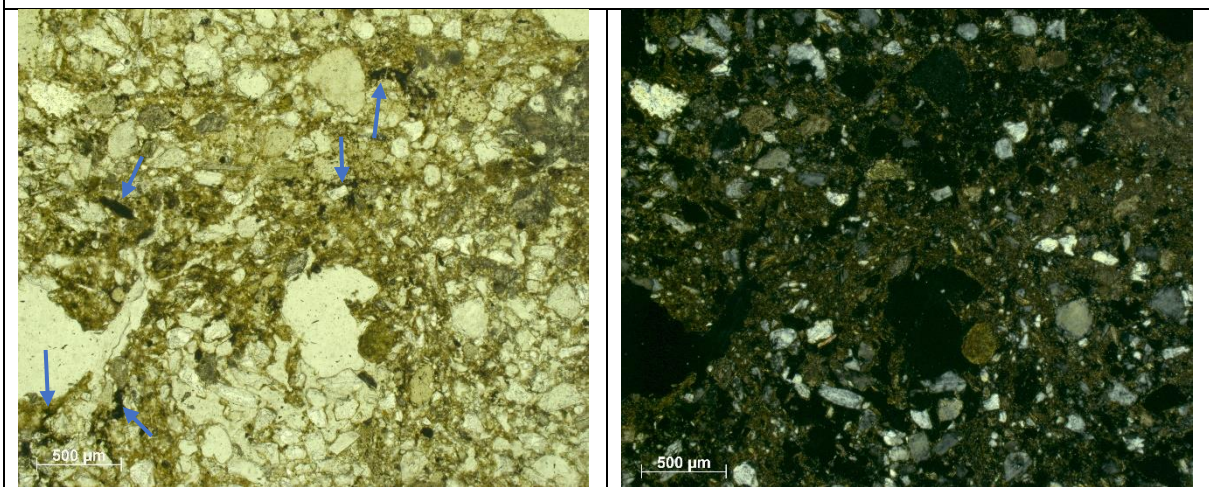


Fig.34: Opaque staining in the micromass (arrows). The mica grains embedded in it are also visible.

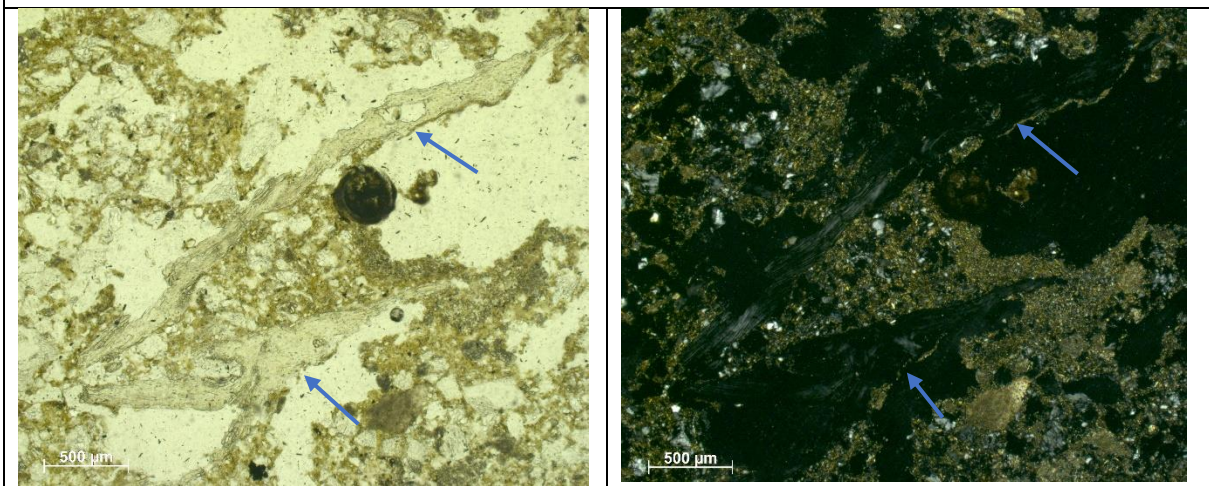


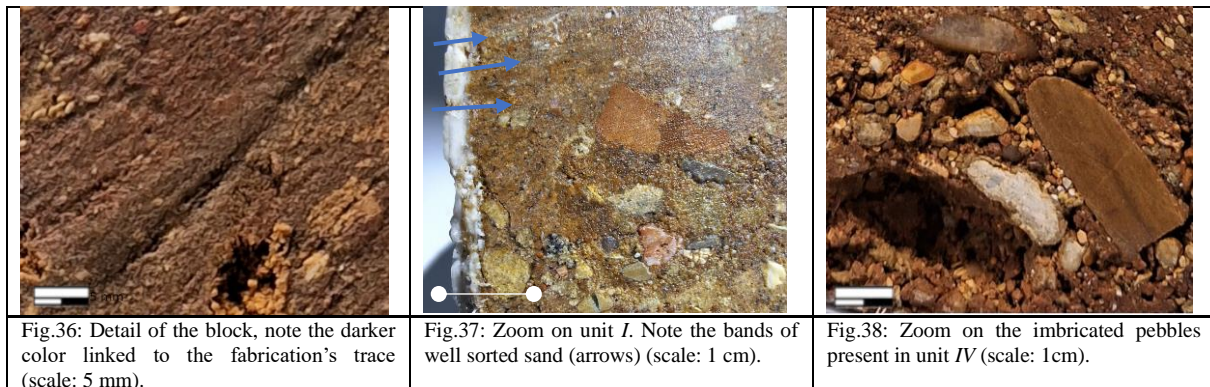
Fig.35: Bone fragments (arrows) with low interference color.

MM2

Stratigraphic description of the block

Block MM2 has heavy traces left by the fabrication of the section, partially obscuring the features on it, making it difficult to observe. The north direction is marked only on the block. The surface of the block presents some issue, which may be linked to the resin which doesn't seem to be well solidified, and so creating false color on its surface; notably is clearly visible that on the traces of fabrication a darker color is displayed (fig.36). For the stratigraphical observations the block has been divided into four units, from top to bottom we find (fig.39):

- I. A banded fabric is slightly visible in this unit, which results to be composed by an alternation of well sorted sand bands and bands of sand embedded in fine material (fig.37).
- II. Unit which has been isolated from the others mostly due to the high presence of fabrication marks, also here a banded fabric is slightly visible (more appreciable with the use of a lens) but the fabrication marks are too heavy to give a better observation.
- III. Unit composed of rounded gravel elements (pebbles) embedded in a fine material matrix displaying a dark brown color. No laminations have been identified.
- IV. Unit composed of fine material matrix displaying the same characteristics of unit III and incorporating small lenses of well sorted sand and coarser elements (coarse sand / fine gravel).
- V. The lowermost unit present in the block results to be composed of rounded gravel and sand; few fine materials is present between the coarser elements. To be noted the characteristic *imbricated* structure displayed by the bigger pebbles at the bottom of the block (fig.38-39), this structure is a clast fabric in which pebbles and particles with tabular shape “tilt in the same direction”, pointing to fluvial or debris-flows deposits (Major, 1998).



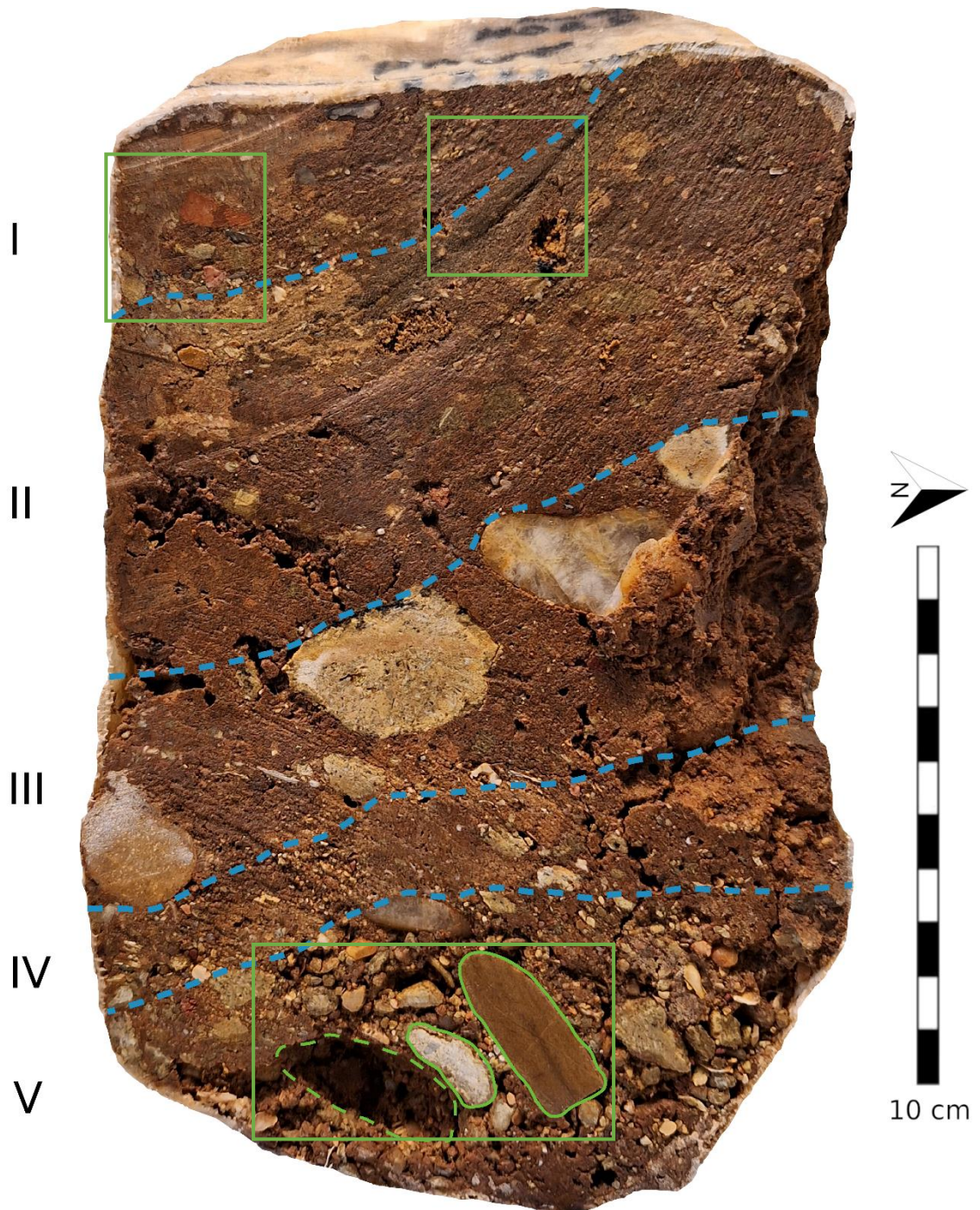


Fig.39: MM2 block. The blue dashed lines indicate the contact between the identified units. In green are marked the imbricated clasts, the dashed one indicates a clast which is missing, probably due to fabrication issues. The green rectangles indicate the areas from which the previous pictures were taken.

Mesoscopic description of the thin section

Unfortunately, the north is not marked on the thin section. From a mesoscale point of view the thin section has been divided into five different facies. From top to bottom we find (fig.40):

e) The facies present a banded fabric composed by three different bands which progressively (from bottom to top) present coarser.

d) Quite homogenous facies presenting a porosity change between its left and right sides (higher on the left). Its mesoscale aspect is very similar to facies *b*, but it present coarse elements as the ones present in *e*.

c) Particular facies with a lenticular shape. It results to be very compact and presents sharp boundaries.

b) Very homogenous at this scale of observation. Doesn't present any bands and it results to be mainly composed of fine fraction, only few coarse elements are present. Traces of bioturbation from mesofauna activity are visible at this scale of observation (*bow-like feature*, fig.59), (Kooistra and Pulleman, 2010). The porosity results to be composed of channels and one big mammillate void (fig.58). The color of the facies is not homogenous throughout all the facies, changing from pale yellow to brownish (going upwards). The sides of the facies result to be too thin to be observed.

a) From a mesoscale point of view the facies results to be characterized by a banded fabric composed of the alternation of bands of fine and coarse material (always in the size range of sand, with few fine gravel elements).

Based on these observations, we can assume the relationships between the section and the block. In particular, facies *e* of the section should be approximately relative to unit *I* of the block. Facies *d*, *c* and *b* should therefore be representative of unit *II* and *III*, to be noted that the differences between these units could be not visible at the scale of the section, since (from a macroscale point of view) the difference between the units results to be mainly related to the presence/absence of big pebbles, which may not have been included by the section cut (also note the reduced width of the observable facies due to the reduced thickness present at its sides). The lowermost facies of the section (*a*) should than be related to unit *IV*. To be noted that this hypothesis is uncertain and difficult to confirm.

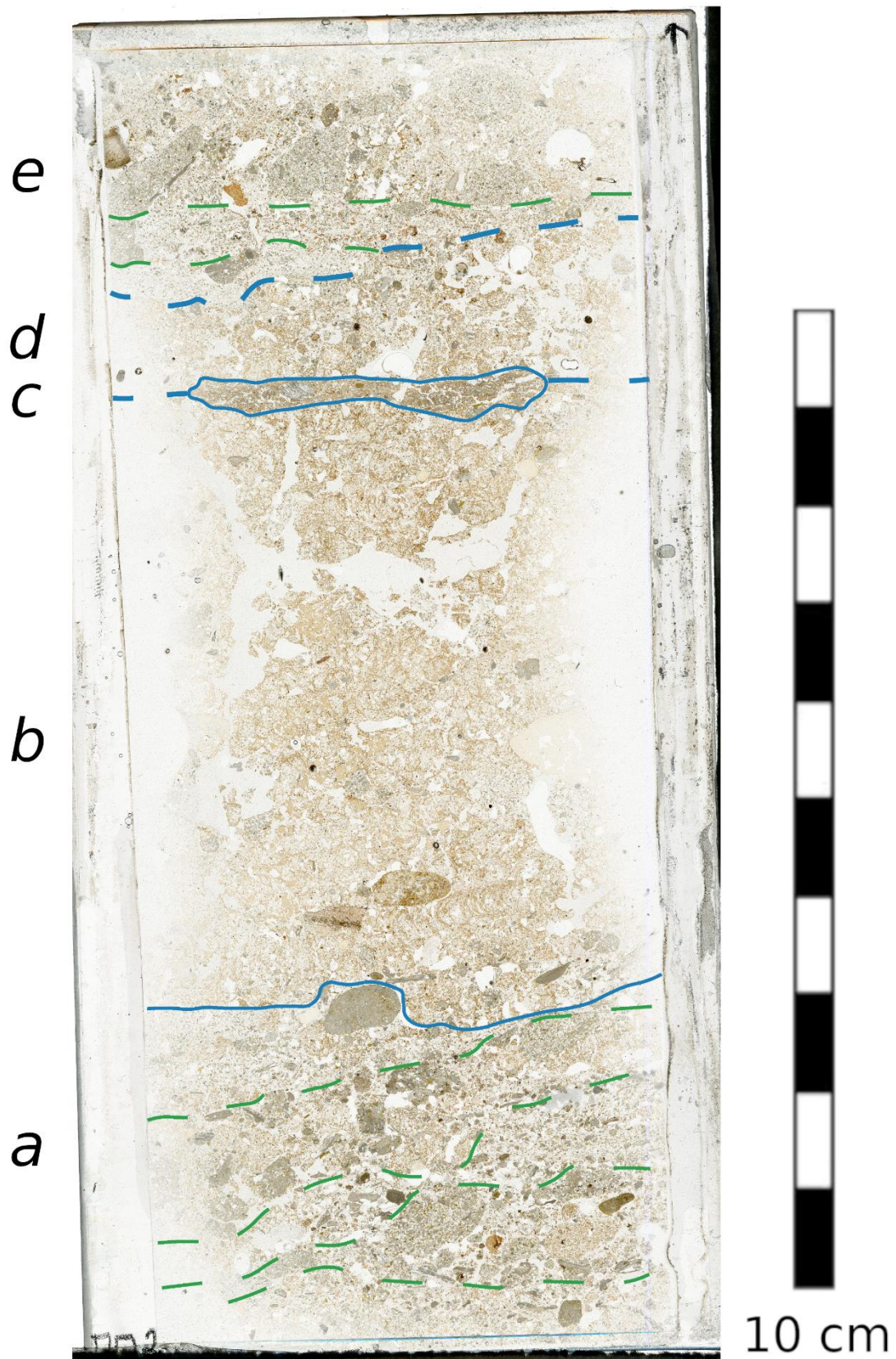


Fig.40: MM2 section's scan. The blue lines indicate the contact between the identified facies, the straight ones indicate abrupt contacts while the dashed a comfortable one. The green dashed lines indicate the bands identified in the facies displaying a banded fabric. Note the irregular shapes of facies *a*'s bands.

Microscopic description of facies

e)

In order to describe the banded fabric that characterizes this facies three partial fabric (each bands) have been described individually and named after their most representative size class, The coarse/fine limit is set at 20 μ m. From bottom to top we find:

- *Fine sand's band*: the band present a lenticular shape (in fig.40 note the lowest band in facies e). No micromass is present, giving the unit a basic microstructure. The porosity is composed of simple packing voids and one horizontal planar void, separating elements with different size (fig.41). The solid phase that constitutes the facies is mainly composed of quartz grains (fine sand size) and some carbonate rocks, which are well rounded and often sub-spherical.
- *Medium sand's band*: an intergrain microstructure is present in the facies. The porosity (beyond simple packing voids) is composed of channels, often presenting micromass typic coating on their walls (fig.43). The solid phase of the unit is composed of aggregates and single grains, therefore, giving rise to an equal to coarse enaulic related distribution pattern (fig.42). These aggregates are composed of reddish micromass with a speckled b-fabric, they embed small micas and quartz grains and often have a sub-spherical shape (fig.44), their size range from fine to medium sand. The coarse fraction is composed of quartz grains and few carbonate rock fragments, their sizes mainly fall into medium sand's size.
- *Very coarse sand's band*: uppermost unit of the facies. It results to be mostly composed of coarse elements (very few micromass is present, often under aggregate from, as for the previous unit). It displays a channel to vughy microstructure, these poroids often presents micromass coatings on their walls (fig.45). The coarser elements that characterize the unit are carbonate rocks fragments and aggregates of cemented calcitic matrix (micrite showing calcitic crystallitic b-fabric) falling into the size class of coarse sand (fig.46). The space present between these elements results to be filled by grains of quartz and carbonate of medium sand size (with the same characteristic presented in the previous unit).

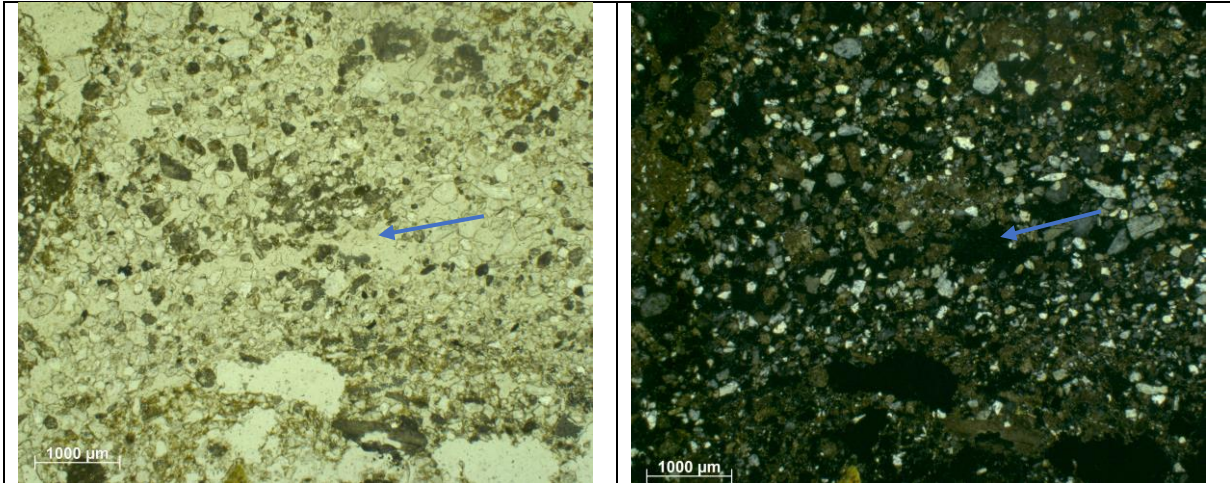


Fig.41: Micrograph of the *fine sand's band*, the blue arrow marks the planar void, note how the elements are coarser above it compared to those below it.

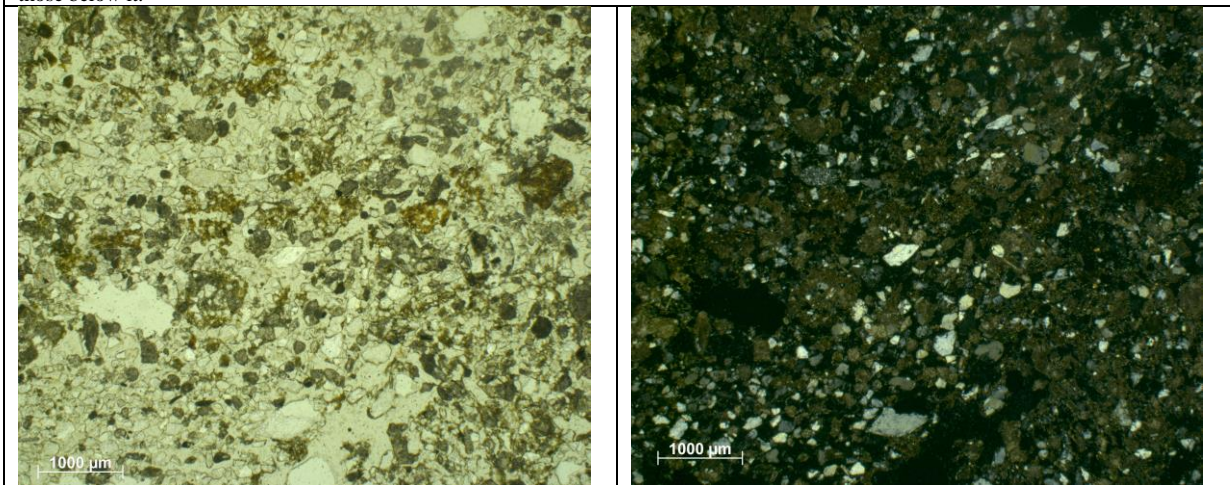


Fig.42: Enaulic related distribution pattern.

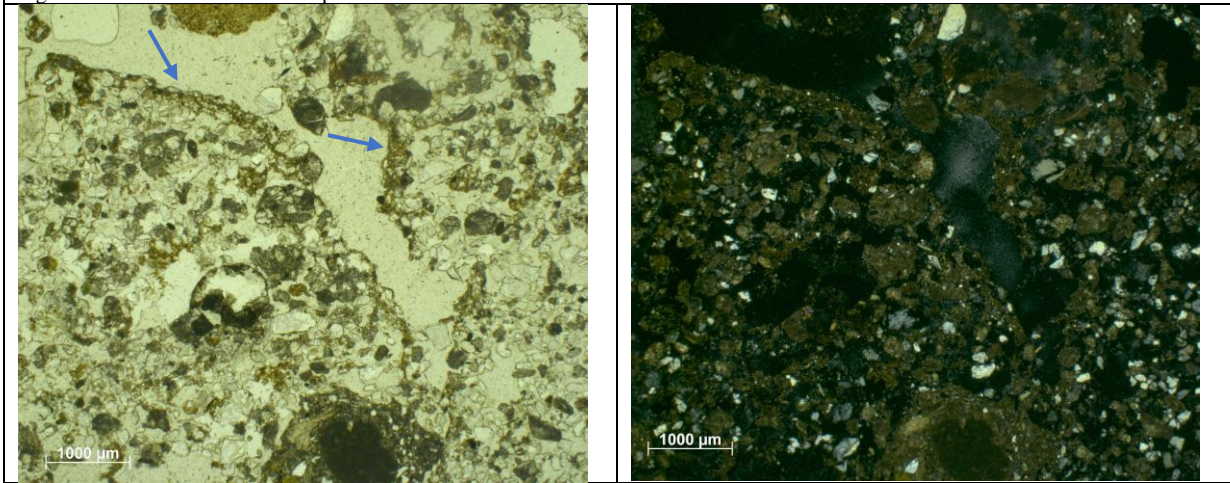


Fig.43: Micrograph of a channel, note the micromass typic coating present on its walls (arrows).

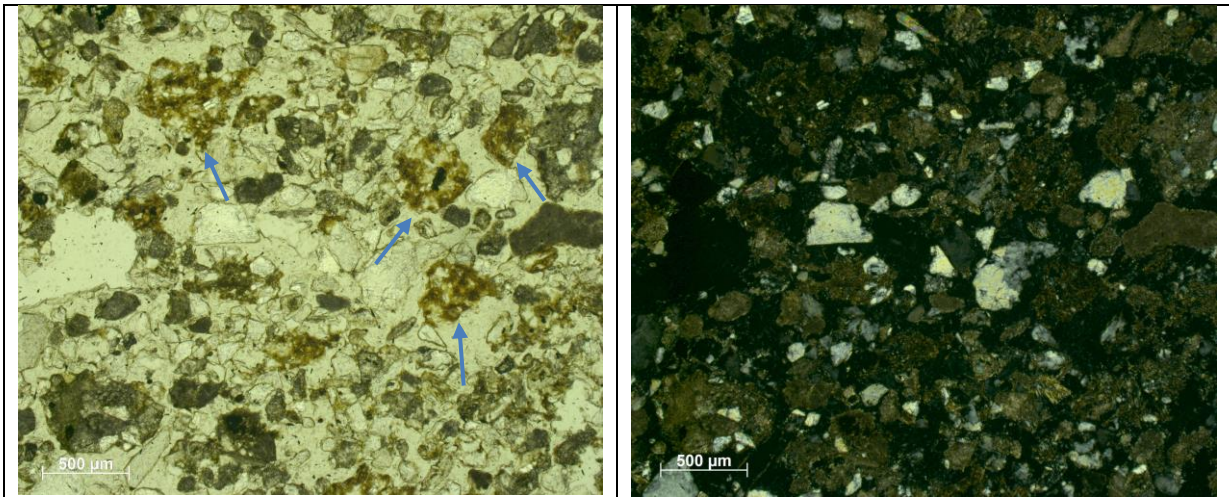


Fig.44: Micrograph of the reddish aggregates (arrows), note their rounded and sub-spherical shapes.

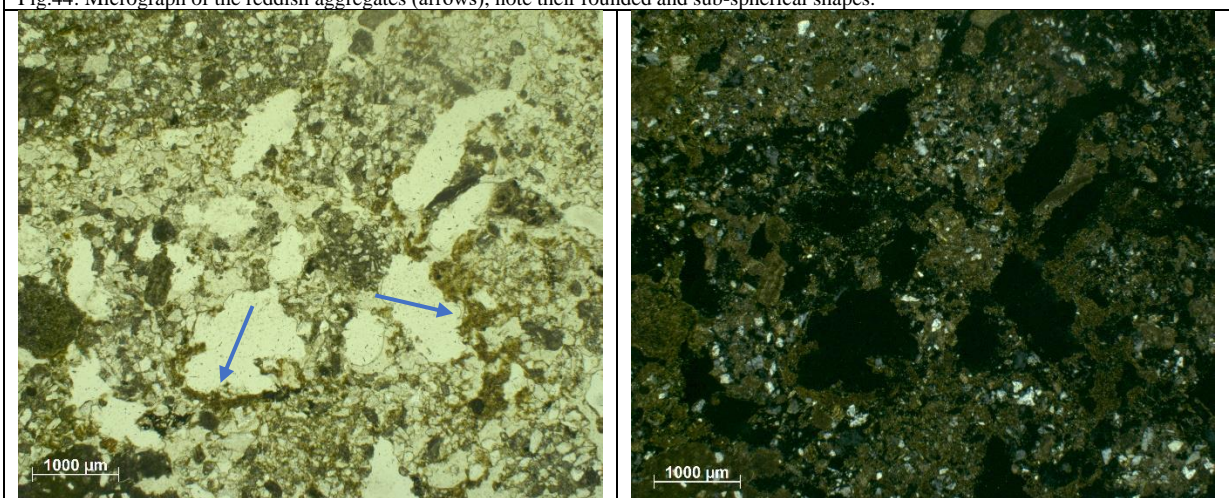


Fig.45: Channel microstructure, note the micromass coatings present on their walls (arrows).

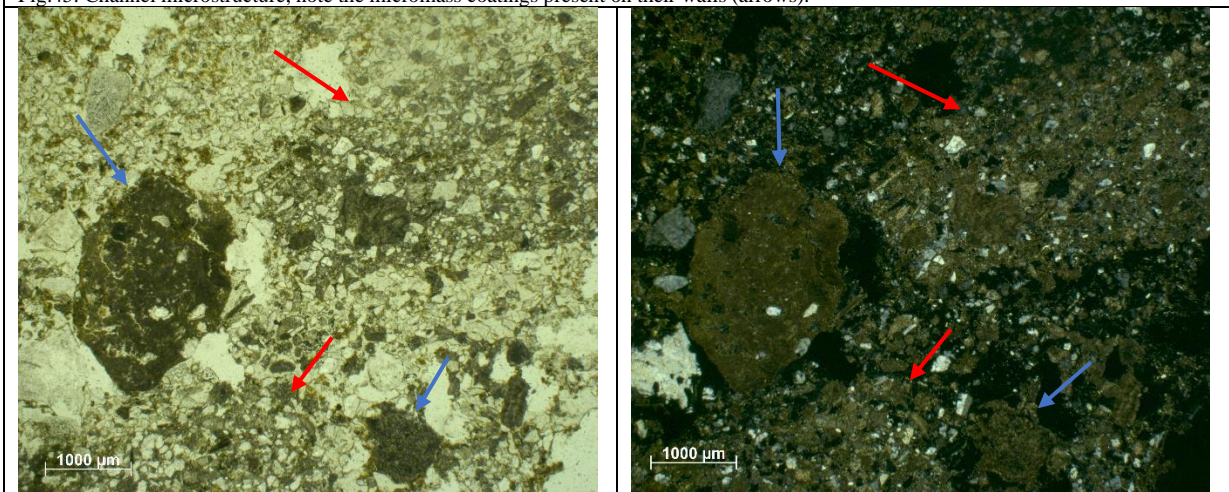


Fig.46: Carbonate rocks fragments (blue arrows) and aggregates of cemented calcitic matrix (red arrows).

d)

The microstructure of the facies range from channel to vughy, the porosity results to higher on the left side of the facies (in fig.40 compare the left and right side of facies *d*), sometimes the channels present typic coatings composed by micromass with a porostriated b-fabric (fig.47). The related distribution pattern ($c/f_{20\mu m}$) results to be basic (sandy material) with few areas presenting a porphyric to gerufic one (fig.47). The micromass shows a brownish to dark brown color and presents opaque staining in it with a random distribution pattern, it has a fibrous aspect given by the linear aggregation of the micromass with a random orientation and distribution pattern (fig.48); the b-fabric is speckled. The opaque material displays a reddish to orange color in OIL (fig.51). The coarse fraction presents a high degree of heterogeneity, both in size and lithology, while the shapes of the elements is almost always sub-spherical, only few elements have a tabular shape. It is composed of quartz grains (fine to medium sand and few coarse sand size), aggregates of cemented calcitic matrix (micrite) (fig.49), and carbonates rock fragments. These last elements present a high degree of size heterogeneity ranging from fine to very coarse sand size; a pattern in the shape of these elements has been identified, in general the smaller the elements are, the more spherical shape they have. Alongside with these elements, phosphatic grains (fig.47-50) and micas grains (fine sand size) have also been identified, the latter are mostly present embedded in the micromass (fig.48).

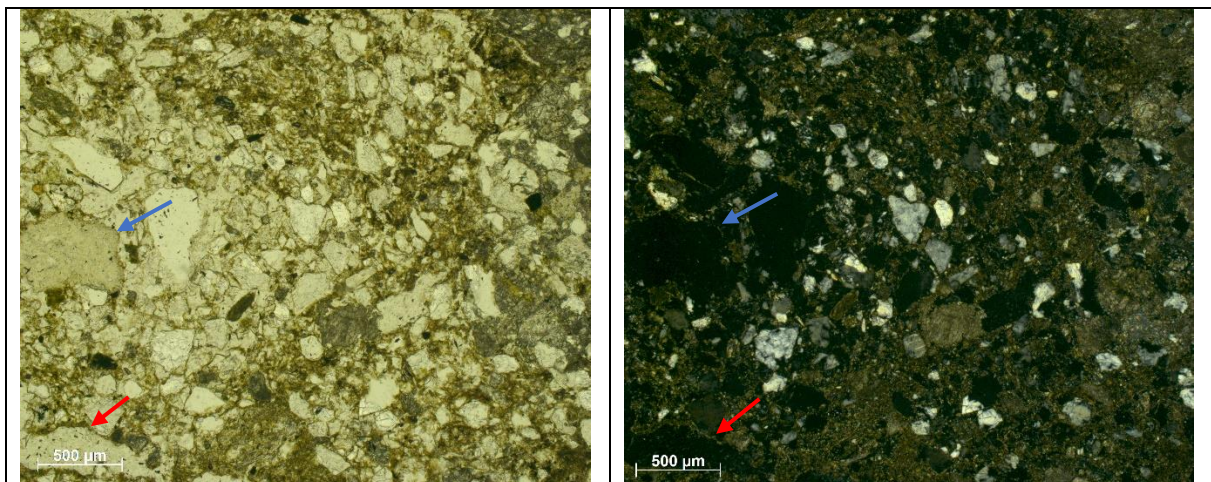


Fig.47: Porphyric to gerufic related distribution pattern. A channel micromass coating is visible at the bottom right part of the micrograph (red arrow). Also note the presence of a phosphatic grain (blue arrow).

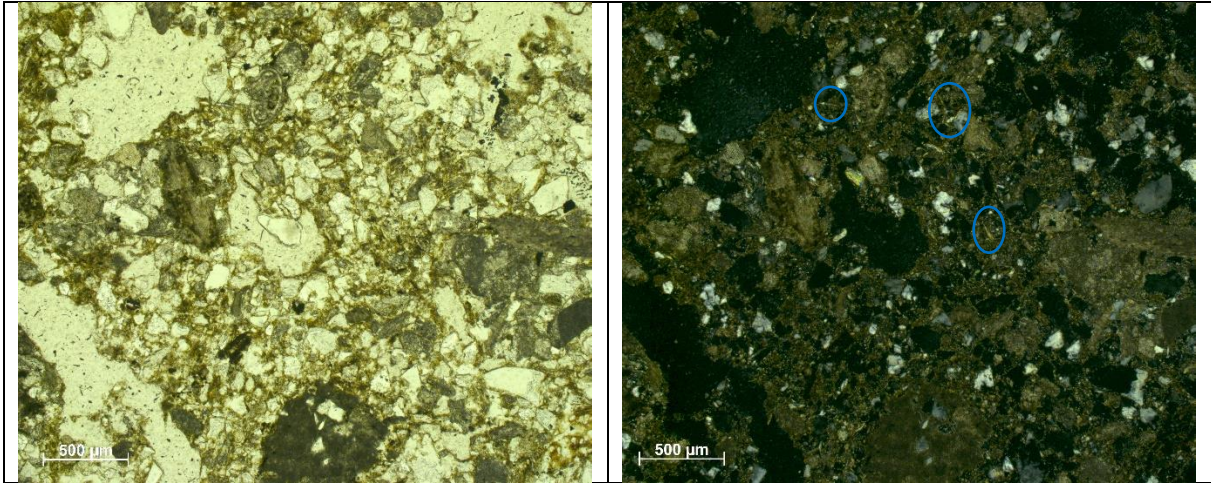


Fig.48: Fibrous aspect of the micromass, note the linear accumulation of the latter displaying a random distribution and orientation pattern. Few micas grains are also visible (blue circles in XPL).

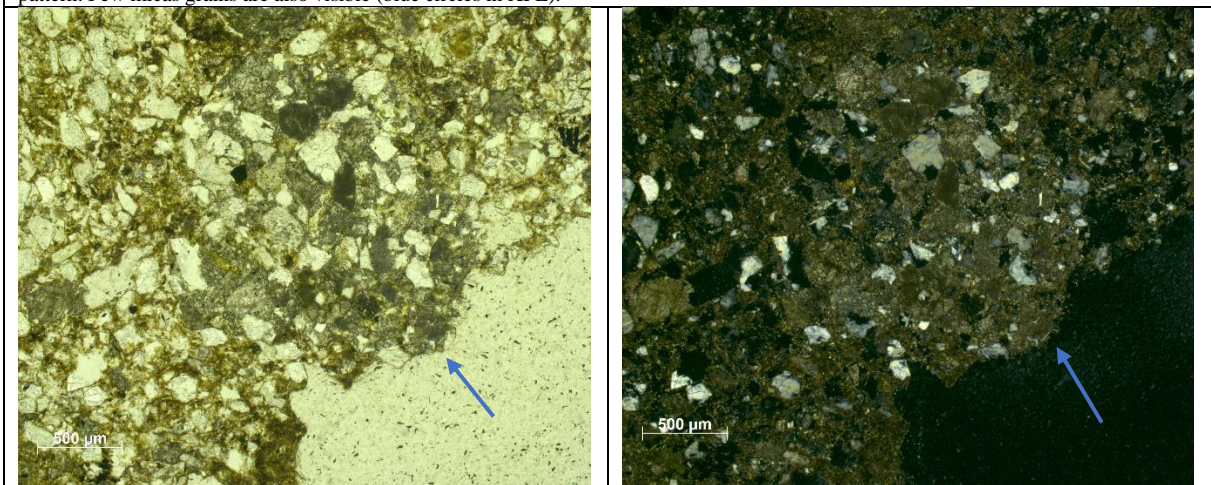


Fig.49: Aggregates of cemented calcitic matrix (arrows). Note the characteristic calcitic crystallitic b-fabric in XPL.

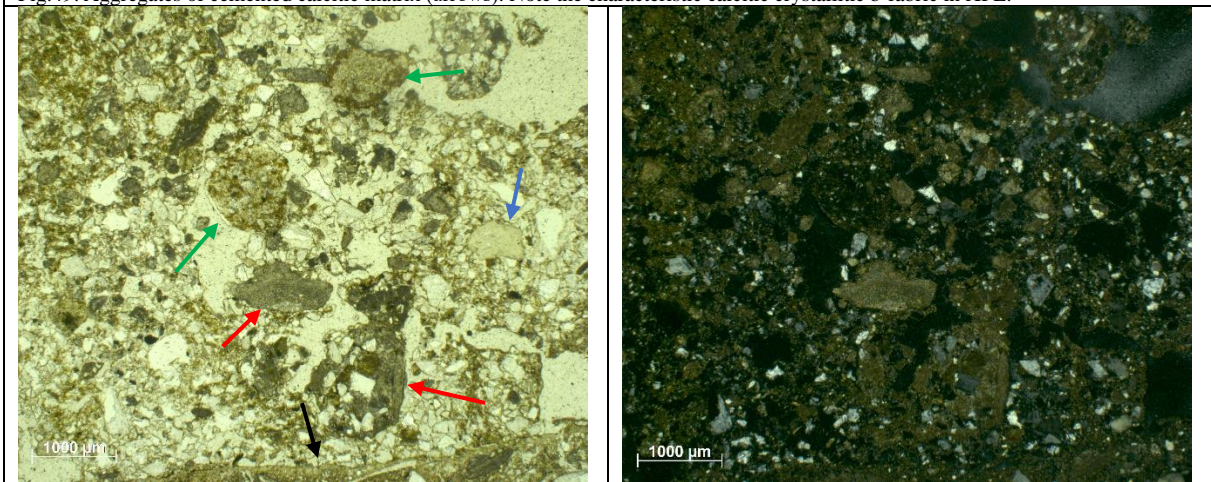


Fig.50: Coarse fraction of the facies, note the high degree of heterogeneity. Note a phosphatic grain (blue), carbonate rocks (red) and unidentified lithologies (green). At the bottom part note the sharp contact with facies c (black arrow).

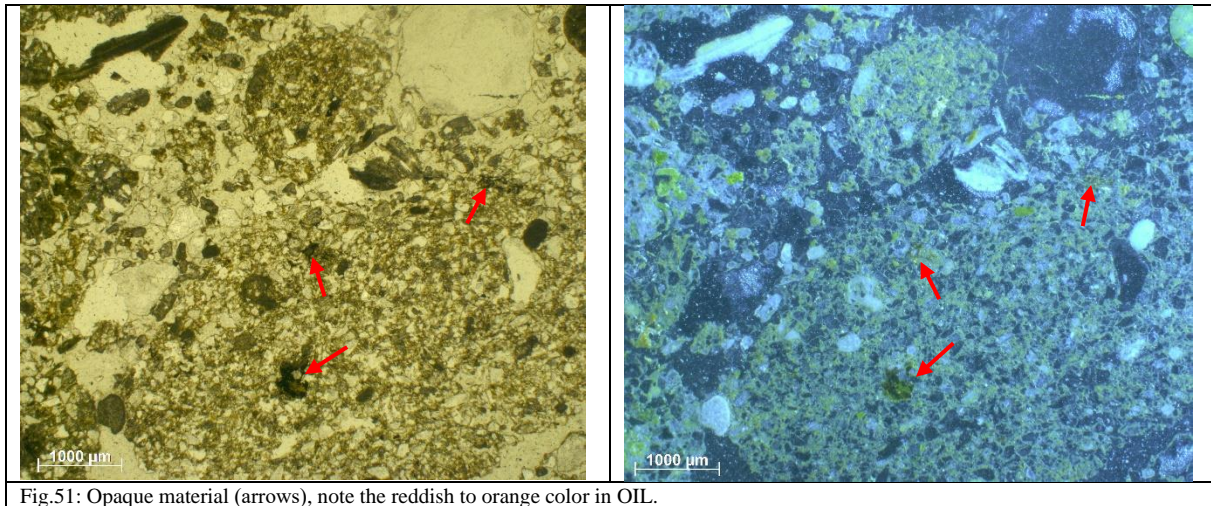


Fig.51: Opaque material (arrows), note the reddish to orange color in OIL.

c)

Facies with a lenticular shape (fig.52), as said in the mesoscale description it presents very sharp boundaries with the other facies (fig.50). It displays a high degree of heterogeneity in its aspect. It results to be composed of a yellowish rim present all along its surface. The thickness of the rim changes in the facies and follows the lenticular shape of the letter. Inside the rim we find a grayish calcitic matrix with a calcitic crystallitic b-fabric (fig.53-54), at the edges of the facies this calcitic matrix is absent and the facies results to be composed only by the rim's material (fig.55). The calcitic matrix often embeds quartz grains of fine to very fine sand with a porphyric to chitonic related distribution pattern (fig.54). Inside this calcitic matrix areas of yellowish matrix are also present (with the same aspect of the rim's one, fig.56). The porosity of the facies is also very heterogenous, it is mostly composed of vughs and planar voids (some of which are in continuity with the upper facies (fig.52). To be noted the presence of a calcitic structure presenting a fabric and a porosity very similar to a vegetal structure (notably wood). This feature could be seen as a wood fragment which underwent a complete combustion, leaving in place ash which still keeps the wood structure aspect (fig.57).

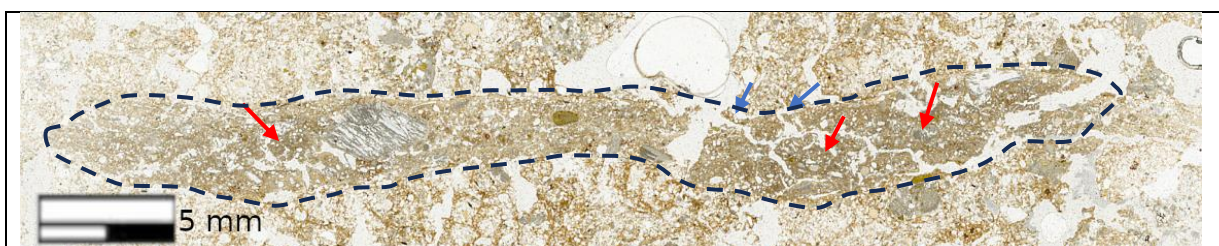


Fig.52: Facies c (delimited by the dashed black line), note the lenticular shape and the sharp boundaries. The channels in continuity with the upper facies are indicated with the blue arrows. Also note the grayish matrix inside the yellowish rim (red arrows).

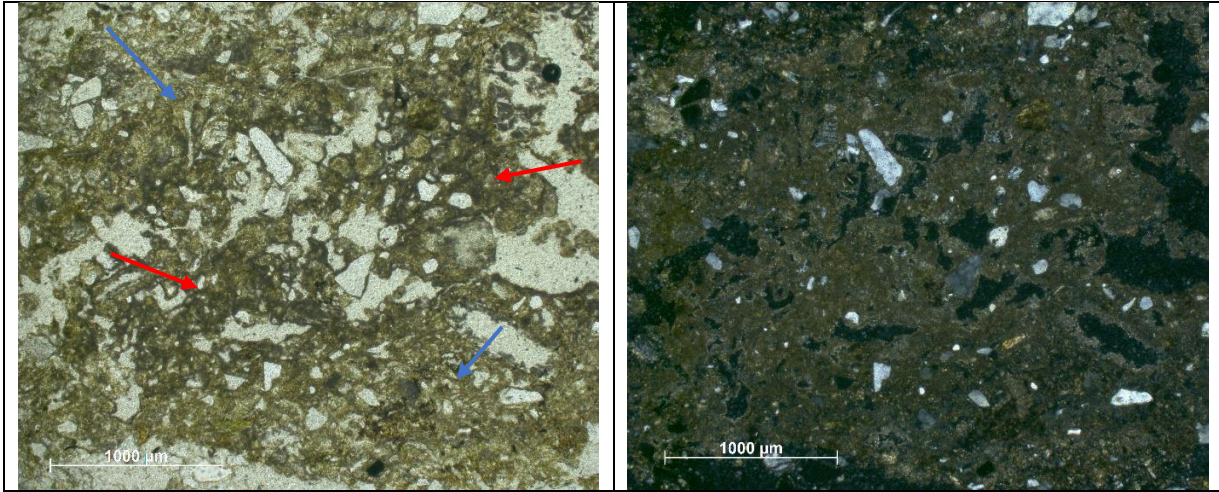


Fig.53: Note the grayish matrix with a chitonic related distribution pattern (red arrow) surrounded by the yellow rim displaying a porphyric related distribution pattern (blue arrow). In XPL note the quartz grains embedded in the matrix.

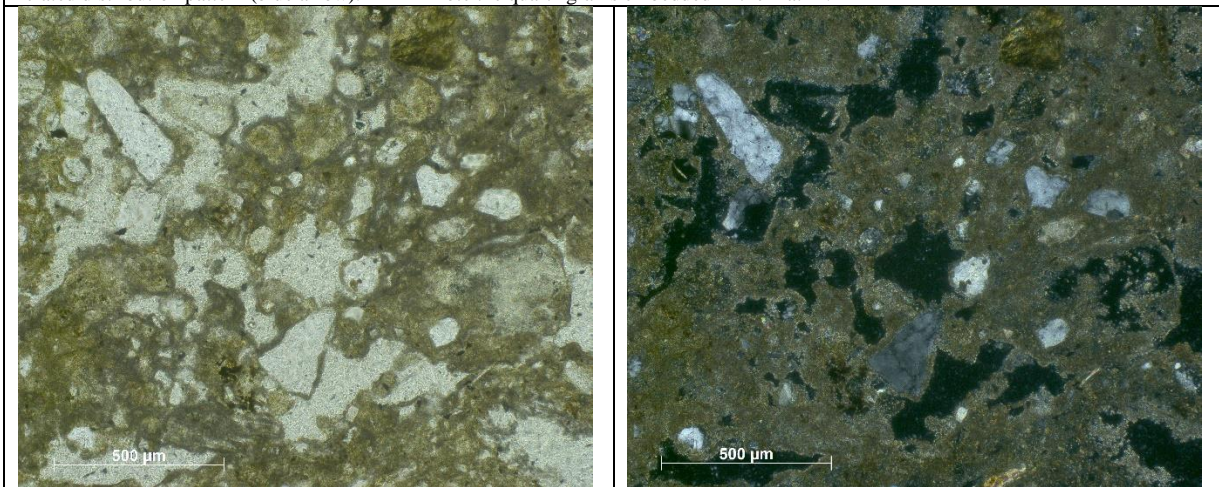


Fig.54: Zoom of fig.17, note the chitonic related distribution pattern in PPL and the calcitic crystallitic b-fabric in XPL.

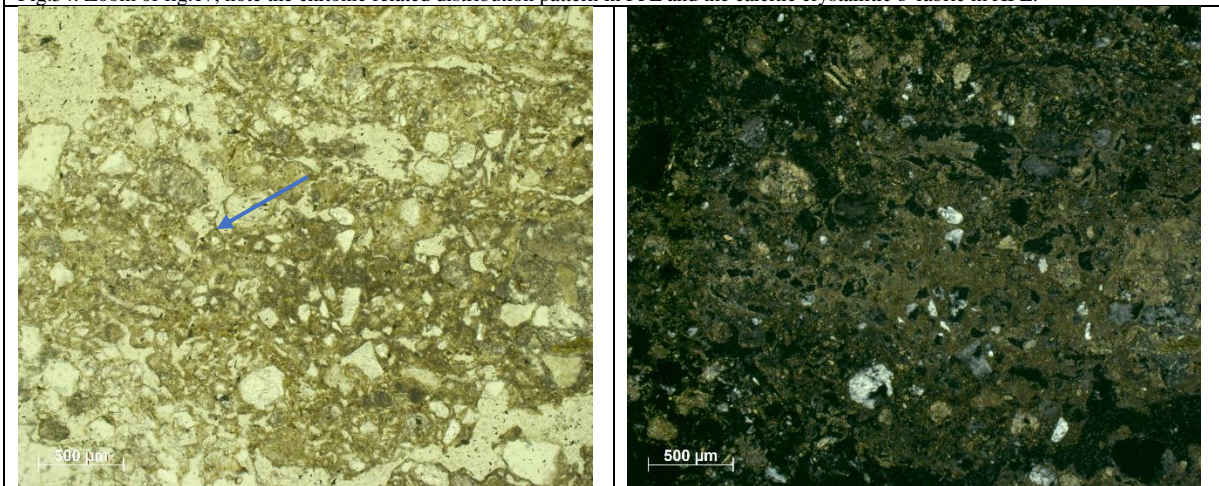


Fig.55: Right edge of the facies, note how the inner grayish matrix becomes progressively smaller until only the yellowish one is left (arrow).

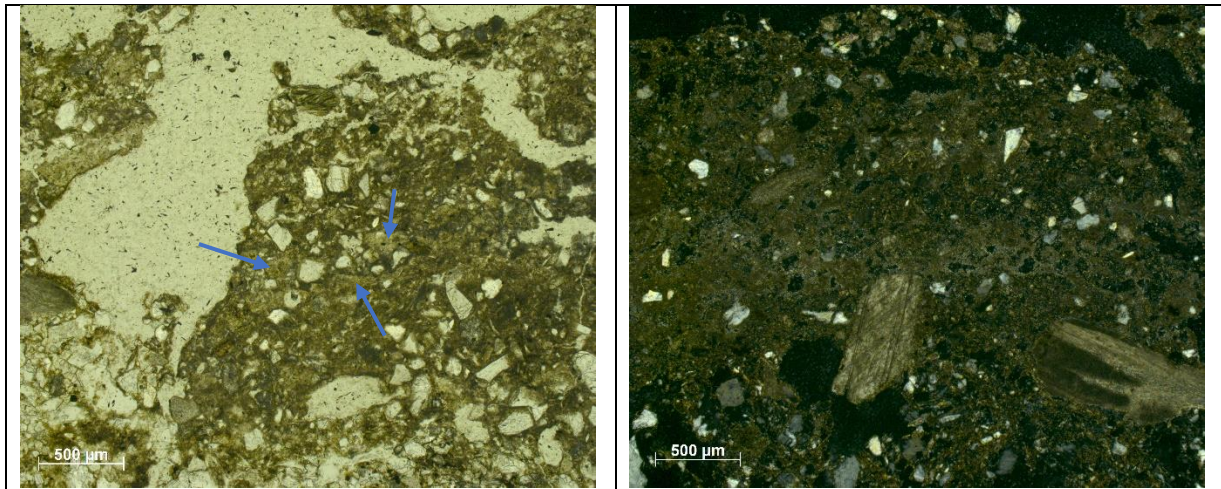


Fig.56: Note the yellowish areas (blue arrows) embedded in the grayish matrix.

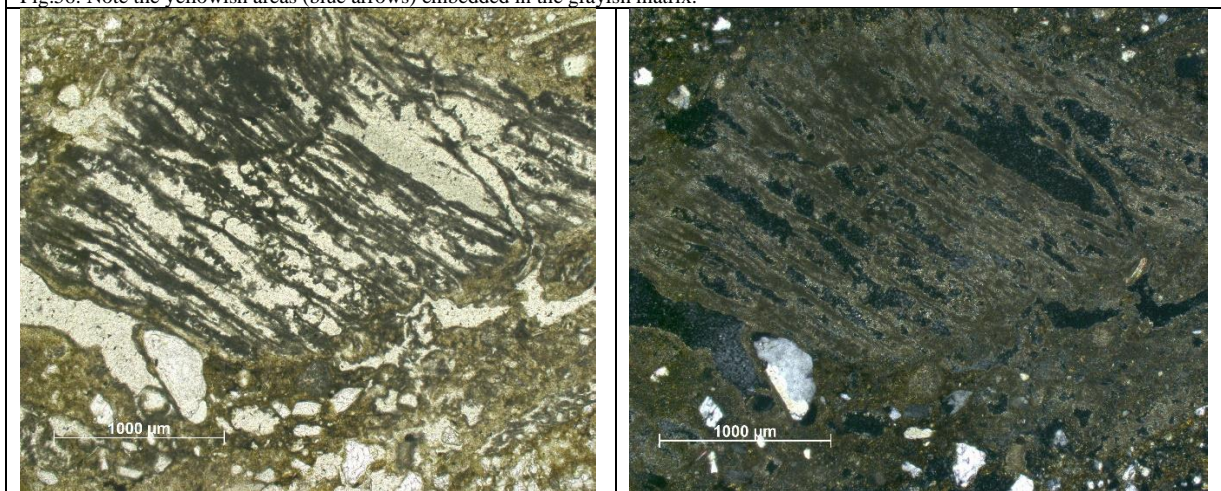
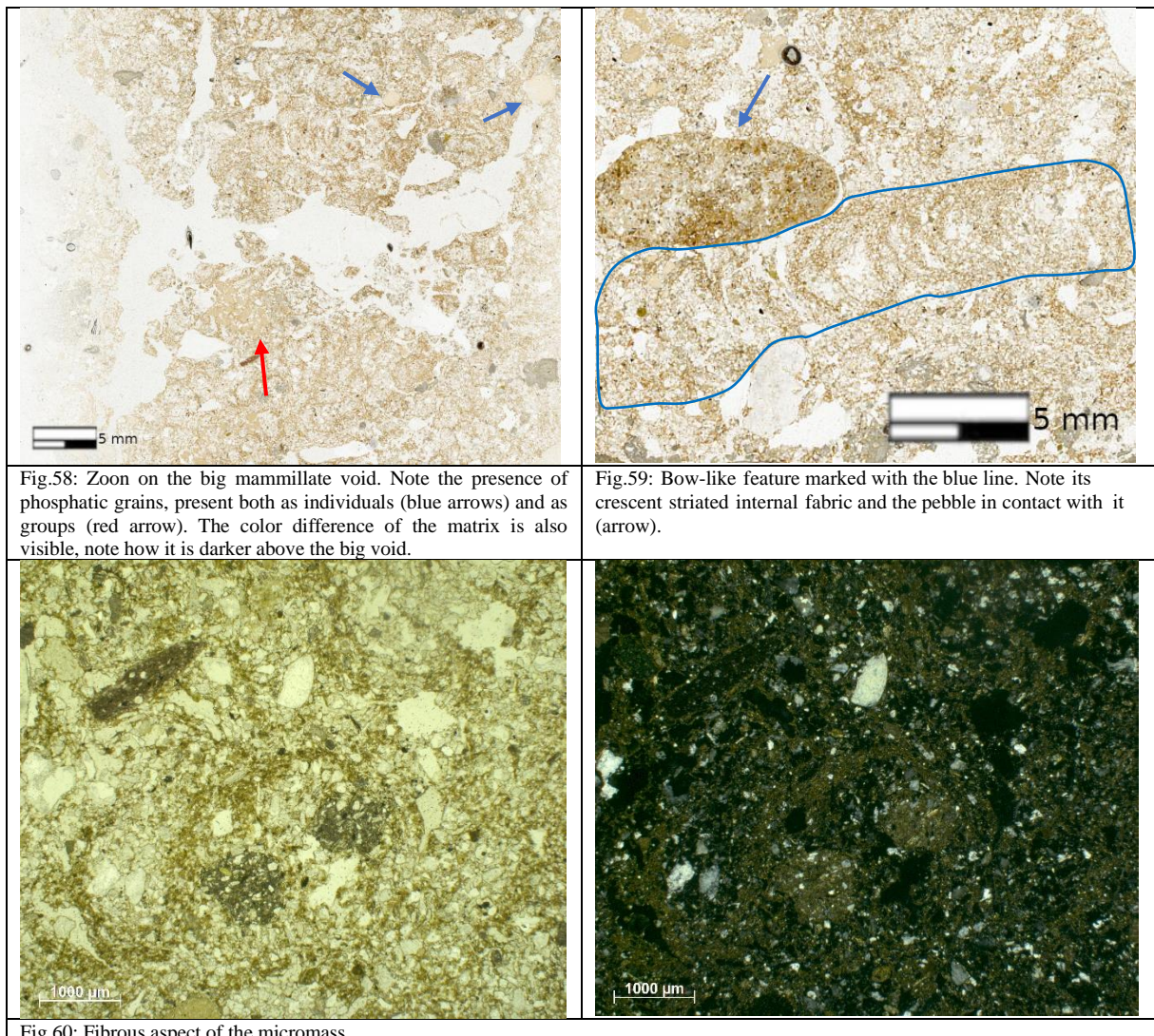


Fig.57: Hypothesized wood-like structure. Note the calcitic crystallitic b-fabric of the feature in XPL.

b)

The facies present a channel to vesicular microstructure, the porosity results to be composed of channels and big irregular poroids (fig.58), all of them displaying no accommodation. The solid material that composes the facies presents a close porphyric related distribution pattern ($c/f_{20\mu m}$), with sporadic areas presenting a gerufic to chitonic one. Two types of micromass have been identified, one presenting the same characteristic of the micromass presented in facies *d* (brownish to dark brown color, speckled b-fabric and fibrous aspect, fig.60), and the other one presenting a yellowish color and a crystallitic b-fabric. The first type of micromass is mostly present in the upper part of the facies while the second one in the lower part (the big mammillate void results to be the boundaries between the two, fig.58). The coarse fraction is mostly composed of quartz grains with sizes ranging from very fine to fine sand, in the same class size also some carbonate rock fragments and micas grains have been identified (fig.61).

Two coarser elements are also visible at the bottom of the facies (fine gravel size), they result to be in contact with a bioturbation feature (fig.59). Alongside with these elements aggregates of cemented calcitic matrix (fig.62), digested bones (fig.63), and a high presence of phosphatic grains have also been identified. The phosphatic grains present a high degree of heterogeneity in their size (ranging from 100 to 1000 μm), on the other hand their shape results homogenous, ranging from spherical to sub-spherical and always with a well-rounded surface (fig.62). A clustered to linear distribution pattern of these elements have been identified, in the groups the elements are often in contact with each other, also isolated phosphatic grains are present (fig.58). For what concerns the pedofeatures micromass typic coatings of voids (fig.64) and mesofauna activity's features are present (bow-like structure, fig.59).



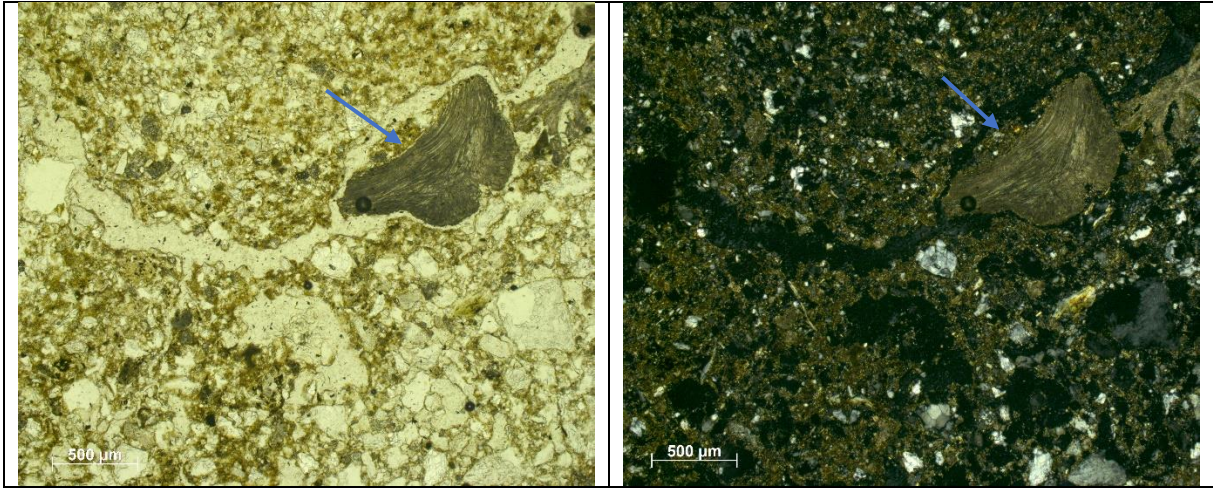


Fig.61: Planar void with a low degree of accommodation. Also visible a carbonate rock fragment (arrow).

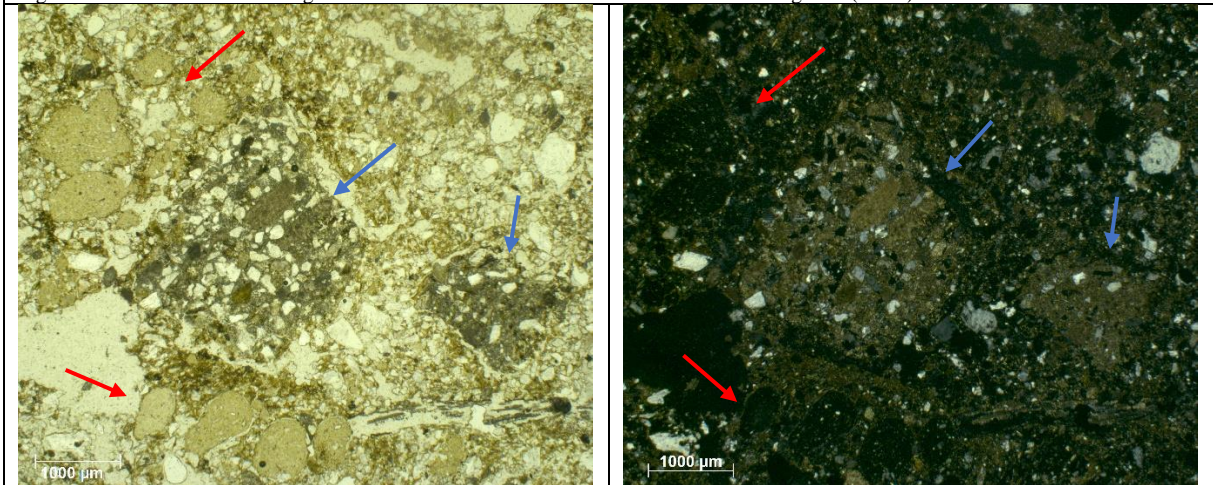


Fig.62: Aggregates of cemented calcitic matrix (blue arrows) and phosphatic grains, note their sub-spherical, rounded shape and their clustered distribution (red arrows).

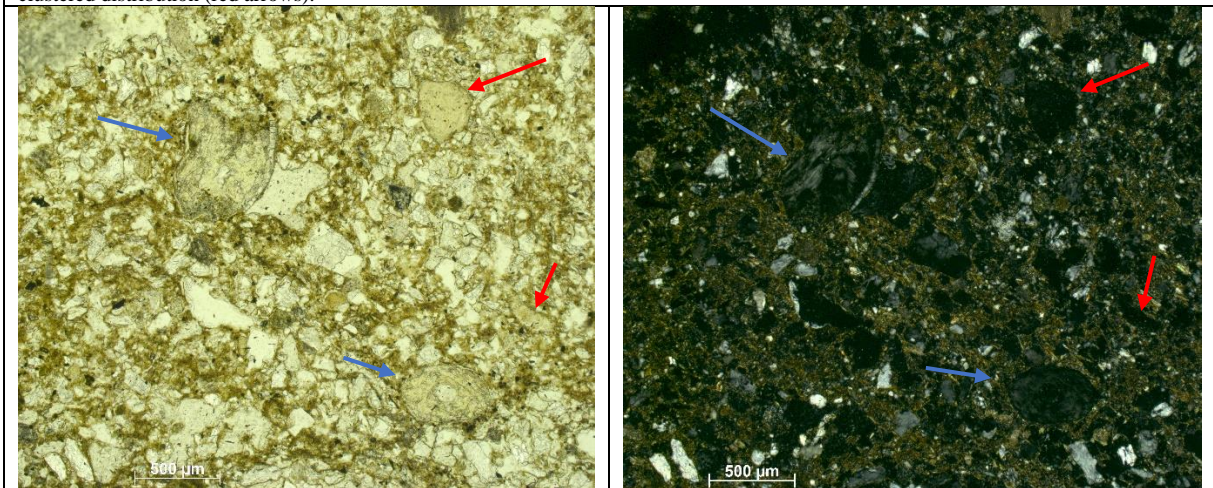


Fig.63: Isolated phosphatic grains (red arrows) and digested bones, note their low interference color pointing to the digestive process (blue arrows).

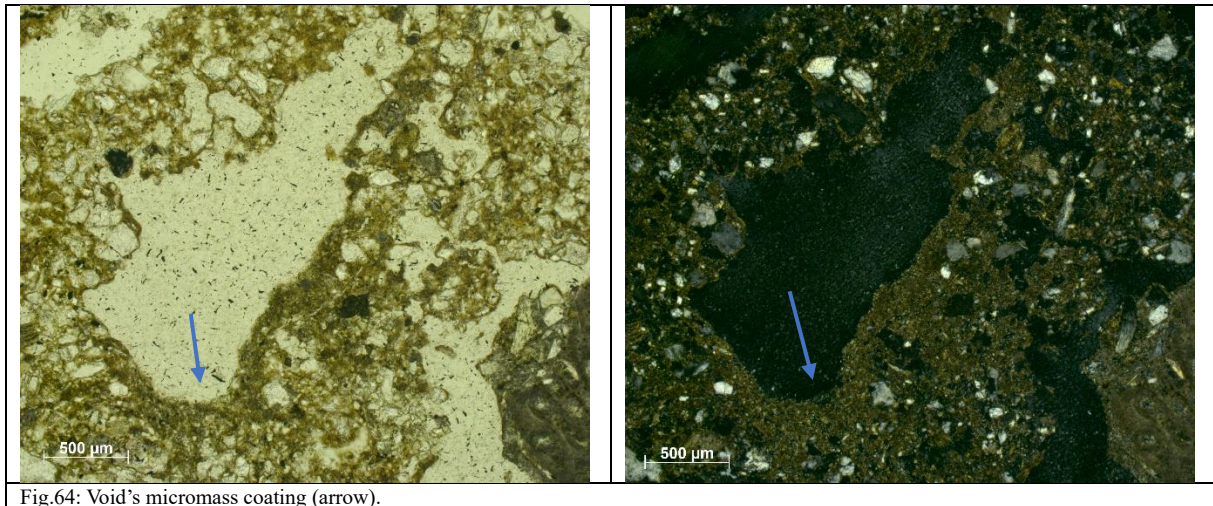


Fig.64: Void's micromass coating (arrow).

a)

The facies presents a banded fabric composed of partial fabric very similar to the one present in facies *e*. The banded fabric is generated by an alternation of coarse and fine sand bands, the shape of these bands is not regular (fig.40), the size of the elements is the only difference identified between the bands. Few micromass is present in the facies giving rise to a dominant basic microstructure (fig.65) with sporadic areas presenting a bridged to intergrain microaggregate microstructure (monic to enaulic related distribution pattern) (fig.66). The porosity is composed of simple packing voids and vesicles, the latter presenting a sub-horizontal distribution pattern (fig.65). The few micromass of the facies is often present under aggregates form, usually well rounded and sub-spherical, with a brownish color and often embedding in them quartz and micas grains (fig.66). The coarse fraction is composed of sandy material of heterogenous size (from fine to coarse sand size), the distribution pattern of the material's size classes gives the facies the banded fabric, each band has a different sorting size (fig.40). The lithology of the coarse fraction is mostly composed of quartz grains, carbonate rock fragments (often presenting fossils inside, fig.67-68) and aggregates of cemented calcitic matrix (micrite) (fig.69). These last two elements are the coarser ones, reaching coarse sand size (sporadically also fine gravel size), and composing the coarser bands, the space between these elements is filled by finer material and small aggregates.

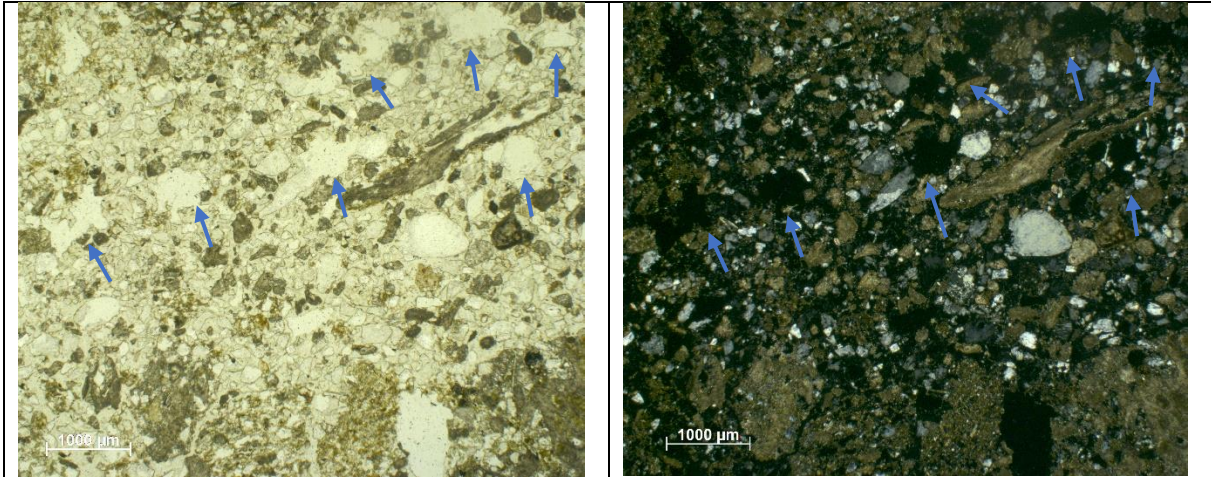


Fig.65: Basic microstructure. Note also the sub-horizontal distribution pattern of the vesicles (arrows).

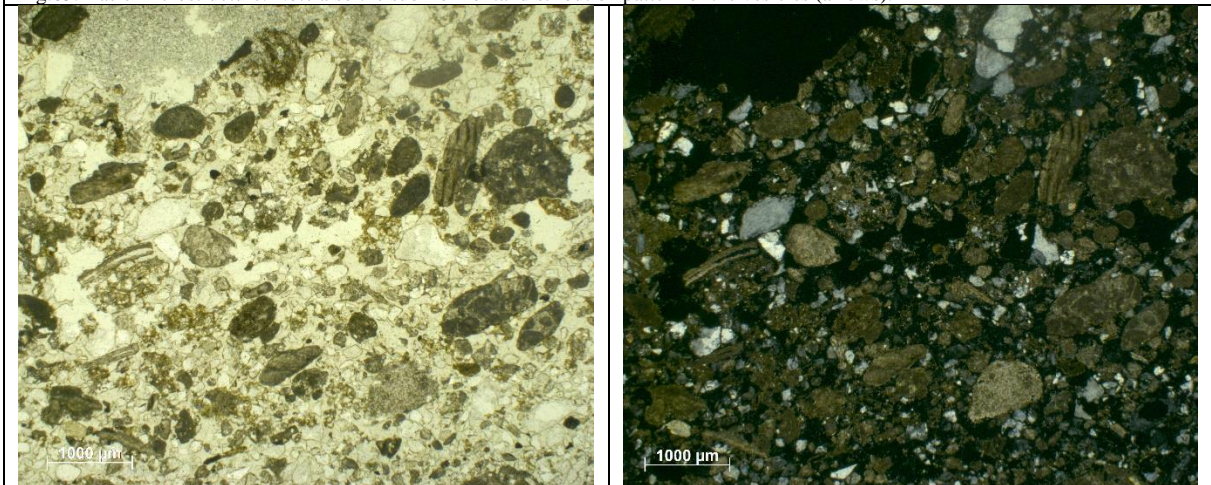


Fig.66: Intergrain microaggregate microstructure.

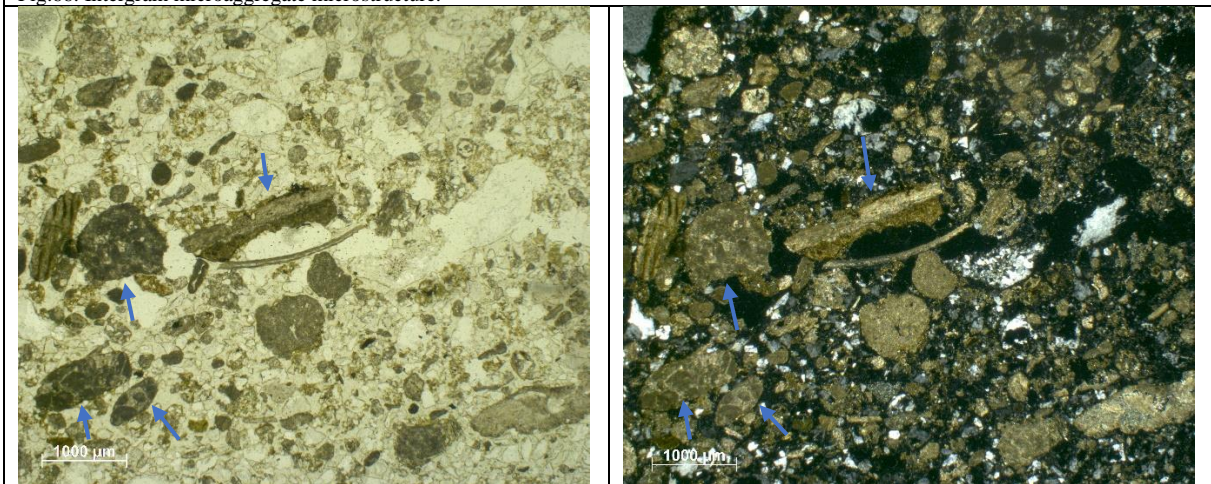


Fig.67: Carbonate rock fragments presenting fossils inside (arrows).

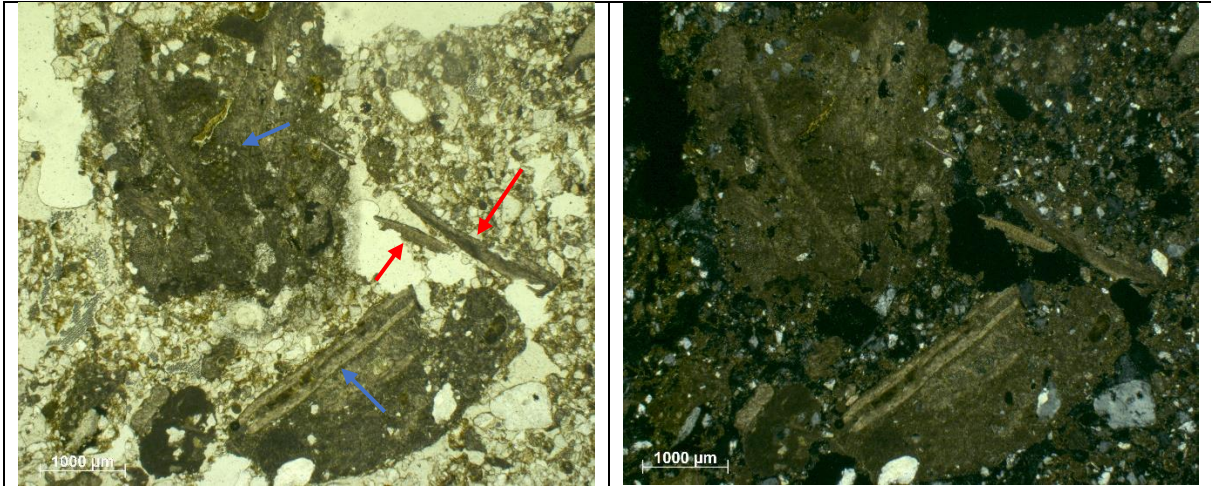


Fig.68: Carbonate rock fragments with fossils residues inside (blue arrows). Isolated fossils are also present (red arrows).

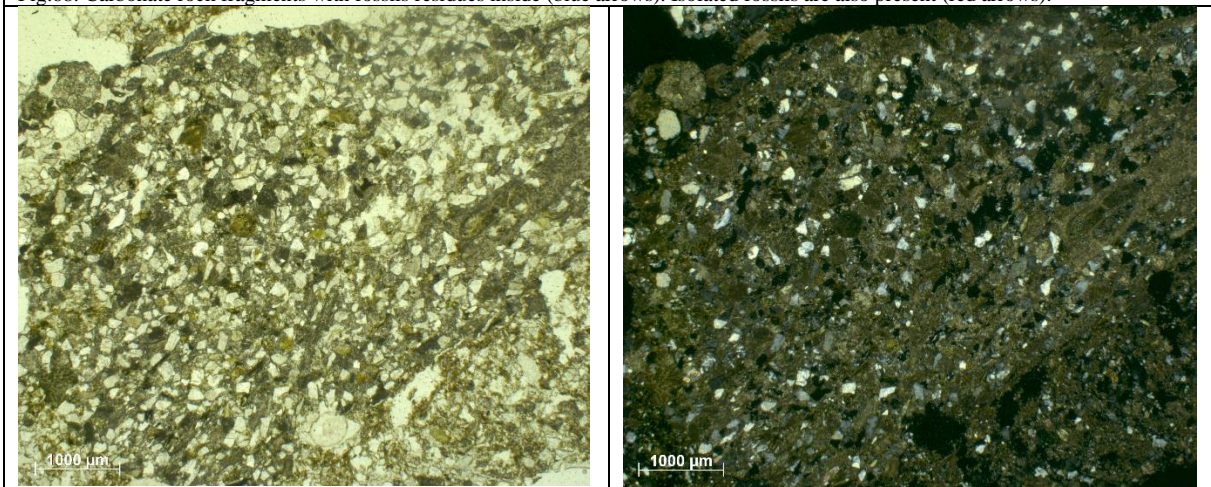


Fig.69: Aggregate of cemented calcitic matrix (micrite) note the calcitic crystallitic b-fabric.

MM3

Stratigraphic description of the block

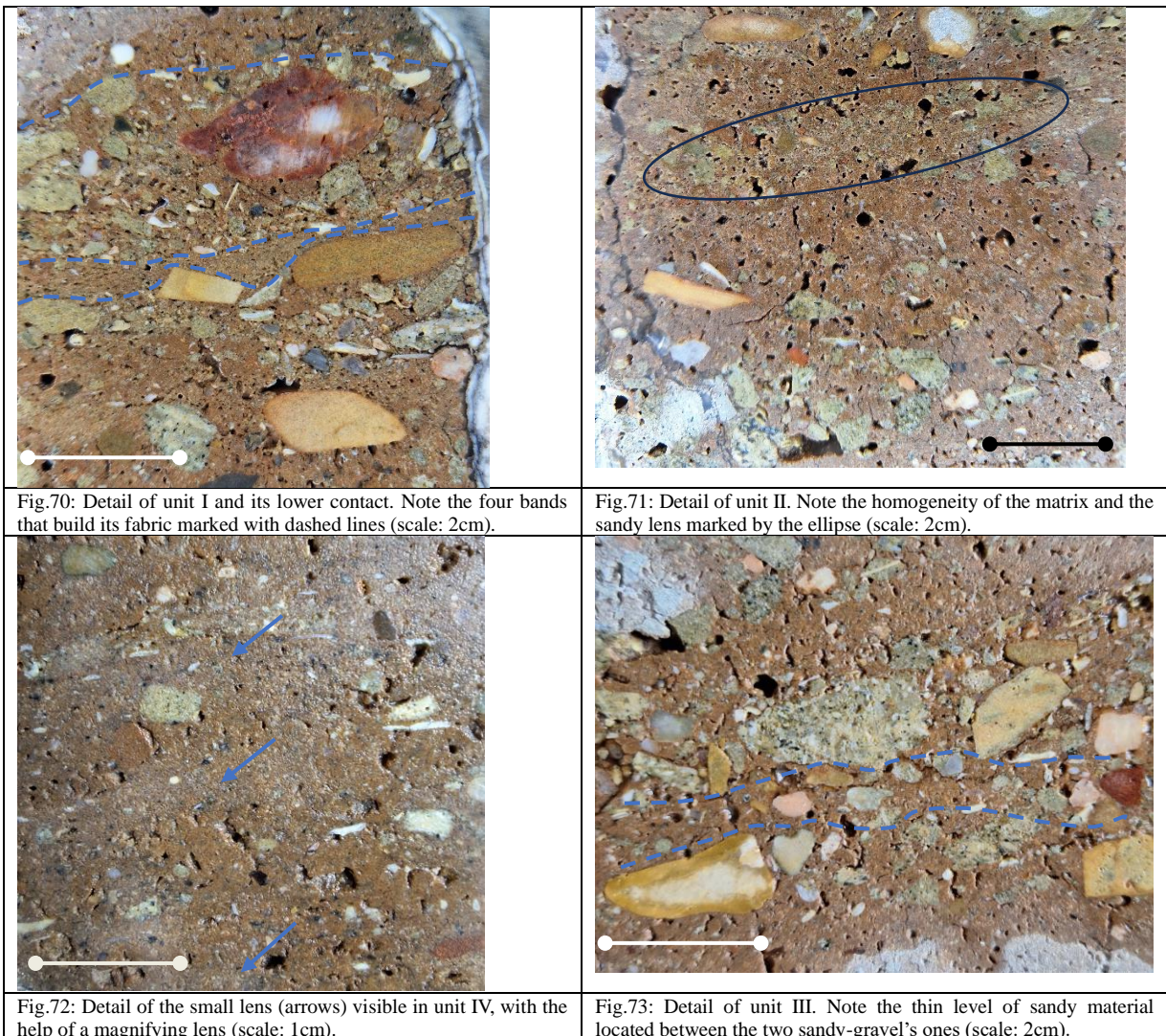
MM3 block results to be well made, easily observable, and the north direction is marked on both the block and the section. One downside of the analysis for what concerns MM3 is the size of the block in comparison to the section's one. The height of the block is in fact almost the double of the section, making it so difficult to find the correct position of the letter on the block.

The general aspect of the block, from a stratigraphical point of view, displays a well visible stratification composed by an alternation of sandy, fine material and sandy-gravel levels. For its description it has been divided into four different units (fig.74). From top to bottom we find:

- I. The unit present a banded fabric composed by a clearly visible alternation of two main kind of bands, one sandy-gravel and one sandy-fine material (fig.70). The thickness of the different levels is variable. Four main bands have been identified, from bottom to top we find (fig.70):
 - Level composed of gravel and sand. The maximum thickness is around 1 cm. The gravel presents a high heterogeneity in its lithology, the gravel's elements that present a tabular shape have a sub-horizontal orientation pattern. The presence of shells fragments has also to be noted.
 - Level composed of sand and fine material. The thickness is also around 1 cm, decreasing towards north. At this scale of observation, it results to be very homogenous and doesn't present any coarse elements.
 - New level composed of gravel and sand. The thickness results to be higher (up to 2 cm). A sorting in the distribution of the elements is visible, at the bottom part of the level we find the smallest elements (sand), while going upwards the elements progressively become bigger, and reach their maximum size at the very top of the level (up to 3cm). In this level (as of the first level described) the tabular elements present a sub-horizontal orientation pattern.
 - The uppermost level of the block results to be again composed of sand and fine material and presents the same characteristic of the one described before.
- II. The unit is mostly composed of a fine material matrix embedding coarser tabular elements which float freely in the matrix, in particular some gravel elements are present at the contact with the upper and the lower unit (fig.74). At this scale of

observation, no bands are visible, only a sandy lens (displaying a clearer color) has been identified (fig.71). A high presence of shell's fragments has been noted.

- III.* Sandy-gravel unit composed of an alternation of levels displaying different sorting. In particular a thin level of sandy material results to be located between two sandy-gravel levels (fig.73). A planar fracture between the uppermost sandy-gravel and the sandy levels has been identified. The lithology of the coarser elements presents a high degree of heterogeneity and the orientation of these elements with a tabular shape is still sub-horizontal.
- IV.* The unit has a very homogenous aspect. It results to be composed of fine material matrix embedding few coarse elements, these elements often present a tabular shape and sub-horizontal orientation pattern. At this scale of observation, the unit doesn't present any bands, even though with the help of a magnifying lens it was possible to identify small lens displaying a different color in comparison to the general matrix of the unit (fig.72).



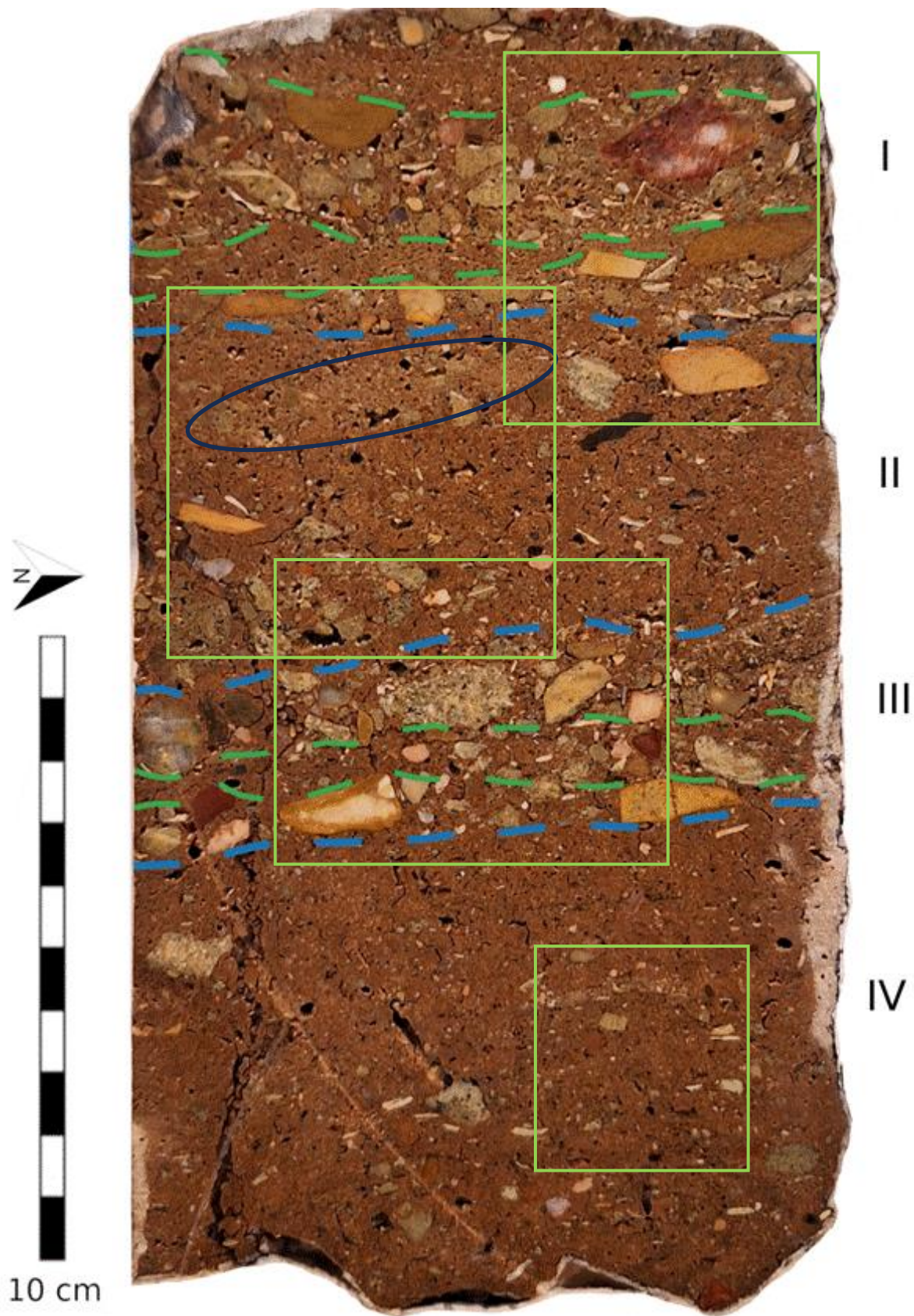


Fig.74: MM3 block. The dashed blue lines mark the units identified in the block, while the dashed green lines mark the subdivision in levels of facies *I* and *III*. The ellipse marks the sandy lens identified in unit *II*.

Mesoscopic description of the thin section

The overall aspect of the section has been subdivided into five different facies (identified with lowercase letters) based on homogeneity and heterogeneity. The facies will first be described at the mesoscopic scale of observation, from top to bottom we find:

- e)* This facies displays a complex structure. A high degree of inner heterogeneity is present. The overall porosity of the facies is moderate (with a degree that could be described between facies *c* and *a*), it seems to be composed of both packing voids and channels/vughs with none of them taking over the other, to be noted that the degree of porosity increases in the right part of the section. A banded fabric (blue arrow in fig.) is clearly visible on the left side of it (less visible on the right one), it is composed of two different types of partial fabric alternating each other with a difference in size, is visible the interbedding between a fine parallel banded partial fabric and a homogenous sand size one (described later respectively as sandwich and sandy partial fabric). On the right side of the section the bands are less visible, which could be linked to the higher porosity (notably channels) of this side. The matrix of this facies also displays a high degree of heterogeneity, the color ranges from brownish to reddish, the color changes seem to have a random distribution and orientation pattern.
- d)* An abrupt contact characterizes the beginning of the next facies. A clear change in elements' size and degree of homogeneity is clearly visible. The facies *d* is composed almost exclusively of sand size grains (exception for one coarser element in contact with the lower facies). It displays a lenticular shape and a high degree of inner homogeneity. The porosity results to be composed mostly of packing voids, very few coarser voids are also present (channel in the middle of the facies and vughs, the latter displays an horizontal distribution pattern and seem to be present exclusively close to the contacts of the presented facies (both upper and lower contact). The upper contact results to be abrupt too.
- c)* This facies presents a higher degree of textural porosity accompanied by bigger (in comparison with facies *b*) vughs and vesicles. The matrix results to be composed of coarse elements of heterogeneous sizes embedded in a fines matrix. An interbedded fabric between coarser and finer elements may be present. At this scale of observation have also been identified two small lenses (ellipses in fig.75) composed of very homogeneous sizes elements; these lenses display a high aspect similarity to facies *d*.

- b)* This facies doesn't present any coarser elements and its porosity is mostly related to the presence of channels and vugs. The matrix aspect presents a pale-yellow color and a massive microstructure in the areas where voids aren't present. At this scale of observation, the facies display a high degree of homogeneity. A gradational contact is present with the upper facies consisting in the progressive decreasing of the micromass and increasing of the coarser fraction.
- a)* This facies seems to be in continuity with facies *b* (comfortable contact between the two facies). It is characterized by a relatively low degree of porosity, the visible voids at this scale of observation are mostly channels and chambers with a random distribution. Few coarser elements are visible. Notably we have two rock fragments at the bottom right of the section whose size result impossible to be identified due of not being integrally present in the section; and three coprolites (*c* in fig.75), two of them are located at the top of the facies and vary close to each other while another one (the smallest) is embedded in the matrix at the center of the facies. The aspect of the matrix seems to be massive with its continuity interrupted by the presence of the channels previously nominated and displays a brownish to yellowish color (to be noted that the yellowish color is barely only present close to the lateral limits of the section, so it may be a consequence of the decrease in the section thickness (Stoops, 2021, p. 64). The inner variability of the facies is moderate and mostly related to the porosity which increases upwards.

Based on these observations we could try to create a stratigraphical connection between the block and the section. Facies *c* seems to be related to unit *III*, they both in fact present a similar thickness and are located between two thick layers of fine material. In this case facies *b* and *a* should fall into unit *IV*, while facies *e* into unit *II*.

This hypothetical position seems to be the most plausible, even though it must be noted that in this case the two pebbles present at the very bottom of facies *a* (fig.75) don't find any correspondence in unit *IV*, not presenting any elements of that size.

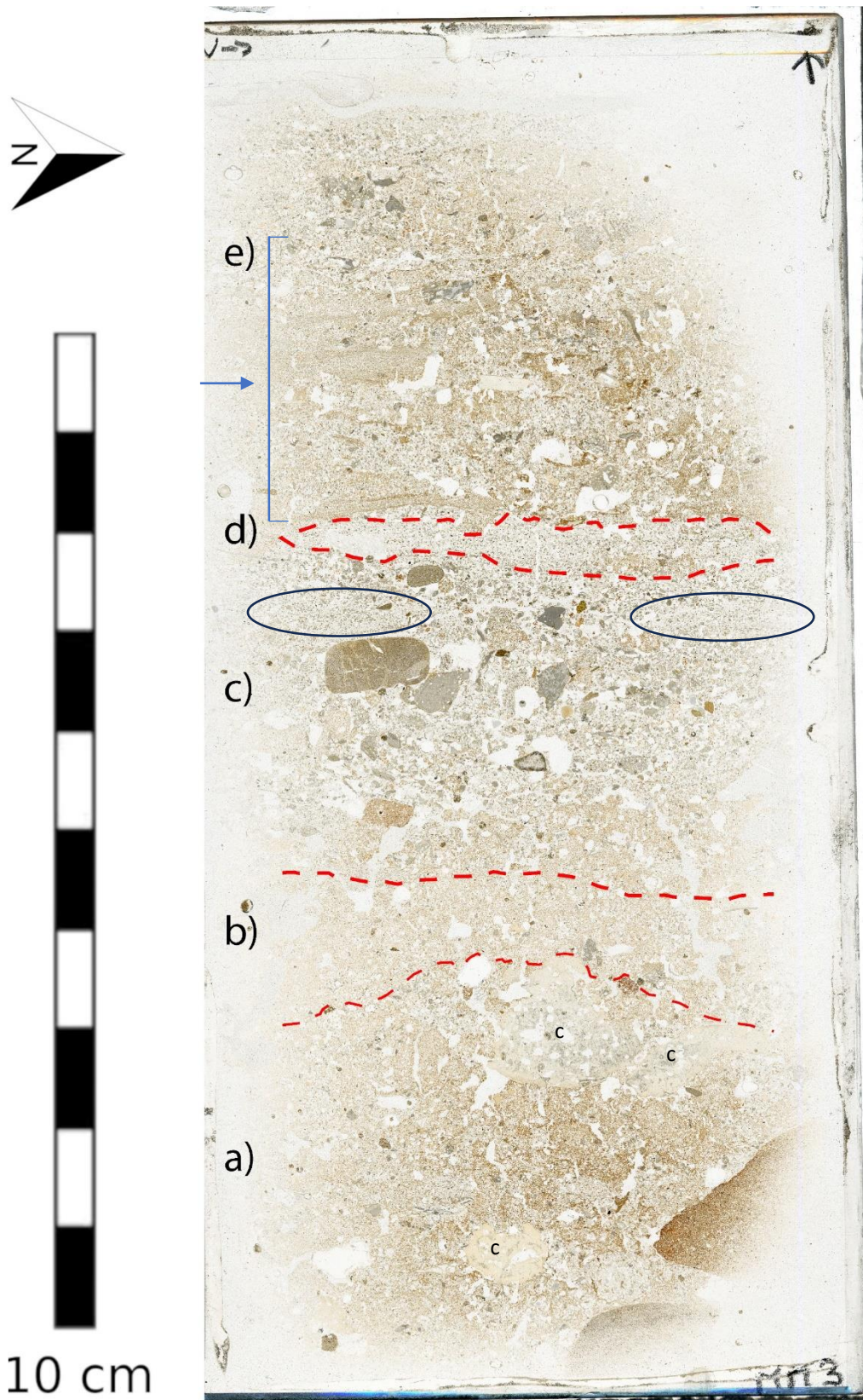


Fig.75: MM3 section's scan. The dashed lines indicate the contact between the identified facies. The ellipses mark the two small lenses composed of very homogeneous sizes elements described in facies c. The blue arrow marks the banded area of facies e.

Microscopic description of facies

e)

This facies is characterized by a complex microstructure, the overall aspect of the facies is quite heterogeneous so, in order to describe it, it has been divided in partial fabric, each of which will be described separately. Throughout all the description the coarse / fine limit will be 20 μm .

1. *Sandwich partial fabric*: it shows a banded fabric composed of three layers giving rise a “sandwich” aspect (fig.77-80-82) with a columnar shape, the orientation and distribution patterns this partial fabric are sub horizontal to the section; they all have more or less the same inclination (compare the figures).

The “bread” of the sandwich shows a massive microstructure composed of dark brown micromass with a banded aspect and a monostriated to parallel striated b-fabric; small aggregates of isotropic micromass are also present. Elongated grains of micas (size from 20 to 150 μm) compose the coarse fraction and show a sub horizontal referred orientation and distribution pattern; few quartz grains are also present (heterogenous shape and medium size slightly smaller than micas’) The c/f related distribution pattern results to be close to single spaced porphyric.

The “inside” of the sandwich instead shows a spongy microstructure. The micromass is less present and displays a yellowish color with a speckled b-fabric; as for the *bread* also small aggregates of isotropic micromass are present. The coarse fraction is composed of micas and quartz grains, few rock fragments are also present; it shows a high degree of homogeneity in size and the elongated grains (mostly micas) show a sub horizontal referred orientation and distribution pattern. The c/f related distribution pattern range from chitonic to gerufic.

A medium degree of variability exists among these fabric units, notably about the degree of porosity of the *inside*, some result very compressed while other with a more open microstructure (fig.80). In addition, the micromass can show some differences, in particular some present also calcareous micromass accumulation between the *bread* and the *inside* (fig.81), this micromass keep displaying a mono to parallel striated b-fabric.

The partial fabric is not always found complete, sometimes only parts of it are found, still displaying the same characteristics described above (fig.77 to 83).

2. *sandy partial fabric*: the microstructure ranges from bridged to intergrain microaggregate microstructure (fig.83-84-85) with few areas displaying a single grain basic microstructure. The coarse fraction is mostly composed of quartz grains (homogenous size that ranges from very fine to fine sand, few grains over 200 μm); and carbonate rocks fragments, the most represented size is fine sand but some coarser element also present; the average shape of the coarse material is sub-spherical and sub-rounded (for the carbonates, while the quartz show a sub-angular shape). This partial fabric is very similar to the facies d), the main difference is the presence of coarser carbonates grains and of the micromass (not always present). The micromass has the same aspect of the one present in the *bread* described above, sometimes also micas grains are embedded in it. The porosity is mainly characterized by vesicles and channels.

An interbedding between these two firsts partial fabric is clearly visible only on the left side of the section (fig.83).

On the other side of the section the microstructure is more complex, the partial fabrics described earlier are still present but less defined. In addition other partial fabric have been observed:

3. *reddish aggregates* (fig.86): composed of brownish to dark reddish micromass embedding a coarse fraction composed of mostly quartz grains of heterogenous size and phosphatic grains (to be confirmed). The micromass shows a striated to speckled aspect and a speckled b-fabric. The inner c/f related distribution pattern range from close to double spaced porphyric, the porosity is composed of vughs, and their shapes remember the ones of the mineral quartz grains (star shaped vughs). The sizes and the shapes of these aggregates is highly heterogeneous.

The rest of the groundmass (mostly present in the space between the partial fabrics previously described) is composed of a brownish and black micromass with a fibrous aspect and a speckled to striated b-fabric; it is related to the coarse fraction with a pellicular to bridged grain basic microstructure (chitonic to gerufic c/f related distribution pattern). The coarse fraction is mostly composed of sand size quartz grains and carbonate rock fragments (same as the one of the *sandy* partial fabric); few coarser elements are also present, their optical characteristics have been associated with carbonate rock fragments with quartz grains and fossils integrated inside, their shapes are quite heterogenous and their surface results to be very rough, characteristic which may be pointing to dissolution processes (fig.87).

Other coarser elements present in the facies are (presumed) phosphatic spheroids (fig.88) very close to each other sometimes in contact and covered by micromass with granostriated b-fabric. one platy bone fragment horizontally orientated (fig.89) with a low interference color (being it very close to the left side of the section it could be linked to the thickness of the letter) and an isotropic element with a particular angular shape (fig.91).

For what concerns the pedofeature (exemption for the aggregates described earlier) a calcite void coating with a perpendicular referred orientation pattern and a parallel referred distribution pattern of the crystals (fig.90), and aggregates of yellow micromass (fig.91) that form an isolated area with a granular microstructure have been identified. Fecal pellets inside channels are also present (fig.92).

The overall aspect of the facies can so be divided in left and right sides (fig.76). On the left side, as said earlier, an interbedded fabric is displayed composed by the alternation of *sandwich* and *sandy* partial units. On the other side of the section in comparison, the arrangement of the elements seems more random, it also presents a higher degree of porosity, mostly composed by vughs (both regular and star-shaped) and channels. To be noted how on the right side of the section the elements of the *sandwich* partial fabric, when in contact with channels, tend to blend with the rest of the groundmass (fig.82).

Throughout all the facies the presence of opaque material has also been identified, it displays a reddish to orange with areas of metallic blue color in OIL (fig.93).

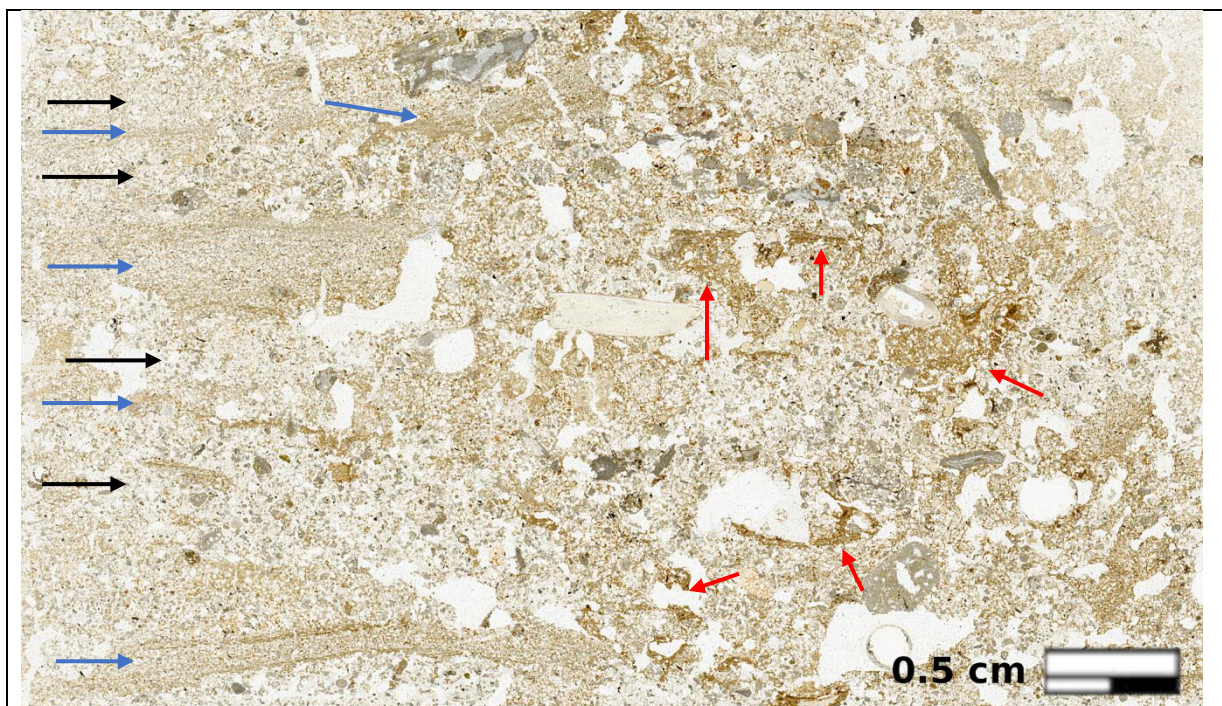


Fig. 76: Zoom of facies *e*. On the right side note the interbedding between the sandy (black arrows) and the sandwich partial fabrics (blue arrows). On the left side note the reddish aggregates (red arrows).

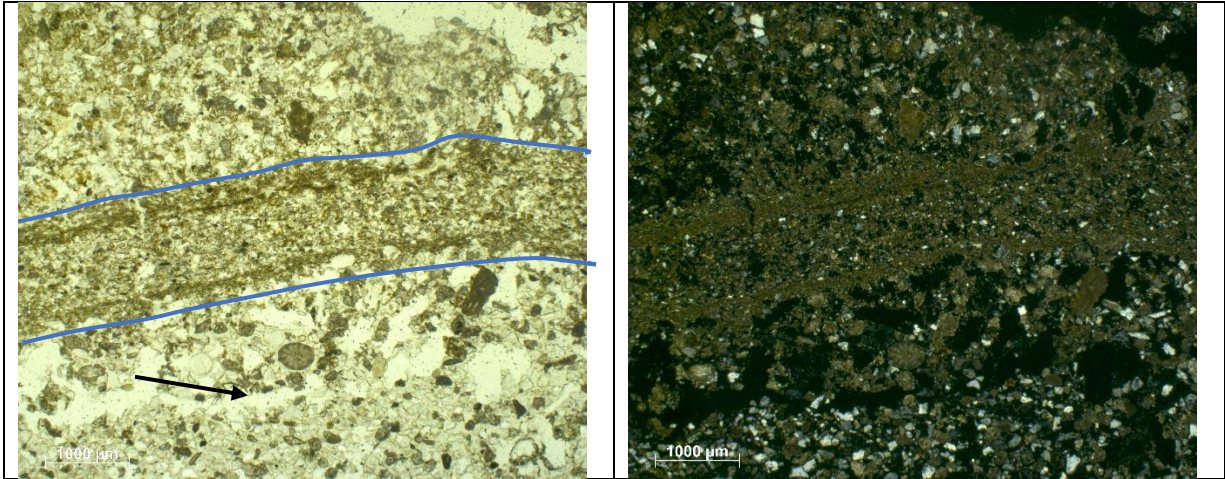


Fig.77: Sandwich-like fabric unit (in blue). Contact between facies d and e at the bottom of the micrograph (black arrow).

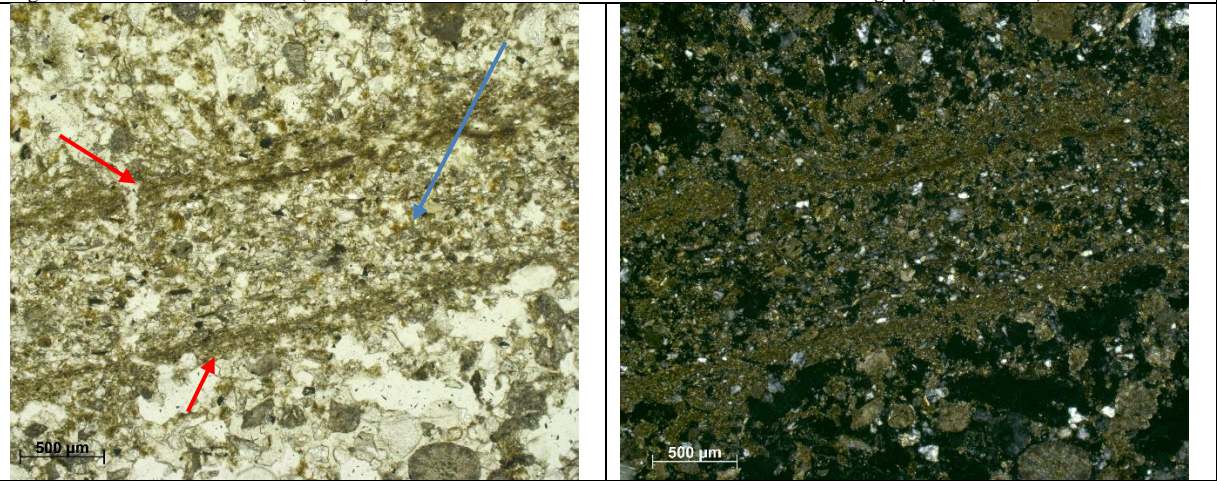


Fig.78: Zoom of fig.31, note the differences between the bread (red arrows) and the inside (blue arrow) explained in the text. In XPL note the monostriated (bottom bread) and parallel striated (top bread) b-fabric.

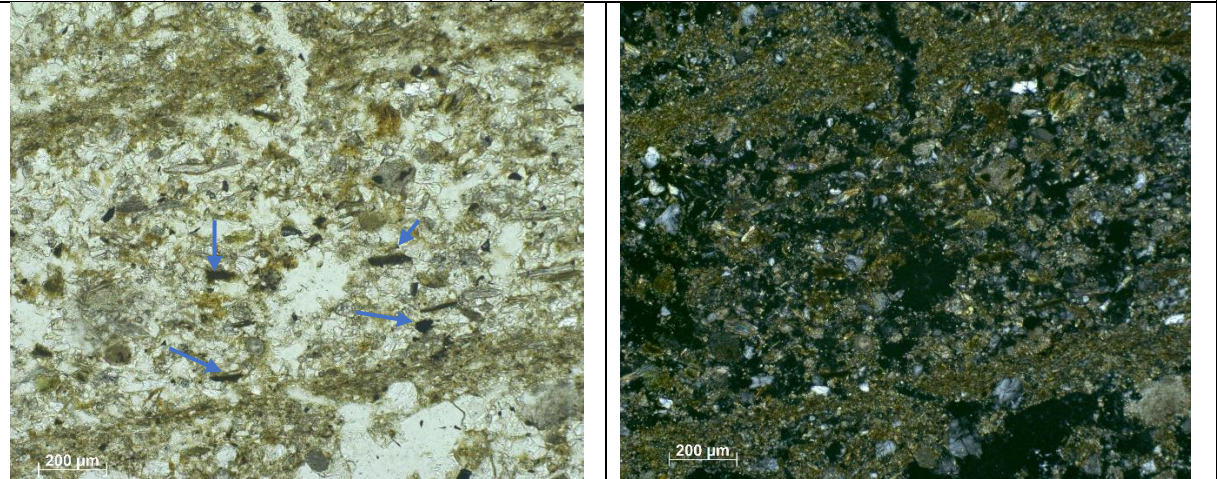


Fig.79: Zoom of fig.32. Note the sub-horizontal distribution and orientation of the elongated particles (mostly micas). Note the small aggregates of dark micromass with isotropic behavior in XPL (arrows).

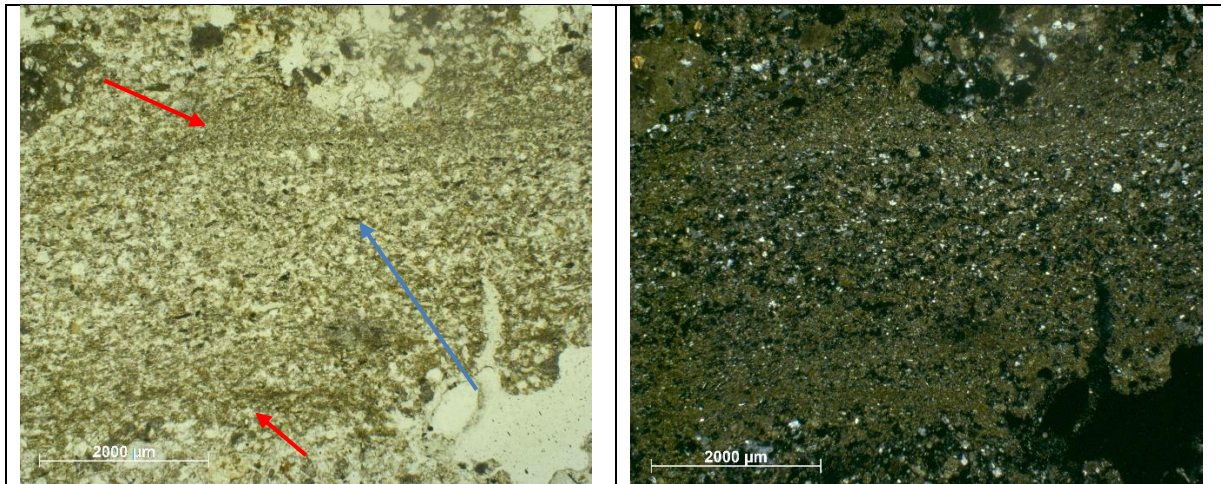


Fig.80: Sandwich fabric unit. Note the differences between the bread (red arrows) and the inside (blue arrow).

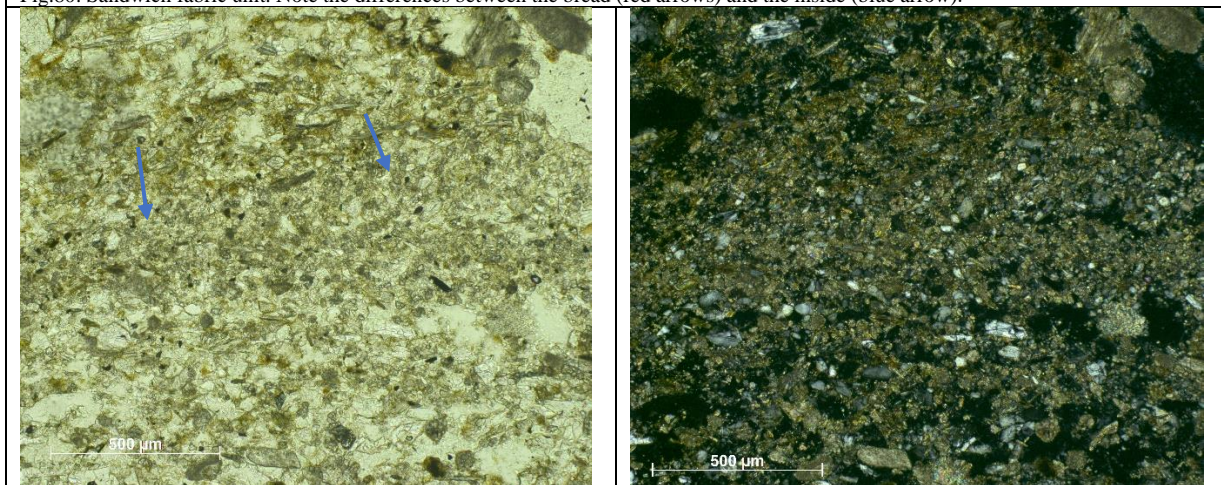


Fig.81: Zoom of fig.34. Note the calcareous micromass accumulation (arrows) between the bread (top) and the inside (bottom).

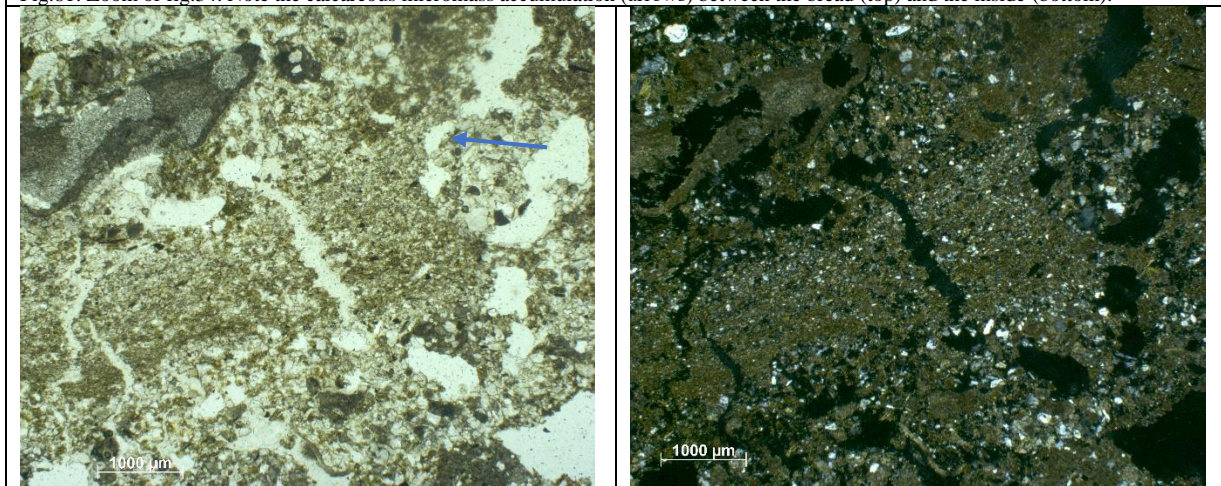


Fig.82: Sandwich fabric unit which is missing the upper bread. Note how its blending in contact with the channel on the right of the micrograph (arrows).

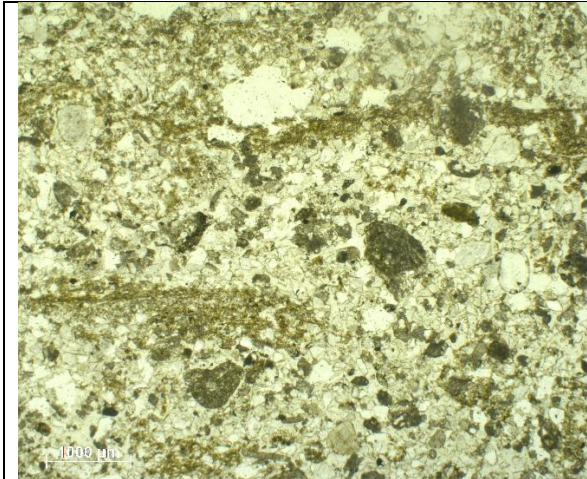


Fig.83: Interbedding between sandy and bread fabric units. Note the high vesicular porosity of the sandy fabric unit.

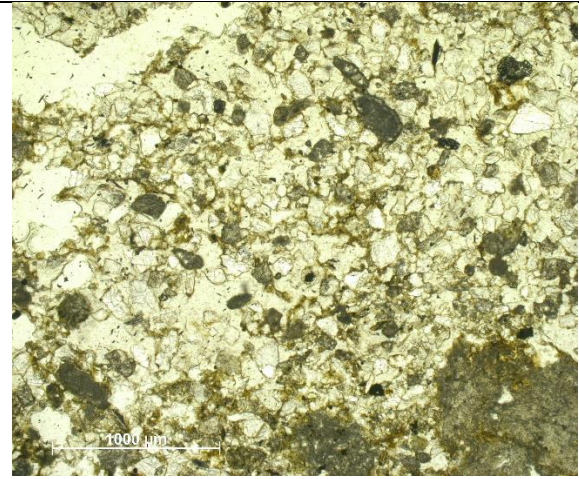


Fig.84: Bridged to intergrain microaggregate microstructure of the sandy fabric unit.

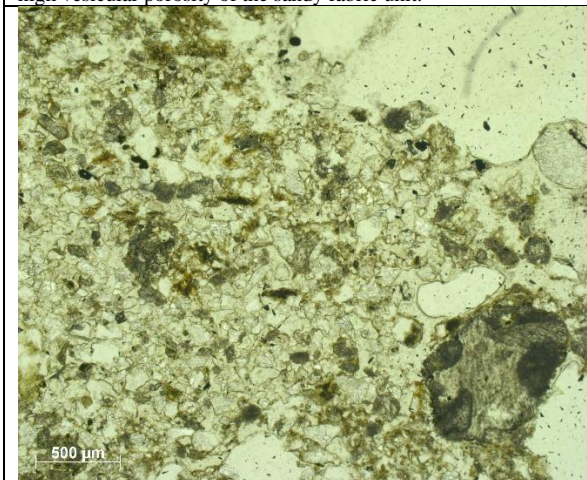


Fig.85: Sandy fabric unit. Note how the r.d.p. changes from coarse monic (absence of micromass) to a gerufic one. Note also the microaggregate of black micromass that show undifferentiated b-fabric in XPL.

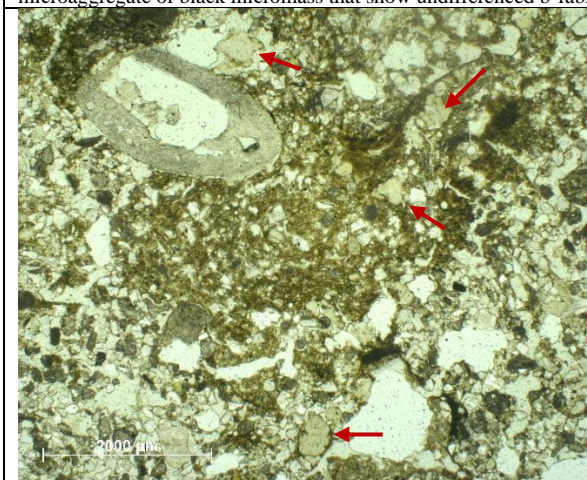
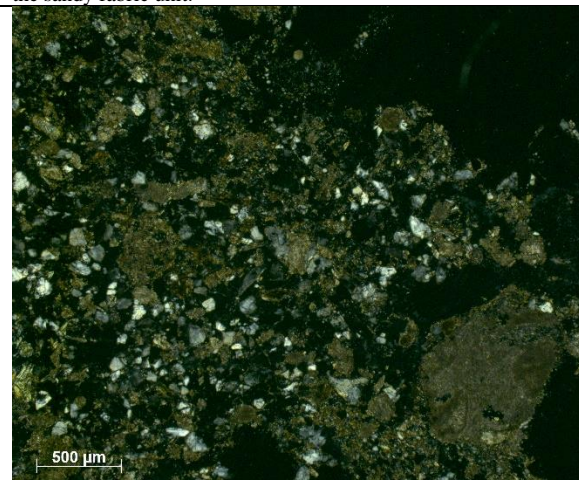
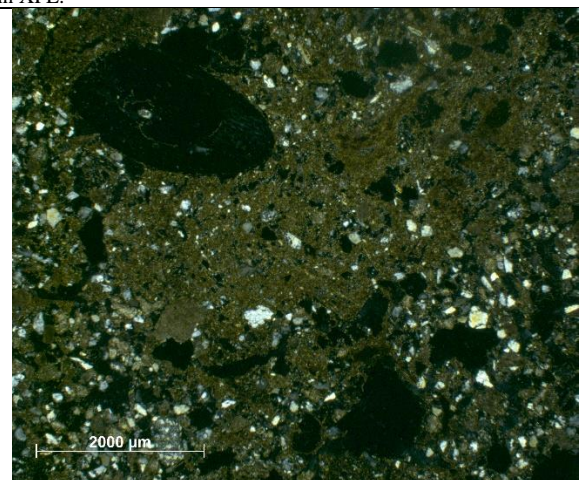


Fig.86: One of the aggregates that compose the aggregates partial fabric. Note the presumed phosphatic grains showing a pale-yellow color in PPL and their isotropic nature in XPL (red arrows).



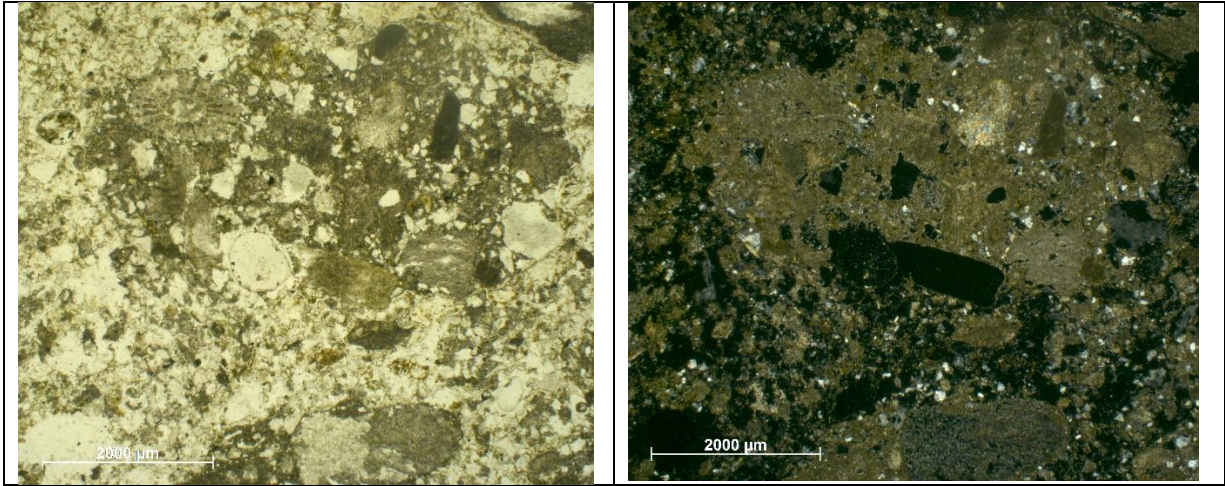


Fig.87: Carbonate rock fragments integrating quartz grains and fossils. Notice the rough surface, that may be pointing to dissolution.

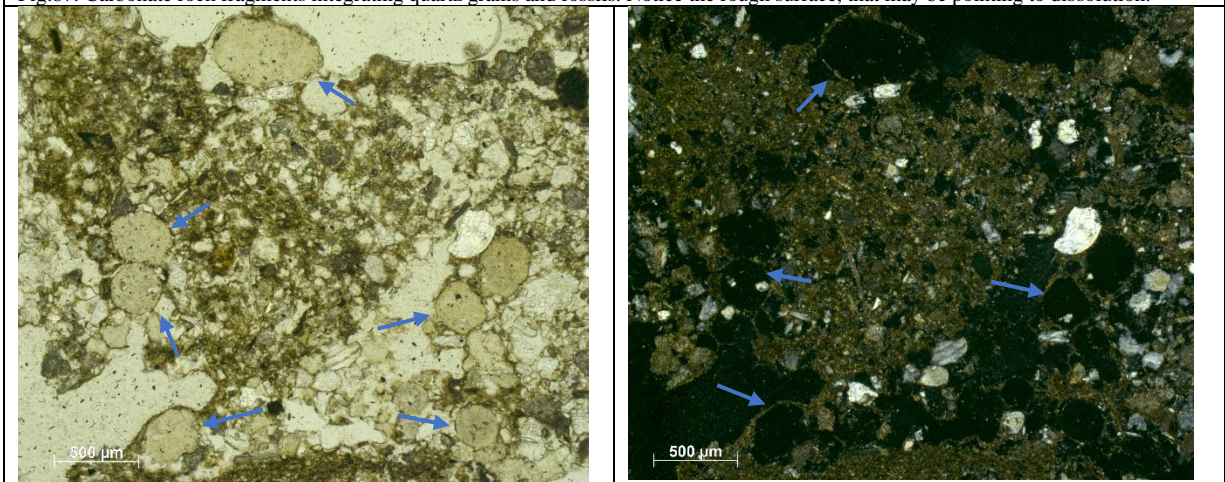


Fig.88: Hypothetical phosphatic spheroids (arrows). Notice the granostriated b-fabric in XPL.

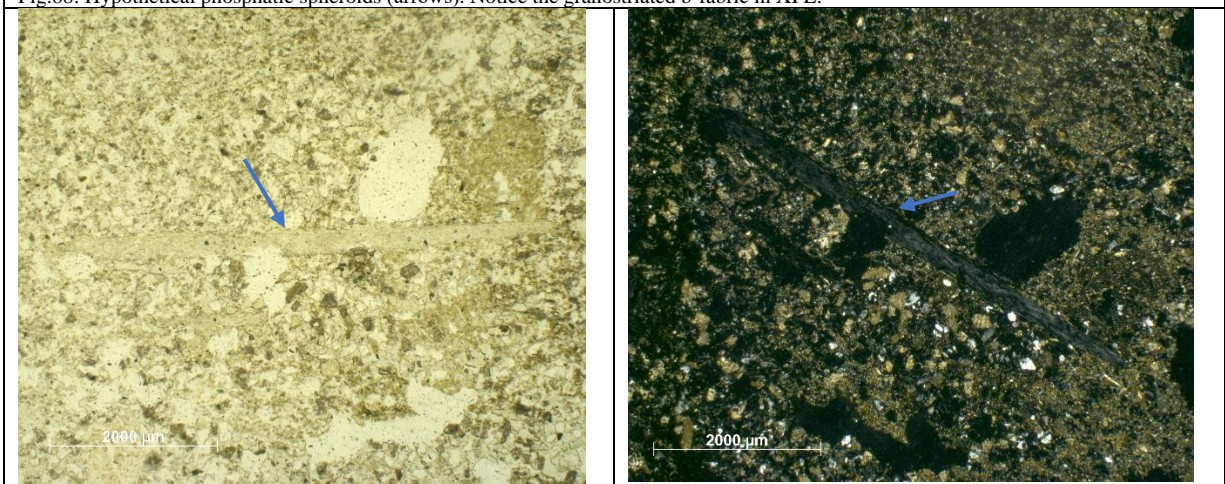


Fig.89: Elongated bone fragment (arrow), the original inclination is in the micrograph in PPL. Notice the weak interference color in XPL.

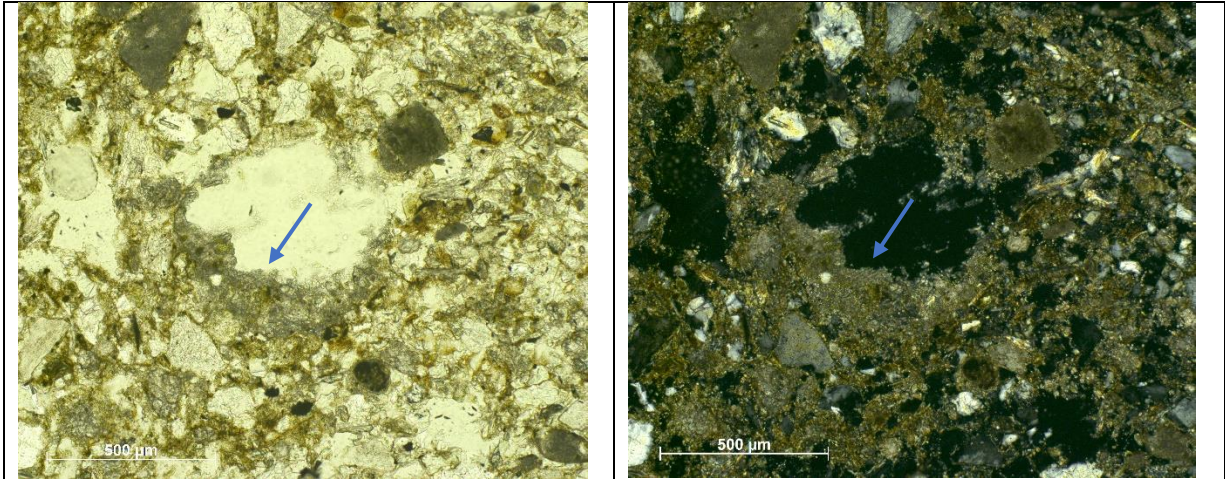


Fig.90: Calcite void coating (arrow), which may be pointing to a secondary calcite deposition.

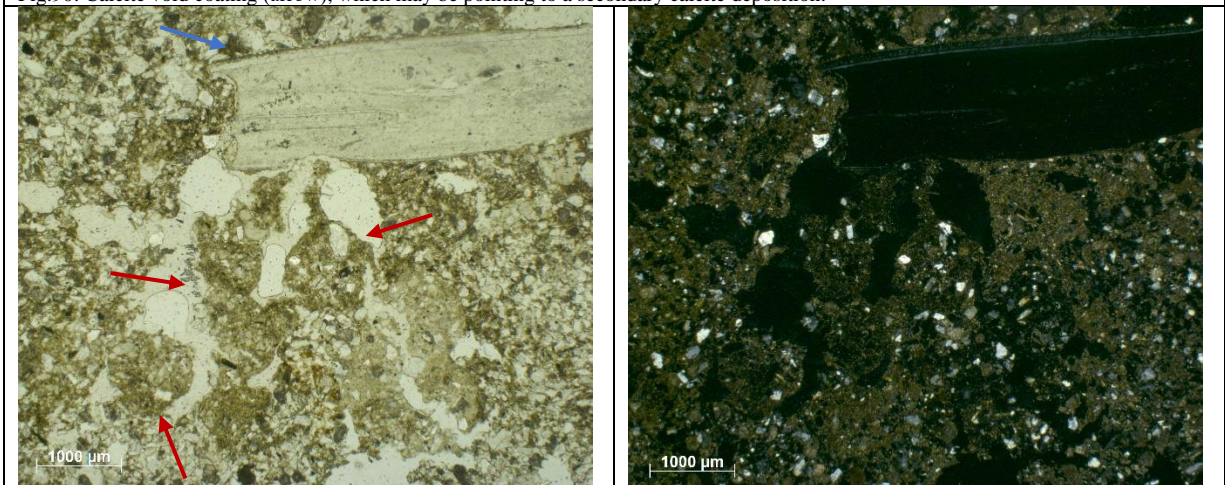


Fig.91: Yellowish sub-spherical aggregates (red arrows) and platy isotropic element (blue arrows).

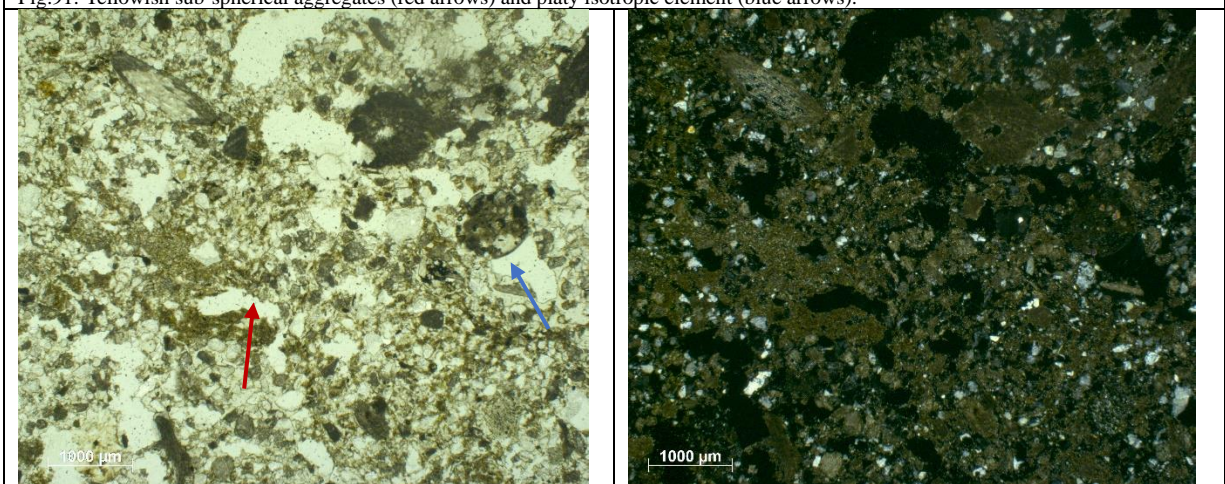


Fig.92: Fecal pellet inside a channel void (blue arrow). Visible also the matrix of the sandwich partial fabric dispersing in the groundmass (red arrow).

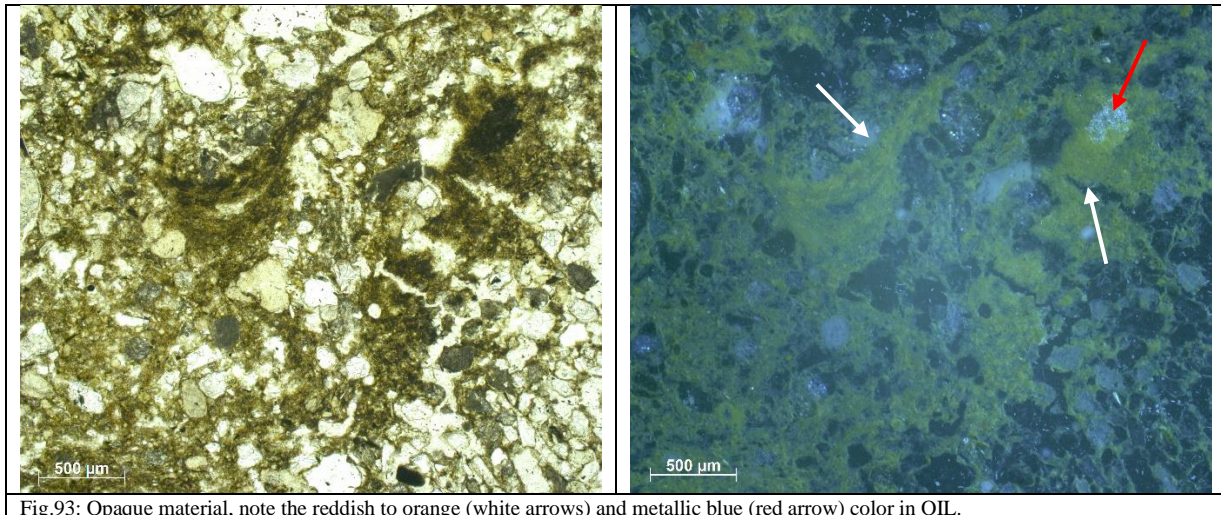


Fig.93: Opaque material, note the reddish to orange (white arrows) and metallic blue (red arrow) color in OIL.

d)

This facies has a lenticular shape and is characterized by a single grain basic microstructure. The size of the elements has a high degree of homogeneity (very well sorted, fine sand) (fig.94). The lithology of the grains is of two different types: quartz grains and carbonate rocks fragments. The quartz grains are the most representative (80-90 %), they present a high shape heterogeneity; while the carbonate rocks have a average size slightly bigger compared to the quartz, and their shape is more homogeneous (rounded and sub-spherical). Some shell fragments are also present. To be noted a big quartzite pebble in the left part of the facies, positioned in contact with the lower facies *c*. The elements that present an elongated shape (despite their lithological type) have a parallel distribution and orientation pattern (referred to the lenticular shape of the facies).

The micromass is absent (sandy material, c/f related distribution pattern coarse monic) throughout all the facies, exception for the top part: the contact between *d)* and *e)* present some micromass coming from the upper facies.

The structural porosity of the facies is composed of simple packing voids (which represent the dominant voids) while channels and vesicles (with sub-horizontal referred distribution pattern) are also present (fig.95).

Pedofeatures observed:

1. Bow-like feature (fig.96) at the lower contact of the facies (probably due to earthworms' activity), composed of brown micromass with a semielliptical crescent fabric. In proximity of the feature also two phosphatic grains are present (completely absent in *d)*)
2. Coating of voids by upper facies' micromass (fig.97)

The upper contact seems quite abrupt and related to the presence of micromass (fig.97)

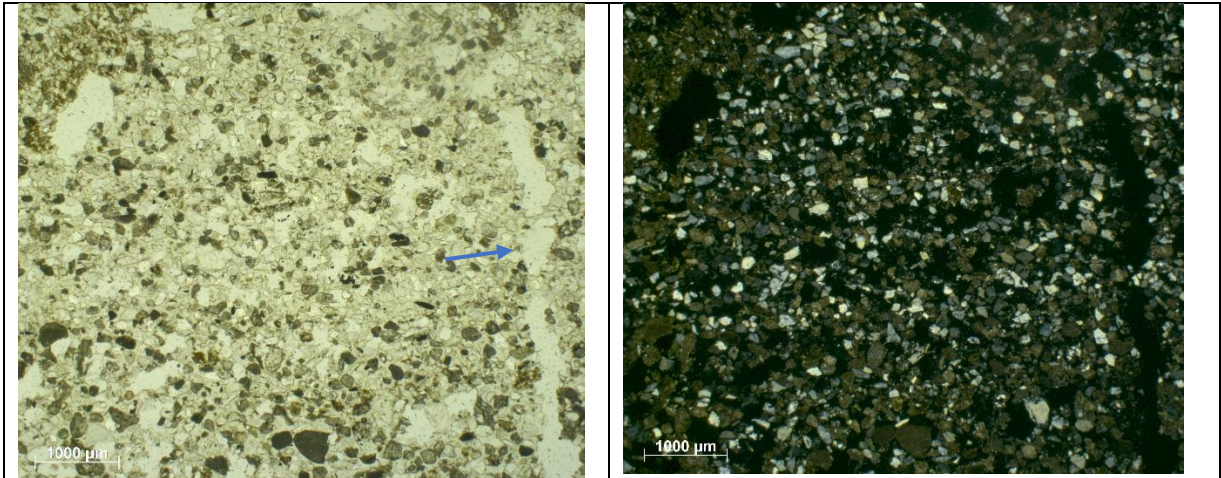


Fig.94: Single grain microstructure, note the homogeneity in size, the high presence of quartz grains and the absence of micromass. A channel (arrow) that cut through all the high of the facies is visible on the right.

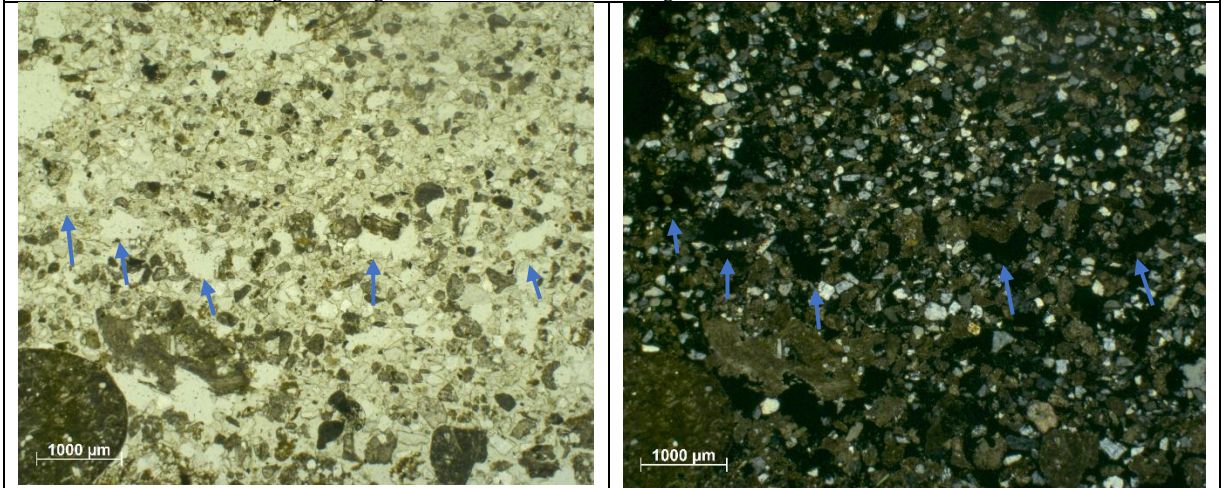


Fig.95: Sub-horizontal referred distribution pattern of the vesicles (arrows).

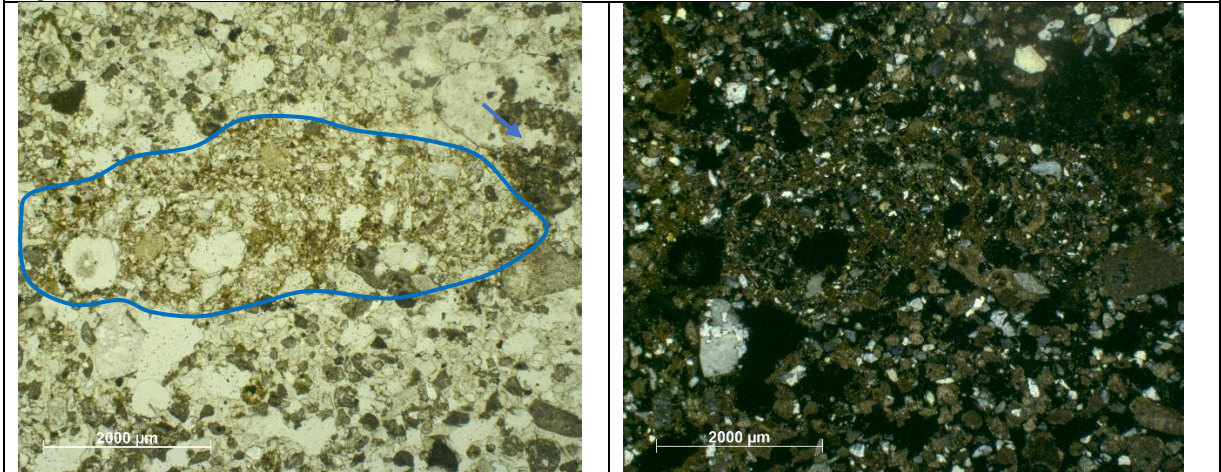


Fig.96: Bow-like feature (in the blue line), at the right edge of the is visible also an earthworm fecal pellet (arrow).

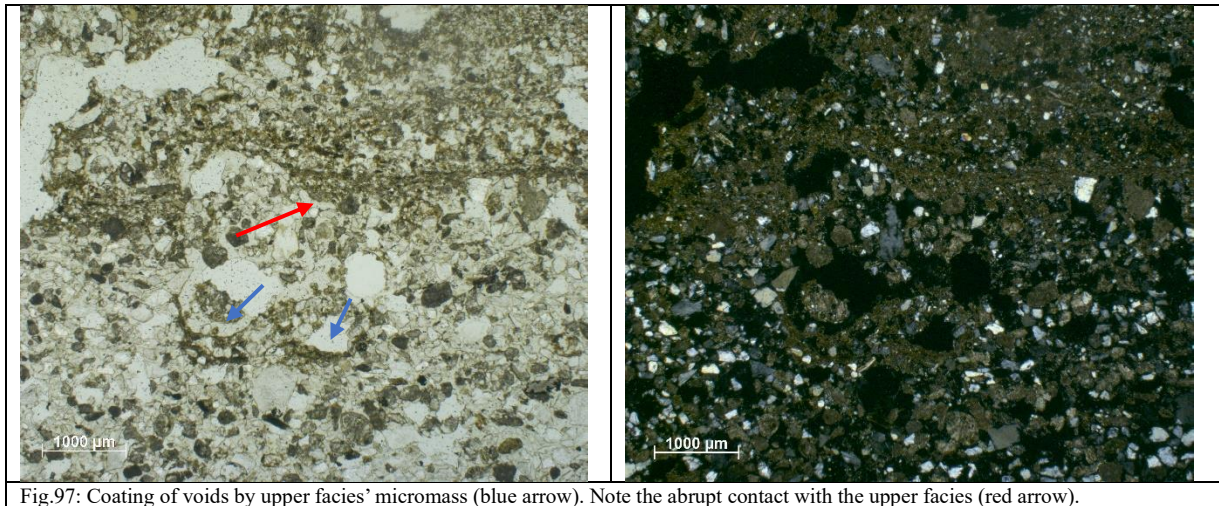


Fig.97: Coating of voids by upper facies' micromass (blue arrow). Note the abrupt contact with the upper facies (red arrow).

c)

This facies present a banded fabric and its microstructure ranges from vughy to vesicular (fig.98-99). The porosity is high and mainly composed of vesicles and vughs with both regular and star shapes, clearly seeable under the microscope are also coarse elements in transition to vughs (fig.100), while vesicles have a sub-horizontal referred distribution pattern (fig.98-99); few channels are also present.

The fine fraction ($c/f_{40\mu m}$) occurs mostly as aggregates of heterogenous size (fig.98-99) which present an inner spongy microstructure and often quartz grains (size $<150 \mu m$) embedded in them. The micromass color ranges from light to dark brown and presents a fibrous aspect referred to the color change (the darker micromass displays a fibrous pattern), the micromass b-fabric has been identified as speckled (fig.104).

The coarse/fine related distribution pattern range from enaulic to coarse monic, the coarse: fine ratio is very high.

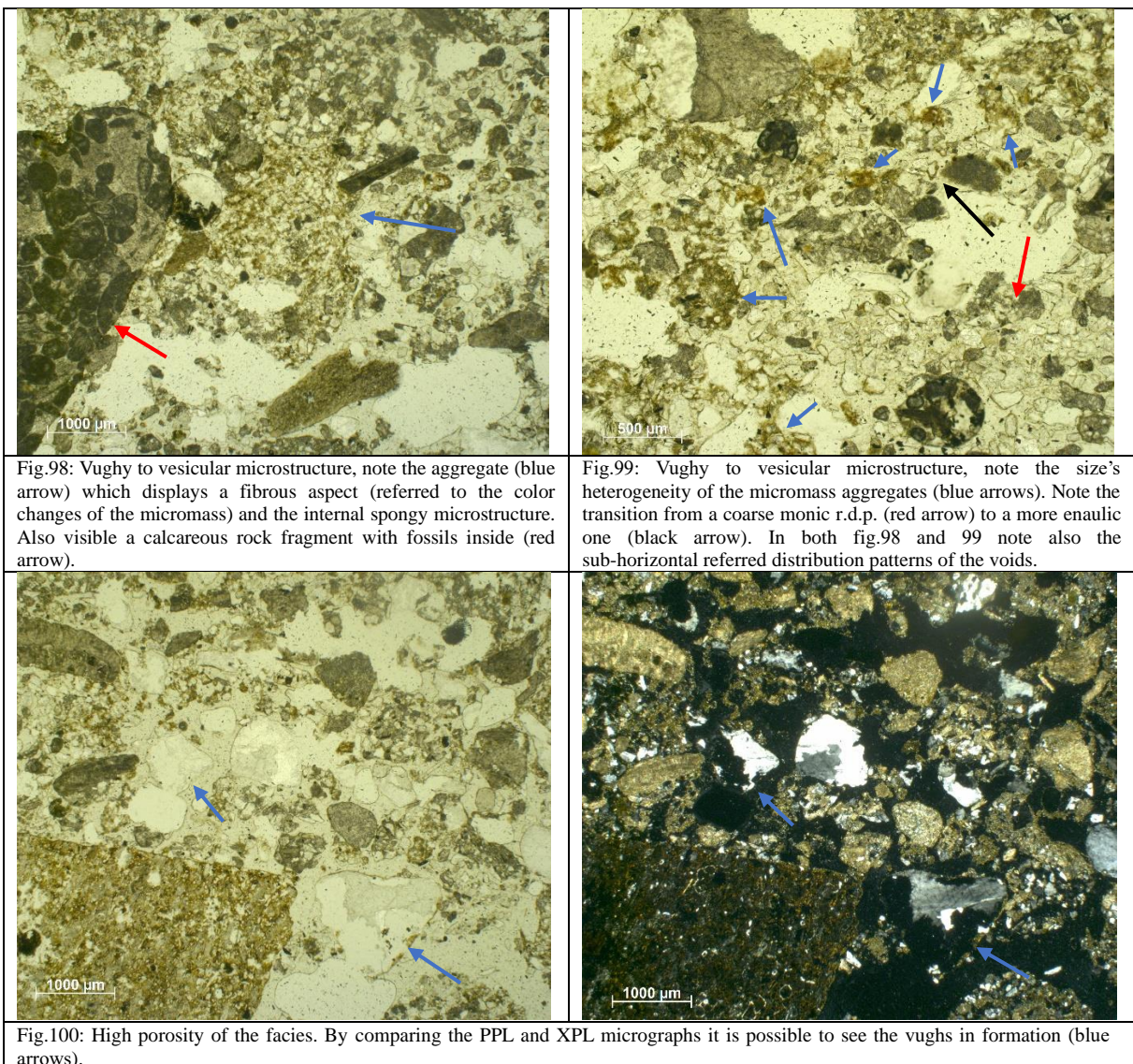
The coarse fraction has been divided into two different partial fabrics:

1. same lithology, arrangement and sizes of the facies *d* but here it presents a higher degree of porosity.
2. coarser elements (medium to very coarse sand size): they show a high heterogeneity in both lithology and size. On the opposite side the shapes of the elements are quite homogeneous (high degree of sphericity) except for some elongated grains (probably related to their structural inner morphology). Some lithological types that were possible to distinguish are: carbonate rock fragments (some fossiliferous) with different grained textures; silicates rock fragments (flint in particular) and quartz minerals. All these

elements show a high degree of weathering. The carbonate rocks seem under dissolution (fig.103) and those with a coarser grained texture (possibly dolomite) show often a micritic capping (fig.102). The silicates rocks often present an alteration rim (fig.101); while the alteration of some quartz grains seem to be leading to the formation of star-shaped vughs voids (fig.100).

3. Aggregates of cemented calcitic matrix (micrite showing calcitic crystallitic b-fabric, fig.105).

For what concern the pedofeatures earthworms' fecal pellet and silt cappings have been identified (fig.102-103).



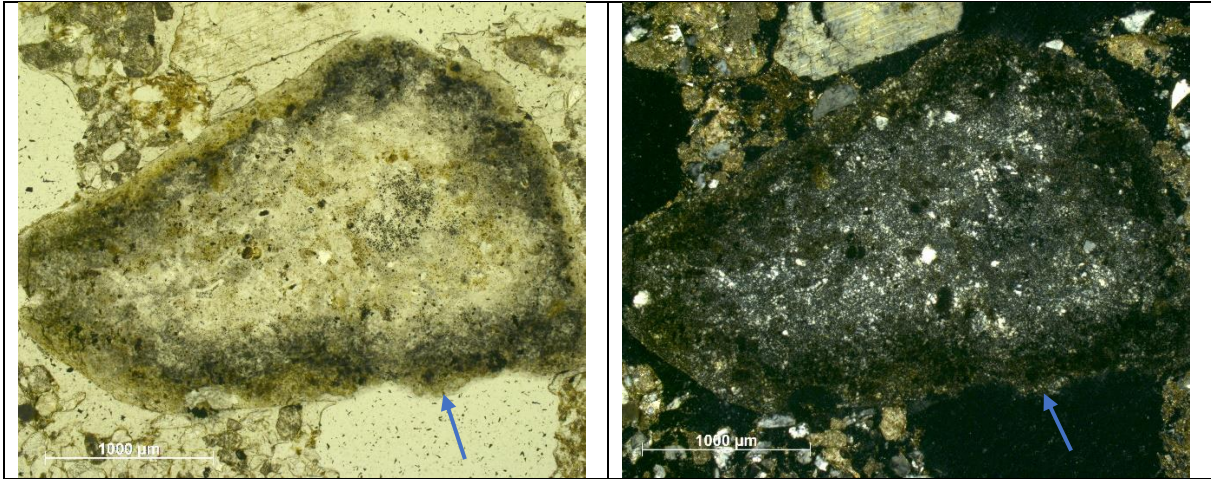


Fig.101: Flint rock fragment with a well-developed alteration rim (blue arrow).

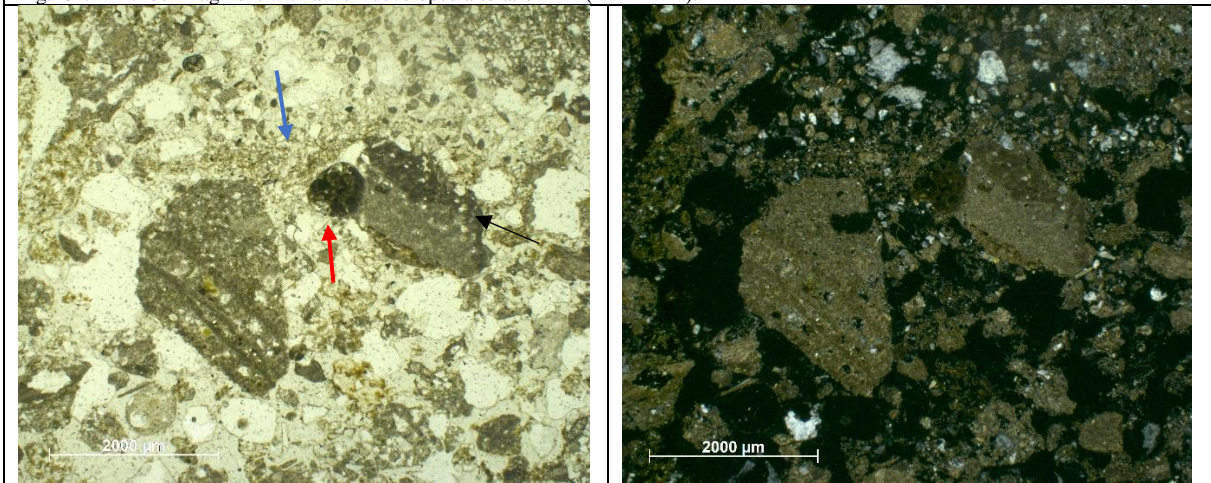


Fig.102: Silt link capping on two carbonate rocks (blue arrow). Fecal pellet (red arrow) in contact with the fragment on the right. The same fragment show also a micritic capping (black arrow).

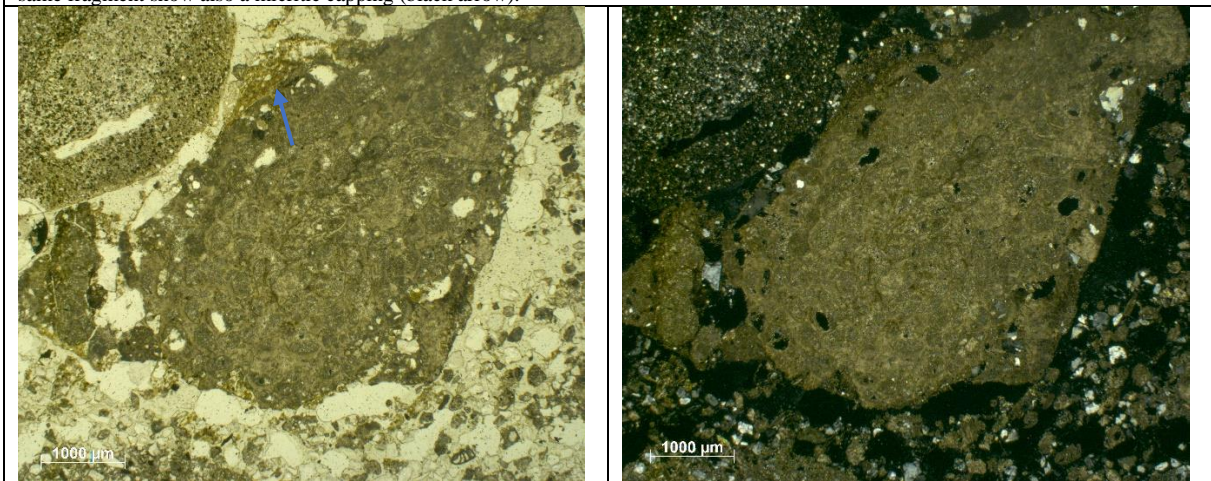


Fig.103: Silt capping (arrow) on carbonate rock fragment under dissolution (roughness of the surface).

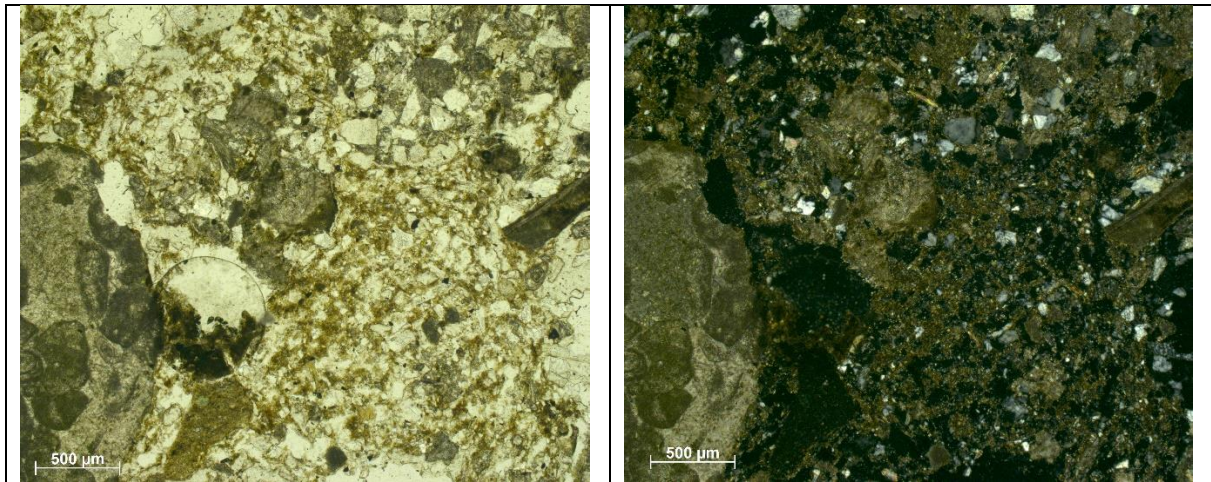


Fig.104: Same aggregate showed in fig.98, note the spackled b-fabric in XPL.

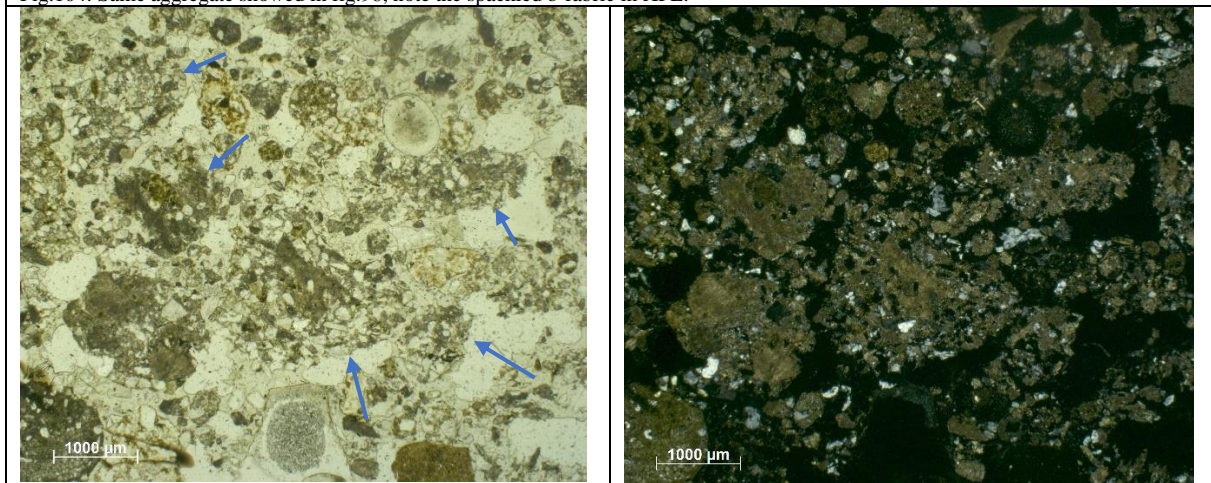


Fig.105: Aggregates of cemented calcitic matrix (blue arrows).

b)

This facies is highly homogeneous compared to the other facies present in the section.

The groundmass of this facies is composed of a yellow to brownish micromass with a speckled aspect and crystallitic b-fabric (fig.106). As for the previous described facies the fine fraction also includes quartz grains smaller than 50μm (fig.106).

In this micromass are embedded coarser elements ($c/f_{50\mu m}$) of two different types:

1. quartz grains bigger than 50μm (poorly represented).
2. carbonate rock fragments (fig.107). Characterized by a high homogeneity in the lithology and a high heterogeneity in sizes (up to 2,5 mm, only few elements overcome 500 μm), the coarser elements present quartz grains and often fossils inside; they present an angular to sub-angular shape and a degree of sphericity that increases with the decreasing of the sizes, they seem under weathering conditions due to the rough aspect of the surface (probably dissolution). All the coarse elements have a

random basic distribution pattern.

The c/f related distribution pattern result to be open porphyric. This facies express a spongy microstructure in all its area whose continuity is often interrupted by channels and vughs of high heterogeneous sizes (the porosity of the facies is more appreciable in the scan). The coarse:fine fraction ratio is very low.

Fecal pellets are present, often inside channels (fig.108).

The upper contact with facies *c* is gradual and characterized by a progressive increase in the size of the quartz grains and a contemporaneous decrease in the micromass (fig.109).

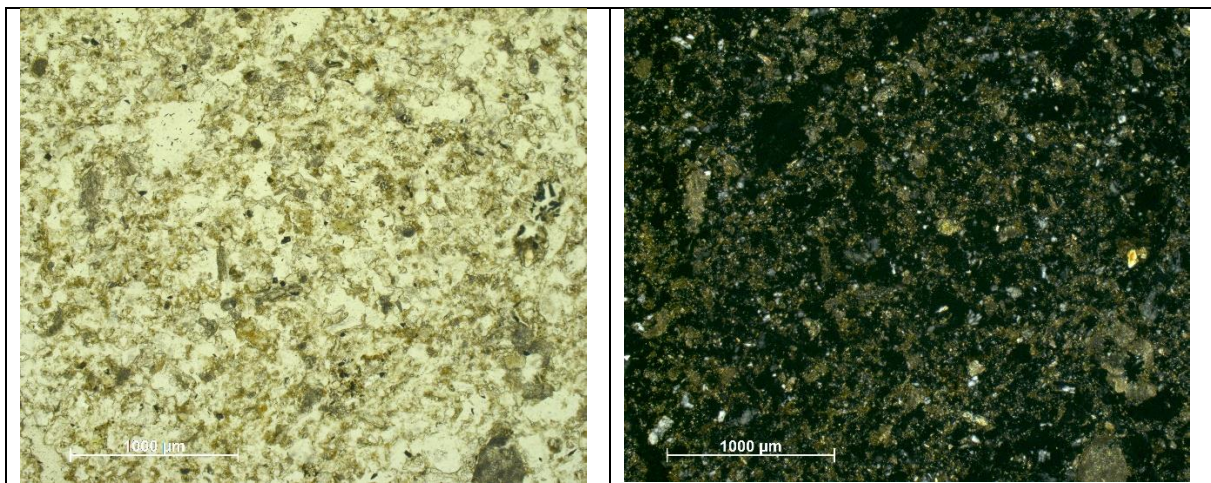


Fig.106: Spongy microstructure. Note the yellow to brownish micromass with a speckled aspect in PPL, and the small quartz grains described as part of the fine fraction. The crystallitic b-fabric is visible in XPL. Some coarse elements (carbonate rock fragments) are also present (open porphyric r.d.p.).

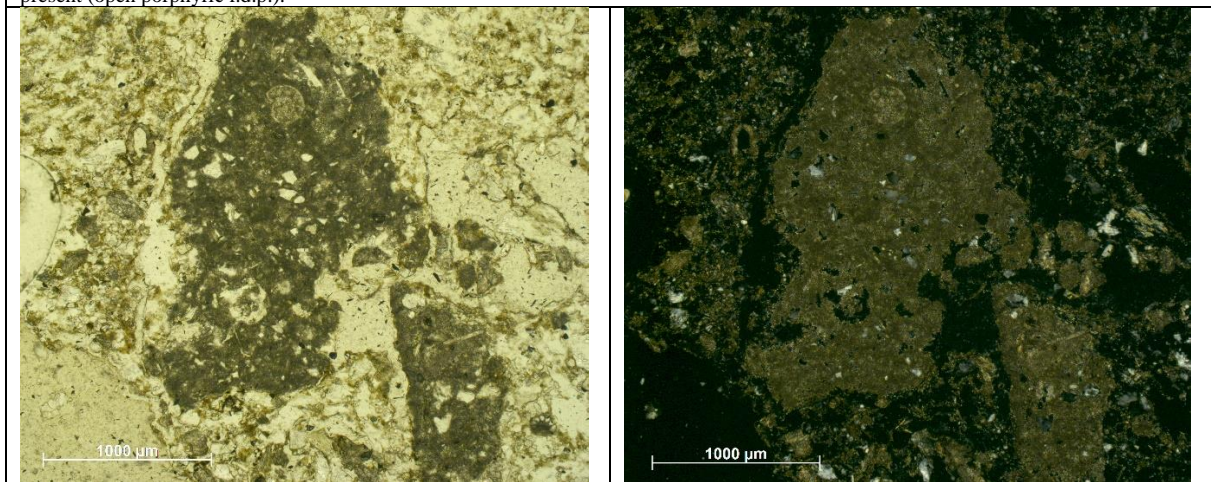


Fig.107: Carbonate rocks fragments. Note the quartz grains and the fossil present in them and the rough surface which may indicate a dissolution.

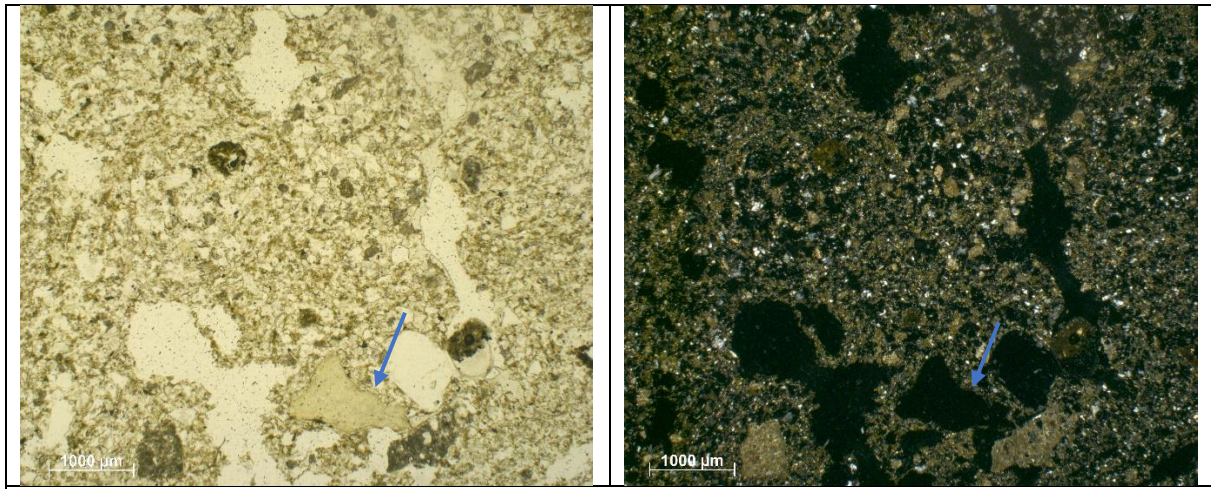


Fig.108: Spongy microstructure with channels and vughs overlapping. Note the phosphatic grain (arrow) which could be in second position due to bioturbation (the micrograph is taken close to the lower contact of the facies).

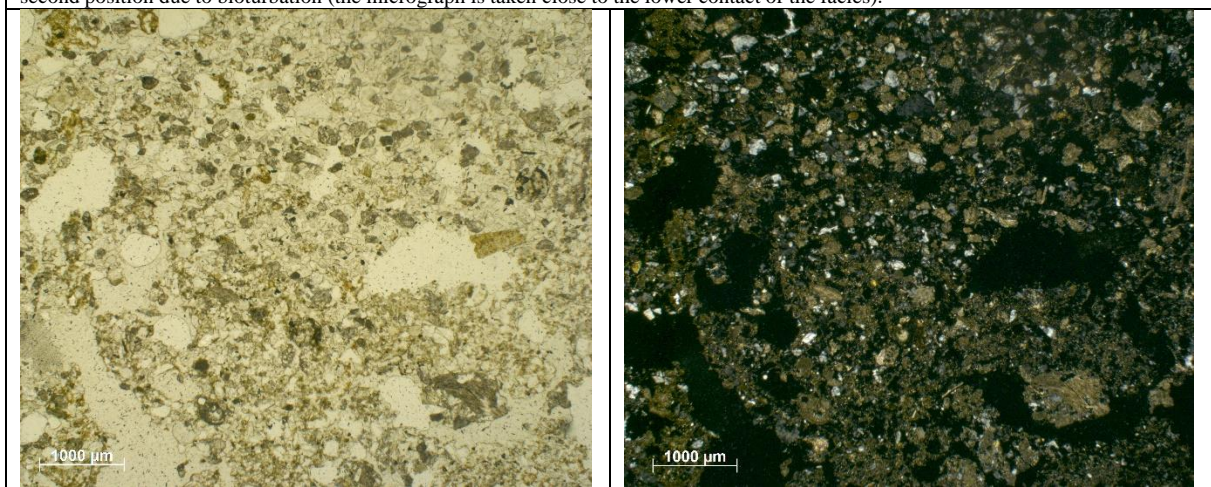


Fig.109: Upper contact of the facies, note the progressive increase in quartz grain sizes and the progressive decrease of the micromass.

a)

The facies at the bottom part of the thin section has a dominant spongy microstructure (fig.110). The continuity of it results to be often interrupted by bigger poroids, channels and voughs (more appreciable looking at the section's scan).

The groundmass ($c/f_{50\mu m}$) is composed of a light brown to dark brown micromass with a straited aspect and a crystallitic b-fabric (exception for the dark brown part of the micromass that shows a monostriated to undifferenced b-fabric).

Three type of c/f related distribution pattern have been identified: fine monic, open to single spaced porphyric and close coarse monic. The coarse monic could be seem like a depletion matrix pedofeature but it is present throughout all the section and seems to have its own depositional origin. These three patterns have been described as three different partial fabrics:

1. Close coarse monic (fig.111): identified by a basic single grain microstructure, the

micromass result to be completely absent. The coarse fraction is mostly composed of quartz grains of homogenous size (mostly fine to medium sand) and high heterogenous shape; other lithotypes are also present (carbonate rock fragments), compared to the quartz fraction they present an overall slightly bigger size (mostly medium sand) and a rounded shape. The porosity of the unit is mostly composed of simple packing voids, few vughs are also present (up to 300 μm). The distribution and orientation patterns of the elements is random. While the partial fabric as a whole has a clustered distribution pattern, whose groups present a lenticular shape.

2. Fine monic (fig.110): the micromass color range from light brown to dark brown and the change in color seems to have a discontinuous banded basic distribution pattern (fig.112) (with random orientation). In addition to the micromass also quartz grains smaller than 50 μm have been considered part of the coarse fraction. A high porosity characterizes this partial fabric, the spongy microstructure is often overlapped by channels and vughs.
3. Porphyric (fig.112): appears between the two fabric unit described above as a transitional unit.

The fine monic fabric is highly more present compared to the coarse monic.

Biogenic coarse elements: four coprolites are present in the section, three of them (fig.113-114-119) seem so be hyena's due to the pale yellow-grayish color of their groundmass, the isotropic behavior in XPL, the presence of bone fragments and quartz grains embedded in them, and their porosity composed of numerous vesicular pores (Brönnimann et al in Nicosia Stoops, 2017). These vesicles are often interconnected by cracks and channel-like voids some of which present micromass coating with a porostriated b-fabric (fig.118).

The fourth one is quite different from the formers, notably in size and porosity, it is quite smaller (1,5 mm max. measurement) and doesn't present vesicular voids but elongated ones (its identification results more difficult).

To be noted: three coarser rock fragments are visible at the very bottom of the section. Presence of phosphatic grains (fig.113-116) (to be confirmed) that range from 940 to 460 μm , located close to the coprolites described above. They have been identified as phosphatic grains based on their color (yellowish), isotropic behavior in XPL and the presence of coprolites (quite often their presence is associated also with the presence of phosphatic grains (Horwitz and Goldberg, 1989; Friesem et al., 2022) but without using the blue-light fluorescence technique it seems difficult to confirm this hypothesis.

Pedofeature: fecal pellets produced by earthworms are present in channel voids (fig.117).

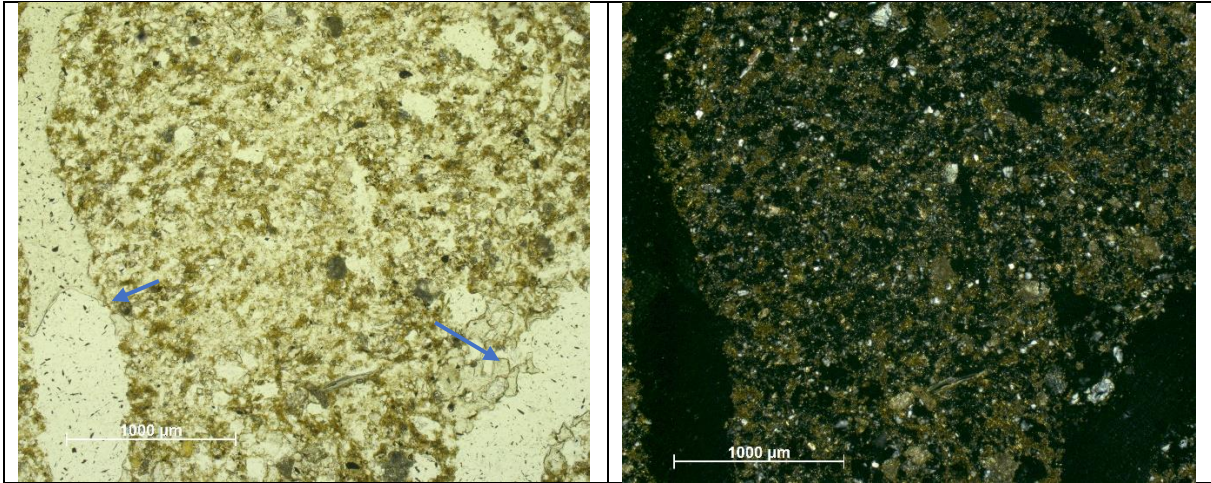


Fig.110: Spongy microstructure and channels (arrows). The light brown color is noticeable in PPL while the crystallitic b-fabric is noticeable in XPL.

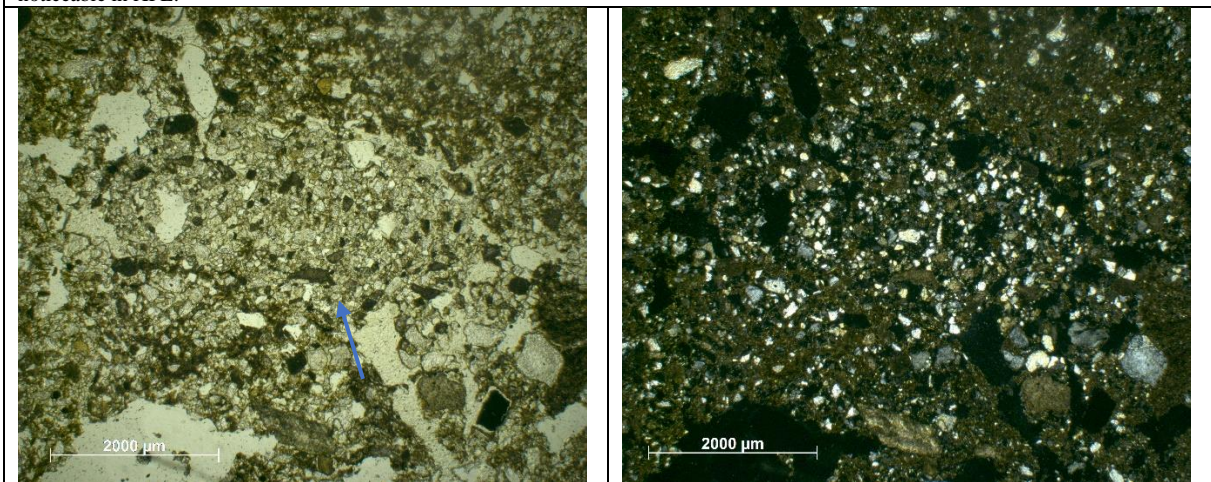


Fig.111: Single grain microstructure (arrow), note the absence of micromass and the homogeneity of the sizes.

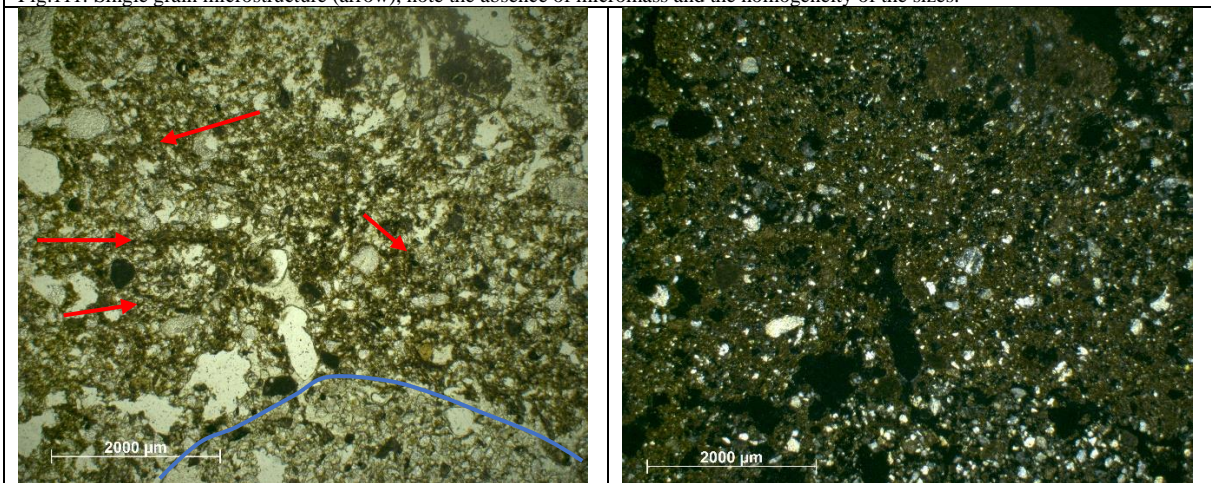


Fig.112: Porphyric and coarse monic related distribution patterns contact marked by the blue line. The banded basic distribution pattern of the darker micromass (red arrows) is noticeable in PPL.

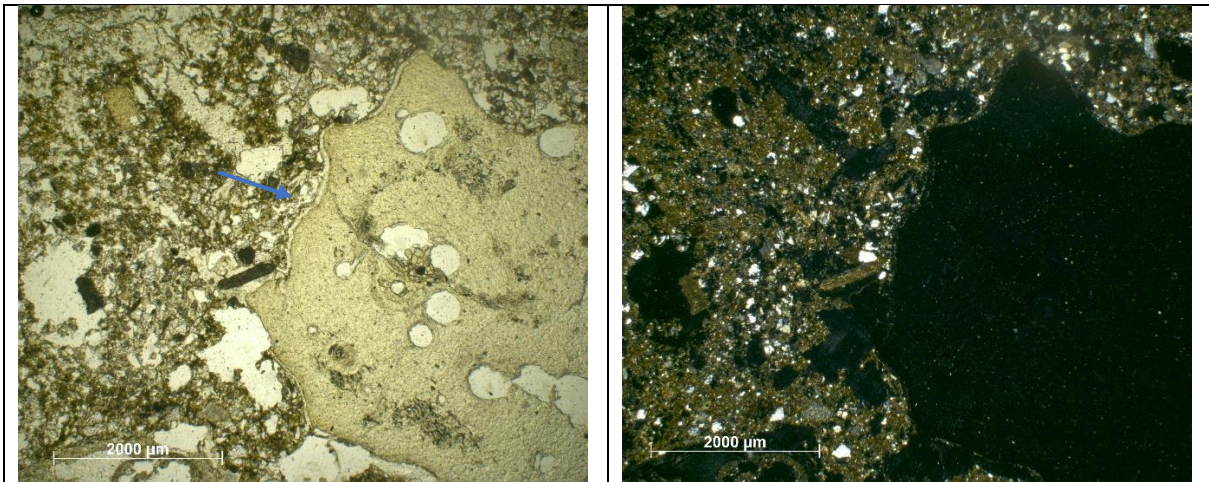


Fig.113: Presumed hyena's coprolite and phosphatic grain (arrow). Note the characteristic vesicular porosity of the coprolite in PPL and the isotropism of both elements in XPL.

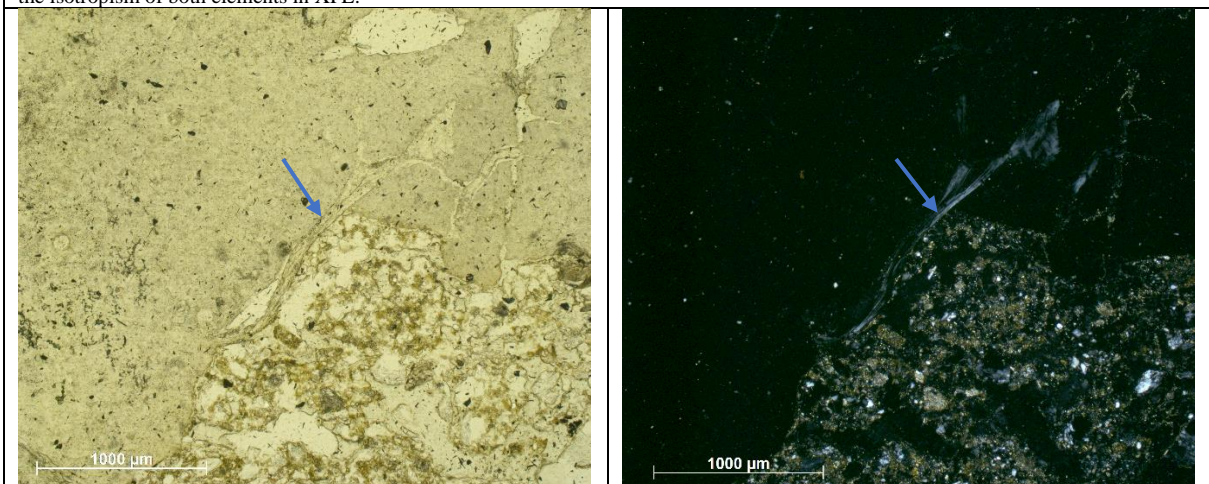


Fig.114: Particular of a bone preserved in the hyena's coprolite (arrow). Note the low interference color of the bone in XPL due to the alteration undergone during digestion, the fibrous fabric of the bone are still clearly visible.

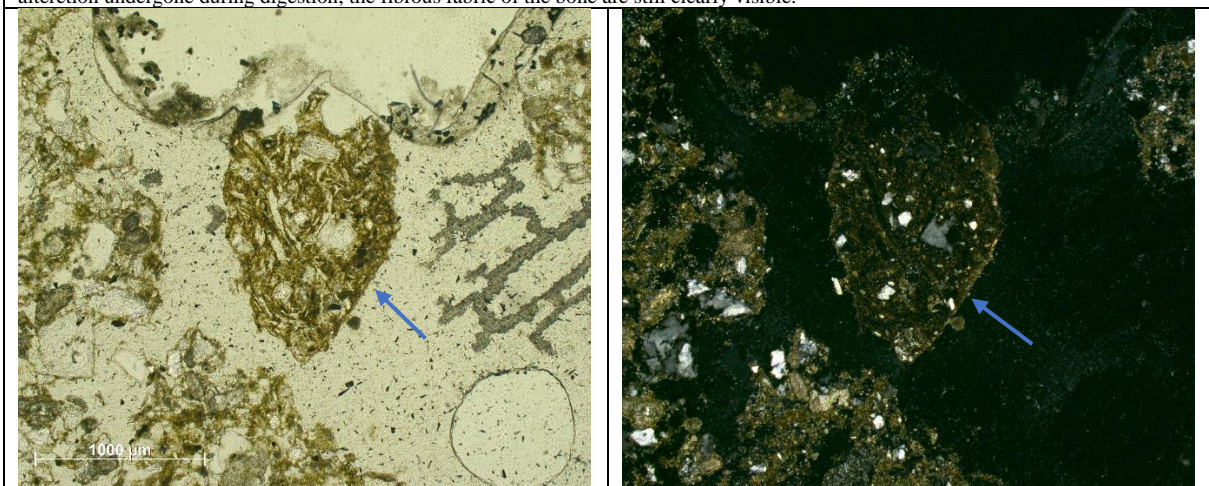


Fig.115: Unkown coprolite (arrow).

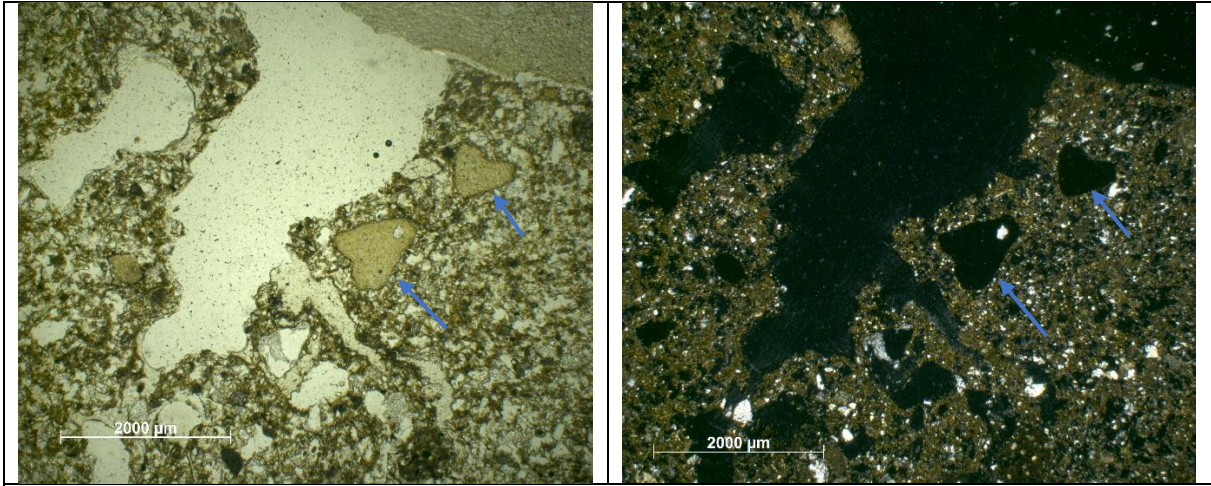


Fig.116: Two presumed phosphatic grains (blue arrows), top right of the section is visible a part of a hyena's coprolite. Note the isotropism of both elements in XPL.

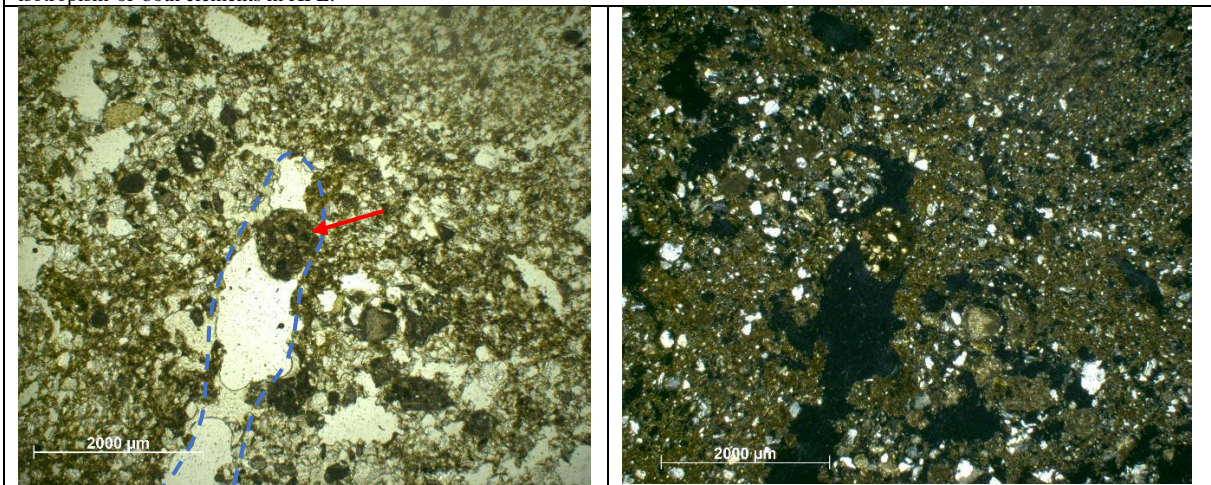


Fig.117: Fecal pellet (arrow) in a channel (dashed line). Appreciable also the complexity of the microstructure. Top right: spongy microstructure and fine monic r.d.p. becoming more porphyric going thword the center (just above the fecal pellet). Note also the banded basic distribution pattern of the darker micromass (in PPL).

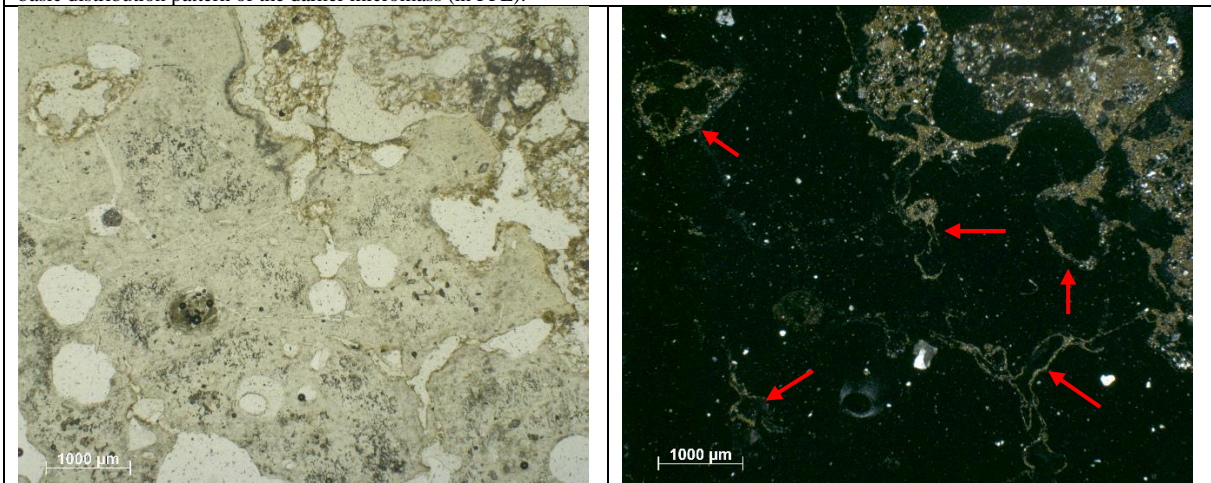


Fig.118: Presumed hyena's coprolite, note in the micromass coatings in the coprolite's voids and its porostriated b-fabric in XPL (red arrows).

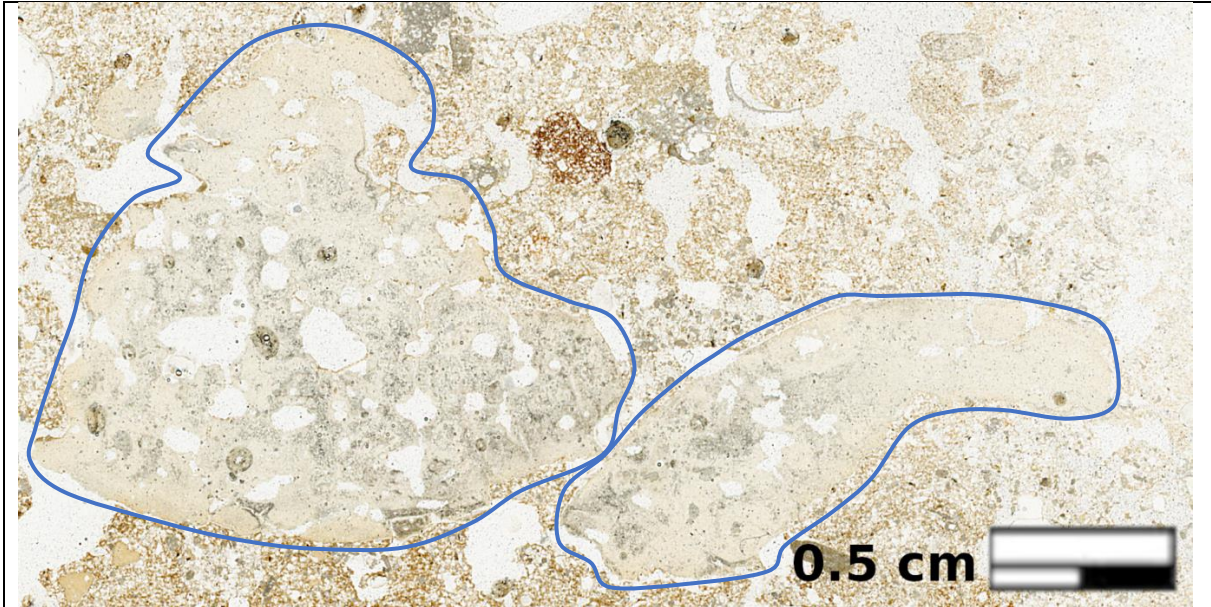


Fig.119: Hyena coprolites (marked by the blue lines). Note their characteristic vesicular porosity and their yellowish-greyish color.

MM4

Stratigraphic description of the block

There have been some difficulties encountered in observing the MM4 block.

The block (as also the section) doesn't present the orientation mark (north direction), but it was possible to reconstruct it. The back side of the block results to be in fact the one exposed during the sampling, it therefore results to be the block's side facing east. Looking at the front of the block, the north should then be on its left side.

Another difficulty in the observation has been related to the block's face. The block in fact doesn't present a flat and homogenous surface, as visible in fig.124, which made it difficult to identify the units in that area. This structural problem could be related to a problem in drying the block before impregnation with resin, which for this reason may have partially failed in the coarse fraction layers.

On the other side the height of the block match perfectly with the height of the section so, despite the observational problems of the block, we know for sure that the section is representative of all the stratigraphy present in the sample.

From a stratigraphical point of view the block has been divided in four units, one of which (unit *III*) has been isolated only in function of the structural problem (described before) of the block. From top to bottom we find:

- I.* The unit is quite homogeneous at this scale of observation, it presents a brownish matrix incorporating few lighter bands. Black stains have also been observed with the help of a magnifying lens.
- II.* The unit present coarse elements, in particular we find pebbles (fine gravel size) at the top and sandy material at the bottom (fig.120). The pebbles are well rounded and often present black staining at their borders (fig.120). High heterogeneity in the element's lithology is noted. The lower contact of this unit is marked by a crack (fig.124-120), which is present also in the section (fig.125-127). The origin of the crack could be linked to the sampling or still to fabrication problems.
- III.* A banded fabric is visible at this scale of observation (fig.121), composed by an alternation of fine sand and fine material in the top part and a layer of coarse material at the bottom. Here, too, the coarse elements present a great heterogeneity in their lithology, but they appear to be less spherical. The lower contact of the unit is abrupt and defined by the beginning of the block's structural problem. Due to this condition, it is difficult to understand the real continuity and vertical extension of this unit.

- IV. Unit isolated due to the absence of a flat surface to be observed. The unit results to be composed of gravels and sand with a random distribution (this, though, could be linked to the difficulty in the observation). Some bands are slightly visible (fig.122), marked by a difference in color. The presence of any other bands results to be difficult to observe.
- V. The beginning of this unit is marked by the end of the structural problem, and so by a new well observable surface. The geometry of the unit is then to be related to the morphology of the latter. The unit present a banded fabric composed of fine bands (sand and fine material, fig.123). The gravel's class size is totally absent in this unit. The coarser elements present (medium sand) displays a tabular shape and a sub-horizontal distribution pattern.



Fig.120: Detail of units *I* and *II*. Note the homogeneity of *I*'s matrix, the sandy layer at the bottom of *II* (blue arrow). Note also the black capping on the reddish pebble (red arrows).



Fig.121: Detail of unit *III*. Note the banded fabric.

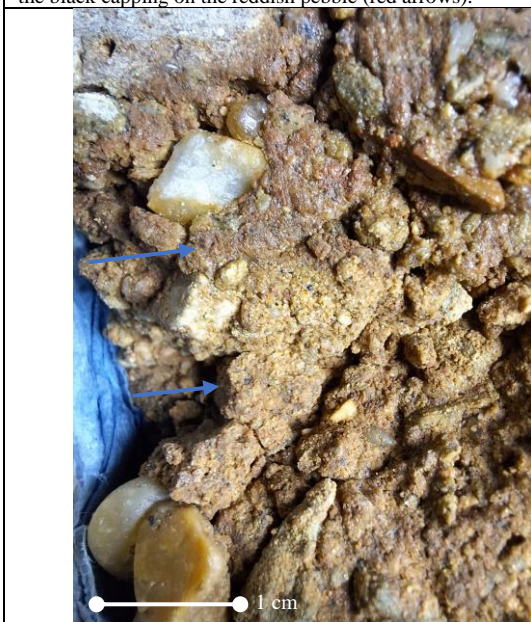


Fig.122: Detail of unit *IV*, marked by the absence of a flat surface. Slightly visible the color bands (arrows).



Fig.123: Banded fabric present in unit *V*.

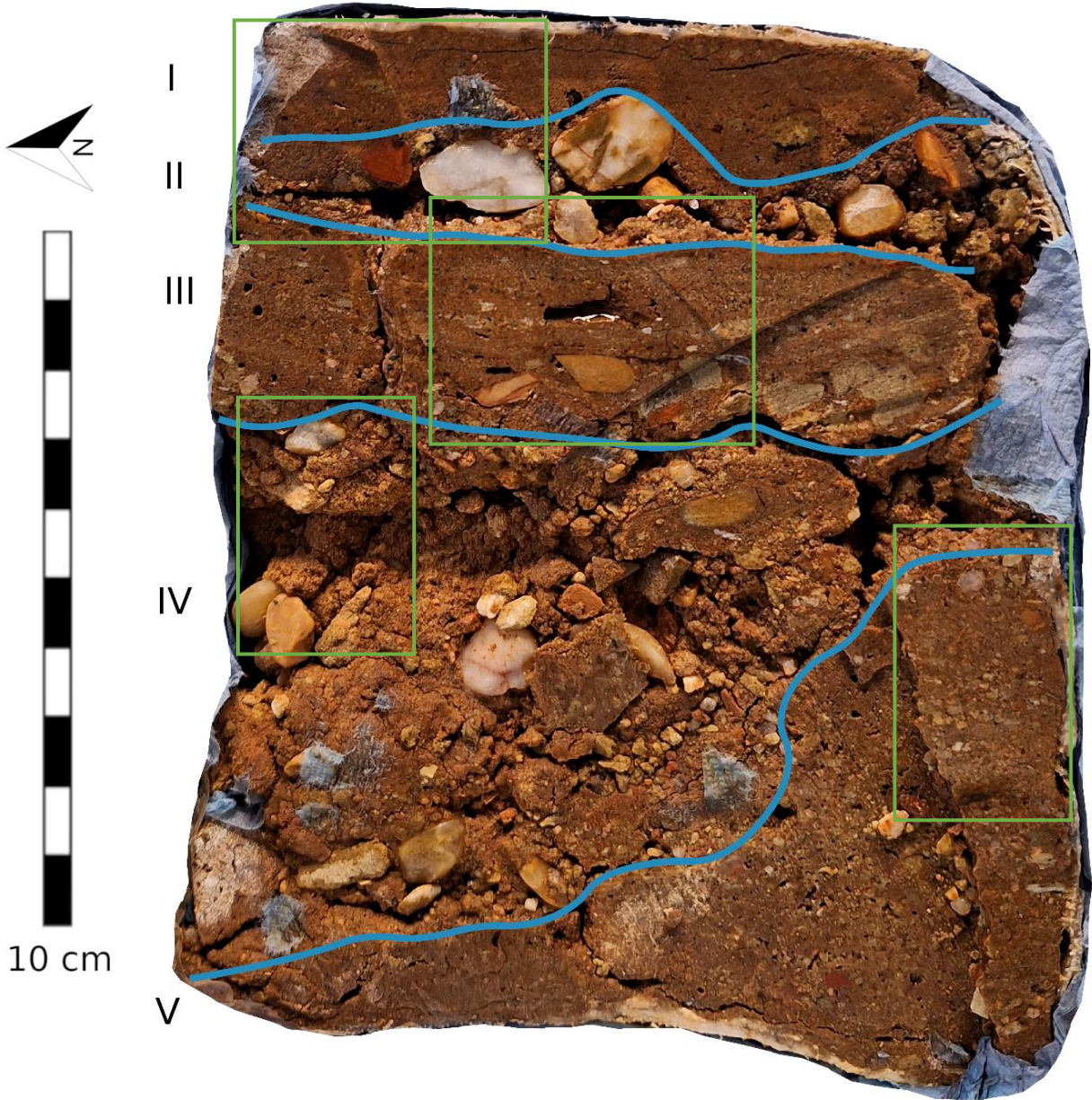


Fig.124: MM4 block. The blue lines indicate the contact between the identified units. The green rectangles indicate the areas from which the following pictures were taken.

Mesoscopic description of the thin section

From a mesoscale point of view the section has been divided in four facies. Their subdivision was based mostly on the degree and type of porosity displayed, and the fabrics mesoscopically visible.

From top to bottom we find:

d) This facies is characterized by banded fabric. The porosity visible at this scale of observation is composed of linear plane voids running horizontally and vertically throughout the facies. One of these horizontal planes is clearly visible also in the block (fig.124-125-127).

Few coarser elements are present in the facies with a random distribution pattern, the elements that present an elongated shape present a sub-horizontal orientation pattern. The bands that give rise to the banded fabric differ between each other (at this scale of observation) on granulometry and fine fraction's color. On the top part of the facies the bands present darker lines (black color). Going upwards the fabric of the sediment seems to change but the section is too thin to be observed.

c) This facies has been isolated from the other on the base of the great void which occupies almost 50% of this area. The facies has a granular structure at this scale of observation. The solid phase is composed of aggregates (highly heterogeneous in size) and few single elements (rocks and minerals) floating with a random pattern in the void's area. Looking at the uppermost aggregates present in the facies it is possible to identify some continuity in the fabric with the lowermost part of facies *d* (fig.126). In the biggest aggregates also, inner banded fabrics are visible, still very similar to the one present in *d*.

b) The porosity of this facies is well distributed in the facies' area. The structure can be described as granular (c/f rdp coarse to fine enaulic), and the elements (both aggregates and grains) seem to never be in contact with each other (as for *c* all the elements float in the voids' space). Also, here a slightly visible bedding is present, linked to the presence of a brownish micromass (in form of aggregates, but with a linear distribution pattern).

a) This facies present a complex structure that ranges from channel to vesicular. These two types of voids are the most present in the facies and their spatial distribution is characteristic, the channel structure is mostly present on the low and right part of the facies while the center and upper-left part of it presents a vesicular one. At this scale of observation, the channels present a sub-parallel basic orientation pattern, most of them presenting the same degree and orientation of inclination with reference to the thin

section. The matrix present in the facies is composed of a fine fraction with colors that range from pale yellow to brownish, few small reddish aggregates are also present. The coarse fraction (always at this scale of observation) is composed of two types of elements (differentiation based on their shape). We find rounded elements that seems to have a random distribution in the facies and elongated ones that displays a sub-parallel basic distribution pattern with a low degree of inclination in the same direction of the channels and vesicles (described earlier).

The lowermost part of the section seems to present a change in the fabric but is too thin to be described, in addition the changes could be related simply to the thickness variable.

Based on these observations we can assume some connection between the block and the section. In particular on the upper part of both of them we find the same crack. On the block this crack is related to the lower contact of unit *II*, whose abrupt contact could have acted as a line of fragility and generated the crack during the sampling.

For what concerns the structural problem presented during the block's description, the area of unit *IV* of the block seems to match with the facies *b* and *c* of the section, which display a high degree of porosity and a granular microstructure composed of aggregates freely floating in the void's space. Based on these observations we could argue that the fabric displayed in these facies of the section could be linked to a problem in the fabrication of the latter, mostly because the large aggregates present in facies *c* exhibit a banded fabric that appears to be in continuity with that of facies *d*, and they display only a very low degree of rotation (fig.126). Besides these observations the facies will still be described as the others.

For the other connections, facies *d* has been related to unit *II* and *III*, while facies *a* to unit *V*.

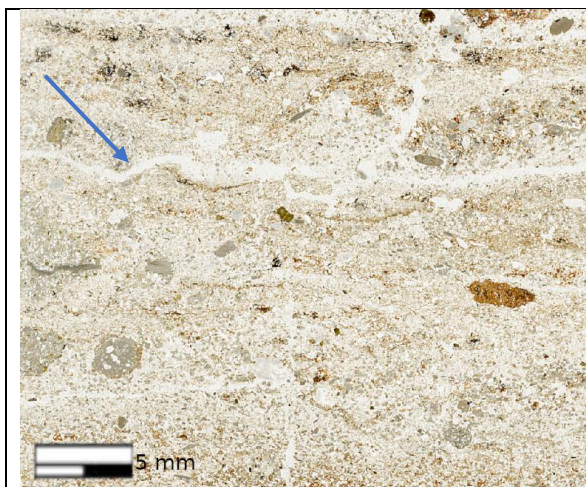


Fig.125: Detail con the section's scan. Note the banded fabric of facies *d*, and the horizontal planar void shared with the block (arrow).

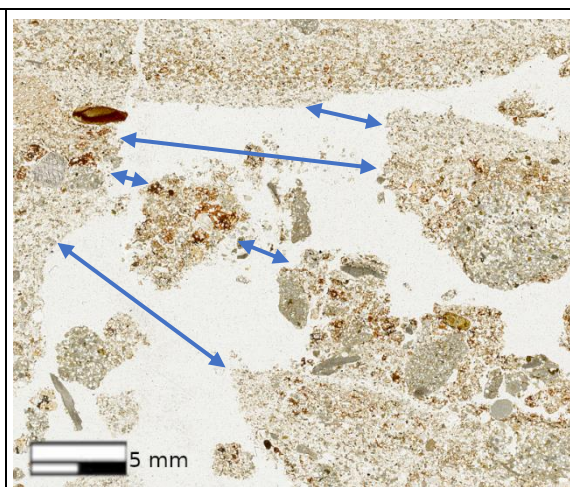


Fig.126: Detail of *d-c* contact. Note the continuity (marked by the arrows) of the banded fabric between facies *d* and the inner fabric of facies *c*'s aggregates.

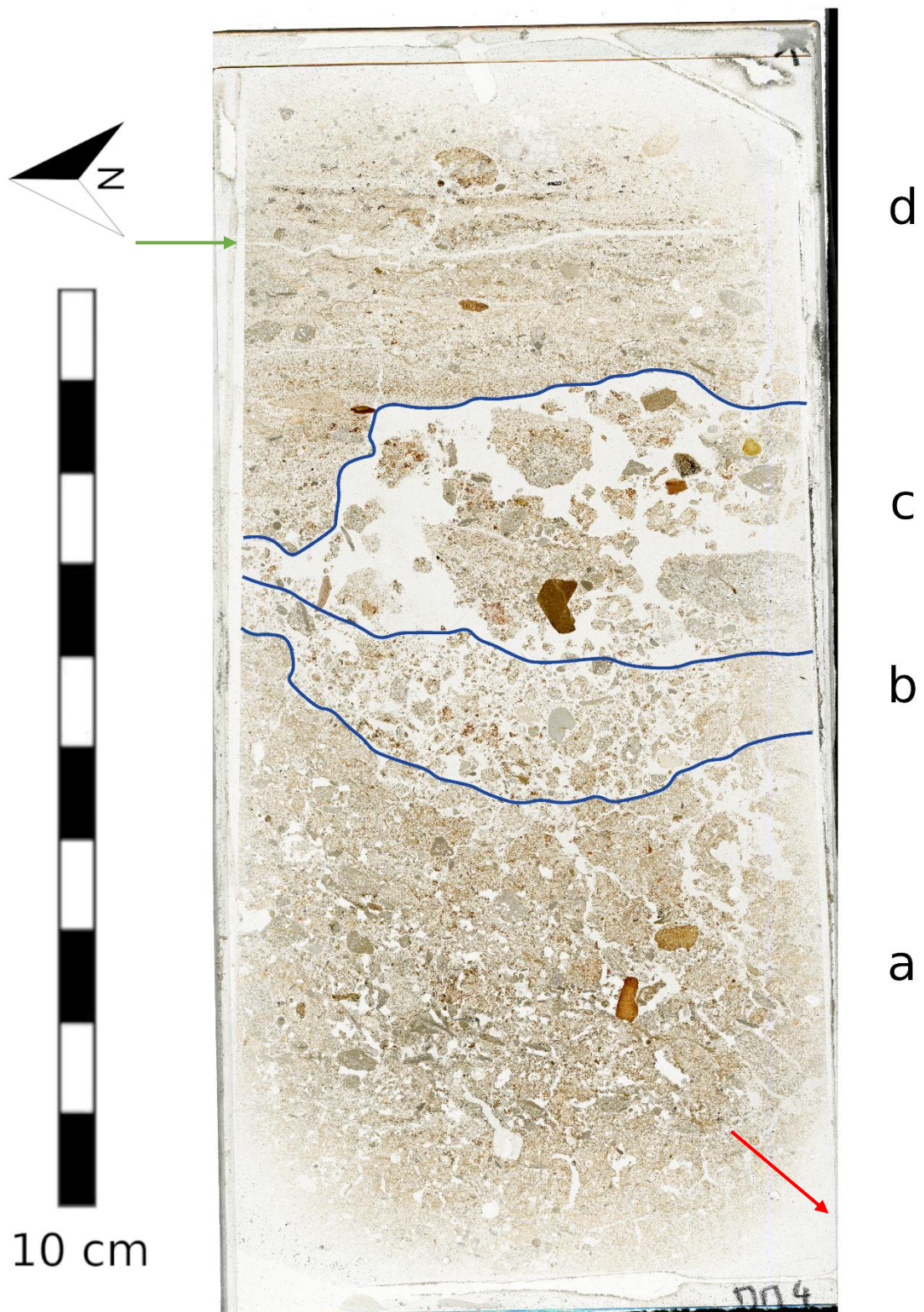


Fig.127: MM4 thin section, the continuous lines mark the limit between the facies. In facies *a* note the common degree of inclination (approximate inclination indicated by the red arrow) of the channels. In facies *d* the green arrow marks the horizontal linear plane void shared with the block.

Microscopic description of facies

d)

The facies present a banded fabric composed of an alternation of bands of *sandy material* and *micromass* (fig.125). These two have been described as different partial fabric.

- *Sandy material's bands*: this partial fabric is characterized by a dominant basic microstructure (fig.128) with few areas showing an intergrain micro-aggregate microstructure. Beyond simple packing voids the porosity of the facies present also straight planes voids (more appreciable looking from a mesoscale point of view), they show a moderate to low degree of accommodation (fig.128). The sandy material close to these planar voids present a lower degree of compactness. Very few micromass is present in the facies (c/f $_{20\mu\text{m}}$), mostly under aggregate form (coarse enaulic, fig.129), and in the contacts with the *micromass bands*. The micromass displays a general brownish color, with stains of opaque material. This opaque micromass is mostly present under two different forms: as cores of some aggregates and as coatings or crusts (fig.129).

For what concerns the coarse fraction all the elements are sub-rounded and sub-spherical. An inner variability of the partial fabric is present in their lithology: the lowest bands present a high degree of heterogeneity (quartz, carbonate rocks, micas and other unidentified elements), while going upward the lithology tends to become more homogeneous, towards a higher percentage of quartz grains. All the elements fall between the size classes of fine sand and medium sand (with few elements of carbonate rock, of medium sand size). The size distribution of the elements presents a banded distribution pattern, the arrangement of the size classes is never random (fig.128).

- *Micromass' bands*: this partial fabric results to be composed mostly of micromass but presents a high degree of inner variability. Three different types have been identified:
 - On the uppermost part of the facies the *micromass' bands* present a massive microstructure with a porphyric coarse/fine related distribution pattern (c/f $_{20\mu\text{m}}$). The micromass presents a brownish to reddish color with a speckled to striated b-fabric, alongside with this type of micromass also an *one* is present, the latter mostly coming as elongated crusts and void coatings (fig.130-132). Both of them embed sand size elements, presenting the same characteristics described above.
 - Going downwards the presence of the opaque micromass decreases leaving place to a higher presence of brownish to reddish micromass, which presents itself also under aggregate form (fig.133-134), the biggest aggregates of this micromass often

shows an opaque core.

- Crusts of silty material often embedding micas grains.

Summarizing these observations, the facies show a constant presence of sandy material (well sorted with a banded pattern), which sometimes is present alone, sometimes alongside with aggregates (intergrain micro-aggregates microstructure) and sometimes embedded in fine material (porphyric related distribution pattern and massive microstructure). Between these bands, crusts of silty material or opaque micromass are often preset. Throughout all the facies the opaque material displays a reddish to orange with areas of metallic blue color in OIL (fig.135).

To be also noted, throughout all the facies, the presence of aggregates of cemented calcitic matrix (micrite showing calcitic crystallitic b-fabric, fig.133-134).

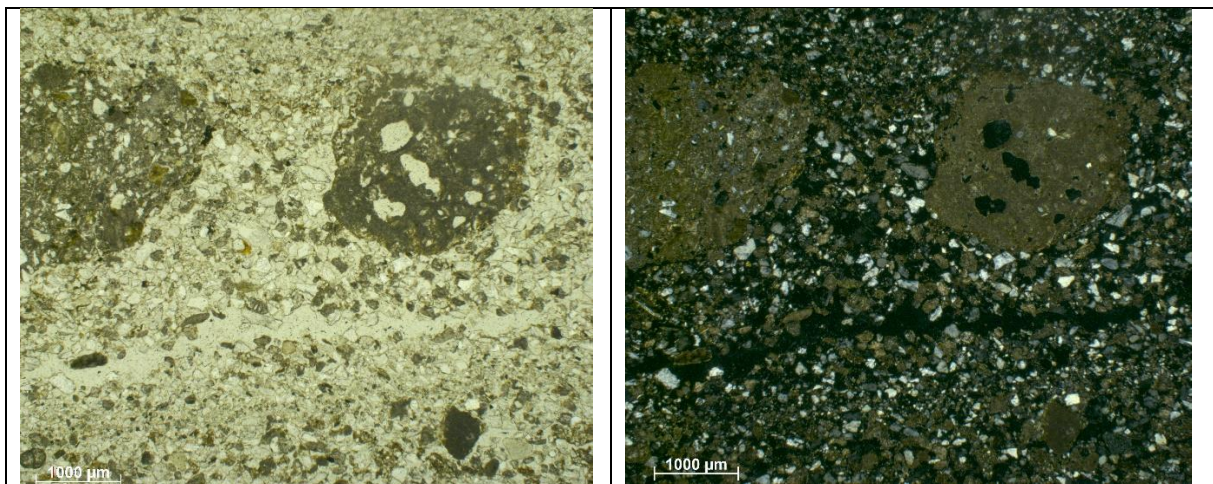


Fig.128: Basic microstructure of the *sandy material's bands*. Note high degree of sorting of the sand and the banded distribution pattern of their sorting (going upwards the elements becomes bigger).

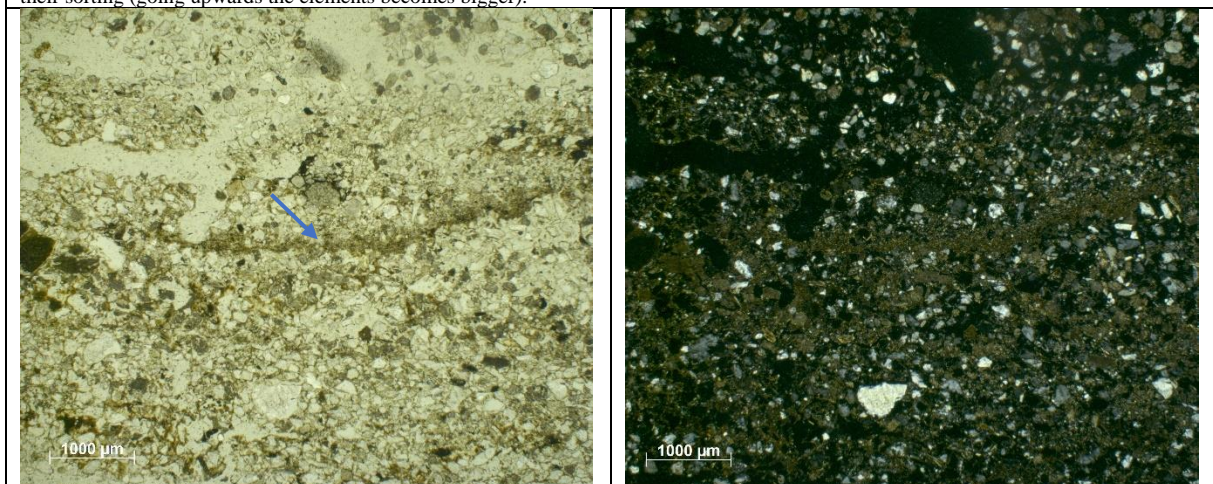


Fig.129: Silty crusts (arrow). Note the presence of small micromass's aggregates giving rise to sporadic areas with enaulic related distribution pattern.

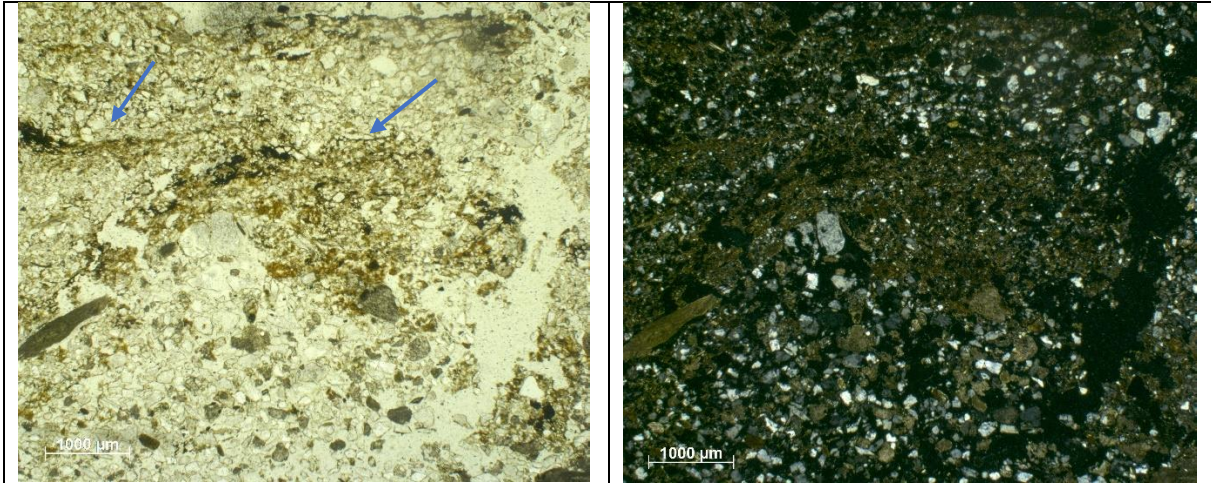


Fig.130: Silty crusts (arrows). Note the two different kinds of micromass: the opaque one and the brownish to reddish one. Note how the opaque micromass creates a sort of capping on the silty crusts.

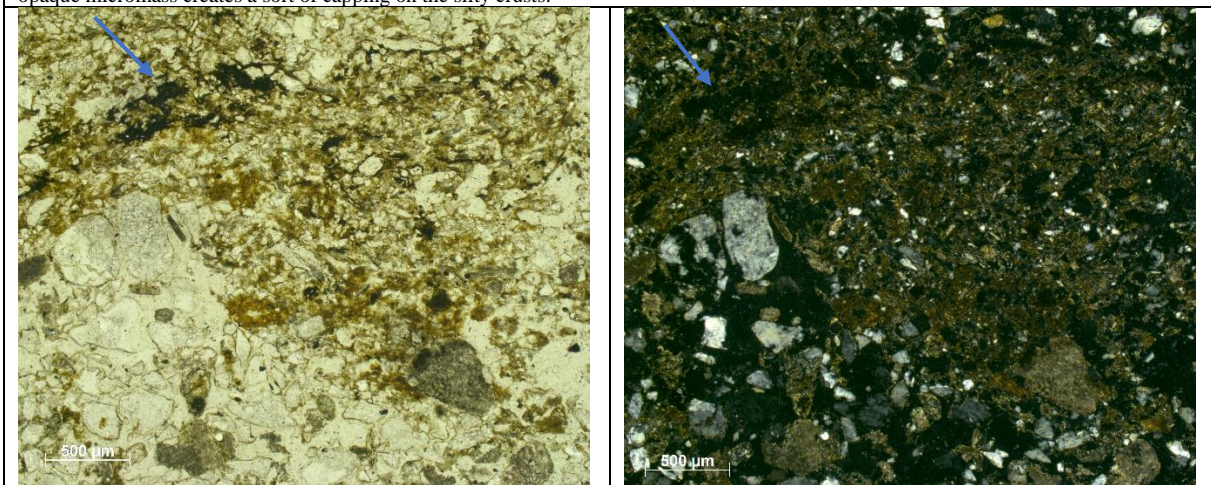


Fig.131: Zoom of fig.130. Note the opaque behavior of the micromass (arrow).

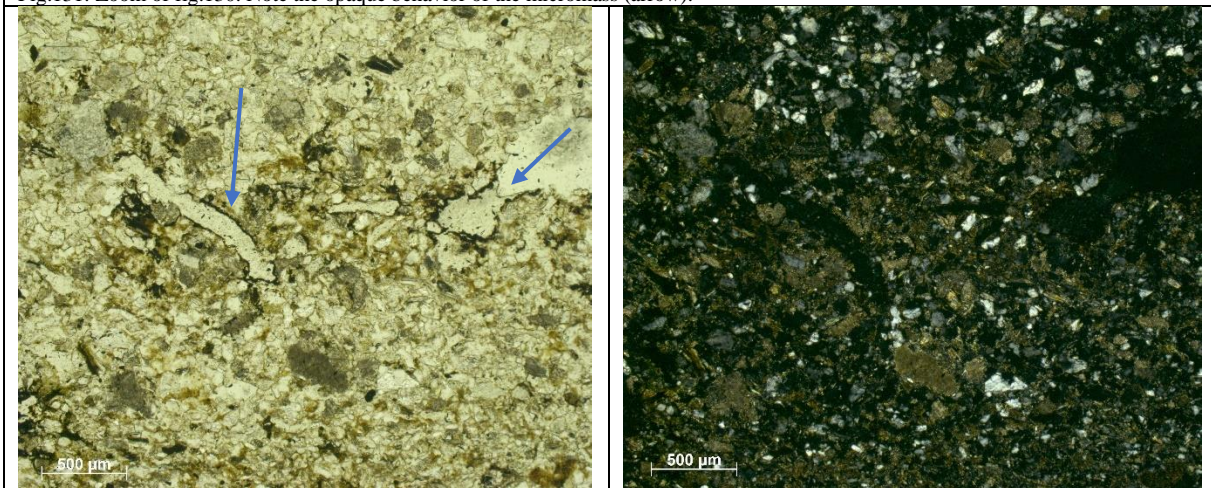


Fig.132: Void's coating by the opaque micromass (arrows).

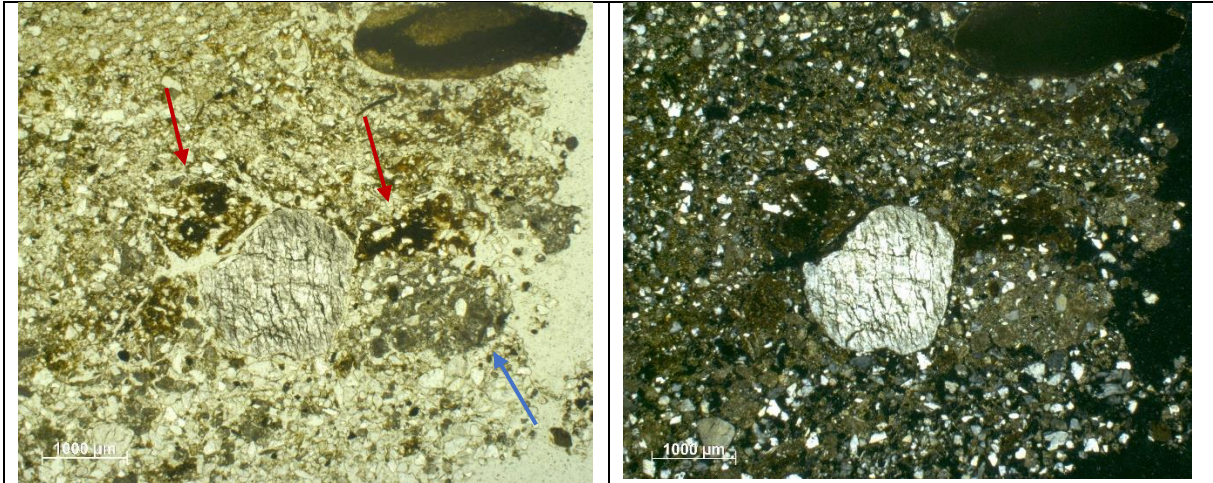


Fig.133: Aggregates of cemented calcitic matrix (blue arrow) and aggregates with opaque core (red arrows).

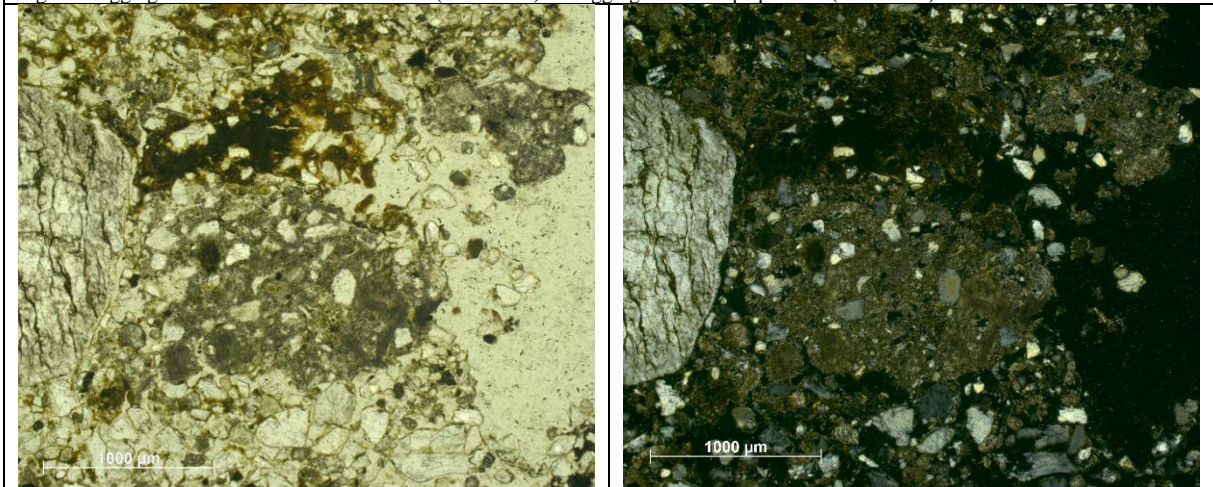


Fig.134: Zoom of aggregates of cemented matrix and aggregate with opaque core present in fig.133.

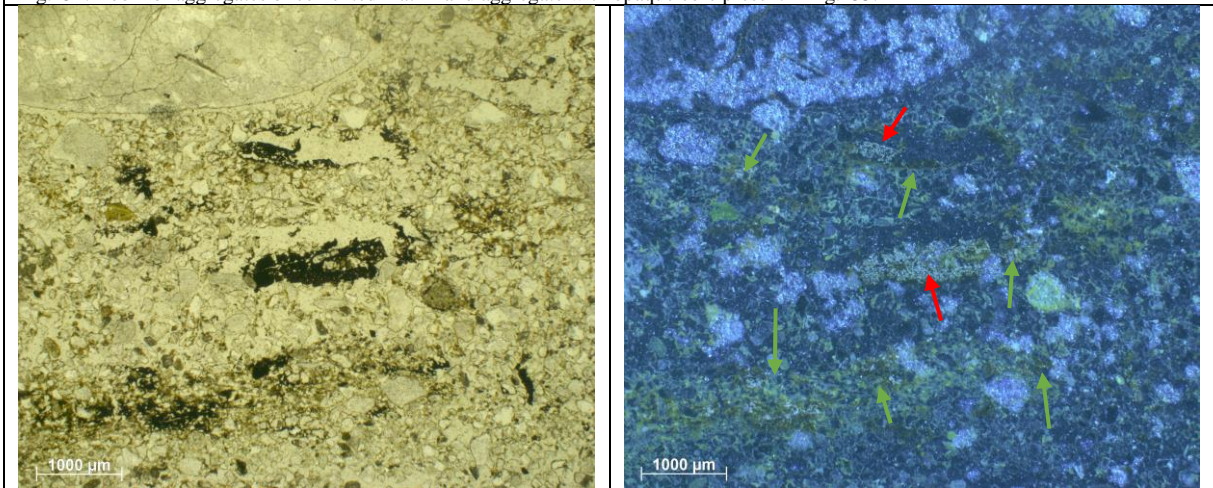


Fig.135: Opaque material, note the reddish to orange (green arrow) and metallic blue (red arrow) color in OIL.

c)

A granular microstructure (fig.136-137) characterizes this facies. The porosity is very high and the aggregates that make up the solid phase of the facies float freely in the space with a random distribution pattern and are never in contact with each other (fig.136). The aggregates display a high heterogeneity in both size, shape, and inner fabric. The aggregates present on the upper part of the facies present an inner fabric equal to the fabric present in the lower part of facies *d*, this characteristic of the facies is more appreciable at a mesoscale point (fig.126) of view or comparing the micrographs from the two facies (fig.139). To be noted that the aggregates do not seem to have rotated much, the inclination of the inner bands is sub-parallel to the bands of the upper facies (fig.126). On the lower part of the facies, alongside with aggregates also grains are present, the aggregates become progressively smaller until giving way to the next facies. The lower contact is very comfortable. To be noted the presence of aggregates of cemented calcitic matrix (fig.139-140) and biospheroids (fig.138) on the upper contact of the facies.

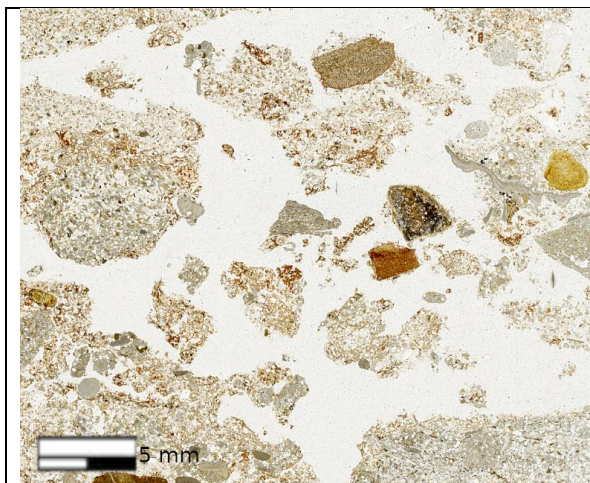


Fig.136: Detail of section's scan. Aggregate microstructure of the facies, note how the aggregates float freely in the void's space without touching each other.

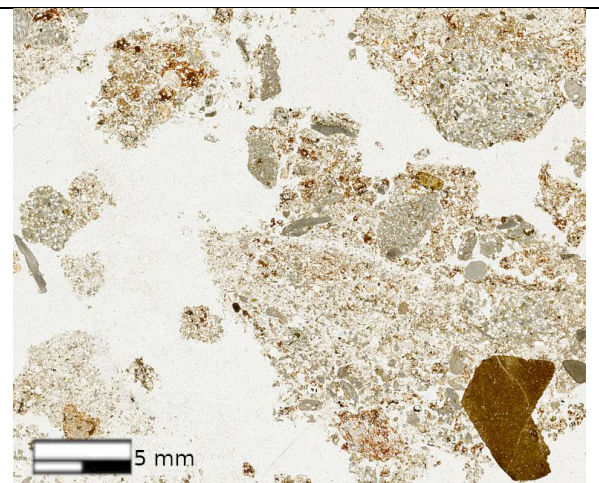
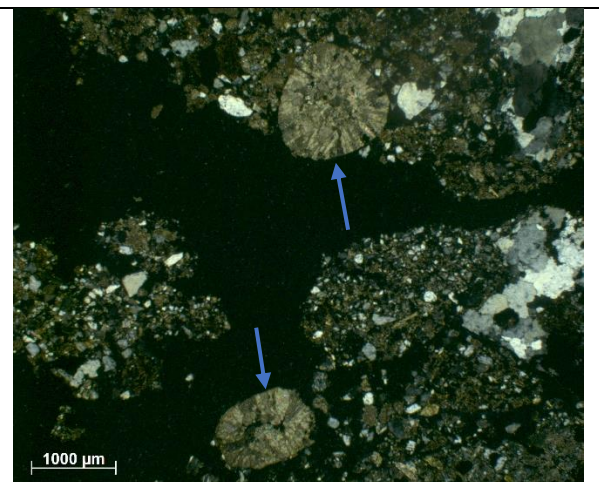


Fig.137: Detail of section's scan. Note the high degree of heterogeneity in the aggregates' sizes.



Fig.138: Biospheroids produced by earthworms (arrows).



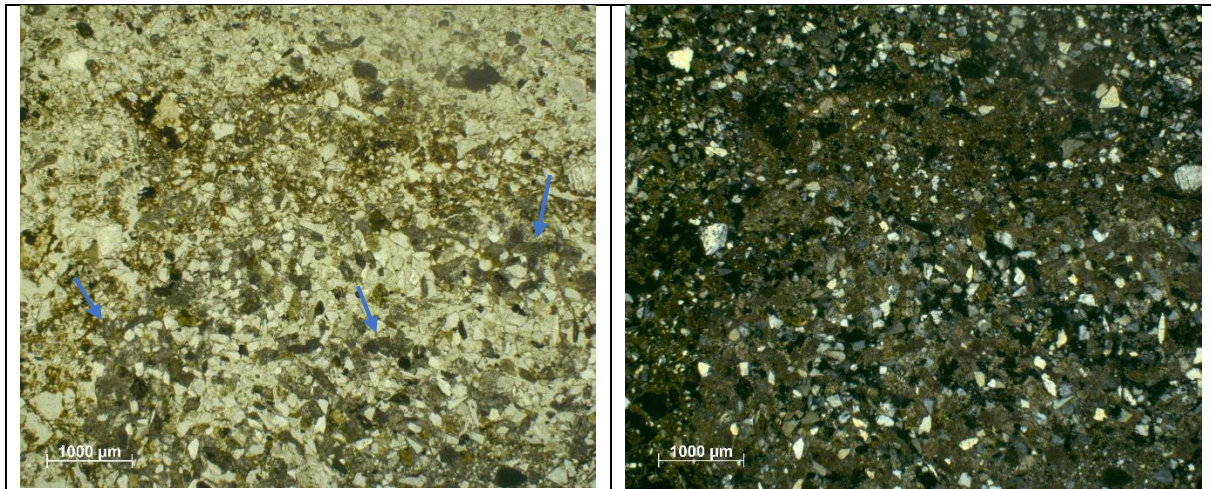


Fig.139: Inner fabric of one of the biggest aggregates. Note the similarity with facies *d*'s fabric (compare with fig.11-12). In the bottom part of the micrograph aggregates of cemented calcitic matrix are also visible (arrows).

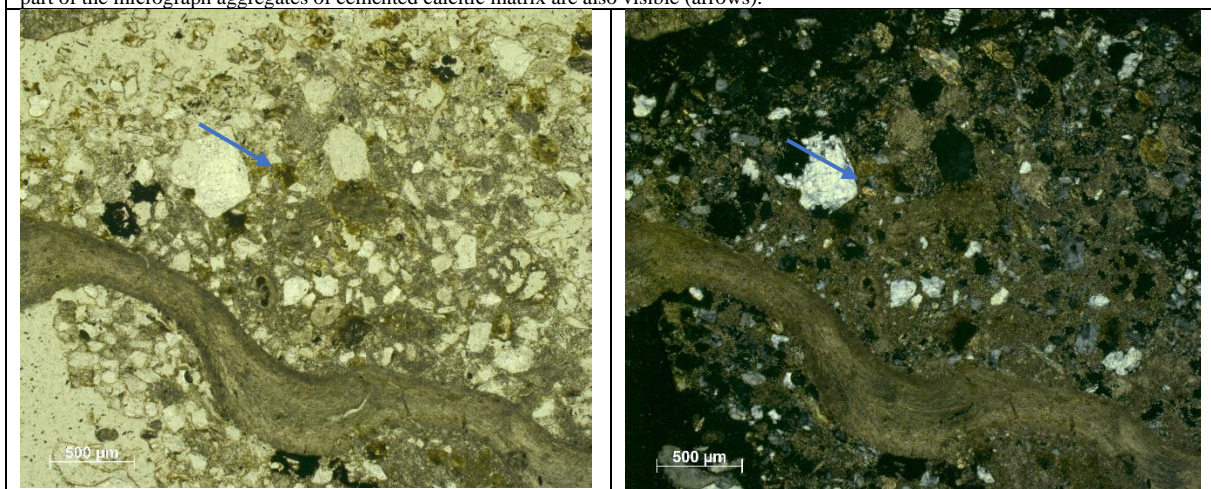


Fig.140: Aggregates of cemented calcitic matrix.

b)

The microstructure of the facies is composed by grains and aggregates floating freely in the space, no accommodation of voids is present and the elements are never in contact with each other (equal enaulic coarse/fine related distribution pattern). The porosity is than composed of compound and simple packing voids and is not homogenous throughout all the facies, going downwards the degree of compaction increases. Different types of basic components have been identified (no micromass in the space between them is present):

- *Minerals and rock fragments*: very heterogeneous size (all the classes from very fine to coarse sand are present; fine to medium sand size is the most present). For what concerns the lithologies we find quartz grains as the dominant lithology, alongside with micas, silicious and carbonate rock fragments. Other unidentified lithologies are also present.
- *Aggregates*: three types of aggregates have been distinguished. Aggregates of cemented calcitic matrix (fig.141) embedding minerals (mostly quartz and few micas) and carbonate

rock fragments, they display a very high heterogeneity in both shape and size (up to 3.5 mm). Aggregates of reddish micromass (fig.142), showing stains of opaque micromass inside, these too present a high degree of size heterogeneity but they are smaller than the previous ones (up to 1.5 mm). Aggregates of sandy material, presenting no micromass and a basic microstructure. Some aggregates show a mixture of the features described above (fig.143).

- *Biogenic elements*: coprolites fragments (fig.144) and fecal pellets (fig.145) have been identified.

In this case too all the opaque material in the facies displays a reddish to orange with areas of metallic blue color in OIL (fig.146).

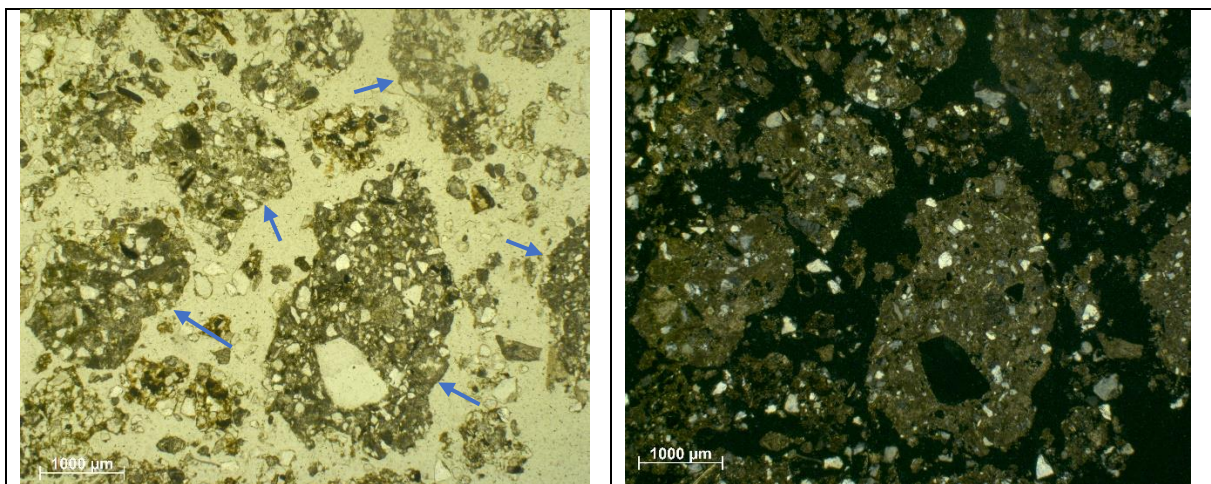


Fig.141: Aggregates of cemented calcitic matrix (arrows). Note the calcitic crystallitic b-fabric of the matrix in XPL.

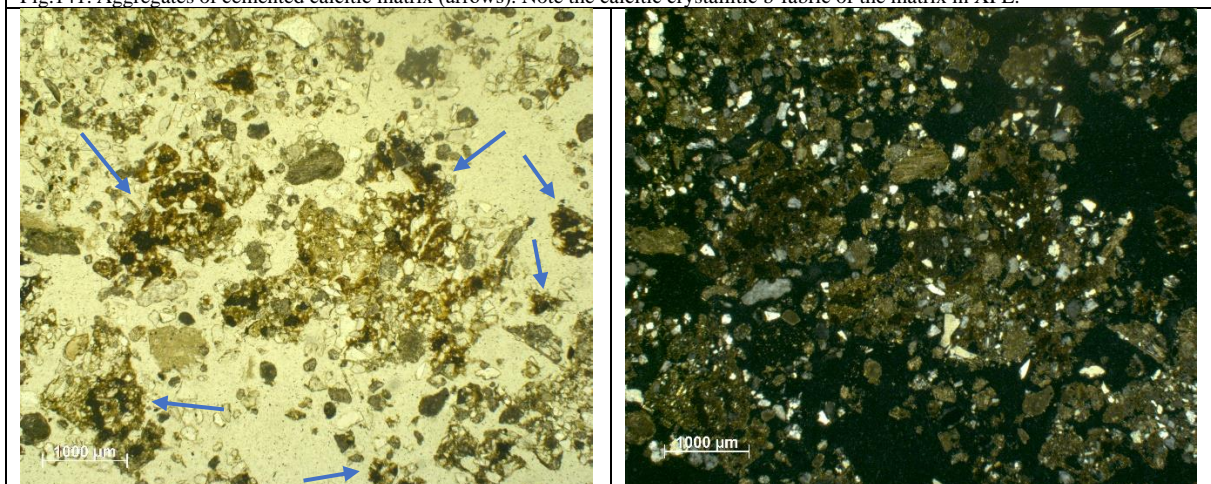


Fig.142: Aggregates of reddish micromass (arrows). Note the opaque staining present in them and the high degree of sizes heterogeneity.

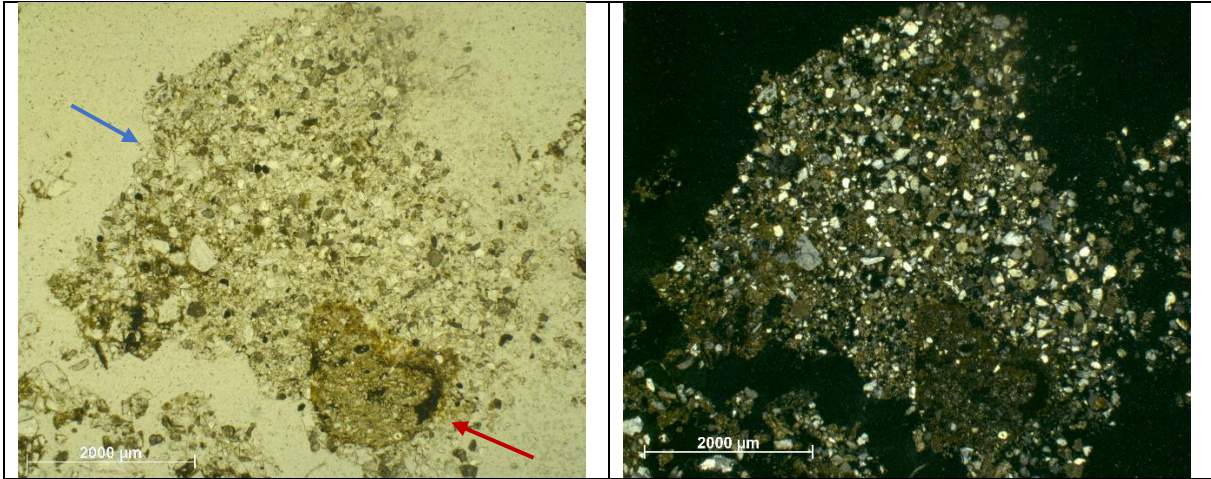


Fig.143: Complex aggregate, composed exclusively of sandy material on the top part (blue arrow) and of micromass at the bottom part (red arrow).

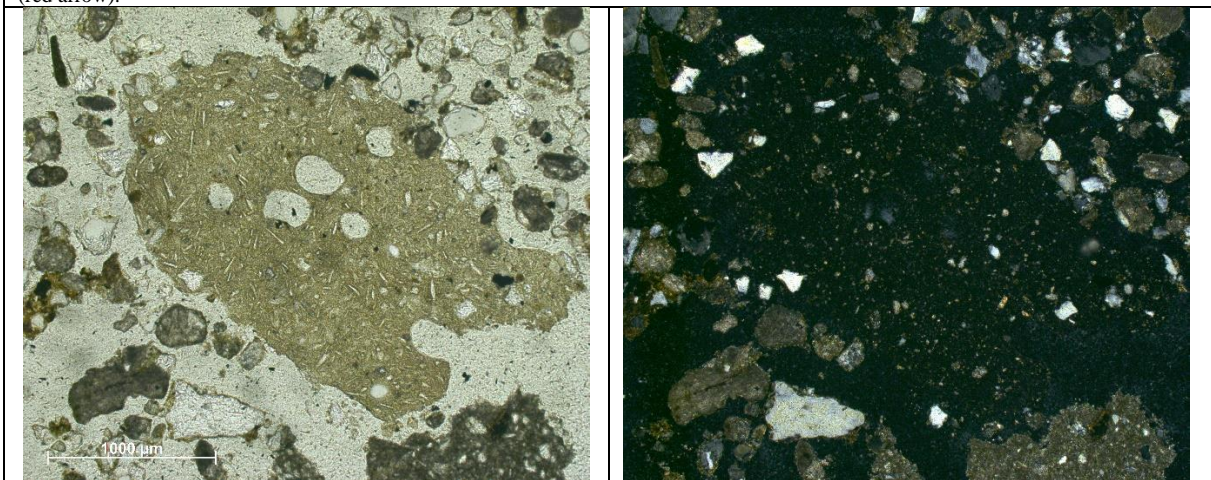


Fig.144: Coprolite fragments. Note its characteristic inner porosity composed of round vesicles and small tabular poroids.

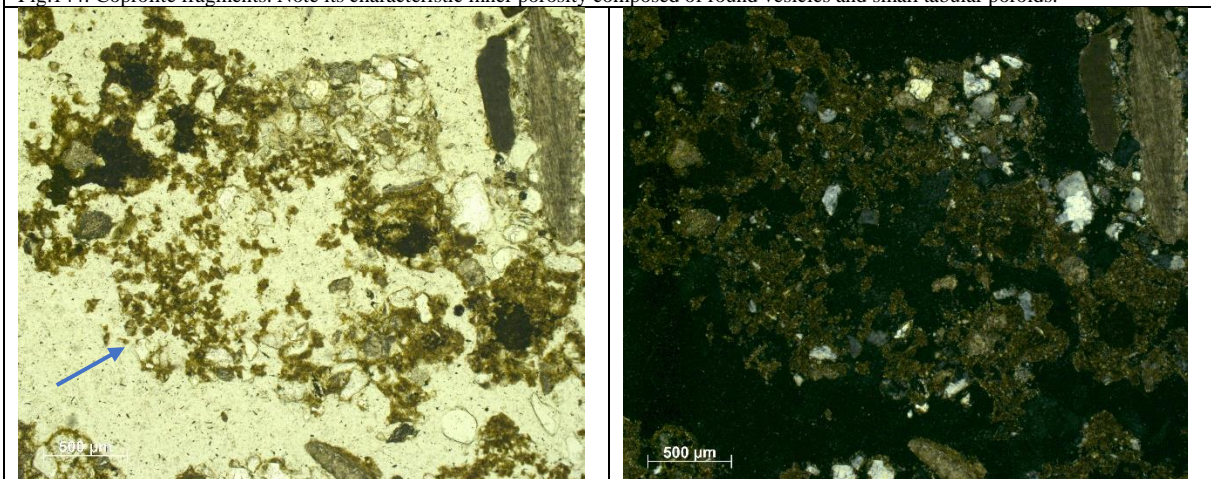


Fig.145: Fecal pellets (arrows). Note their characteristic granular microstructure.

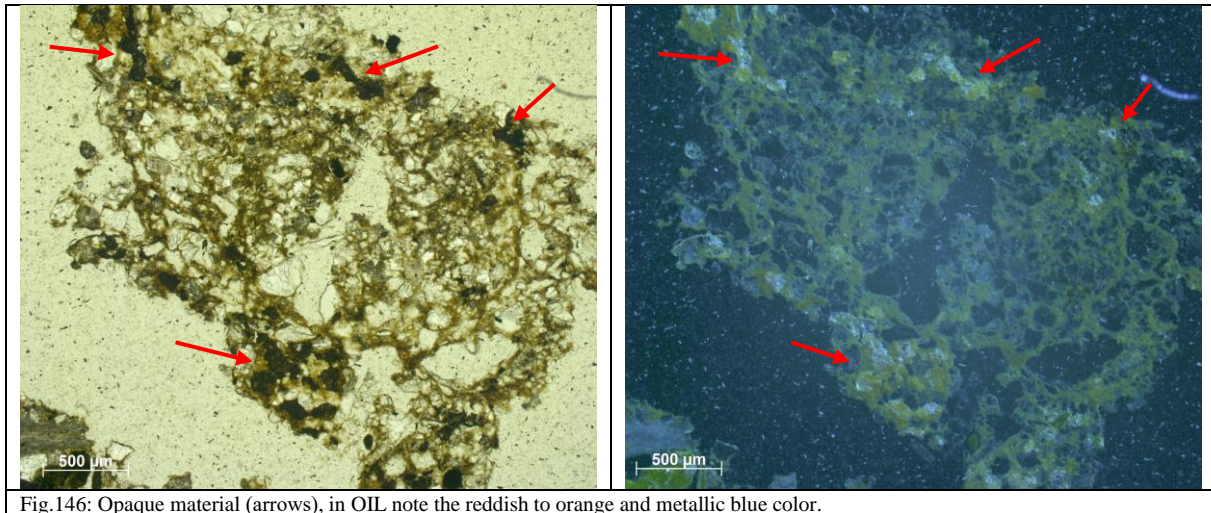


Fig.146: Opaque material (arrows), in OIL note the reddish to orange and metallic blue color.

a)

The facies present a complex microstructure. A dominant channel/vesicular microstructure (fig. 147-148) is present at a low degree of magnification (mesoscale), zooming in the porosity becomes more variable: alongside with big channels and vesicles also planes become appreciable (which differ from channels as they exhibit at least one sharp edge, fig.150). All the poroids present in the facies present a high degree of size heterogeneity and no accommodations.

Setting the coarse/fine limit at 40 µm two pattern of coarse/fine related distribution have been found. Areas with close to single spaced porphyric (fig.150) give rise to a massive microstructure, while areas with gerufic to enaulic (from fine to coarse, fig.149) to a basic microstructure. None of these features is dominant on the others and their continuity results to be interrupted by the elongated poroids (channels and planes).

The micromass present in the facies range from reddish to brownish and present some areas of opaque material (fig.151), a speckled aspect and a speckled to monostriated b-fabric characterize it. The arrangement of the micromass is characteristic: it is often present as lines and accumulation (fig.152) randomly distributed, or as aggregates. The linear accumulation of the micromass have different aspect, notably related to their boundary's sharpness, those who present a high degree of sharpness results to be very similar to the *bread* of the *sandwich features* identified in MM3's facies e (fig.154). The aggregates (as for the previous facies) often show a core of opaque material (fig.153). In this case too all the opaque material in the facies displays a reddish to orange color in OIL (fig.157). Aggregates of cemented calcitic matrix have also been identified (fig.155).

The coarse fraction presents an high degree of heterogeneity both in size and in lithology, it has been divided into two size classes:

- The elements $< 500 \mu\text{m}$: mostly composed of quartz grains with few carbonate rock fragments and micas grains (mostly in relationship with the micromass), fig.150.
- Elements $> 500 \mu\text{m}$: mostly carbonate rock fragments, some of which presents fossils inside. Their shape is very heterogeneous, ranging from sub-spherical to tabular, fig.147-148.

Alongside with these geogenic component also some biogenic elements have been identified, notably phosphatic grains (fig.154-156).

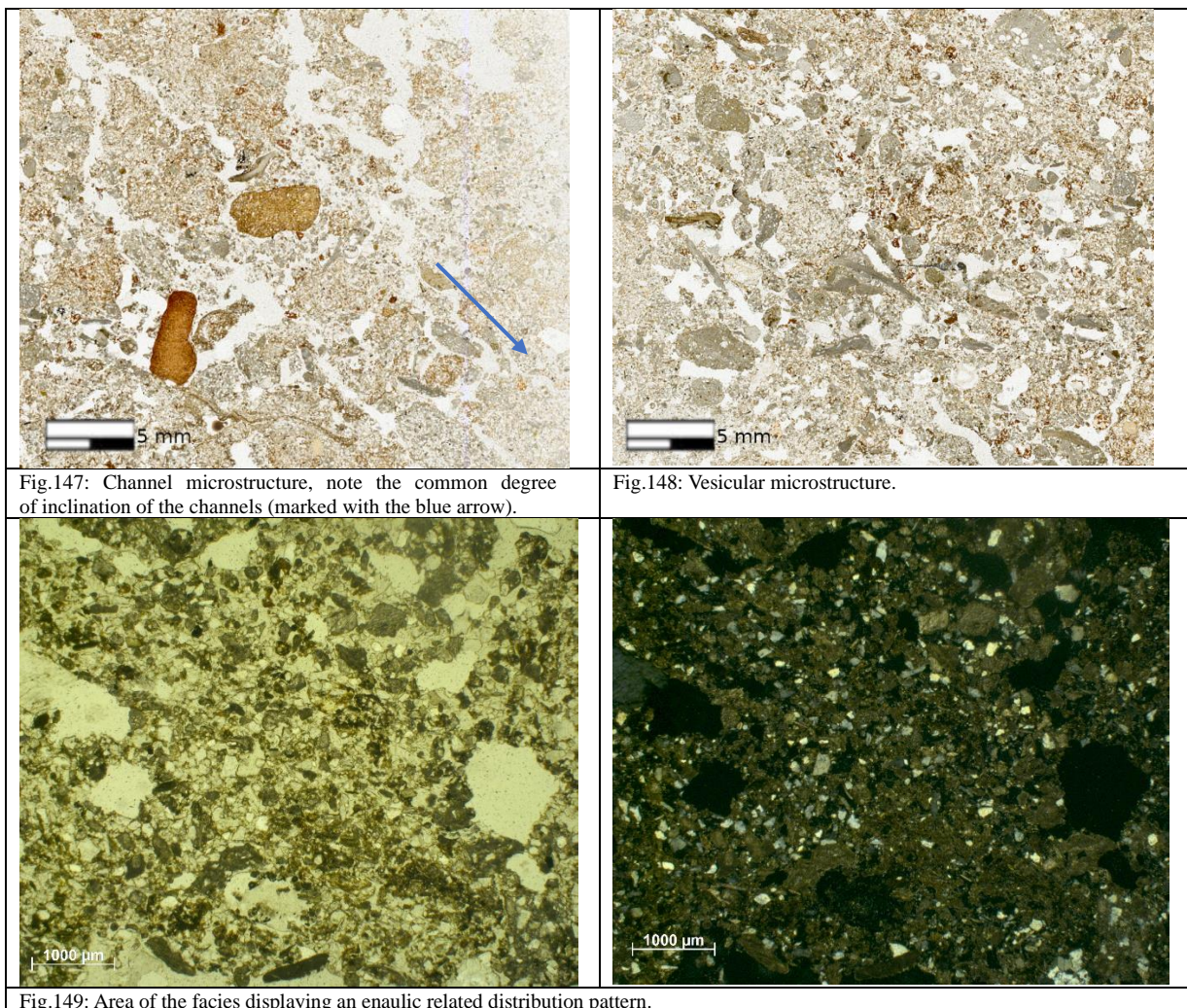


Fig.147: Channel microstructure, note the common degree of inclination of the channels (marked with the blue arrow).

Fig.148: Vesicular microstructure.

Fig.149: Area of the facies displaying an enaulic related distribution pattern.

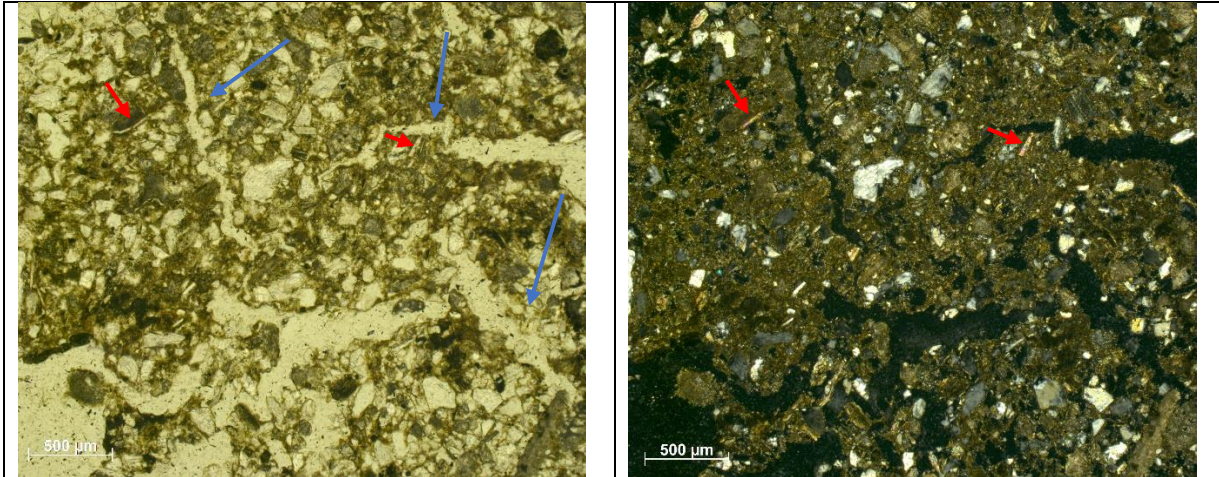


Fig.150: Massive microstructure and porphyric related distribution pattern. Note how at this scale of observation the continuity of the material is interrupted by planes voids (blue arrows). Also note the coarse fraction < 500 µm, mostly composed of quartz grains and micas (red arrows).

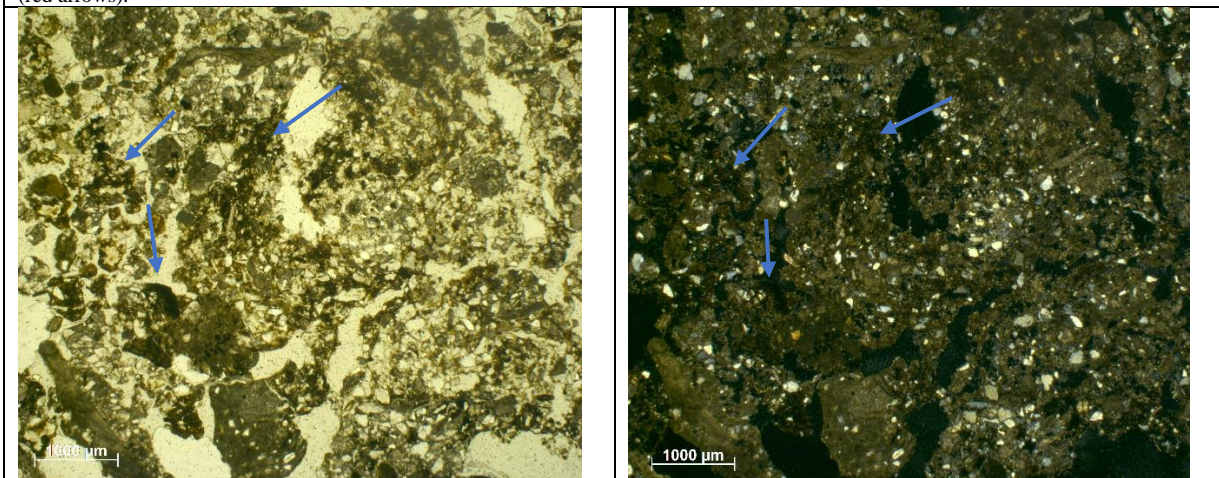


Fig.151: Reddish micromass. Note the opaque staining in it (arrows).

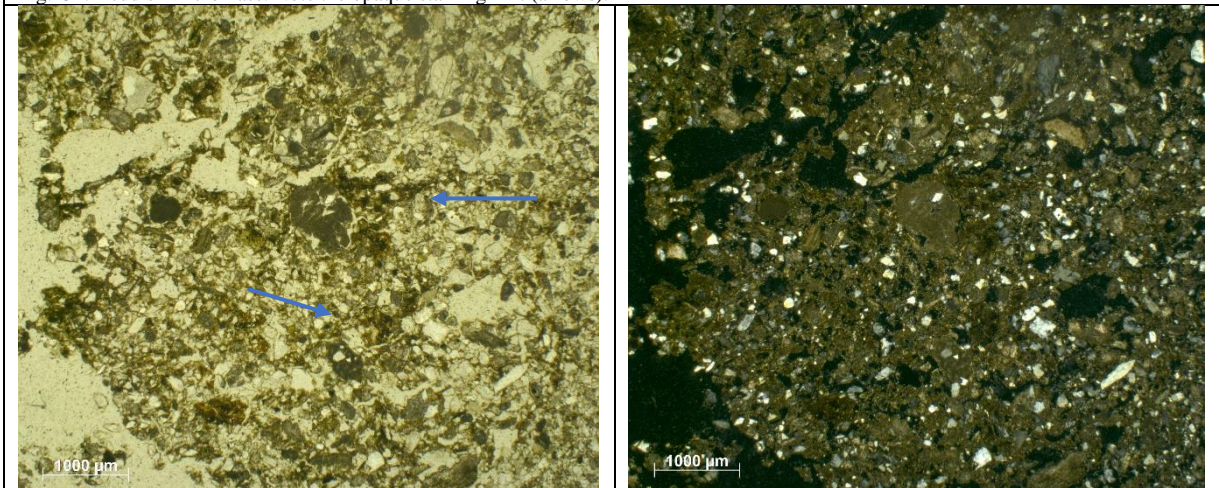


Fig.152: Reddish micromass. Note the characteristic distribution in the form of bands with random orientation (arrows). In this case the bands lack sharp boundaries.

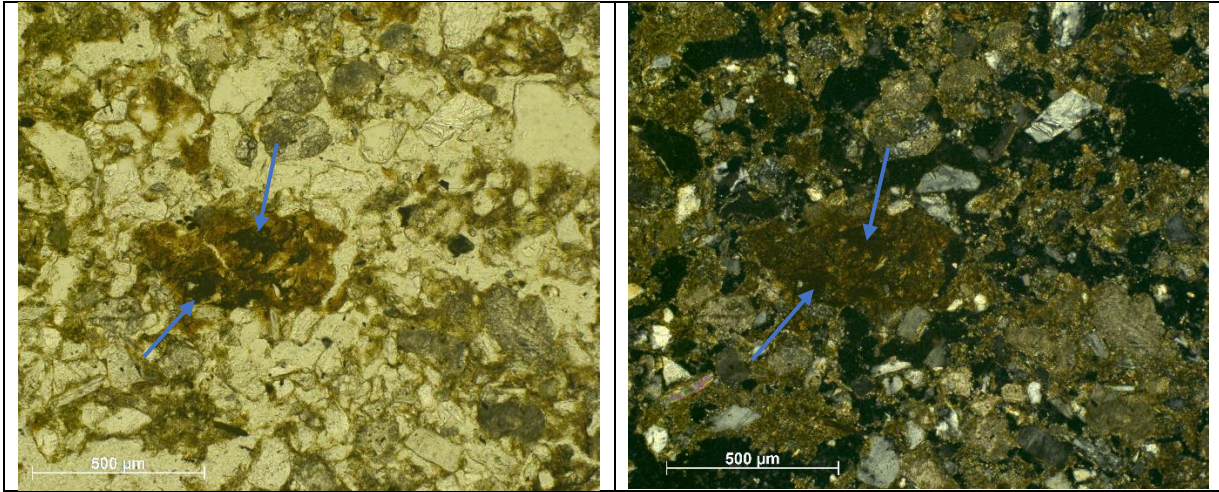


Fig.153: Aggregate of micromass presenting opaque staining (arrows).

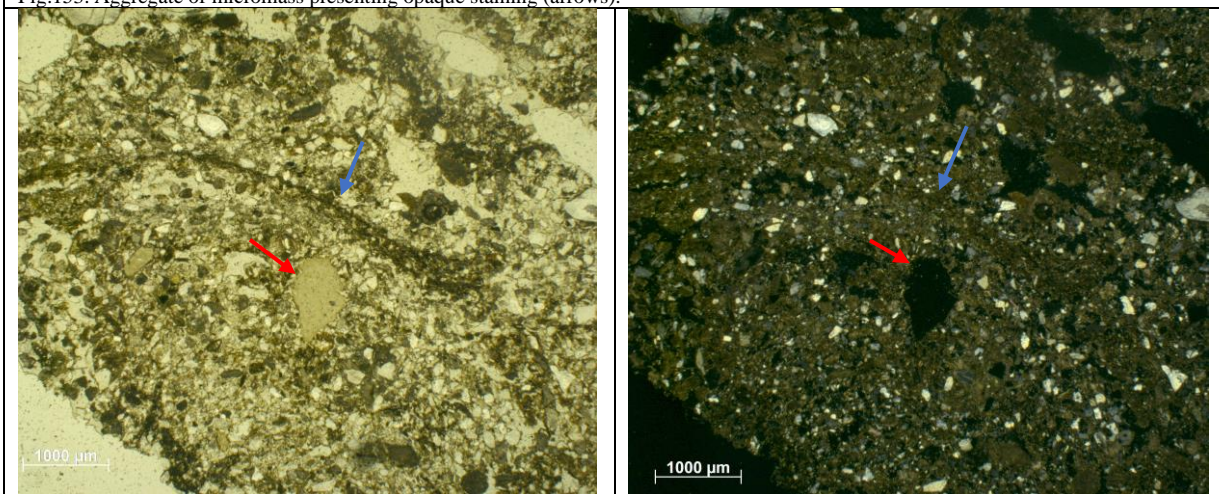


Fig.154: Bands of micromass showing sharp boundaries (blue arrow) and phosphatic grain (red arrow).

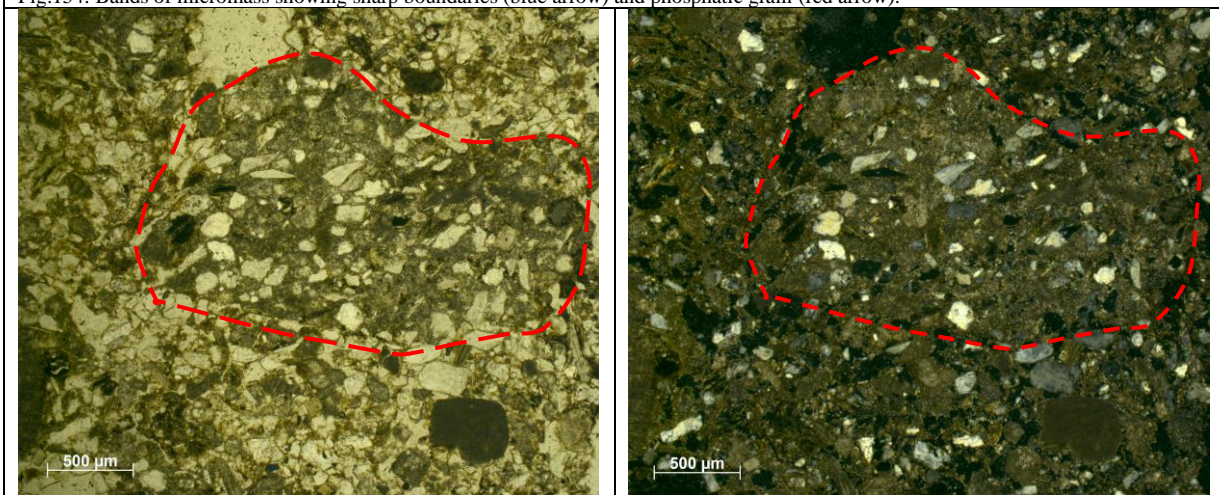


Fig.155: Aggregates of cemented calcitic matrix, approximately indicated by the dashed line.

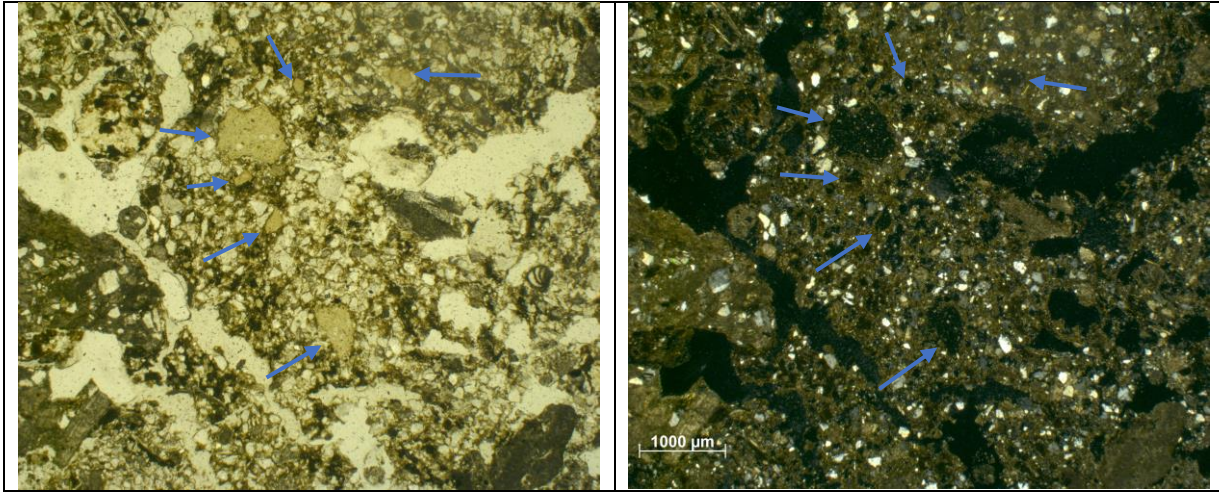


Fig.156: Phosphatic grains (arrows). Note their high presence a localized area. For the scale of the micrograph in PPL refer to that in XPL.

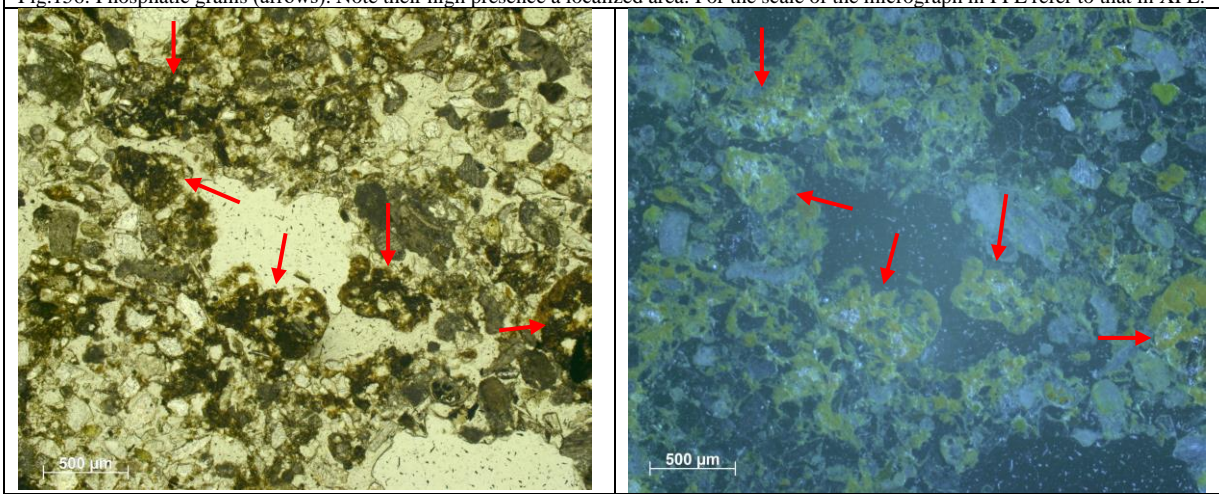


Fig.157: Opaque material (arrows), in OIL note the reddish to orange and metallic blue color.

MM5

Stratigraphic description of the block

The MM5 block result to be well made exception made for the central top part (fig.158), the upper part is still very visible on both sides, so it was still possible to observe its integrity.

It has been subdivided in four different units, from top to bottom we find:

- I. This unit present a banded fabric, composed of an alternation of sandy bands and fine material bands (fig.159).

The sandy ones display a pale color (yellowish grayish) and results to be well sorted, only few coarser elements are embedded in sandy matrix (up to 0,5 cm). These coarser elements often present a tabular shape and an orientation and distribution pattern sub-horizontal and sub-parallel to the bands; the coarser elements which don't displays this shape present a sub-spherical and sub-rounded one.

The fine material ones show a brownish color, are very well sorted and thinner that the sandy ones. The contact with the lower unit is composed of very fine and very well sorted sand, visible with the aim of a magnifying lens.

- II. Sandy unit, also displaying a banded fabric, it has been subdivided in two subunits (fig.160):

The upper part is composed of a relatively thick level of sand which displays three internal layers: a coarser one between two finer ones (in terms of observable granulometry). The overall color is yellowish/grayish.

The lower part still presents a banded fabric, but the sandy bands are coarser (medium sand) and are interspersed by fine material ones. This part shows a decreasing in thickness from the right to the left of the block, almost disappearing on the extreme left of the latter.

- III. Fine material unit, displaying a brownish color, no bands are visible at this scale of observation (fig.161). Few coarse elements (sand size) are embedded in the matrix displaying a random distribution pattern. A high porosity is also visible in the block.

- IV. Fine material-sandy unit, embedding gravels. The fine material shows the same characteristic as the previous one. It presents in it lenses of sandy material sub-parallel to the surface (fig.162); and coarser elements (fine gravel size) with a linear distribution pattern and displaying sub-rounded and sub-spherical shapes.

To be noted: the biggest element presents a black alteration rim over its entire surface.

The decreasing in thickness of the lower part of unit II presented in the block may show the complex geometry of the real, three-dimensional, extension of the levels.

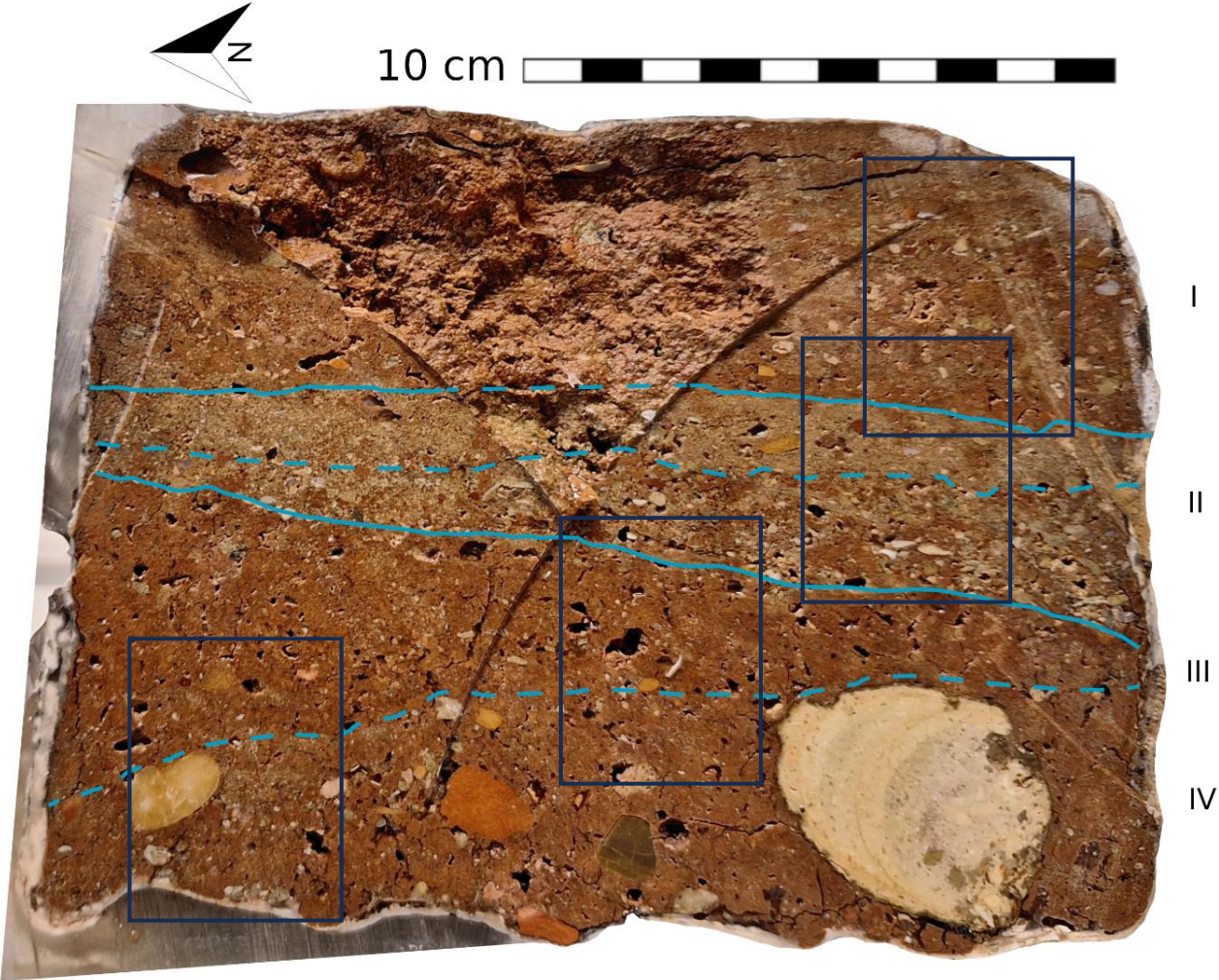


Fig.158: MM5 block. The continuous lines show an abrupt contact while the dashed ones a comfortable one. The dashed line present in relationship with unit II shows the subdivision of the it described in the text. The squares indicate the areas of the next pictures.



Fig.159: Detail of unit *I*. note the banded fabric (scale: 1cm).

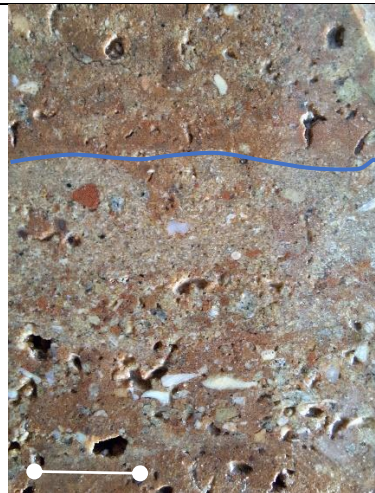


Fig.160: Contact between unit *I* and unit *II* (line). Visible also the subdivision of unit *II* (scale: 1cm).



Fig.161: Detail of unit *III*. Note the homogeneity of the unit (scale: 1cm).



Fig.162: Detail of unit *IV*. Note the sandy lens embedded in the fine matrix and in touch with a gravel size element (scale: 1cm).

Mesoscopic description of the thin section

From top to bottom (fig.163):

- c) The facies develops itself with a clear banded fabric, showing the alternation of bands composed of fine sand, coarse sand and fine material. An abrupt change defines the beginning of this facies (lower contact), marked by a low presence of micromass which leave place to a sandy material.
- b) The contact with *a* and *b* is comfortable and marked by an absence of coarse fraction. A channel to vesicular structure is displayed at this scale of observation. Few coarser elements are present, to be noted one hourglass-shaped red elements, and a dark brown element (isotropic nature under the microscope) which seems to be chitin (fig.176).
- a) The facies displays a banded fabric, composed by the alternation of two type of bands: a coarser bands, which present a high degree of porosity, (with poroids that range from channels to vesicles and vughs) and displays a grayish color, linked to the high presence of rounded and sub-spherical calcareous rock fragments. And finer bands marked by an abrupt decreasing in the porosity of the material and in the coarse fraction, they display a compact structure.

On the base of these observations, it was possible to create a link and connect the thin section with the block. The facies *c* seems to correspond to unit *I*. Facies *b* to the upper portion of unit *II*. While for facies *a* the upper band seems to correspond to the lower portion of unit *II*, while the rest of the facies to both unit *III*. If this is the case the lower unit of the block could have been lost on the section due to the extreme thinness of the lower part of the latter, which results to be unreadable. It was not possible to find the exact position of the section on the block but the height of both coincides, so the section turns out to be representative of the whole block.

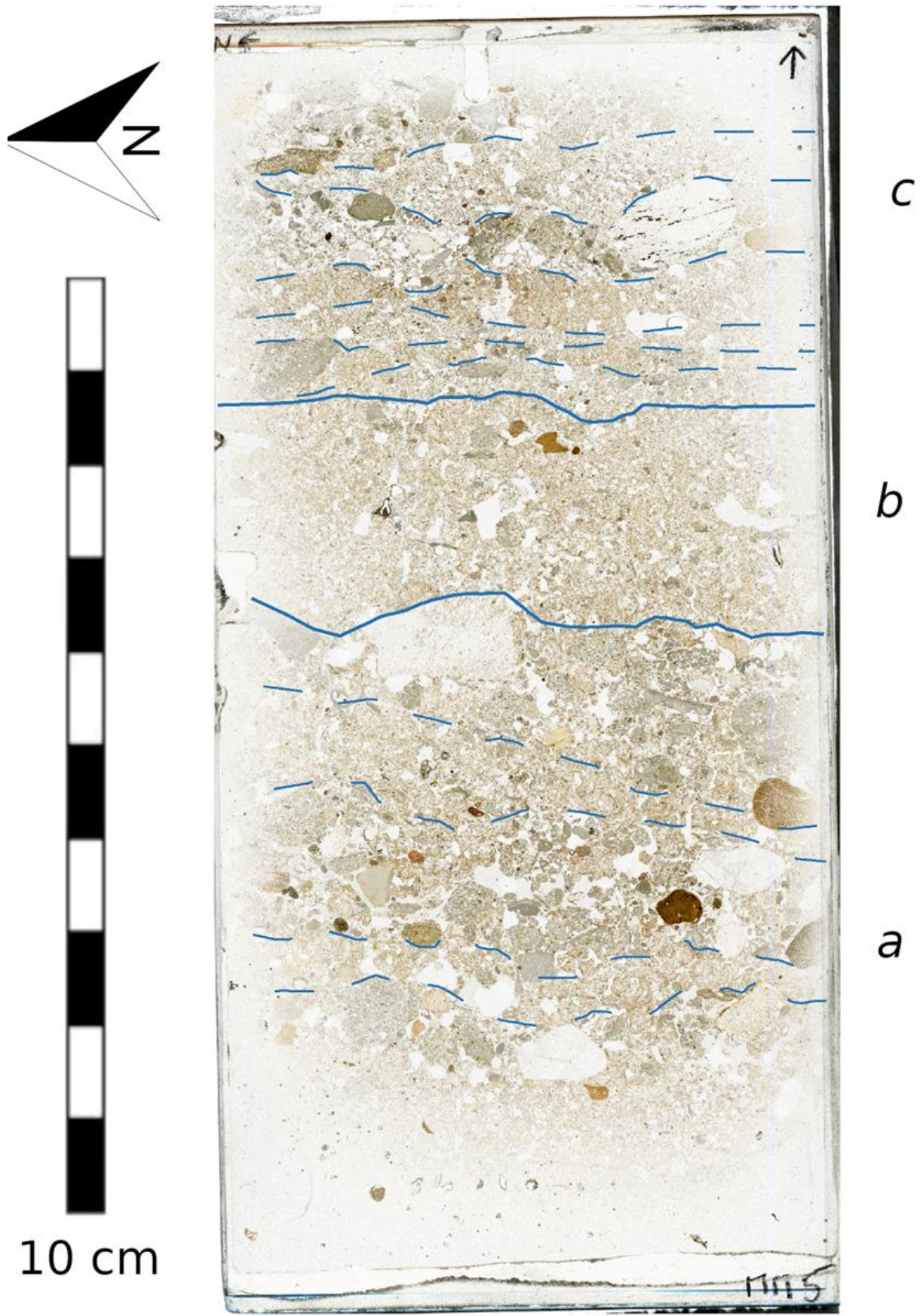


Fig.163: MM5 thin section, the continuous lines mark the limit between the facies while the dashed ones the bands which compose the banded fabrics.

Microscopic description of facies

c)

In order to describe the facies, it has been divided into three different partial fabrics which alternate each other, creating the banded fabric described during the mesoscale description.

These partial fabrics will so be called after their most representative basic component: *fine sand*, *coarse sand*, and *fine material*.

- *Fine sand*: the material that compose this partial fabric is almost exclusively sandy material, displaying few or no micromass (fig.164). A vesicular microstructure has been identified, the porosity results in fact to be composed of simple packing voids between the basic components (sandy material) and vesicles, the latter often displaying a sub-horizontal referred distribution pattern (fig.165). The coarse fraction (sandy material) is composed of very well sorted sand size grains (mostly fine sand with sporadic elements of medium sand), the lithology present in this fabric is composed mostly of quartz grains and carbonate rock fragments, and few micas grains. The few micromass is very low and is mostly present close to the contact with the other bands of the facies (fig.166-167), showing a related distribution pattern with the sandy material that range from gerufic to porphyric. For what concerns the inner variability of the partial fabric it must be noted the lower porosity of the lower fabric unit, which still displays vesicles, but they are relative smaller and less abundant.
- *Fine material* (fig.168): in this fabric unit the ratio between the coarse fraction and the micromass is very low (the micromass is dominant). The microstructure ranges from massive to vesicular, the porosity is composed of small vesicles with a random distribution pattern. The micromass displays a color that range from pale to dark brown and a crystallitic to speckled b-fabric. The coarse fraction is composed of very fine sand quartz and micas grains, and of fine sand carbonate rock fragments. To be noted that the micas grains present in this partial fabric are smaller but relatively more present than the ones present in the sandy partial fabrics. The coarse/fine related distribution pattern range from close to open porphyric.
- *Coarse sand*: a basic microstructure is displayed in this partial fabric, no micromass is present. The coarse sand that composes the units is heterogenous in lithology and shape. The most represented lithology are carbonate rock fragments (others, less represented lithologies, are quartzite and flint). The shapes range from tabular (only for what concerns the carbonate fraction) to sub-spherical (fig.169). These elements are not in touch with

each other, and the space between them results to be filled by fine sand (fig.170), which displays the same characteristics showed in the *fine sand* partial fabric; exception made for the porosity, which in this case is very high: the simple packing voids between the sandy elements is more open and the vesicles are bigger and relatively more present, showing a clustered distribution pattern.

The order, from top to bottom, of this banded fabric is the following: *coarse sand* (slightly visible at the very top of the section), *fine sand*, *coarse sand*, *fine sand*, *fine material*, *fine sand*, *fine material*, *fine sand* (fig.171-172).

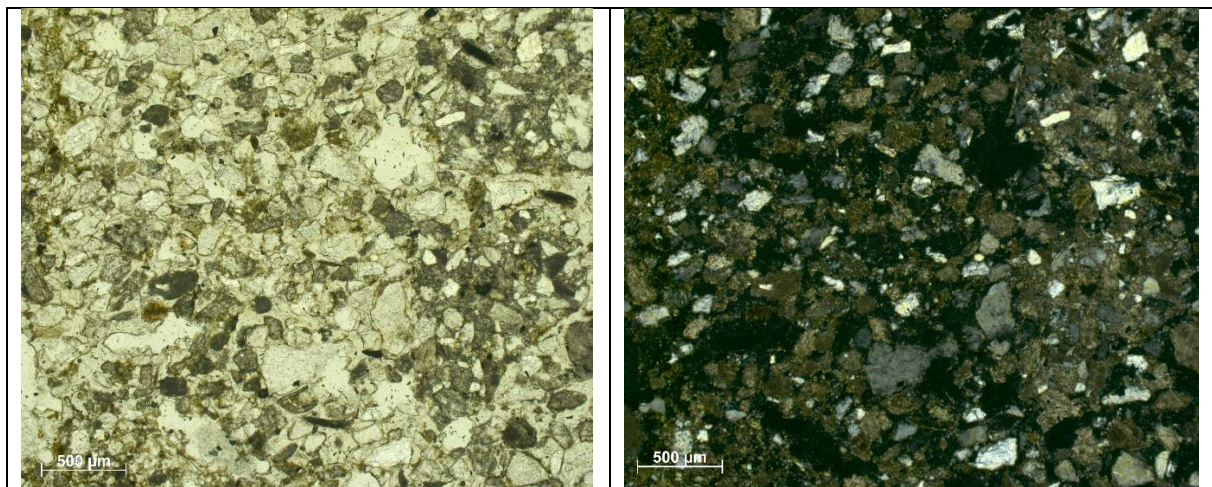


Fig.164: Fine sand fabric unit. Note the absence of micromass and well sorting of the elements.

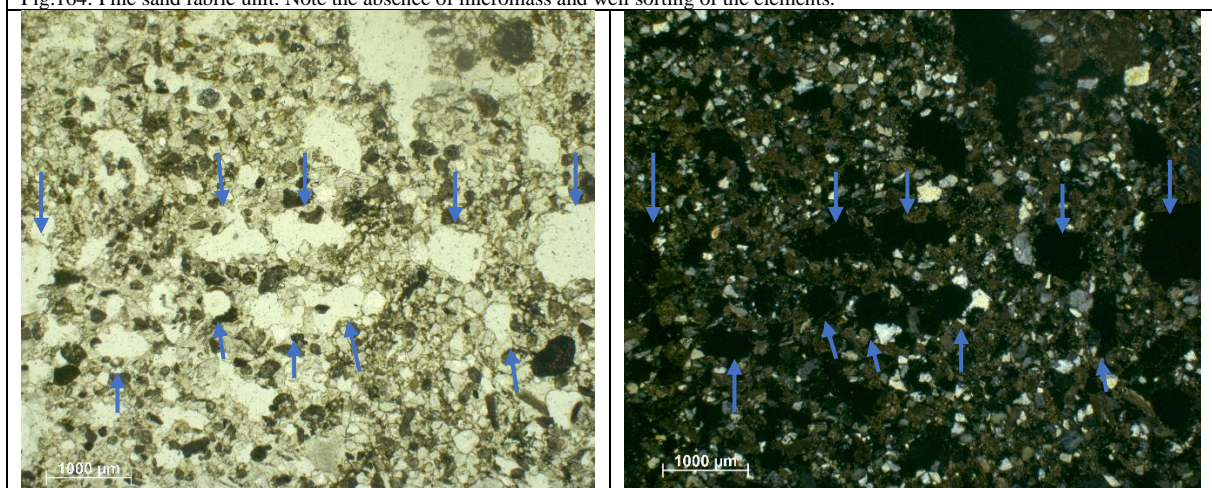


Fig.165: Fine sand fabric unit. Note the sub-horizontal referred distribution pattern of the vesicles (arrows).

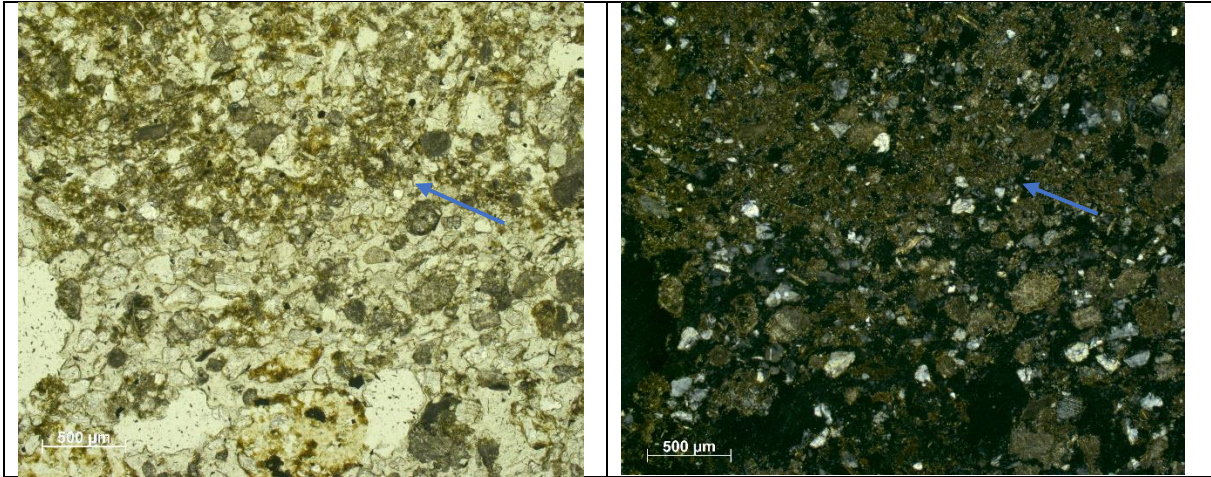


Fig.166: Contact between fine material and fine sand fabric units (arrow).

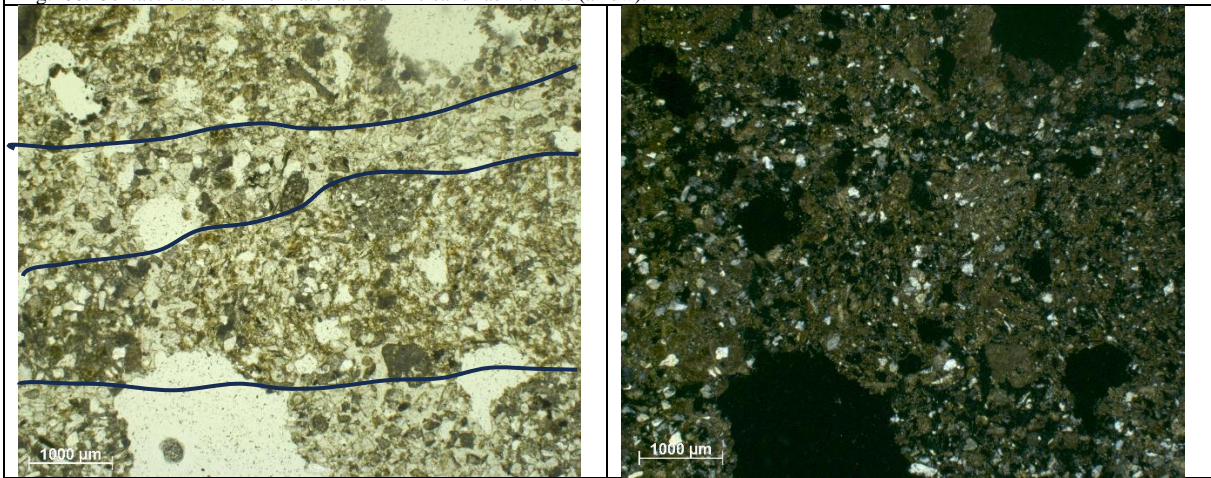


Fig.167: Alternation of (from top to bottom) fine micromass, fine sand, fine micromass and fine sand partial fabric (divided by the lines).

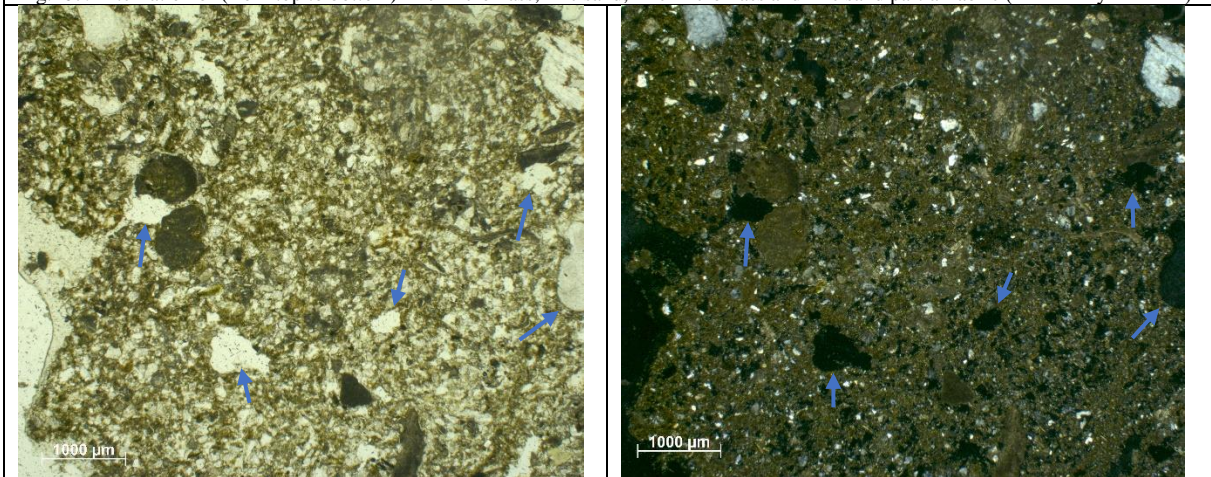


Fig.168: Fine material partial fabric. Note the massive microstructure interrupted by few vesicles (arrows), and the porphyritic r.d.p.

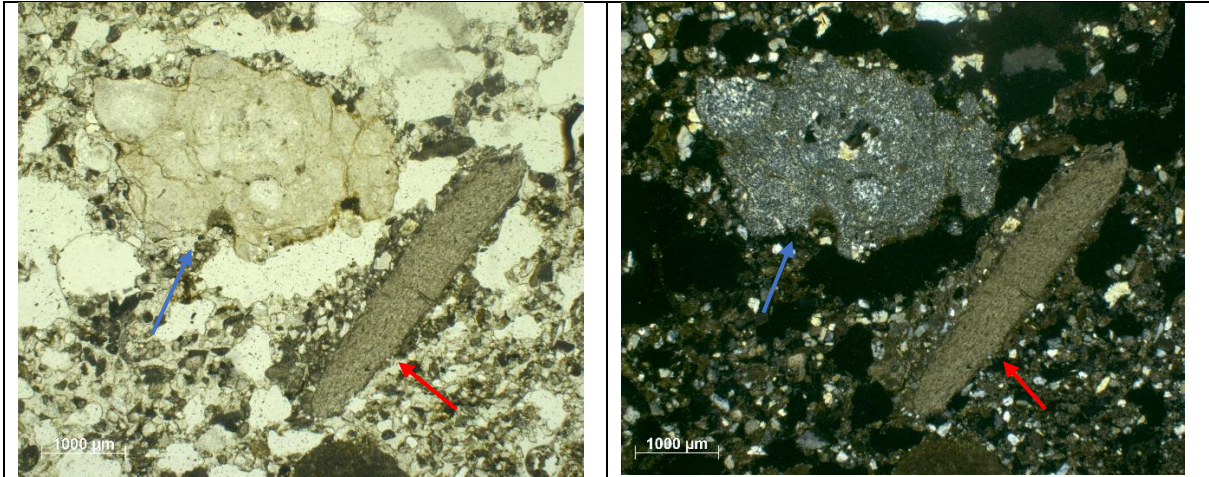


Fig.169: Coarse sand partial fabric. A flint element (blue arrow) and a carbonate rock fragment (red arrow) are visible.

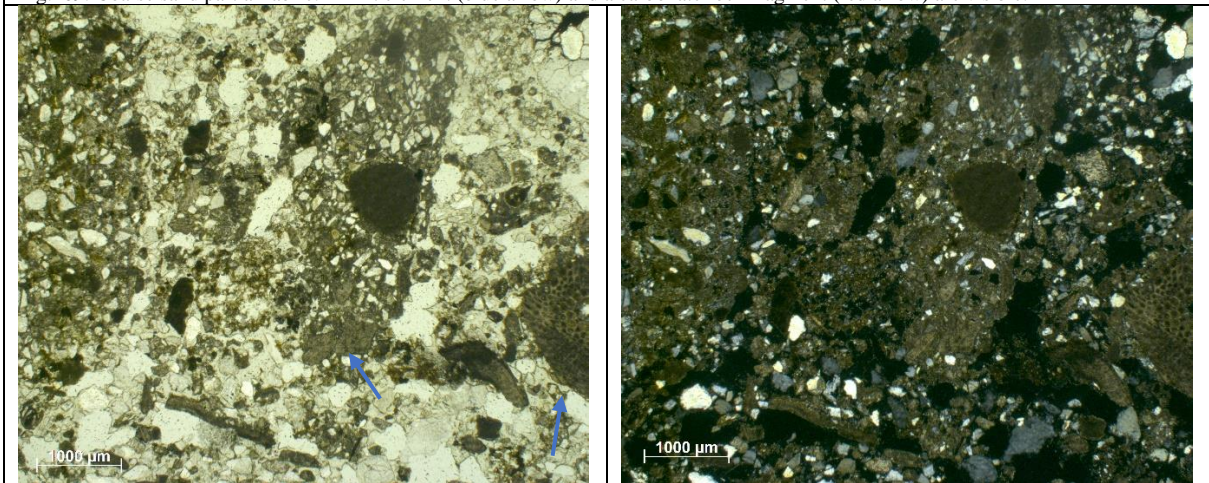


Fig.170: Coarse sand partial fabric. Carbonate rock fragments of coarse sand (arrows), note the fine sand filling the interstitial space.

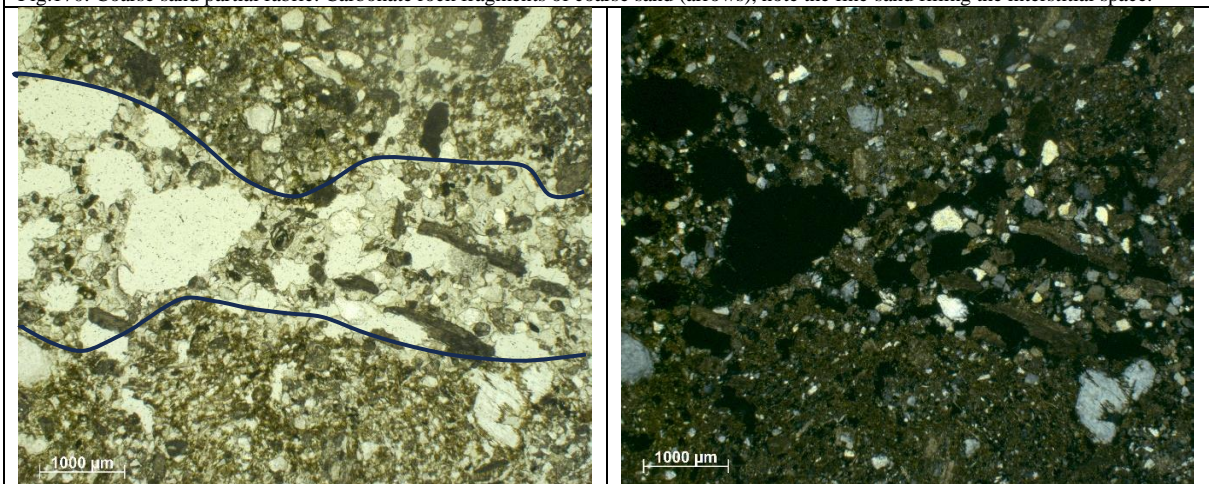


Fig.171: Alternation of (from bottom to top, contacts marked by lines): fine material, fine sand, and coarse sand. Note the high vesicular porosity present in the fine sand partial fabric.

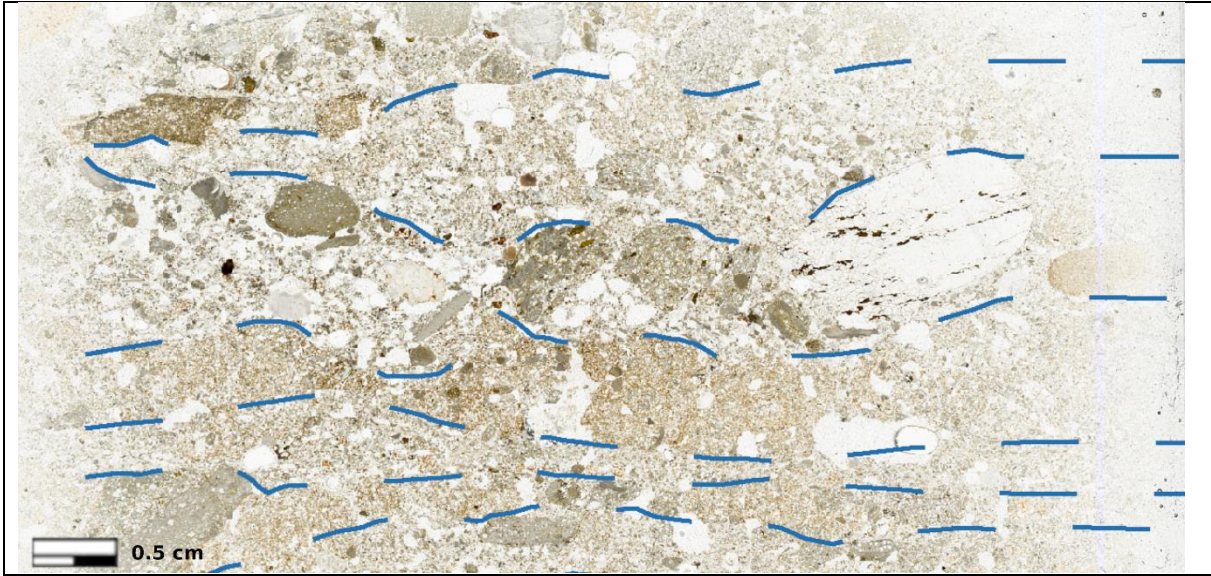


Fig.172: Banded fabric of facies *c*, the dashed lines mark the different bands.

b)

The facies is homogenous and doesn't present any bands. A channel to vesicular microstructure is present (fig.173), other than these voids also few vughs are visible, no accommodation of the poroids is present. Setting the coarse / fine size limit to 20 μm the related distribution pattern range from close to open porphyric. The micromass presents a brown to dark brown color, a speckled b-fabric and, as for facies *a* it embeds micas grains. The coarse fraction is mostly composed of very fine to fine sand quartz grains and carbonate rock fragments. Few aggregates of cemented calcitic matrix (micrite showing calcitic crystallitic b-fabric) are also present (fig.174). In addition to these elements a quartzite rock fragment, and a hourglass shaped red element (described in the mesoscale description), and elements with unidentified lithology (fig.175) are present. A bone fragment has also been identified (fig.177), and a pear-shaped dark brown element with isotropic behavior (hypothesized to be chitin, fig.176). To be noted a channel infilled with sandy material displaying the same characteristics of the *fine sand* partial fabric presented in facies *c*.

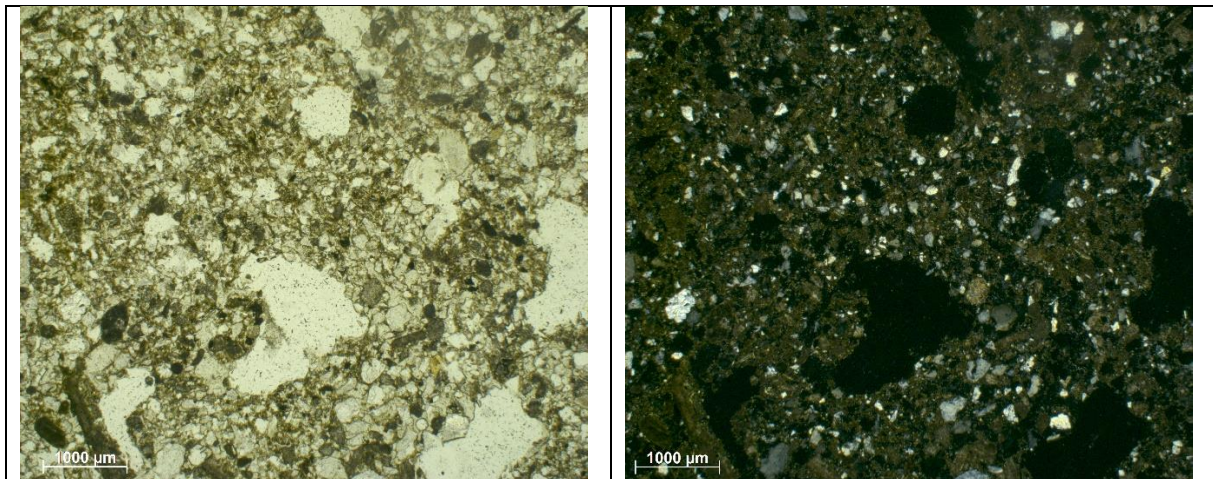


Fig.173: Vesicular microstructure interrupting the material, displaying a close to single spaced porphyric r.d.p. Note the very fine to fine sand quartz grains and carbonate rock fragments embedded in the micromass.

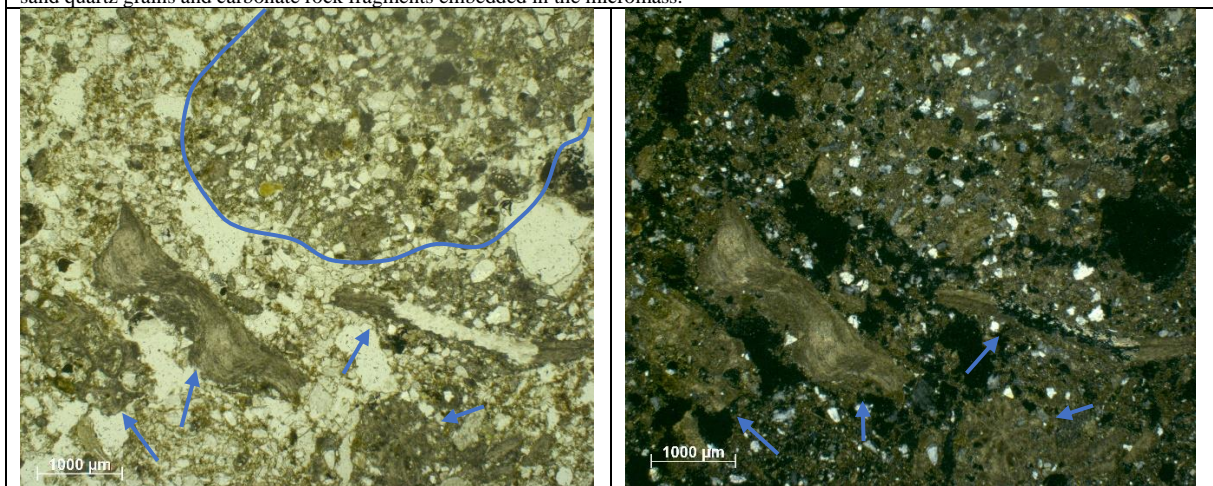


Fig.174: Aggregate of cemented calcitic matrix (inside the blue line), and carbonate rock fragments (arrows).

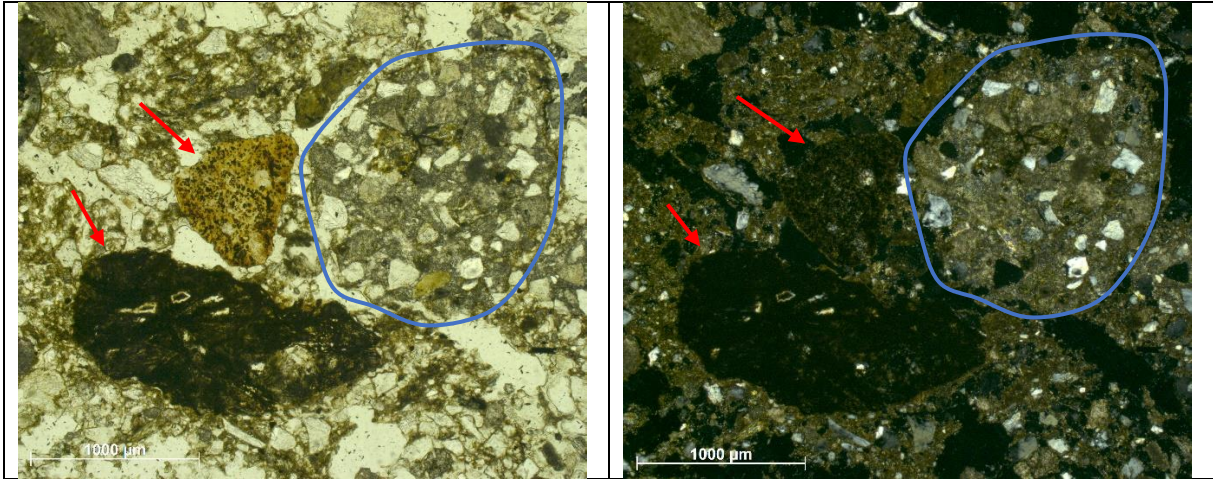


Fig.175: Aggregate of cemented calcitic matrix (inside the blue line) and two elements of unidentified lithology (red arrows).

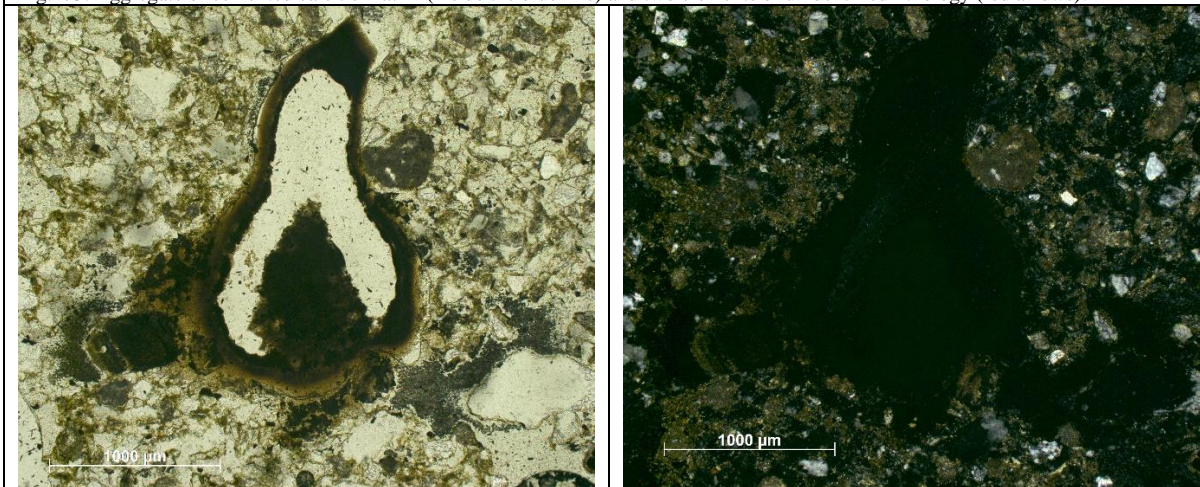


Fig.176: Element of chitin (hypothesized). Note the isotropic behavior.

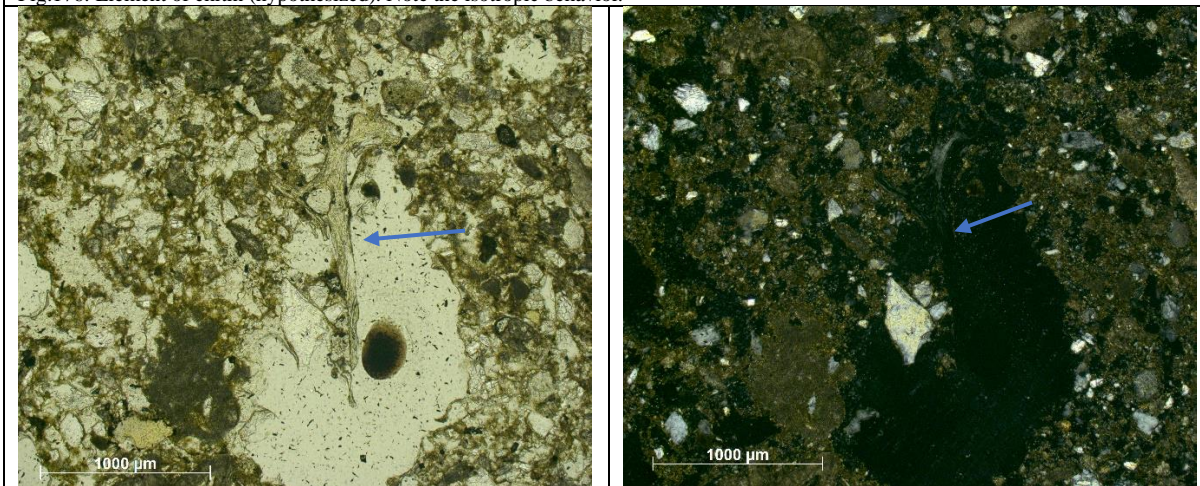


Fig.177: Bone fragment (arrow) showing a very low interference color.

a)

This facies presents a banded fabric composed of the alternation of micromass bands (showing few coarse fraction), and bands which still present the micromass but result to be dominated by the coarse fraction. The basic components that compose the two types of bands are the same, the differences are mainly related to their ratio (between coarse and fine fractions) and the porosity, being it very high in the bands dominated by the coarse fraction and lower on the other ones.

A channel to chamber microstructure is present in the facies, the voids don't show accommodation. The fine fraction ($c/f_{20\mu m}$) shows a fibrous aspect (fig.178) and is composed of brownish micromass embedding micas grains, the b-fabric range from speckled to crystallitic and sporadically also granostriated (fig.181). To be noted also the presence of dots of dark micromass.

The c/f ratio, as said before, is variable, and defines the banded fabric of the facies. In the bands with a low c/f ratio the related distribution pattern is porphyric (fig.179), while the bands with a high c/f ratio presents a chitonic to gerufic pattern (fig.180).

The coarse fraction has been divided in two size classes, setting as limit 200 μm . The finer coarse fraction is composed of very fine to fine sand quartz grains and few carbonate rock fragments. The coarse fraction bigger than 200 μm is instead composed of spherical to sub-spherical and well-rounded elements displaying a high lithological heterogeneity: carbonate rock fragments (the most represented), quartzite, flint and unidentified lithologies. One flint element also displays a surface alteration (fig.186). Also, tabular elements are present, but their shape seems to be strongly connected to their internal structure.

To be noted also the presence of a quartzite rock fragments (fig.187-188-189) which displays a very angular shape and regular and smooth surfaces with sharp boundaries, characteristics that may be pointing to a knapped artifacts (Angelucci, 2017).

Aggregates of cemented calcitic matrix (micrite showing calcitic crystallitic b-fabric) have also been identified, they show a rounded and spherical to sub-spherical shapes, very heterogenous sizes and they embed in them mostly the finer coarse fraction described earlier, sometimes they embed also micromass aggregates.

The pedofeatures that have been observed in this facies are:

- Biospheroids produced by earthworms (fig.183).
- micromass coating of channels (both typic and complete, fig.184).

- cappings on the very coarse fraction (both by micromass and fine coarse fraction, fig.185). Also calcitic cappings have been identified (fig.182)
- aggregates of micromass: these aggregates present themselves as lines of pure micromass displaying the same aspect of the coatings, but they are present without the void association; their distribution and orientation is random, giving the micromass the fibrous aspect described earlier (fig.178).

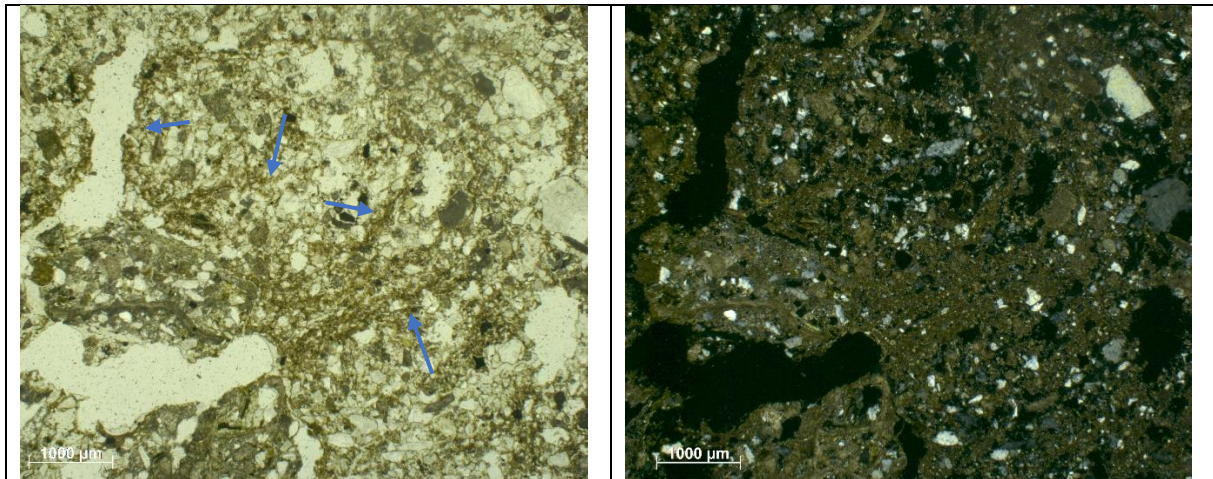


Fig.178: Fibrous aspect of the micromass. Note the random distribution of the linear aggregations of micromass giving the fibrous aspect (arrows), and the finer coarse fraction.

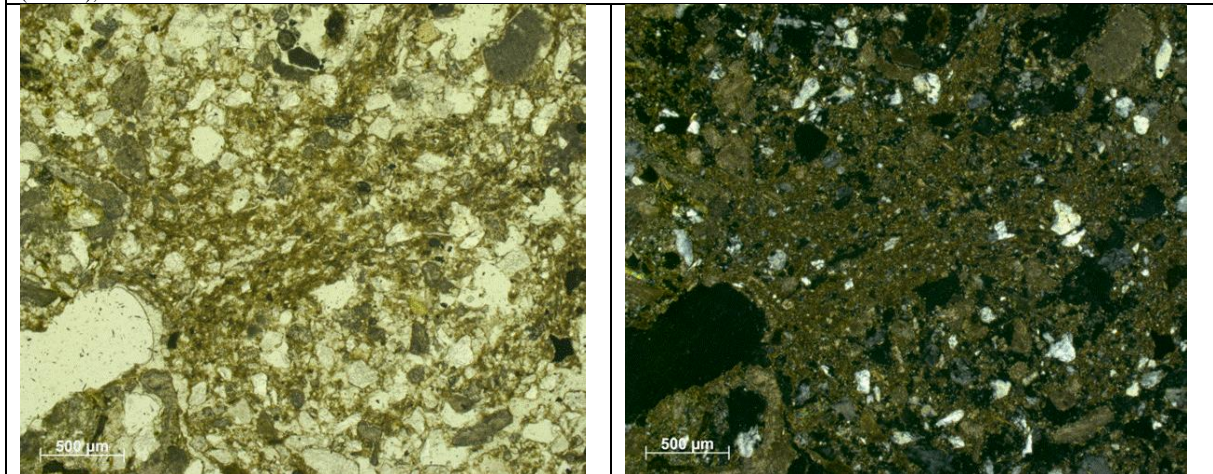


Fig.179: Detail of fig.15. Note the porphyritic distribution pattern

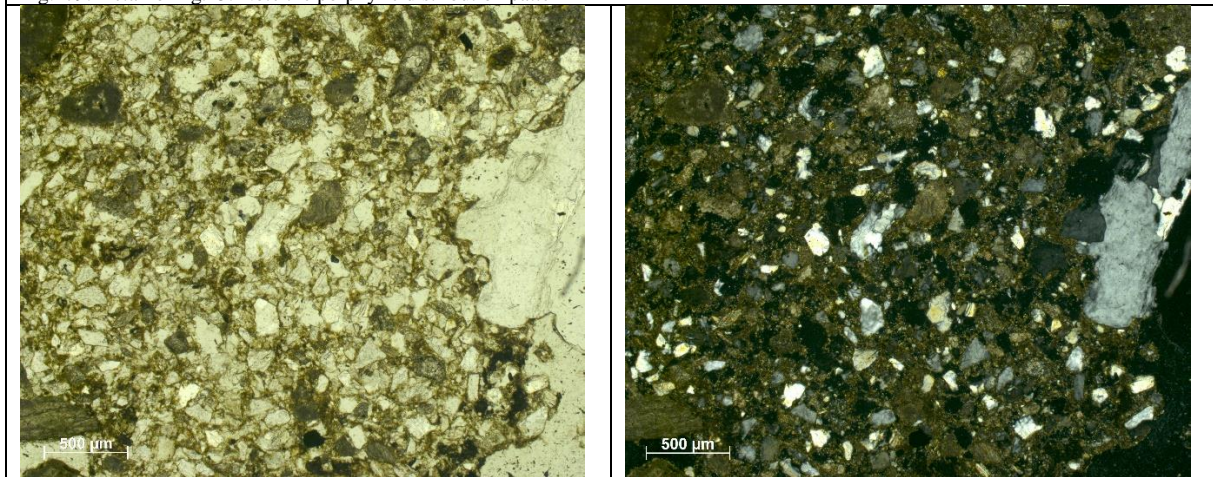


Fig.180: Chitonic to gerufic related distribution pattern. Note how on the top left corner the r.d.p. is still porphyritic.

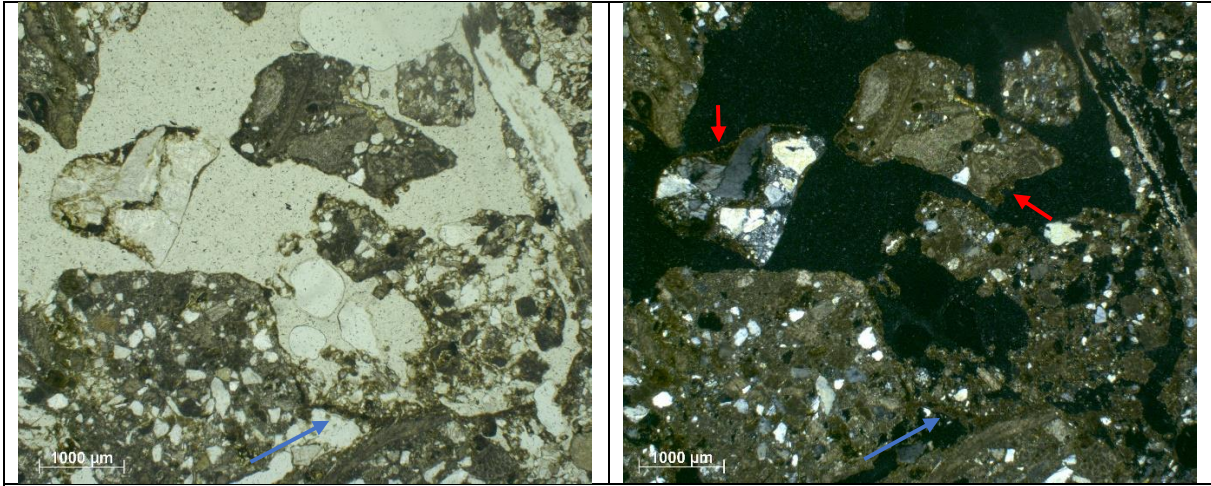


Fig.181: Link capping between two coarse elements (blue arrow). Note the granostriated b-fabric (red arrow) in XPL.

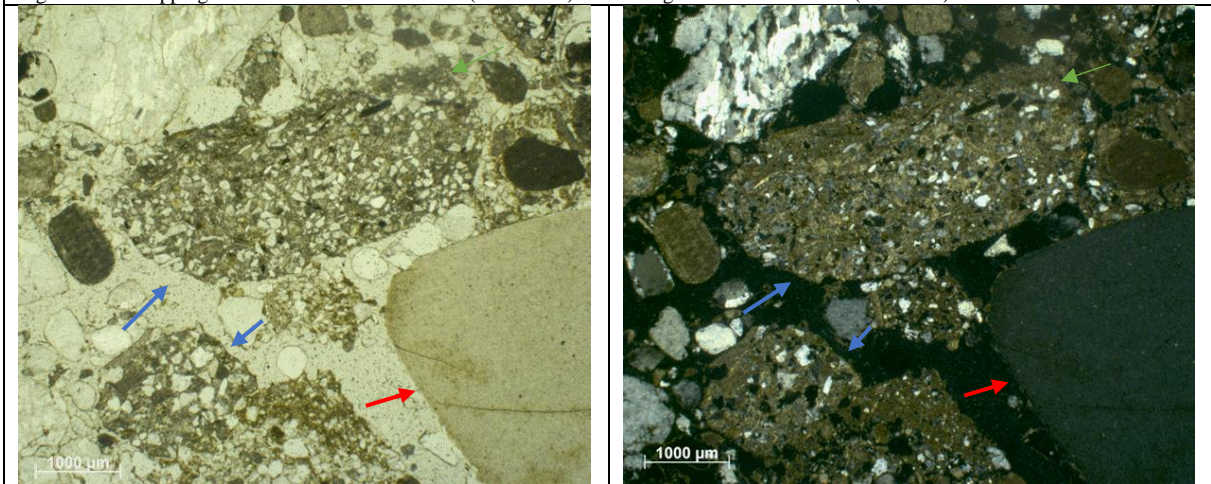


Fig.182: Aggregates of cemented calcitic matrix (blue arrow) with calcitic capping on top (green arrow). Unidentified lithology (red arrow).

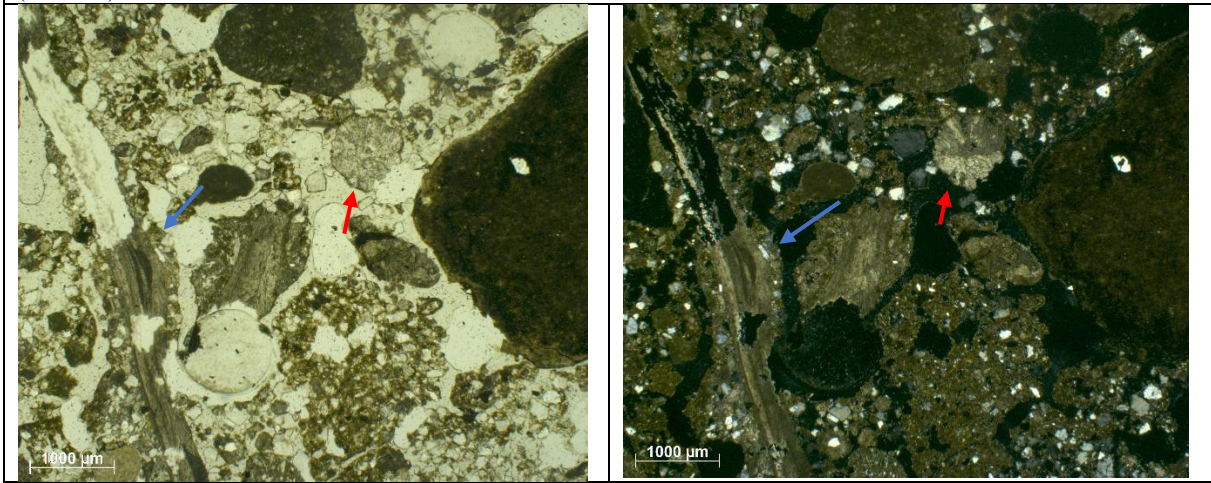


Fig.183: Tabular carbonate rock fragment (blue arrow) and biospheroid (red arrow).

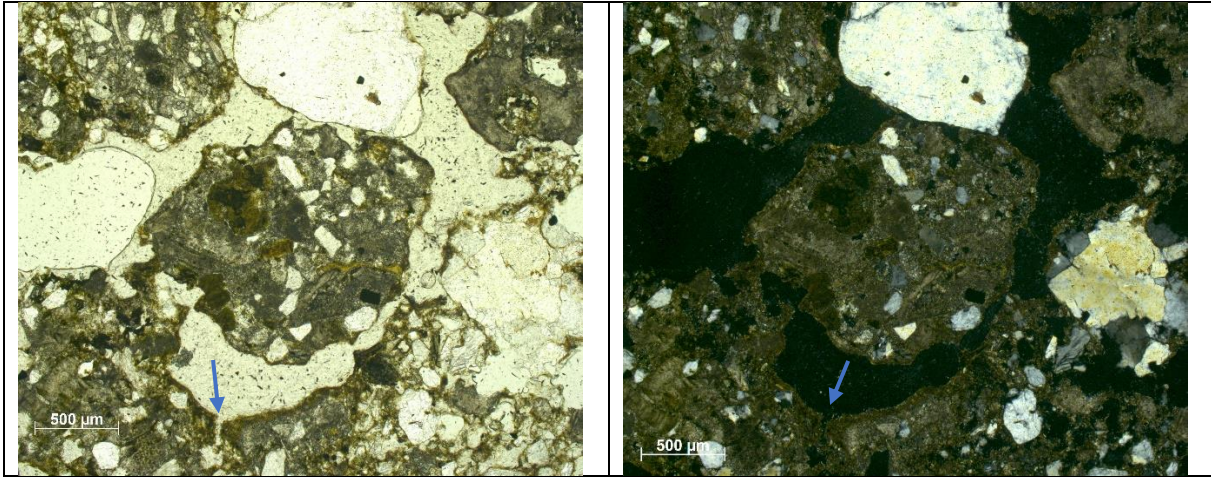


Fig.184: Typic micromass coating of void (arrow).

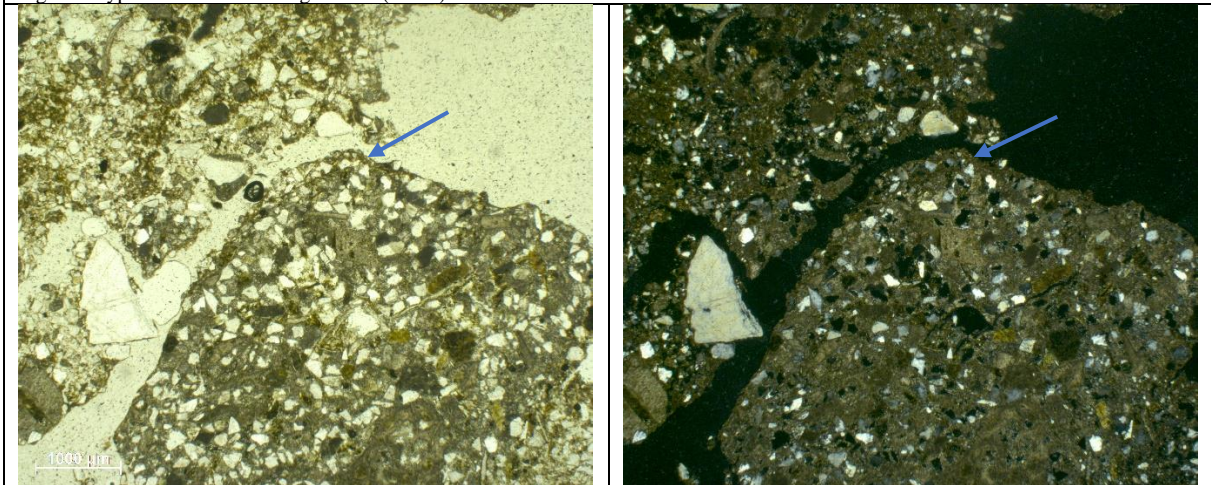


Fig.185: Capping of fine fraction (arrow) on aggregate of cemented calcitic matrix.

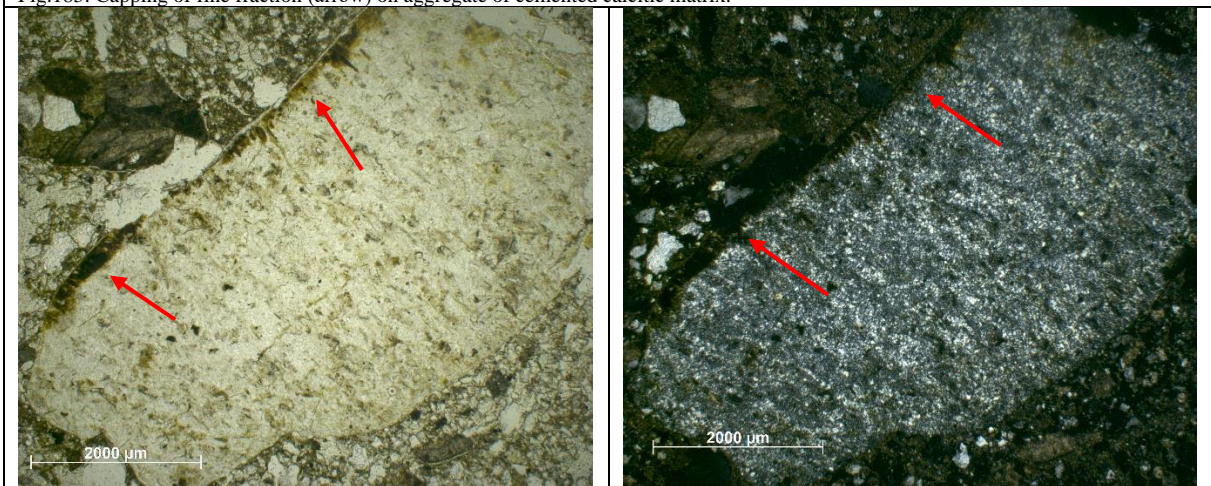


Fig.186: Flint with surface alteration (arrow).

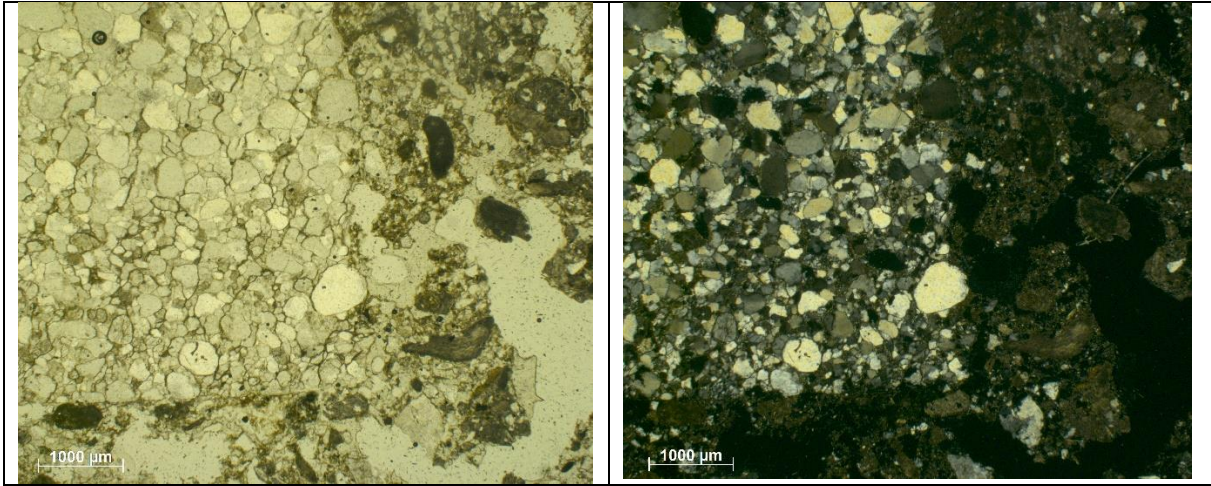


Fig.187: Quartzite rock fragments displaying a very angular shape and regular and smooth surfaces with sharp boundaries.

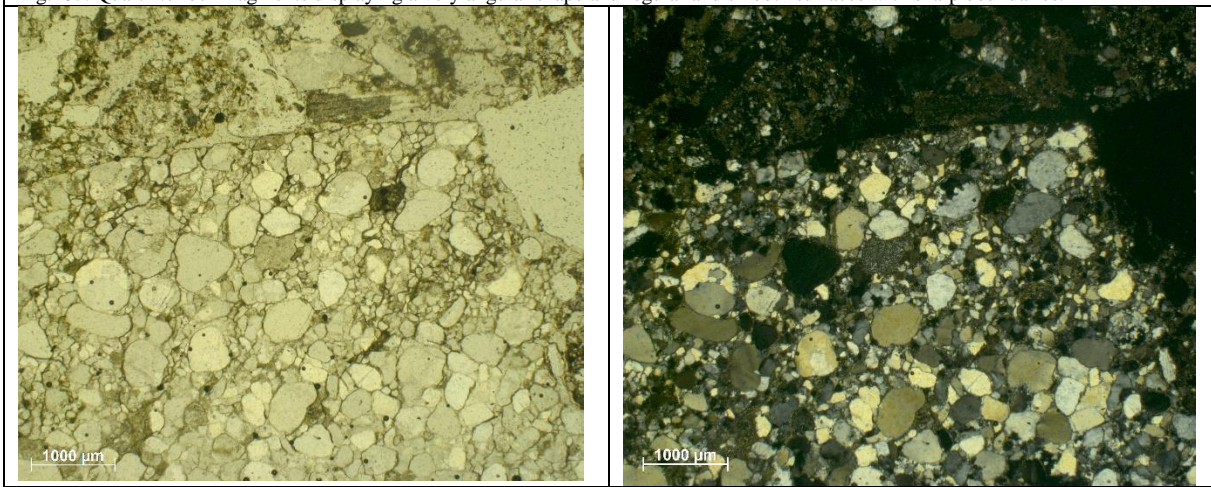


Fig.188: Same element presented in fig.29

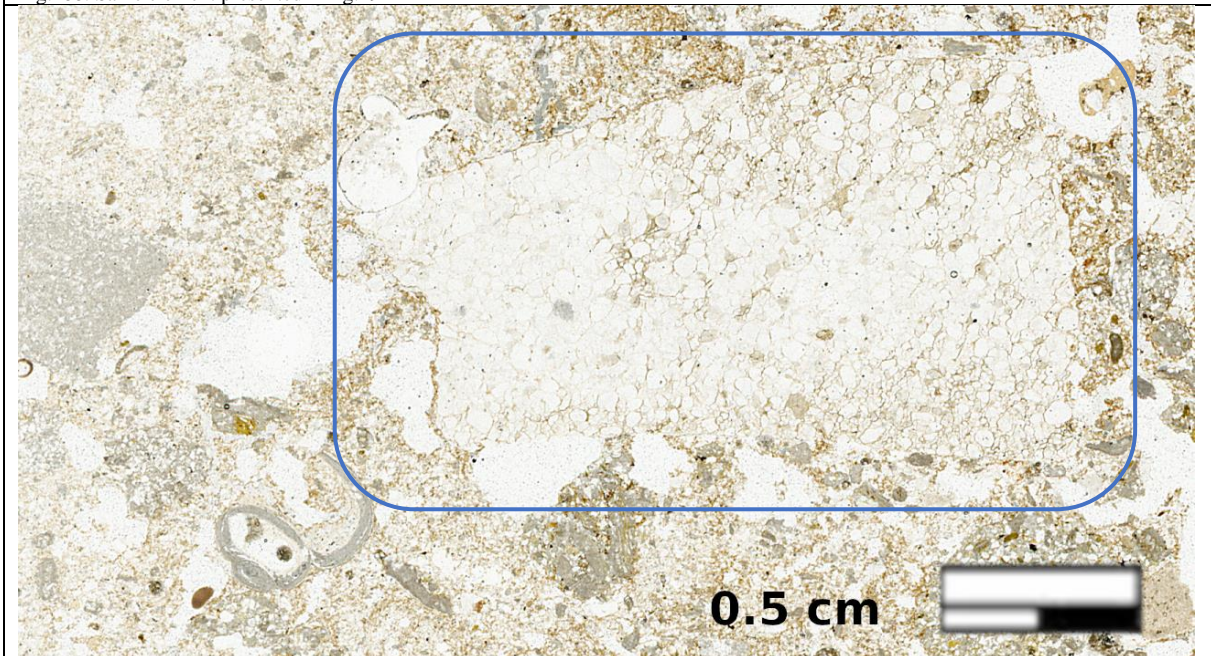


Fig.189: Quartzite rock fragments, note the very angular shape and the regular and smooth surfaces with sharp boundaries. Characteristics not present in other elements and often pointing to a knapped artifact.

Appendix bibliography

Angelucci, D.E., 2017. Lithic Artefacts. In: Nicosia, C., Stoops, G. (Eds.), *Archaeological Soil and Sediment Micromorphology*. John Wiley & Sons, Ltd, Chichester, UK, pp. 223–230. doi:10.1002/9781118941065.ch27

Friesem, D.E., Shimelmitz, R., Schumacher, M.L., Miller, C.E., Kandel, A.W., 2022. A micro-geoarchaeological view on stratigraphy and site formation processes in the Middle, Upper and Epi-Paleolithic layers of Sefunim Cave, Mt. Carmel, Israel. *Archaeological and Anthropological Sciences* 14, 222. doi:10.1007/s12520-022-01686-0

Horwitz, L.K., Goldberg, P., 1989. A study of Pleistocene and Holocene hyaena coprolites. *Journal of Archaeological Science* 16, 71–94. doi:10.1016/0305-4403(89)90057-5

Kooistra, M.J., Pulleman, M.M., 2010. Features Related to Faunal Activity. In: *Interpretation of Micromorphological Features of Soils and Regoliths*. Elsevier, pp. 397–418. doi:10.1016/B978-0-444-53156-8.00018-0

Major, J.J., 1998. Pebble orientation on large, experimental debris-flow deposits. *Sedimentary Geology* 117, 151–164. doi:10.1016/S0037-0738(98)00014-1

Acknowledgements

I would like to thank Laurent Bruxelles for providing me with the opportunity to study the beautiful archaeological site of Mas Des Caves (Lunel-Viel, Hérault), for installing in me a passion for the subterranean world and for guiding me within the scope of this Memoire project.

I would like to extend my thanks to Mathieu Lejay for his precious advice, for introducing me to archaeological micromorphology and for the essential technical support given during the micromorphological analysis.

I also wish to thank Federica Fontana and Michele Bassetti for the support from the other side of the Alps and for the theoretical and practical background they transmitted to me last year.

I want to express my gratitude to the Research Project on the archeo-paleontological cave-site of Mas Des Caves. This project has been supported by the French Ministry of Culture and SRA-DRAC Occitanie through the 'Fouilles programmées' since 2019, led by Jean-Philippe Brugal (UMR 7269, LAMPEA, Aix-en-Provence), whom I would also like to thank for his hospitality in Lunel Viel.

In January 2023, with the help of Laurent Bruxelles and Jean-Philippe Brugal, we collected block samples for the micromorphological analysis. These samples were then sent to the PACEA laboratory in Bordeaux (UMR 5199), where they prepared the thin sections, thanks to funding from the Mas Des Caves research project. By April 2023, we had the five thin sections ready for study, which was made possible thanks to the TRACES laboratory.

Finally, I would like to express my gratitude to the Double Degree program between Università degli Studi di Ferrara and Université Toulouse Jean Jaurès, and to the Bando Vinci from the Università Italo-Francese for allowing me to attend this year in Toulouse.